DOCTOR OF BIOMEDICAL AND PHARMACEUTICAL SCIENCES

New insights into therapeutic strategies for obesity-induced chronic kidney disease
Is there a central role for AMP-activated protein kinase?

JUSZCZAK, Florian

Award date:
2022

Awarding institution:
University of Namur
Université de Mons (UMons)

New insights into therapeutic strategies for obesity-induced chronic kidney disease:

is there a central role for AMP-activated protein kinase?

Dissertation originale présentée par **Mr. Florian Juszczak** en vue de l'obtention du grade légal de **Docteur en Sciences Biomédicales et Pharmaceutiques**

Promoteur :
Prof. Anne-Emilie Declèves — Laboratoire de Biochimie Métabolique et Moléculaire, Institut de recherche en sciences et technologies de la santé, Faculté de Médecine et Pharmacie, UMONS

Co-promoteur :
Prof. Nathalie Caron — Laboratoire de Physiologie Générale, Unité de Recherche en Physiologie Moléculaire, NARILIS, UNamur

Membres du jury :
Prof. Jean-Marie Colet (UMONS) - Président
Dr. Alexandra Tassin (UMONS) - Secrétaire
Prof. Thierry Arnould (UNamur)
Prof. Charles Nicaise (UNamur)
Dr. Benoit Viollet (Institut Cochin, Paris, France)
Prof. François Jouret (ULiège)

Année académique 2020-2021

Remerciements

C'est avec émotion que se termine mon parcours de doctorat, la concrétisation de quatre années de recherche et plus généralement l'aboutissement de neuf années d'études autant intenses que passionnantes.

J'adresse mes premiers remerciements aux membres de mon jury de thèse, lecteurs avertis de ce présent ouvrage. Merci au Prof. François Jouret et au Dr. Benoît Viollet, membres externes, pour leurs regards critiques et distanciés vis-à-vis des données de recherche ainsi que pour leur participation dans l'élargissement des discussions et perspectives de ce travail. Je remercie également le Dr. Alexandra Tassin, le Prof. Charles Nicaise, le Prof. Jean-Marie Colet et le Prof. Thierry Arnould, membres de mon comité d'accompagnement et de jury de thèse, pour le suivi depuis les prémisses de ce projet jusqu'à sa concrétisation. Je remercie tout particulièrement Alex de m'avoir partagé son expertise du modèle expérimental d'entrainement physique en endurance, ainsi que le Prof. Alexandre Legrand pour m'avoir ouvert les portes de son laboratoire dans lequel j'ai pu réaliser les manipulations *in vivo* présentées dans la première partie de cette thèse. Je remercie par ailleurs très sincèrement Vinciane pour son aide et enseignements des différentes expertises du laboratoire de physiologie ainsi que Sarah et Jérôme pour le soin apporté aux animaux. Je remercie également le Prof. Thierry Arnould pour l'impulsion et expertise scientifique apportée à ce travail concernant l'étude de la Sirtuine 3 dans nos différents modèles expérimentaux. Je ne peux qu'espérer que les collaborations initiées dans les différents projets de recherche de cette thèse pourront se poursuivre et plus amplement se concrétiser dans le temps.

Evidemment, je remercie ma promotrice de thèse, le Prof. Anne-Emilie Declèves. Merci d'avoir cru en moi, de m'avoir donné la liberté de chercher qui m'est essentielle, merci pour ta disponibilité et ton soutien dans les réussites comme dans les échecs. J'espère que tout ceci n'est que le début d'une longue histoire … Je pense aussi à ma co-promotrice, le Prof Nathalie Caron. Ta passion pour la physiologie rénale a été très inspirante pour moi. Merci pour ta gentillesse et ton humanité.

Je remercie tous les membres du laboratoire de Biochimie Métabolique et Moléculaire de l'UMONS, mon labo « d'origine », où j'avais déjà réalisé mon mémoire sous la direction du Prof. Alexandra Belayew, qui m'a notamment donné l'envie de poursuivre mon parcours dans le milieu de la recherche. Pendant donc plus de 5 années dans ce laboratoire, j'ai eu la chance de rencontrer de nombreuses personnes et je garderai évidemment de nombreux souvenirs de cette longue période. Je remercie donc Clothilde, Aline, Manon, Virginie, Carole, Thomas et Frédérique. Je n'oublierai notamment pas mes débuts partagés avec Aline, nos longues conversations souvent scientifiques mais pas que… , nos journées interminables et ponctuées de mille et une questions de la part des étudiants du laboratoire à l'époque très nombreux voire trop nombreux pour nos deux pauvres cerveaux. Clothilde, tu nous as rejoint peu de temps après, reprenant ainsi le dessus des doctorant sur les mémorants dans notre bureau,

avec à la clé un peu plus de sérénité. Merci pour ton grain de folie (raisonnable), ton inventivité et créativité en particulier pour nous créer des super surprises d'anniversaire mais aussi des activités pédagogiques dignes d'un film de science-fiction. Merci à Manon pour ton amitié et nos beaux voyages ensoleillés ou rafraichissants … Merci à Thomas pour son aide technique très utile et au Dr. Frédérique Coppée pour ses feedback scientifiques.

J'ai eu l'opportunité de réaliser ma thèse en cotutelle dans deux laboratoires, à l'UMONS et à l'UNamur. C'est à cette occasion que j'ai pu découvrir une autre université, une autre ville, un autre environnement de recherche ainsi d'autres personnalités. Je n'ai pas souhaité que cette collaboration ne se retrouve uniquement que sur le papier, mais j'ai essayé, non sans difficultés, de m'investir au mieux de part et d'autre de la Wallonie. C'est ainsi que je suis arrivé dans le laboratoire de Physiologie Générale dans lequel j'ai élu domicile à la fin de ma thèse. Merci à Inès, Pauline, Audrey et Olivia de m'avoir directement intégré dans le laboratoire. Inès, je me souviendrai particulièrement de notre beau congrès dans ce magnifique château à Florence, mais aussi de toutes nos conversations sur tous les sujets. Merci à Olivia, notre super-technicienne pour ton aide mais aussi ton sourire et ta bonne humeur en toute circonstance qui rend le travail au quotidien beaucoup plus agréable dans le laboratoire. Pauline, merci aussi pour ton aide et nos échanges de connaissances sur nos modèle expérimentaux et idées de recherche en néphrologie. Je souhaite évidemment la bienvenue dans notre groupe à Louise. Grâce à toi, je sais que la relève est assurée et que nos projets sont entre de bonnes mains. Je te souhaite autant de réussites (et pas trop d'échec) et d'épanouissement qu'ils ont pu également m'apporter. Merci aussi à Olivier de l'URPhyM pour ton amitié.

Au cours de mon doctorat, j'ai pu m'éloigner encore un peu plus de Mons et de la Belgique en général lors d'un séjour de recherche à l'Université de Zurich. À cet égard, je remercie le Prof. Olivier Devuyst de m'avoir accueilli dans son laboratoire et de m'avoir donné le champ libre pour réaliser les différentes expériences que j'avais imaginées. Un très grand merci au Dr. Alessandro Luciani pour la supervision scientifique et à Huguette Debaix pour l'aide technique très précieuse durant ce séjour. Merci aussi à Alex, mon colocataire expatrié en Suisse pour m'avoir fait découvrir le pays et les randonnées dans les montagnes …

Pendant le doctorat, il nous est aussi demandé d'encadrer des étudiants et de superviser leurs mémoires/travaux de fin d'étude. J'ai donc eu la lourde tâche de suivre pas plus de 7 étudiants aux personnalités très variées. Heureusement, vous avez été plus que motivés et investis dans les travaux que je vous ai confiés. Merci donc à Maud, Céline, Margaux, Anne-Laure, Pauline, Tim et Morgane pour leurs contributions à ce travail.

Bien sûr, je ne vais pas oublier de remercier tous mes proches qui m'ont soutenu pendant tout ce parcours. Mes amis d'enfance, de toujours, de fac et du hasard de la vie (pour ceux que je n'ai pas encore cités) … Laetitia, Laure, Maïté, Marie, Myrtille, Pauline, Tiffani … vous savez déjà tout ! Je suis très fier de vos parcours respectifs dans la vie et je serai là pour vous supporter

comme vous l'avez fait pour moi. Merci à Emilien de m'avoir soutenu ces longs derniers mois d'écriture qui ont été particulièrement pénibles. Je te souhaite beaucoup de réussite pour ta thèse.

Je terminerai par remercier mes parents qui ont toujours suivi mes choix, qui ont absorbé le stress et l'inquiétude à ma place mais qui ont toujours eu confiance en moi et en ce que je pouvais accomplir. Merci à ma grand-mère et à ma marraine (ma bonne fée), grandes supportrices toujours présentes dans les moments importants. Finalement, merci à ma sœur dont l'esprit cultivé et l'intelligence continueront de m'inspirer.

De près ou de loin, vous avez tous contribué à ma réussite.

Florian

À la mémoire de

Claude Luc

et de

Huguette Dubois

Summary

Since the last decades, obesity has become epidemic worldwide largely due to the combination of our sedentary lifestyle, associated with a high caloric intake and the lack of physical activity. Obesity is associated to a wide variety of health complications such abdominal adiposity, hyperlipidemia, hyperglycemia, hyperinsulinemia and hypertension that may impair health. Accumulating studies have reported that obesity is a significant risk factor for chronic kidney disease (CKD) and the second most highly prognostic factor to predict end-stage renal disease. Characteristic features of obesity-induced CKD include obesity-related glomerulopathy associated to glomerulomegaly and, ultimately, focal glomerulosclerosis. We particularly demonstrated ectopic lipid depositions in proximal tubular cells, suggesting a role of fat accumulation in the development and progression of CKD. This ectopic lipid accumulation impairs fatty acid β-oxidation in kidney cells and tissue. Moreover, evidence of a dysregulation of AMP-activated protein kinase (AMPK) activity in podocytes and proximal tubular cells in obesity condition has been demonstrated by our group and others. AMPK is a central mediator of energy homeostasis responsive to nutritional and metabolic stress such as obesity but is also a key regulator of autophagy and mitochondrial homeostasis. Despite considerable efforts in the development of new therapeutic strategies for obesity-related diseases, there is still a lack of effective treatment without strong side effects, particularly for obesity-induced CKD. This highlights the urgent need for alternative therapeutic strategies. Particularly, behavioral interventions such as exercise have regained interest and may represent a safer alternative therapeutic approach for the treatment of chronic metabolic disorders. Moreover, the effects of exercise training in obesity-induced CKD remains poorly investigated and the pre-clinical and clinical data are still controversial. Understanding the underlying mechanisms of exercise-based therapy may lead to new therapeutic opportunities for the management of obesity-related disorders.

In view of these points, our objectives were to investigate the effect of exercise training intervention in a mice model presenting obesity-induced CKD. We particularly highlighted potential biomarkers that could be targeted with a dietary compound as an exercise mimetic to treat or prevent obesity-induced CKD. Furthermore, the central role of AMPK pathway regulation in this pathological context and in the responsiveness of each treatment was particularly evaluated. Thus, we firstly investigated an endurance exercise training protocol on a treadmill applied on obese mice presenting CKD. The animals exposed to a HFD for 20 weeks presented the hallmarks of obesity including hyperinsulinemia, glucose intolerance, hyperlipidemia and hepatic steatosis. A delayed endurance exercise training (EET; for the last eight weeks of the protocol) was associated to a strong improvement of glucose tolerance, insulinemia and dyslipidemia without weight loss as well as a drastic decreased in ectopic lipid accumulations in the

liver. Furthermore, exercise in obese mice reduced glomerular impairments, improved kidney function and tubular lipid depositions in the kidney, associated to a decreased fibrosis and inflammation. These results were concomitant with an improvement of the AMPK pathway by exercise in renal tissue as well as an enhanced autophagy flux. Finally, the mitochondrial NAD^+-dependent deacetylase Sirtuin 3 (SIRT3) was found to be decreased with obesity while its expression was enhanced with exercise in kidney tissue.

Based on the EET study, the next step of this PhD project was to investigate SIRT3 as a new potential biomarker or therapeutic target for obesity-induced CKD. We collected kidney and urine samples from obese mice model overexpressing SIRT3. In this section, we evaluated whether overexpression of SIRT3 protected mice from obesity-related CKD. Wild-Type HFD mice presented renal hypertrophy and impaired renal function as attested by an increased albuminuria and proteinuria. Evidence of proximal tubule injury was observed in these mice with the presence of enlarged lipid vacuoles. In addition, these alterations were associated with the reduction of AMPK activity and the relative mRNA and protein expression of SIRT3. Interestingly, renal hypertrophy and impaired renal function were significantly improved in SIRT3 transgenic mice fed a HFD. This was also associated to a reduced number and size of ectopic lipid vacuoles in proximal tubular cells and an enhances AMPK activity. These findings revealed that SIRT3 plays a critical role in ectopic lipid accumulation in proximal tubular cells and impairment of renal function. Activation of SIRT3 normalized the renal alterations observed in HFD WT mice and may thus represent a potential strategy to improve altered lipid metabolism in HFD-induced CKD.

Lastly, the nicotinamide riboside (NR), a NAD^+ precursor, has been used to maintain SIRT3 deacetylase activity both in *in vitro* and *in vivo* models of renal lipid overload. NR-treated cells were associated to an increased level of NAD^+ with a decrease in the accumulation of lipid droplets in renal cells treated with palmitic acid (PA). Moreover, NR treatment prevented mitochondrial dysfunction, oxidative stress and lipid peroxidation in renal cells exposed to lipid excess. Regarding the investigation of NR *in vivo*, wild-type mice were fed either a LFD or a HFD during 20 weeks treated or not with early (at the beginning of the specific diet) or late (starting at week 12) supplementation with NR in the diet. Our results demonstrated that NR supplementation led to an effective activation of SIRT3 in renal tissue, associated to an enhanced AMPK activity. However, the effects of NR on obesity-induced CKD were mitigated. Moreover, our results highlighted an increased ectopic lipid deposition in the liver and in the kidney, suggesting that NAD^+ increase in tissues may reduce metabolic flexibility of the tissue during long-term exposure.

List of abbreviations

ACC	acetyl coA carboxylase
ACE	angiotensin-converting enzyme
AdipoR1	Adiponectin Receptor 1
AdipoR2	Adiponectin Receptor 2
AKI	acute kidney injury
Akt	protein kinase B (PKB)
AMPK	AMP-activated protein kinase
AP1	Activator Protein 1
ATM	adipose tissue macrophages
AUC	area under the curve
BAT	brown adipose tissue
BMI	body mass index
CAMKKβ	calcium/calmodulin kinase kinase β
CD36	scavenger receptor
CFTR	cystic fibrosis transmembrane conductance regulator
CKD	chronic kidney disease
CT	computed tomography
CVD	cardiovascular disease
DAG	diacylglycerols
DRP1	dynamin-like protein 1
DXA	X-ray absorptiometry
EET	endurance exercise training
ENaC	epithelial sodium channel
ER	endoplasmic reticulum
Er-α, -β	estrogen receptor-alpha, -beta
ESRD	end stage renal disease
ETC	electron transport chain
FA	fatty acid
FABP	fatty Acid-binding Protein
FA-CoA	fatty acyl-CoA
FAS	fatty acid synthase
FATP	fatty acid transporter
FFA	free fatty acid
FSGS	focal segmental glomerulosclerosis
FTO	fat mass obesity
FUNDC1	FUN14 domain containing 1
GFR	glomerular filtration rate
GLUT4	glucose transporter Type 4
GTT	glucose tolerance test
GWAS	genome-wide association study
HFD	high-fat diet
HIF1α	hypoxia-inducible factor 1 alpha
HMGCR	HMG-CoA reductase IDH2: isocitrate dehydrogenase
HMW	high molecular weight
HO-1	Heme oxygenase-1
HPA	Human Protein Atlas
IDO	indoleamine 2,3-dioxygenase
IKB	inhibitor of κB

IKK	IκB kinase
IL-1β	interleukin 1 beta
IL-6	Interleukin 6
IRS 1,2	insulin receptor substrates
JNK	c-Jun N-terminal Kinase
kJ	kilo Joules
LCAD	long chain acyl-coA dehydrogenase
LD	lipid droplet
LKB1	liver kinase B1
LMW	low molecular weight
LPL	lipoprotein lipase
MCP-1	Monocyte chemoattractant protein-1
MetS	Metabolic Syndrome
MFF	mitochondrial fission factor
MMP2	matrix metalloproteinase–2
MRI	magnetic resonance imaging
MRS	magnetic resonance spectroscopy
NAD	The nicotinamide adenine dinucleotide (NAD)
NADPH	Nicotinamide adenine dinucleotide phosphate
NADS	NAD^+ synthase
NAFLD	Non-Alcoholic Fatty Liver Disease
NAMN	nicotinic acid mononucleotide
NAPRT	nicotinic acid phosphoribosyltransferase
NEFA	non-esterified fatty acids
NFκB	nuclear factor kappa B
NHE	sodium-hydrogen exchanger
NKA	Na^+-K^+-ATPase
NKCC	Na-K-Cl cotransporter
NMNAT	NAMN transferase
NO	nitric oxide
NR	nicotinamide riboside
NRF-1/2	nuclear respiratory factor 1 and 2
ObR	leptin receptor
ORG	obesity-related glomerulopathy
PA	palmitic acid
PARP	poly adenosine diphosphate ribose polymerase
PAS	Periodic acid shiff
PCT	proximal convoluted tubule
PGC-1α	peroxisome proliferator-activated receptor gamma co-activator 1-alpha
PI3K	phosphatidylinositol-3'-kinase
PKC	protein kinase C
PLIN2	Perilipin2
PP2A	protein phosphatase 2A
PP2C	protein phosphatase 2C
PPARα	peroxisome proliferator-activated receptor alpha
PPARγ	peroxisome proliferator-activated receptor gamma
PT	permeability transition
PTEN	phosphatase and tensin homolog
PUFA	polyunsaturated fatty acids

List of abbreviations

RAAS	renin-angiotensin-aldosterone system
ROS	reactive oxygen species
RSNS	renal sympathetic nervous system
SAT	subcutaneous adipose tissue
SDC1	steroyl CoA desaturase 1
SGLT	sodium-glucose cotransporters
SOD2	superoxide dismutase 2
SREBP-1	sterol regulatory element-binding protein-1
T2D	Type 2 diabetes
TAK1	transforming growth factor (TGF)-β-activated kinase-1
TG	triglycerides
TDO	tryptophan 2,3-dioxygenase
Tfam	Mitochondrial Transcription Factor A
Tg	trangenic
TGFβ	Transforming Growth Factor beta
TLR	toll-like receptors
TNF-α	Tumor necrosis factor α
TRPC6	transient Receptor Potential Canonical Channel 6
TSC2	Tuberous Sclerosis Complex 2
UACR	urinary albumin to creatinine ratio
UCP1	uncoupling protein 1
ULK-1	Unc-51 like autophagy activating kinase
VAT	visceral adipose tissue
WAT	white adipose tissue
WHR	waist-to-hip ratio
WT	wild-type

Table of contents

Introduction

1 Obesity

1.1 Definition and diagnosis

Obesity is fundamentally defined by an excessive fat accumulation as triacylglycerols in the adipose tissue, increasing adipose tissue mass, that may impair health [1,2]. In humans, obesity condition is attested when the body mass index (BMI), which means the body weight in kilograms divided by the height in meters squared (kg/m^2), is greater than or equal to 30 kg/m^2. Obesity is subclassified into class 1 (30–34.9), class 2 (35–39.9) and class 3 (≥ 40) category [3]. Even though BMI is widely recognized to diagnose and classify adiposity, recent clinical practice guidelines promote the waist circumference measurement in routine physical examination as a better indicator of obesity-related health risks [4,5]. Waist circumference (more than 105 for women and more than 110 for men) represents the abdominal adiposity that is associated to a greater risk of death compared to BMI-defined obesity alone, particularly when the BMI is low [6]. Indeed, waist circumference or waist-to-hip ratio more strongly correlate with visceral adipose tissue than BMI [7]. Another argument is that high intra-abdominal fat has been associated to a constellation of other health risk factors that promotes a clinical condition termed the Metabolic Syndrome (MetS) [8]. MetS is characterized and diagnosed with different criteria which have been extensively discussed in the literature (**Figure 1**). Nevertheless, MetS includes abdominal adiposity, hyperlipidaemia, hyperglycaemia, hyperinsulinemia and hypertension [9]. More recently, innovative techniques are used to assess body composition and fat distribution to improve obesity diagnosis limitations such as dual-energy X-ray absorptiometry (DXA), computed tomography (CT) and magnetic resonance imaging (MRI) or magnetic resonance spectroscopy (MRS) scans [10]. The investigation of "obesity biomarkers" such as the plasma level of adipokines (such as leptin, adiponectin and resistin) also represents an interesting way for a more refined diagnosis and prognosis of obesity-related health problems [11].

	WHO (1999)	NCEP-ATP III (2001)	NCEP-R (2004)	IDF (2005)	AACE
Obesity	WHR >0.90(male) >0.85(female) or BMI>30 kg/m2	WC ≥ 102 cm (male) ≥ 88 cm (female)	WC ≥ 102 cm (male) ≥ 88 cm (female)	[REQIREMENT] WC ≥ 94 cm (male) ≥ 80 cm (female)	Overweight/ Obesity BMI ≥ 25 kg/m^2
Serum triglycerides	≥ 150mg/dl	≥ 150 mg/ dl	≥ 150 mg/ dl or medication	≥ 150 mg/ dl or medication	≥ 150 mg/ dl
Serum HDL Cholesterol	< 35 mg/ dl (male) < 39 mg/ dl (female)	< 40 mg/ dl (male) < 50 mg/ dl (female)	< 40 mg/ dl (male) < 50 mg/ dl (female) or medication	<40 mg/ dl (male) <50 mg/ dl (female) or medication	<40 mg/ dl (male) <50 mg/ dl (female)
Blood pressure	≥ 140/ 90 mmHg	≥ 130/85 mmHg or medication	≥ 130/85 mmHg or medication	≥ 130/85 mmHg or medication	≥130/ 85 mmHg or medication
Fasting plasma glucose	[REQUIREMENT] FPG≥110 mg/ dl	≥ 100mg/ dl	≥ 100mg/ dl	≥ 100mg/ dl or previously diagnosed T2DM	110-126 mg/ dl
Other risk factors	Urinary albumin excretion rate ≥ 20µg/ min or albumin / creatinine ratio ≥ 30 mg/g				Family history of T2DM, HTN, or CVD. Polycystie ovary syndrome, sedentary life stly, Advancing age and ethnic groups having high risk for DM or CVD Physician's judgement
Diagnosis	Impaired FPG+any 2 criteria	Any 3 criteria	Any 3 criteria	WC+any 2 citeria	

Figure 1 | Comparison of different diagnostic guidelines of the Metabolic Syndrome from [12].

1.2 Aetiology

To understand the causes of overweight and obesity, we can refer to the first law of the thermodynamics, whereby if the energy intake and energy expenditure are equals, the body weight is stable, which could be termed as the energy balance [13]. The basic components of the energy balance includes energy intake, energy expenditure and energy storage [14]. The energy intake represents the net metabolizable energy from the 3 major macronutrients in food: carbohydrates, proteins and fat. The components of energy expenditure include all the biological processes by which macronutrients are metabolized to produce metabolically useful energy for many processes such as growth, body maintenance, physical activity, high metabolic organs (brain, heart, kidney, liver) or pregnancy. The excess of macronutrients are stored as glycogen in the muscle and the liver and as triglycerides in the adipose tissue [15]. In healthy individuals, the energy balance is tightly regulated to avoid weight loss and to prevent weight gain [16]. The imbalance between energy consumption and energy expenditure in favour of storage is the main driver of weight gain and consequent overweight or obesity (**Figure 2**).

Regarding the energy intake, the efficacy of absorption of dietary energy can vary between individuals and the nature of the food consumed, which impacts the potential metabolizable nutrients. The energy density of foods (the amount of energy (in kJ) per gram of food) is an important factor that significantly influences the energy intake. Particularly, the fat content (37 kJ/g or 9 kcal/g) considerably increases the food density compared to carbohydrates (17 kJ/g or 4 kcal/g) or proteins (17 kJ/g or 4 kcal/g), making high-fat food highly dense. However, studies showed that the quantity of food intake is

relatively constant among day unlike the amount of energy consumed [17]. Therefore, the consumption of fat-rich diet is associated to an extended energy intake that participates to weight gain while low-fat diet or low energy density carbohydrate-rich diet promotes weight loss [18]. Moreover, the dietary composition of fibres (content; soluble or insoluble) and the glycemic index also influence the energy intake [19]. Foods with a high glycemic index result in a high postprandial glycemic load, increasing demand for insulin secretion by β pancreatic cells and a poorer satiety compared to low glycemic foods [20]. In long term studies in experimental animals as well as in epidemiological studies, diets based on high glycemic carbohydrates were associated to weight gain and enhanced fat storage [21]. Lastly, the energy digestibility is largely different between individuals and also depends on dietary composition, affecting net energy intake [22]. In Western countries, high proceed-food rich in fat and sugar, the lack of exercise and a sedentary lifestyle largely contribute to the increased prevalence of obesity [23]. However, increased fat depositions according to the simplistic view of energy imbalance is not sufficient to explain the complex aetiology of obesity. Indeed, this simple equation overrides many inter-individual differences that contribute to the adaptation of weight gain [24]. In fact, many factors such as genetic and phenotypic interactions, individual behaviours, environment, socioeconomic status or gut microbiota affect food intake and differential fat storage (**Figure 2**).

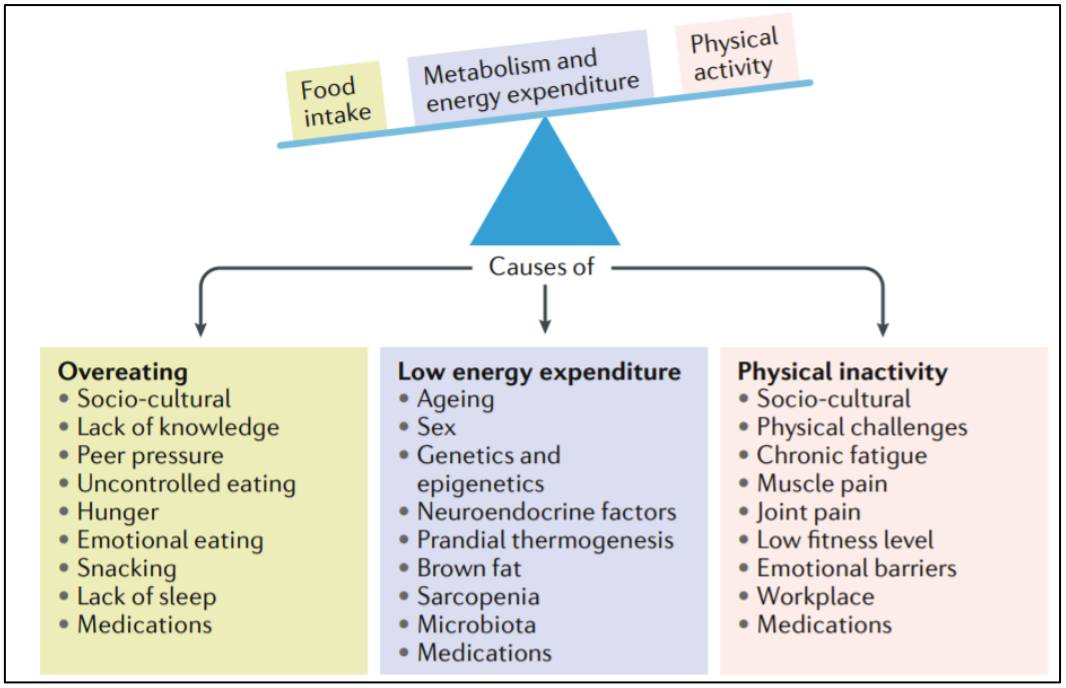

Figure 2 | Factors that can influence the energy balance, thus subsequently causing obesity. Weight gain can result from a combination of increased energy intake, low physical activity and reduced energy expenditure [25].

In addition to environmental factors, obesity has been associated to genetic factors [26]. Particular polymorphisms of specific genes can induce monogenic obesity. In rodents, that includes the gene encoding for leptin (*Lep*) and its receptor (*Lepr*), the melanocortin 4 receptor (*Mc4r*) and pro-opiomelanocortin (*Pomc*) controlling appetite and metabolism. Mutations in the human orthologues of these genes cause monogenic obesity [27]. Actually, more than 150 genetic variants have been robustly associated to changes of BMI [28]. Particularly, a genome-wide association study (GWAS) found a polymorphism (variant rs9939609) in the fat mass obesity (*FTO*) gene that has been consistently associated with a higher BMI and occurrence of type II diabetes [29]. However, the monogenic forms of obesity are considered relatively rare in humans [27,30]. Moreover, the individual impact of each variant on BMI is relatively small and does not explain the explosion of obesity prevalence over the last decades, considering the rapidity with which the incidence of obesity has increased [30]. However, interactions between genetic and environmental factors could explain important individual differences in body weight response to the same environmental exposures. Notably, environmental factors influence epigenetic programming during embryo-foetal and perinatal period of development. For example, maternal obesity has been linked to increased risks of overweight for the offspring [31]. Nogues *et al.* demonstrated that obesity environment for the foetus was associated with DNA methylation of the adiponectin and leptin system [32]. More generally, maternal nutritional status during pregnancy and lactation as well as the perinatal nutrition induce a metabolic imprinting that is being largely investigated [33]. Furthermore, large-scale epigenetic studies identified a large number of DNA methylation sites associated with obesity [34]. However, whether these epigenetic changes are the cause or the consequence is still not clear.

The initiation and development of obesity also vary between genders. Men and women differ in the distribution and proportion of body fat mass. Indeed, the fat distribution is mostly determined by genetic factors and sex steroids production [35]. The percentage of body fat of women measured by computed tomography is more important than for men with a matched BMI [36]. Moreover, women present a lower intra-abdominal/visceral fat mass and have more subcutaneous adipose tissue in the abdominal and in the gluteofemoral area (**Figure 3**), but these differences tend to decrease with age, particularly after menopause [37]. Changes of body fat mass/distribution is an important aspect since it is linked to metabolic significance and associated health outcomes. Central obesity (in abdominal area) has been more associated to metabolic health problems (e.g. diabetes) compared to peripheral fat accumulation, explaining the protective relation between fat deposition in women compared to men [38]. On the other hand, the metabolic function of adipose tissue

differs in males and females. Indeed, a differential gene expression pattern between genders has been highlighted in visceral and subcutaneous adipose tissues, leading to differential adipokine production [39]. Particularly, circulating levels of leptin and adiponectin (discussed later) are increased in women compared to men [40,41]. Moreover, females present a higher mobilization rate of triglycerides (TG) stored in the adipose tissue with an increased lipolysis, while fatty acid (FA) oxidation rate is similar in both sexes, suggesting that females present a more efficient machinery to handle free fatty acids (FFAs) and use it as an energy source under conditions of high energy demands [37].

Differences in circulating gonadal steroid levels play an important role in many sexually dimorphic features. Moreover, estrogens have been widely reported to protect against adipose tissue accumulation. Estrogens act through two nuclear receptors, estrogen receptor-α (Erα) and estrogen receptor-β (Erβ), both of which are expressed in the adipose tissue. Both receptor isoforms are present in mitochondria of white adipose tissue (WAT), suggesting important influences on cell metabolism. Remarkably, loss of ERα also increases the adverse effects of high caloric excess [42].

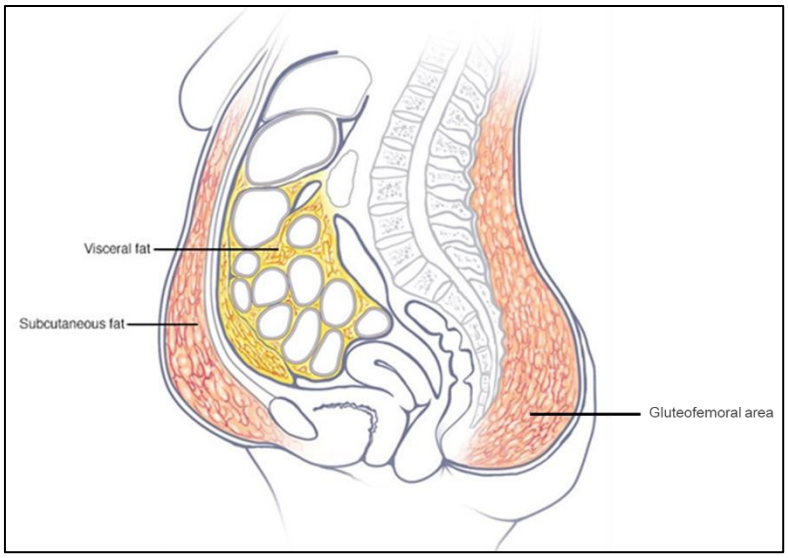

Figure 3 | Anatomical differences in the distribution of subcutaneous adipose tissue (SAT) and visceral adipose tissue (VAT). VAT is mainly present in the mesentery and the omentum while subcutaneous fat is found just beneath the skin, separated by a connective tissue.

1.3 Epidemiology of obesity

The prevalence of obesity has constantly increased over the last decades in both adults and children, in both sexes, globally for all geographical locality, ethnicity and socioeconomic status (**Figure 4**) [43]. However, disparities exist in the general population. The highest rates of obesity are found in Western countries and particularly in the US. In 2015, 39% of the global population were overweight. The prevalence of obesity was 12,5% in 2015, which represent an increase of 80% compared to the prevalence in 1980 [23]. Moreover, 38 million children under the age of 5 were overweight or obese in 2019 (WHO). Projections for 2030 in the US estimate that around 50% of the population will be obese without further political, medical or preventive interventions [44]. Woman are more affected by obesity than man, and the prevalence increases with age for both genders with a greater increase in woman after menopause [43]. Despite biological differences between sexes in terms of fat deposition, adipose tissue storage and metabolism exist, the prevalence of obesity between genders is also the consequence of sociocultural disparities [45]. In low-income countries, obesity is higher among adults from rich and urban environments, whereas in high-income countries, obesity is disproportionately greater in disadvantaged groups [46].

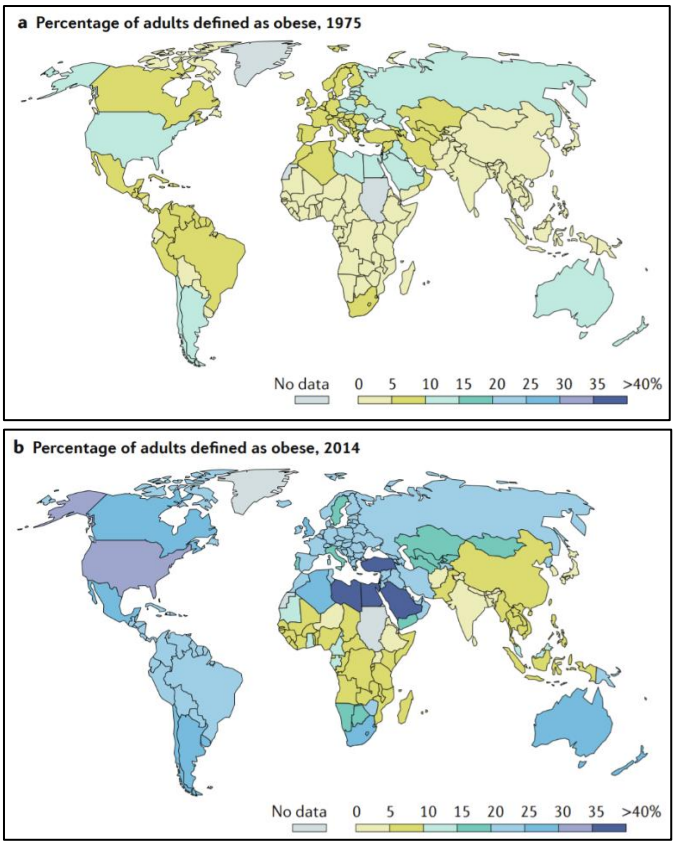

Figure 4 | **Increase in prevalence of obesity over time**. Percentage of adults defined as obese by country in 1975 (part a) and 2014 (part b). The number of adults with obesity increased substantially between 1975 and 2014. Data from the WHO, Global Health Observatory.

1.4 Adiposity: beyond fat accumulation

The adiposity is defined by an excessive accumulation of fat in an expended adipose tissue leading to impairments of the tissue. In fact, obesity-related metabolic disturbance is firstly explained by adipose tissue dysfunction [47].

1.4.1 Healthy adipose tissue

The adipose tissue has not only an important role in energy storage of excess nutrients as triglycerides but also senses energy demands and regulates energy mobilization [47]. The adipose tissue has endocrine, paracrine and autocrine functions and secretes notably cytokines, hormones and lipids to communicate with other tissues [48]. The adipose tissue is mostly composed of adipocytes but it also contains preadipocytes, fibroblasts, macrophages and vascular endothelial cells. There are two types of adipose tissues, the white adipose tissue that stores fat (WAT) and the brown adipose tissue (BAT) implicated in thermogenesis [49]. Another type of AT has been described in mice, the beige adipose tissue, also found in humans [50]. The brown adipocytes are rich in mitochondria with multi-locular lipid droplets and uniquely express the uncoupling protein 1 (UCP1) for heat generation by non-shivering thermogenesis [51]. The white adipocytes present a unique lipid droplet (LD) where is located the storage pool of lipids as TG that plays a crucial role in energy homeostasis [52]. Adipose tissue expansion for storage implicates the increase of adipocytes/LD size (hypertrophy) or the increase of the number of adipocytes (hyperplasia). Hyperplasia mainly occurs when the adipocyte reaches its capacity limit of lipid storage [53]. During positive energy balance, healthy adipocytes hydrolyze excess circulating lipids by the lipoprotein lipase (LPL) releasing non-esterified fatty acids (NEFAs). The NEFAs are re-esterified into TG and stored in the LD. This process is regulated by insulin, secreted during nutrient abundance, that inhibits lipolysis [54]. Moreover, the insulin-dependent glucose transport *via* GLUT4 is required for lipogenesis. During fasting or metabolic stress (e.g. exercise), the TG present in the LD are hydrolyzed into NEFA and glycerol and released in the circulation to be oxidized by other tissues [55]. In healthy WAT, the adipose tissue macrophages (ATM) make around 5% of the tissue mass. The ATM are implicated in the clearance of dead adipocytes during adipocyte turnover to maintain an anti-inflammatory environment [56]. They also play a role in adipocyte lipolysis and in adipogenesis [57]. Despite a high diversity of inflammatory macrophages in the adipose tissue, the ATM display an anti-inflammatory phenotype, close to the “M2 macrophages” in the lean adipose tissue [58].

As mentioned, the WAT is an endocrine organ and synthesize biologically active compounds (hormones, cytokines, growth factors, enzymes, matrix protein) to communicate with other tissues (such as the kidney) or the adipose tissue itself in order to regulate metabolic homeostasis. The cytokines secreted by the WAT are commonly called adipokines. It was particularly demonstrated that the endocrine activity and the expression level and type of adipokines vary between the WAT localization, visceral fat appearing to be more active [59]. Some of important factors secreted by the WAT and their implications in obesity are described below:

Leptin

Leptin is an anorexigenic adipokine that regulates food intake and energy expenditure and, hence, body weight, at the level of the central nervous system (neuroendocrine hormone) by activating its receptor (ObR) in the hypothalamus [60–62]. Leptin increases the sympathetic efferent signal to adipose tissue in order to increase lipolysis [63]. However, leptin receptors are expressed in various tissues as well as in the adipose tissue itself [64]. Leptin functions also include a broad of biological processes such as hematopoiesis, angiogenesis, blood pressure, bone mass, lymphoid organ homeostasis, and T lymphocyte systems [65]. The level of circulating leptin is related to the fat mass [66,67]. Obese individuals present an elevated level of leptin compared to non-obese individuals, suggesting the inability of leptin to exert its functions (with a reduced leptin receptor signaling), defined as leptin resistance [68]. This was also described in animal models of obesity [69,70]. Moreover, exogenous leptin failed to induce anorexigenic effects in obesity conditions [71]. The leptin resistance has been found to be induced by a decreased permeability of leptin for the blood-brain barrier, characterized by an impaired leptin transport [72,73]. Furthermore, chronic low-grade inflammation in the hypothalamus during obesity was suggested to contribute to leptin resistance [74–78]. Recently, Mazor *et al*. established that high-fat diet in mice promoted matrix metalloproteinase–2 (Mmp-2) activation in the hypothalamus, which cleaved the leptin receptor extracellular domain and demonstrated an impaired leptin-mediated activation of its receptor [79].

Adiponectin

Adiponectin is an adipokine with anti-inflammatory and insulin-sensitizing characteristics. It plays an important role in regulating the metabolism of fatty acids and glucose mostly in the liver and in skeletal muscles. Adiponectin is a multimeric protein secreted in different isoforms: trimeric (low-molecular weight; LMW), hexameric (medium-molecular weight; MMW) or high-molecular weight (HMW). Despite the HMW isoform is known to be more biologically active, total and HMW adiponectin have equivalent relevance when assessing adiponectin levels in diseases [80].

Adiponectin signaling is mediated by its two receptors, Adiponectin Receptor 1 (AdipoR1) and Adiponectin Receptor 2 (AdipoR2). AdipoR1 leads to the activation of AMPK pathway and AdipoR2 is associated to peroxisome proliferator-activated receptor alpha **(**PPAR-α) ligand activities. In the same way as leptin, the adipose tissue is the main source of adiponectin and adiponectin release is stimulated by insulin [81,82]. However, contrary to leptin, serum adiponectin level is decreased during obesity in animals and humans although adiponectin-overexpressing mice display an improved insulin sensitivity and protection against steatosis with a High-Fat diet (HFD) [83–85]. The paradoxical decrease of adiponectin is obesity suggest a dysregulation of the adiponectin metabolism. Different studies suggest that visceral fat accumulation in obesity is associated to a decreased in HMW adiponectin level [86,87]. Moreover, oxidative stress, chronic inflammation and pro-inflammatory cytokines such as Tumor necrosis factor α (TNF-α) contributes to the decreased production and release of adiponectin in the adipose tissue [88]. Finally, in addition to decrease in adiponectin concentrations, obesity is also associated to a decline in proper expression of adiponectin receptors on the cell membrane and effective adiponectin binding, so called adiponectin resistance [89].

Monocyte chemoattractant protein-1 (MCP-1)

MCP-1 is a pro-inflammatory adipokine secreted by adipose tissue under hypoxia conditions to recruit and regulate immune cells such as monocytes [90]. MCP-1 is predominantly produced by macrophages and endothelial cells in the adipose tissue and has particularly been linked to atherosclerosis development [91]. Its expression was found to be increased in adipose tissue and in the circulation in many studies on obese animals [92–95]. MCP-1 expression in adipose tissue mostly contributes to the macrophage infiltration but is also implicated in insulin resistance and hepatic steatosis development associated with obesity [96].

Interleukin 6 (IL-6)

IL-6 is a soluble mediator with a pleiotropic effect on inflammation and immune response, and plays a pathological effect on chronic inflammation and autoimmunity [97]. The adipocytes themselves can produce and secrete IL-6, but the main source of IL-6 are WAT macrophages [98]. In the obese WAT, the elevated number of M1 macrophages contributes to the elevated level of local and circulating IL-6 [99]. Whereas physiological expression of IL6 regulates multiple aspects of metabolism, including glucose disposal, lipolysis, oxidative metabolism, and energy expenditure, depending on the environment (e.g. muscle can secrete IL6 following exercise and suppress ATM accumulation in adipose tissue), a dysregulation of IL6 production may lead to insulin resistance and improper inflammatory response [100].

Tumor necrosis factor α (TNF-α)

Tumor necrosis factor α (TNF-α) is a pro-inflammatory cytokine produced by macrophages and implicated in many inflammatory diseases. A systemic increased level of TNF-α as well as its overexpression in WAT have been described in obese humans and animals [101–105]. TNF-α is known to interfere with the insulin pathway by inhibiting the phosphorylation of insulin receptors and therefore, blocking off the activation of insulin-associated transduction signal [105]. In addition, TNF-α plays a role on the regulation of genes encoding key proteins that controls GLUT4 trafficking in WAT and skeletal muscle [106]. This reinforces its implication in the development of insulin resistance. Supporting this, it has also been demonstrated that TNF-α could activate the lipolysis in primary cultures of adipocytes [107]. This was then confirmed in rat where TNF-α infusion induced a rapid increase of pro-inflammatory gene expression in adipocytes along with an increase in plasma concentration of FFA and triglycerides [108]. Consequently, the elevated circulating FFA contribute to the insulin resistance and systemic lipotoxicity.

1.4.2 Unhealthy adipose tissue

The WAT can substantially expend to store energy excess without displaying metabolic disturbance until a certain limit, depending on many factors (inter-individuals disparities, fat localization; described above) [109]. During obesity, unhealthy expansion of the WAT leads to a dysfunctional energy storage, inflammation, fibrosis, hypoxia and altered metabolism of the adipocytes [110]. Indeed, during prolonged energy oversupply, the adipocytes compensate by increasing lipid storage and expending cell size and number [111]. During the WAT remodeling, hypertrophic adipocytes secrete hormones and cytokines to recruit preadipocytes to be differentiated into mature adipocytes. However, different studies have highlighted that hyperplasia is induced in response to dysfunctional hypertrophic adipocytes (lipid-overloaded and insulin-resistant) to recover the pool of metabolically active cells in the WAT [112–115]. Thus, adipogenesis during obesity is limited and adipocyte hypertrophy is the main mechanism of adult fat mass expansion [116].

Alterations in the adipose tissue plasticity are the major trigger of the obesity-associated metabolic complications. In obesity, the inadequate fat deposition in response to caloric overflow leads to systemic metabolic alterations. When the storage capacity of SAT is exceeded, the caloric excess leads to visceral depositions and ectopic lipid accumulations in non-adipose tissues (liver, skeletal muscle, heart and kidney) [117–120]. The caloric overload is induced by dysfunctional hypertrophic adipocytes, leading

to secretion of cytokines and this, in turn, lead to systemic inflammation and impaired adipogenesis [121]. Indeed, the hypertrophic adipocytes present alterations of their cell metabolism. First, lipolysis is elevated in hypertrophic adipocytes in association with an impaired lipogenesis, leading to increased leakage of FFAs [122]. This lipid overload is characterized by an increased level of NEFA and cholesterol in the circulation mediating systemic lipotoxicity and insulin resistance. Moreover, FFAs leakage and the release of pro-inflammatory cytokines by adipocytes promote local and systemic inflammation [123]. Hypertrophy also induces local hypoxia in the adipose tissue. Hypoxia-inducible factor (HIF) 1α is activated and accelerates local inflammation and fibrosis of the adipose tissue [124,125]. Macrophages and T-cells are recruited by the altered secretion of immune-related molecules that promotes infiltration of immune cells [123]. This toxic environment leads to an increased adipocytes death as well as to an accumulation of pro-inflammatory M1-like macrophages, forming a "crown-like structure" around necrotic adipocytes [58]. In addition, M1-polarized macrophages secrete a variety of inflammatory cytokines (interleukin 1 beta (IL-1β), MCP-1, TNF-α, and IL-6) further contributing to local and systemic inflammation and to insulin resistance (**Figure 5**).

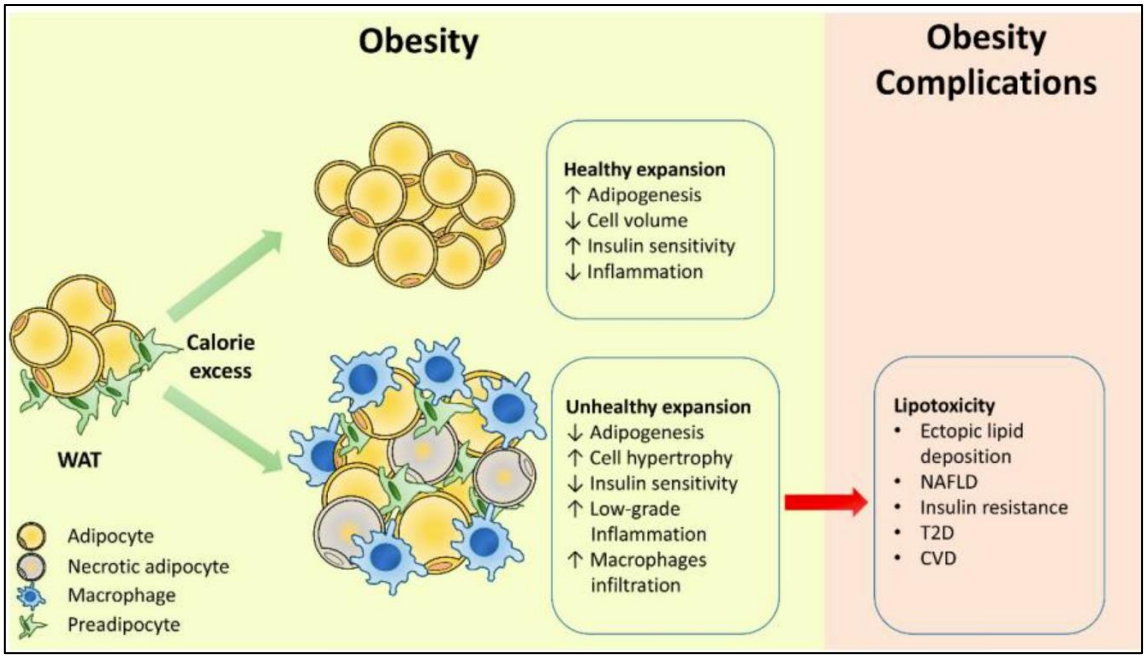

Figure 5 | In obesity context, WAT is characterized by adipocytes hypertrophy and hyperplasia. In addition, the remodeling of WAT is accompanied by a disparity of adipokines secretion and immune cells in favor of pro-inflammatory cytokines and macrophage infiltration. These changes lead therefore to lipotoxicity, development of cardiovascular disease (CVD) or type 2 diabetes (T2D) [47]. NAFLD: Non-Alcoholic Fatty Liver Disease

1.5 The deleterious consequences of obesity

It is widely recognized that obesity is directly associated to increased risks of developing diseases and consequently increased morbidity and mortality (the all-cause mortality rate is doubled or tripled with obesity, depending on the grade) [126]. Obesity causes or exacerbates co-morbidities including type II diabetes, hypertension, and dyslipidemia [127]. Indeed, obesity is the most important risk factor for type II diabetes (60% of patients with type II diabetes are obese) [128]. Abdominal visceral fat tissue accumulation has been strongly associated with insulin resistance [129]. Interestingly, many reports supported that even a moderate weight loss (5-10% of body weight) was associated with an improved insulin resistance in obese and diabetic patients, suggesting that lifestyle interventions such as exercise or decreasing energy intake is a fundamental therapeutic strategy for obesity-related disorders [130–133]. Moreover, epidemiological studies have confirmed that obesity is an independent risk factor for the development of cardiovascular diseases (CVD) (coronary heart disease, arterial fibrillation, hypertension or obstructive sleep apnea) [134]. Being overweight increases the risk of developing a heart failure by 33% [135]. Also, a high abdominal fat accumulation enhances mortality risk for patients with CVD [136]. Obesity especially initiates hemodynamic changes, fat infiltration and fibrosis in heart, inflammation and adipokines dysregulation that promote cardiomyocytes dysfunction [137] and CVD with the involvement of obesity-related atherosclerosis [138].

1.5.1 Chronic low-grade inflammation

Obesity induces a systemic low-grade inflammation state, characterized by elevated circulating pro-inflammatory cytokines, so called meta-inflammation. As described above, the starting signal of inflammation is promoted by obesity in adipose tissue which is the primary site of inflammatory process. Circulating concentrations of plasminogen activator inhibitor-1, angiotensin II, C-reactive protein, fibrinogen, and TNF-α are all related to BMI [139]. Moreover, other pro-inflammatory cytokines such as IL-6, IL-1β, and MCP-1 were described in obese animals and patients [140,141]. In contrast, there is a decrease in anti-inflammatory cytokines (adipokines) such as adiponectin. The inflammatory environment is strengthened by the activation of endogenous inflammatory cells that even recruit other inflammatory cells into the adipose tissue. Indeed, evidence of macrophage infiltration into adipose tissue have been reported in obese human and experimental models [93,94,142]. Moreover, resident M2 macrophages shift to pro-inflammatory M1 macrophages that, in turn, produce a large amount of pro-inflammatory cytokines (**Figure 6**). Consequently, the overall production

of inflammatory cytokines creates a toxic environment in adipose tissue but also in other tissues and organs such as the liver, brain, kidneys, or muscles, promoting the development of insulin resistance and deleterious cellular responses in targeted organs [142–145]. The underlying molecular mechanisms that explain the pathogenesis of obesity-induced inflammation associate different cellular pathways including the activation of toll-like receptors (TLRs; particularly through the TLR4/phosphatidylinositol-3'-kinase (PI3K)/Protein kinase B (Akt) signaling pathway), hyperactivation of c-Jun N-terminal Kinase (JNK)-Activator Protein 1 (AP1) and inhibitor of kB (IkB) kinase (IKK)-nuclear factor kappa B (NFkappaB) pathways [146]. During obesity, the elevated level of cytokines can activate JNK in various tissues. Compared with controls, adipose and liver tissues present increased activation of these signaling pathways and genetic deletion of specific kinases of the pathways demonstrated their implication in inflammatory response in obesity condition [147–149]. Particularly, activation of JNK is implicated in obesity-induced insulin resistance and decreased compensatory insulin secretion, both of which are key features of type 2 diabetes (T2D) [150]. JNK is activated in response to various stress signals, including pro-inflammatory cytokines, FFAs, endoplasmic reticulum (ER) stress and reactive oxygen species (ROS) [151]. In adipocytes, JNK activation causes insulin resistance and the increased expression of pro-inflammatory cytokines. In macrophages, JNK activation causes increased expression of pro-inflammatory cytokines that promotes M1 phenotype, and subsequent recruitment of more M1 macrophages [152]. In the liver, JNK activation causes hepatic insulin resistance and is associated to the development of hepatic steatosis and fibrosis [153]. JNK activation causes also skeletal muscle insulin resistance and reduces insulin secretion in pancreatic ß-cells [154]. JNK activation causes central insulin resistance (in the hypothalamus), which affects general energy homeostasis. Indeed, this kinase can inhibit insulin signaling via serine phosphorylation of IRS-1, thus disturbing downstream insulin actions [155]. Another important hallmark of obesity-induced inflammation is the immune cell infiltration. This occurs not only in the adipose tissue but also in targeted non-adipose tissues. Indeed, evidence of inflammatory processes in liver, skeletal muscle, pancreas, and kidney has been also demonstrated [106,156,157]. In addition, these changes were associated with the increase of lipolysis in the adipocytes leading to the rise of plasma FFA and therefore to the ectopic accumulation of lipids and lipotoxicity in targeted organs [108]. In summary, meta-inflammation induced by obesity is an important driver of peripheral insulin resistance and of the disruption of nutrients and energy metabolism, primarily in the adipose tissue but also in other metabolic tissues. These contribute to the development of obesity-associated complications and diseases.

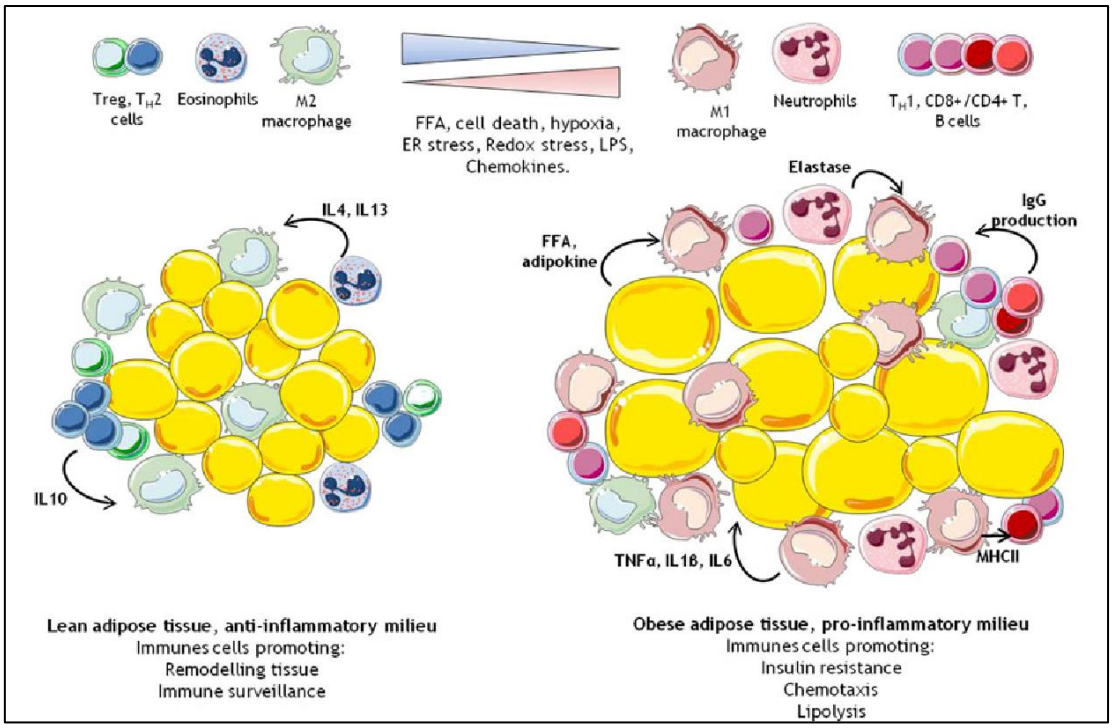

Figure 6 | White adipose tissue (WAT) inflammation. In lean adipose tissue, the crosstalk between adipocytes and immune resident cells maintains tissue homeostasis. In particular, anti-inflammatory cytokines (IL-10 and IL-4) that promote M2 macrophage phenotype, are secreted by Treg cells. Overnutrition results in WAT expansion and adipocyte hypoxia, with consequent production of chemoattractant and infiltration of immune cells. B and T cells become activated, and there is a phenotypic switch from M2 to M1 macrophages, which accumulate around necrotic adipocytes forming 'crown-like structures'. From [158].

1.5.2 Lipotoxicity

Lipotoxicity is defined by the deleterious effects of fat accumulation that can reach a toxic level within non-adipose tissues because of chronic elevation of circulating lipids during obesity. As discussed before, metabolically unhealthy obese patients develop metabolic alterations that are, at least in part, related to alterations in fatty acid utilization and intracellular signaling, while metabolically healthy subjects do not present obvious metabolic abnormalities and associated complications. A key feature to distinguish healthy from unhealthy obesity is the ectopic fat accumulation in non-adipose tissues such as in the skeletal muscles, liver, heart, pancreas, and in the kidney. However, lipotoxicity also participates to chronic inflammation and insulin resistance. The storage of lipid surplus in non-adipose tissues is the consequence of the inappropriate capacity of adipose tissue to expand and consequently to store further lipids, as well as of the excess FFA release by hypertrophic adipocytes. In non-adipose tissues, the main determinant of lipotoxicity is the excessive intracellular FA content, leading to the accumulation of potentially toxic metabolites such as fatty acyl-CoA (FA-CoA), diacylglycerols (DAG), and ceramides [159–163]. Indeed, increased circulating FA concentration induces accumulation of intracellular triglycerides but also metabolites of FA re-esterification including long chain Acyl-CoA and DAG. DAG are activators of protein kinase C (PKC) that are implicated in insulin resistance through inhibitory serine phosphorylation of insulin receptor substrates (IRS 1/2), leading to disruption of insulin signaling pathway [164,165]. The accumulation of various ceramide species in tissues during obesity results in the activation of several different signaling pathways, many of which are detrimental for the organ and tissue functions. In muscle, increased intramuscular accumulation of long-chain acyl-CoA, DAG and ceramide has been reported [162,163,165]. These lipotoxic metabolites interfere with the insulin signaling pathway, induce inflammation and decrease muscle differentiation and regeneration, leading to muscle atrophy [166,167].

In addition, a robust independent marker of obesity complications is the non-alcoholic fat accumulation in the liver (known as the non-alcoholic fatty liver disease; NAFLD, **Figure 7**). NAFLD has been associated with an increased risk of T2D and of CVD [168]. Most patients with NAFLD usually exhibit diseases such as obesity, insulin resistance, hypertension and hyperlipidemia [169]. Moreover, long-term NAFLD may initiate the development of NASH (non-alcoholic steatohepatitis) that likely progresses to cirrhosis and hepatocellular carcinoma in patients [170]. Lastly, cardiac steatosis has been associated with impaired left ventricular function in humans and experimental animals [171]. Fat deposition in the pancreas is particularly associated to β cell dysfunction and therefore to increased risk of diabetes [172]. In pancreatic β cells, the increased

production of ROS along with ER stress have been reported as the major mechanism implicated in their dysfunction [173]. Overall, in targeted-organs and tissues, lipotoxicity induces metabolic overload of mitochondria resulting in an incomplete β-oxidation, accumulation of toxic intermediate metabolites and increase in ROS production that promotes cellular dysfunction into these tissues and organs [174].

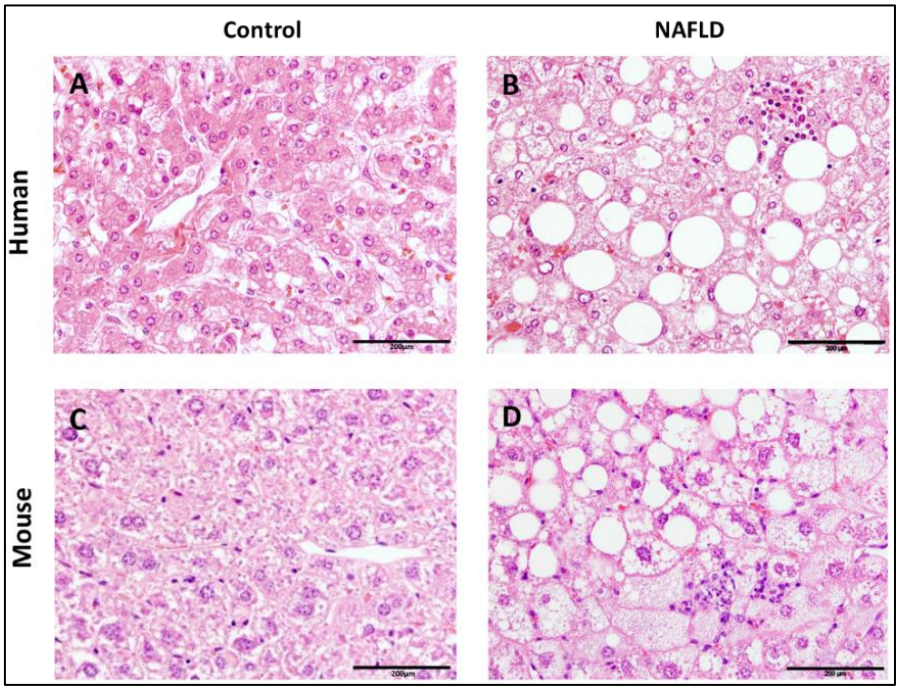

Figure 7 | Liver cross-sections from a NAFLD patient mouse fed a HFD versus control. Macrovesicular steatosis: large lipid droplets are present in hepatocytes; microvesicular steatosis: small lipid droplets are present in hepatocytes. All photomicrographs: Hematoxylin and eosin; magnification 200x. From [175].

Cellular dysfunction induced by lipotoxicity can be schematized in different steps. The fatty acid transporter (FATP) and scavenger receptor CD36, abundantly expressed in tissues with a high capacity for fatty acid metabolism, has been demonstrated to play an important role in fatty acid transport during obesity [176]. Indeed, the inhibition of CD36 has been associated to the prevention of lipotoxicity in multiple tissues such as the liver, muscle, heart and the kidney [177–179]. CD36 is found to be upregulated during NAFLD and in skeletal muscle in response to obesity, especially in response to insulin [180,181]. The FA transport to the cell induces deleterious effects, particularly mediated by mitochondrial impairments. In the early phase, FA overload induces an increased FA oxidation leading to increased production of ROS. The oxidation of FA delivers excess electrons to the electron transport chain (ETC), which thus causes superoxide overproduction. Moreover, FA also increase ROS production by the NADPH oxidases such as NOX4 [182,183]. This FA-induced oxidative stress leads to alterations of the mitochondrial structure and function, mostly as a consequence of the uncoupling oxidative phosphorylation. Mitochondrial dysfunction decreases β-

oxidation and may elevate plasma FFA concentration, thereby aggravating lipotoxicity. At the last step, the deterioration of mitochondrial function induces permeability transition (PT) pore opening followed by caspase activation and apoptosis [184,185]. The accumulation of lipids in the form of neutral lipids (TG or cholesterol esters) in lipid droplets is in the first instance an adaptative mechanism by which the cells protect themself against FA-induced lipotoxicity to keep low concentration of lipid intermediates [186,187]. However, increased lipid droplet formation is a hallmark of cellular stress [188]. Indeed, dysfunction of lipid droplet turnover consequent to mitochondrial dysfunction abolishes the ability of cells and tissues to fight against lipotoxic damage and increased accumulation of DAG and ceramide [189,190].

2 Obesity-induced chronic kidney disease

2.1 Introduction

The specific components of the kidney are the nephrons and a unique microvasculature. The human kidney contains about one million of nephrons, already established during prenatal development. A nephron is composed of a renal corpuscle (glomerule) connected to a complex tubule that finally drains into a collecting duct. The glomerule comprises a tuft of specialized capillaries attached to the mesengium, enclosed in the Bowman's capsule, an extension of the tubule. The renal tubule is subdivided into several distinct segments: the proximal tubule, a convoluted section followed by a straight section (the proximal tubule is also divided into S1, S2 and S3 segments), the loop of Henle, which has two parts, the descending loop of Henle and the ascending loop of Henle ("ascending loop"), the distal convoluted tubule and the connecting tubule. The last part of the nephron is the collecting ducts. The glomerule represent the filtering unit of the nephron. The blood is filtered across the capillary walls through the glomerular filtration barrier which is composed of pedicles of podocytes, the glomerular basement membrane (GBM) or basal lamina, and the fenestrated endothelium of glomerular capillaries that finally selectively filters molecules based on size (70 kDa), electrical charge (the more cationic, the more permeable), and capillary pressure. Reabsorption occurs in the renal tubules and is either passive, due to diffusion, or active, due to pumping against a concentration gradient. Secretion also occurs in the tubules and is active. The kidneys ensure multiples functions from excretory to endocrine functions in order to maintain the whole-body homeostasis. Indeed, they maintain a constant volume and composition of the body fluids by regulating the excretion of water, electrolytes as well as organic molecules. In addition, the kidneys eliminate metabolic wastes such as urea, creatinine, and uric acid. It also plays an osmoregulatory role and contributes to the maintenance of the acid-base balance. Finally, the kidneys synthetize and secrete hormones that influence renal hemodynamics (renin, angiotensin II and prostaglandins), the erythropoiesis (erythropoietin or EPO) and the phosphocalcic metabolism (1,25-dihydroxy-cholecalciferol or calcitrol). Because of these crucial functions, damages in the kidneys can be dramatic.

2.2 Kidney Disease

The Global Burden of Disease (GBD) study has estimated in 2015 that 1.2 million people died from kidney disease [191]. Kidney disease is defined as an alteration in the functioning of the renal system. The progressive decline of renal function results in a decrease of the glomerular filtration rate (GFR) along with the blood accumulation of toxins and metabolic products such as urea and creatinine.
Kidney diseases are among the diseases with the highest morbidity and mortality rates in the world. Kidney diseases can be divided into two major categories:

- *Acute kidney injury* (AKI), characterized by a sudden loss of kidney function, that usually occurs over the course of hours to days [192];
- *Chronic kidney disease* (CKD), which is defined by the progressive loss of a tremendous number of nephrons, leading to the decline of kidney function that persist for >90 days [192].

2.2.1 Acute kidney injury

AKI is a complex syndrome that often happen in hospitalized patients, or in patients admitted to the intensive care unit with a prevalence estimated up to 15% and 60% respectively [193–195]. In AKI, the deterioration of renal function occurs quickly and involves both structural and functional alterations. However, AKI has rarely a single and distinct pathophysiology but occurs as a combination of etiologies such as sepsis, nephrotoxins and ischemia [196–199]. AKI is classified into three categories: pre-renal azotemia, intrinsic AKI (acute tubular necrosis, acute interstitial nephritis, acute glomerular renal injury) and postrenal obstructive AKI and is often transient [196–199]. However, patients who have had an AKI episode are more likely to develop CKD, especially with age.

2.2.2 Chronic kidney disease

CKD is characterized by a progressive and irreversible loss of kidney function. The overall prevalence of CKD in the general population is about 14% and has become a major burden on quality of life and for the economy [200]. CKD is diagnosed by indicators of kidney function (measurement of the GFR) and structural kidney damages (by medical imaging or measure of albuminuria) [201]. Therefore, CKD is defined by a GFR lower than 60 ml/min/1.73 m^2, or markers of kidney damage for a period equal to or greater than three months. It is considered that a patient with a GFR less than 15 ml/min per 1,73 m^2, corresponding to the stage 5, has reached the end stage renal disease (ESRD); at that point the patient requires renal replacement therapies (dialysis and renal

transplantation). Compared to AKI, the development of CKD is more insidious. Indeed, in its early stages, individual has no symptoms while symptoms might only appear when the disease is very advanced.

CKD is divided into five stages, according to the GFR and proteinuria (**Figure 8**) [201]:

Stage 1: Kidney damage with normal kidney function (estimated GFR ≥90 mL/min per 1.73 m^2) and persistent (≥3 months) proteinuria.
Stage 2: Kidney damage with mild loss of kidney function (estimated GFR 60-89 mL/min per 1.73 m^2) and persistent (≥3 months) proteinuria.
Stage 3: Mild-to-severe loss of kidney function (estimated GFR 30-59 mL/min per 1.73 m^2).
Stage 4: Severe loss of kidney function (estimated GFR 15-29 mL/min per 1.73 m^2).
Stage 5: Kidney failure requiring dialysis or transplant for survival. Also known as ESRD (estimated GFR <15 mL/min per 1.73 m^2).

Prognosis of CKD by GFR and Albuminuria Categories: KDIGO 2012				Persistent albuminuria categories Description and range		
				A1	A2	A3
				Normal to mildly increased	Moderately increased	Severely increased
				<30 mg/g <3 mg/mmol	30-300 mg/g 3-30 mg/mmol	>300 mg/g >30 mg/mmol
GFR categories (ml/min/ 1.73 m^2) Description and range	G1	Normal or high	≥90			
	G2	Mildly decreased	60-89			
	G3a	Mildly to moderately decreased	45-59			
	G3b	Moderately to severely decreased	30-44			
	G4	Severely decreased	15-29			
	G5	Kidney failure	<15			

Figure 8 | Stages of CKD. Reprinted with permission from KDIGO 2012 Clinical Practice Guidelines for the Evaluation and Management of Chronic Kidney Disease. 32 GFR, glomerular filtration rate; KDIGO, Kidney Disease: Improving Global Outcomes. Green: low risk; Yellow: moderately increased risk; Orange: high risk; Red: very high risk.

In 2015, the number of people receiving renal replacement therapy exceeded 2.5 million. This number is projected to double to 5.4 million by 2030 [202].
The clinical risk factors to develop CKD include a previous episode of AKI, aging, the CVD, high blood pressure, diabetes, and obesity [9]. Moreover, with the expected continuous rise in diabetes and obesity, and the delay between their onsets and the late stage complications, the probability that the prevalence of CKD will increase even more drastically in next few years is very high [203]. In addition, it has been demonstrated that obesity is strongly associated with the development of CKD and ESRD. In the general population, obesity is the second most highly predictive factor to predict end-stage renal disease, even independent of diabetes and hypertension [204]. In addition, obesity not only induces kidney disease, but also worsens and accelerates the progression of pre-existing kidney diseases such as glomerulonephritis, age-related kidney disease or following renal transplant or nephrectomy [205–207].

2.3 Obesity-induced kidney disease

The mechanism by which obesity causes CKD is certainly multifactorial. However, it is now well considered that a high BMI or waist-to-hip ratio (WHR) are among the strongest risk factors for developing CKD [208,209]. However, it is worth to also note that a part of obese individuals never develop CKD and about 25% of obese individuals are considered as metabolically healthy (as described in the previous chapter) [210,211]. Therefore, increased body weight cannot explain the whole pathophysiology of the development of kidney damages. Indeed, obesity-related kidney disease occurs as a result of complex interactions between metabolic and hemodynamic factors and is characterized by functional and structural changes such as impairment of renal perfusion, vascular dysfunction, as well as albuminuria, glomerulosclerosis, tubular atrophy and tubulointerstitial fibrosis [120,212–215].

2.3.1 Glomerular hyperfiltration and subsequent glomerulomegaly and glomerulosclerosis

The increased obesity epidemic is correlated to the increased incidence of obesity-related glomerulopathy (ORG). The mechanisms involved in ORG are complex and other comorbidities may also contribute to its onset such as hypertension, diabetes, or insulin resistance. The progression of ORG is influenced by many factors such as pro-inflammatory adipokines and cytokines, lipotoxicity, the renin-angiotensin system, sympathetic nervous system, inflammation, and oxidative stress [213,216]. ORG consists in glomerulomegaly, defined as the glomerular hypertrophy, with or without the presence of focal segmental glomerulosclerosis (FSGS). The kidney hypertrophy

(glomerulopathy) is partly due to an increased renal plasma flow, an increased GFR and an increase in tubular sodium reabsorption, overall leading to an increased intraglomerular pressure [215,217]. This glomerular hyperfiltration might be a compensatory mechanism necessary to meet the high metabolic demands of extensive increased body weight. However, this mechanism leads to maladaptive consequences on glomeruli and tubular structures [215,218] Indeed, the glomerular hyperfiltration is also associated to damages on glomerular basement membrane (GBM) and podocytes (**Figure 9**). Widening of GMB is observed along with podocyte hypertrophy. Consequences of podocyte hypertrophy is the progressive foot process effacement and podocyte dysfunctions [219]. However, the chronic mechanical stress induced by the glomerular hyperfiltration on podocytes leads to podocyte detachment, enlarged glomerular capillaries with damages of endothelial cells and mesangial expansion which in turn lead to FSGS [219–223].

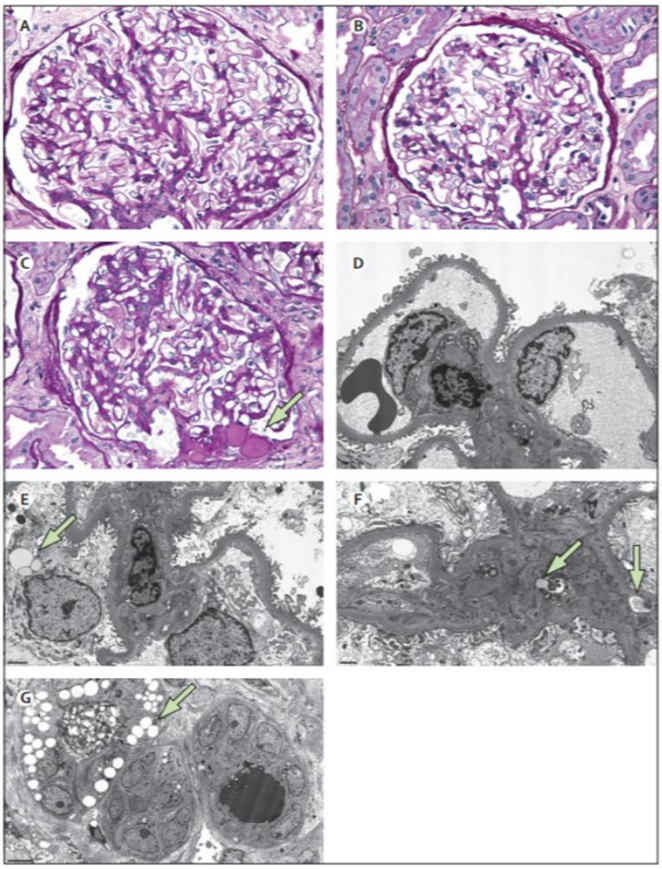

Figure 9 | **Pathology of obesity-related glomerulopathy**. Light microscopic and electron microscopic findings showing glomerulomegaly (A) by comparison with an age-matched normal control glomerulus (B) and perihilar hyalinosis with loss of overlying podocytes and adhesion to Bowman's capsule, forming a lesion (arrow) of focal segmental glomerulosclerosis (C) (A–C, periodic acid-Schiff , magnification ×400). By electron microscope, there is mild glomerular basement membrane thickening, mesangial sclerosis, and foot process effacement (D, magnification ×5000). Lipid droplets (arrows) are present in the cytoplasm of podocytes (E, magnification ×6000), mesangial cells (F, magnification ×10 000), and tubular epithelial cells. A lipid-laden degenerating epithelial cell has been shed into the tubular lumen (G, magnification ×3000)

2.3.2 Hemodynamic changes in obesity and renal consequences

In obesity, many vascular and tubular factors may cause hemodynamic changes, promoting an increase in glomerular pressure and therefore, hyperfiltration that consequently increases tensile stress applied to the capillary wall structures (**Figure 10**). In spite of the contribution of elevated blood pressure, obesity-related hyperfiltration is primary associated to renal afferent vasodilatation that is caused by multiple factors such as the compression of the renal tubules, hyperglycemia, a high protein intake, hyperinsulinemia and impaired renal autoregulation [224]. Particularly, increased tubular sodium reabsorption has a key role in initiating obesity-associated hyperfiltration. In obese conditions, the renal sympathetic nervous system (RSNS) is overactivated and is link to increased sodium reabsorption and hypertension [225,226]. This overactivation of the RSNS has been shown to be related to increased leptin production by the adipose tissue during the development of obesity. Hyperleptinemia increases sympathetic nerve activity through the binding of its receptor in the central nervous system which, in turn, promotes renal sodium reabsorption by stimulating renin release and consequently activating the renin-angiotensin-aldosterone system (RAAS) [227,228]. Activation of the RAAS leads to increased formation of angiotensin II and aldosterone, which both stimulate renal tubular sodium reabsorption. Angiotensin II is involved in the control of blood pressure and sodium homeostasis but can also induce cell proliferation [229], ROS production [230,231] and promote interstitial fibrosis [232,233] in pathological conditions. In the progression of obesity and diabetes related kidney disease, this system has been demonstrated to be overactivated [234,235], leading to vasoconstriction effects on the efferent renal arteriole which is expected to increase GFR [236]. Moreover, angiotensin II increases sodium tubular reabsorption through the stimulation of the luminal NA^+-H^+ exchanger and the basolateral Na^+-K^+-ATPase in the proximal tubule and through the activation of the epithelial Na^+ channel (ENaC) in the distal tubule [237]. This, in turn, leads to an impairment in natriuresis, to volume expansion, and hence to hyperfiltration and hypertension [238]. In addition, the role of insulin in renal vasculature has been pointed out [239]. Insulin induces vascular relaxation by promoting nitric oxide (NO) production and bioavailability through the phosphatidylinositol 3-kinase (PIK3-Akt) signaling pathway. In addition, it is thought that insulin may exert physiological role on kidney structure. Indeed, mice lacking insulin receptors specifically in their podocytes present podocyte foot process effacements and glomerular matrix expansion along with albuminuria [240]. However, in context of insulin resistance, the beneficial role of insulin on renal vasculature is compromised. Moreover, glomerular hyperfiltration also creates a mechanical stress on proximal tubular cells that generates a biochemical signaling to promote sodium

reabsorption through the luminal NH3 transporter and the basolateral $Na^+/3HCO_3^-$ cotransporter [241].

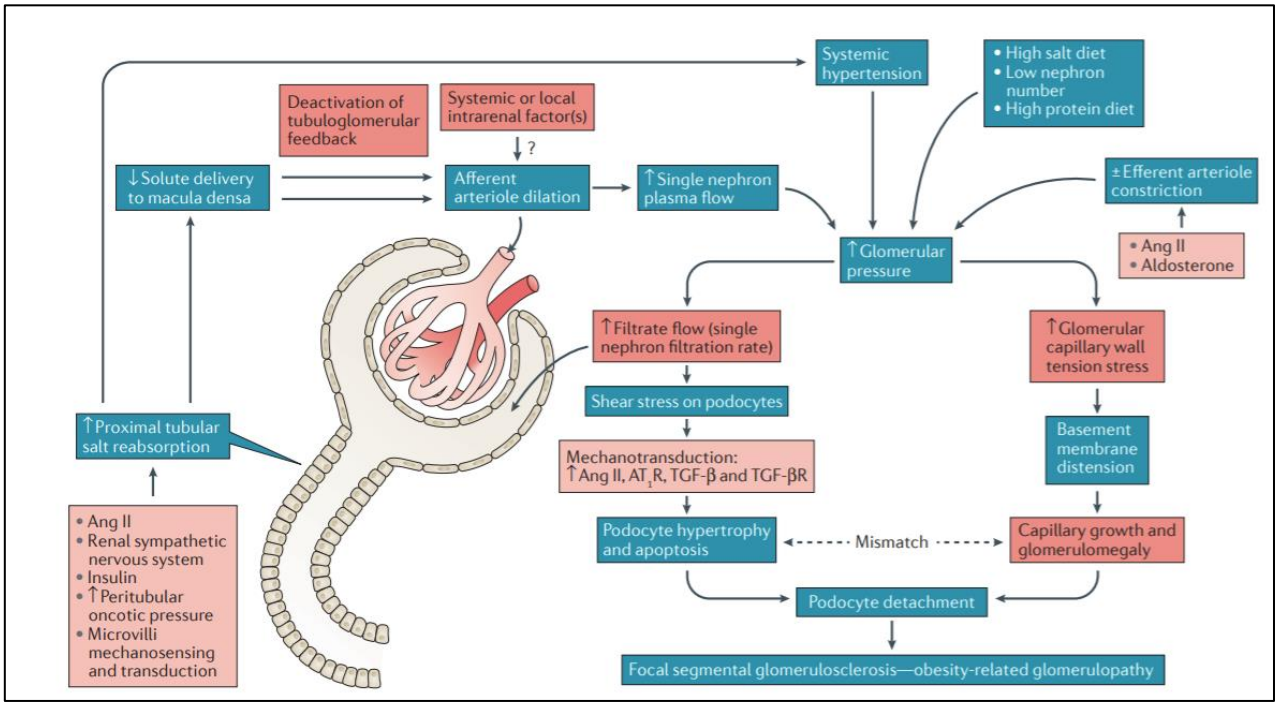

Figure 10 | Hemodynamic alterations in obesity. Primary dilatation of the afferent arteriole and variable constriction of the efferent arteriole via activation of angiotensin II (Ang II) and aldosterone contribute to increases in single nephron plasma flow, glomerular intracapillary hydrostatic pressure, and filtration rate. The major driver of afferent arteriolar dilatation is unknown, but deactivation of tubuloglomerular feedback via increased proximal tubular salt reabsorption and decreased delivery to the macula densa likely has a role. A host of factors, including Ang II, the renal sympathetic nervous system, insulin, an increase in postglomerular oncotic pressure due to increased filtration fraction, and mechanosensors of tubular flow rates, mediate the increased tubular reabsorption of sodium. The increase in filtrate flow (single nephron filtration rate) in turn promotes glomerular capillary wall stretch tension, glomerulomegaly, and maladaptive podocyte stress leading to obesity-related glomerulopathy and focal segmental glomerulosclerosis. AT1R, type 1 angiotensin II receptor; TGF-β, transforming growth factor β; TGF-βR, TGF-β receptor. From [216].

As a consequence of enhanced tubular sodium reabsorption, the delivery of NaCl to the *macula densa* is decreased, leading to the compensatory tubulo-glomerular feedback-mediated dilatation of the afferent arterioles, increasing GFR and renal blood flow [242,243]. Finally, hypertrophy of proximal tubules is also observed as a consequence of increased amino acids and upregulation of transporters such as sodium-glucose cotransporters (SGLTs) and sodium-hydrogen exchanger 3 (NHE). The increased amino acid concentrations into tubular cells promote the activation of mTORC1 which, in turn, induces cell growth [244]. The chronic consequences of these changes are progressive loss of nephrons and decline of GFR reflecting the loss of kidney function to end-stage renal disease (**Figure 11**) [245].

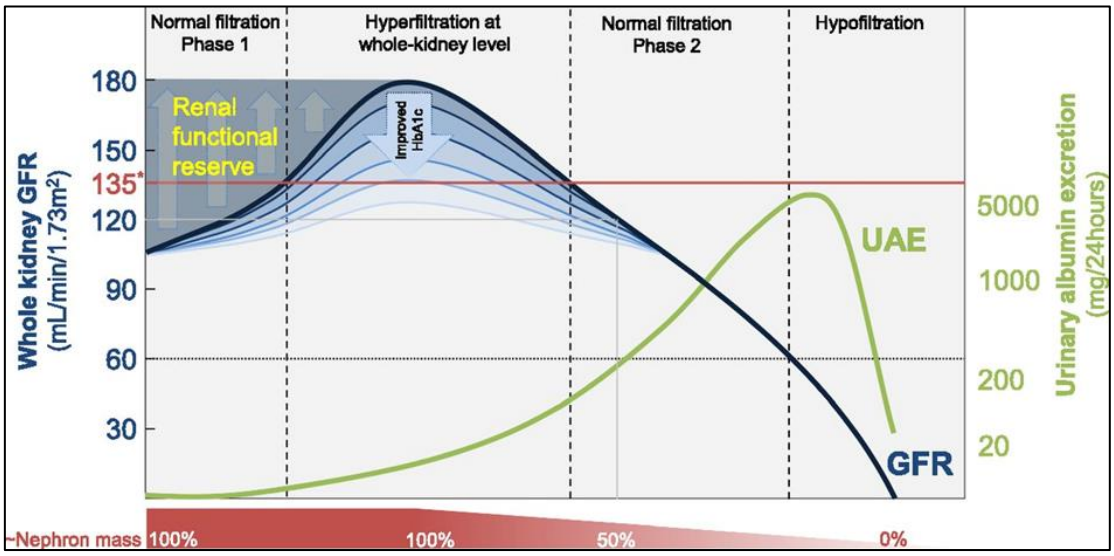

Figure 11 | Classic course of GFR and UAE according to the natural (proteinuric) pathway of diabetic nephropathy. Whole-kidney hyperfiltration is generally defined as a GFR that exceeds approximately 135 ml/min, and is indicated with the red line. From [246].

2.3.3 Microalbuminuria and advanced proteinuria

Albuminuria is generally the earliest sign of impaired kidney function and is related to a higher risk for developing cardiovascular disease [247]. Albuminuria is increased because of glomerular vascular permeability due to glomerular hypoperfusion, hyperfiltration and hypertension, that result into podocyte foot process effacements [248]. Urinary albumin excretion is even considered as preceding the progressive decline of GFR. In the early stage of obesity, glomerular hyperfiltration induces an increased glomerular permeability of albumin. This is associated to an enhanced tubular flow, resulting in impaired reabsorption of albumin by the proximal tubules and the so-called micro-albuminuria (range 30 to 300 mg/day). In advanced stage of the disease, obese individuals may develop FSGS along with heavy proteinuria, including protein-bound lipids, cytokines, and growth factors. Thus, the adaptative reabsorption of proteins by the proximal tubule contributes to tubular oxidative stress, hypoxia, tubulo-interstitial fibrosis and apoptosis (tubular atrophy) [249]. These changes also conduct to decreased renal function and ultimately end-stage renal disease.

2.3.4 Low-grade inflammation and oxidative stress and subsequent renal fibrosis

Rapid expansion of adipose tissue results in an aberrant production of pro-inflammatory adipokines that leads to a state of low-grade inflammation [93]. As already mentioned, during obesity, an imbalance in the production of anti-inflammatory adipokines (adiponectin) and pro-inflammatory adipokines is observed. Therefore, pro-inflammatory adipokines (MCP-1, TNF-α) are increased and participated to the chronic inflammation of the adipose tissue [250,251].

Evidence of inflammation in kidney has been demonstrated and associated to the progression of the obesity-related CKD [252]. First, the role of adiponectin has been highlighted by the group of Sharma's lab. Adiponectin has a protective effect on podocyte structure and function. Sharma et al. (2008) identified that low levels of circulating adiponectin correlate with low grade albuminuria in obese patients and that the adiponectin knockout mice developed low grade albuminuria without co-existent obesity, hypertension or hyperglycemia [253]. The protective effects of adiponectin has been shown to involve reduction of oxidant stress, possibly by inhibition of NADPH oxidases as it has been shown in endothelial cells and in podocytes [253]. Fang et al. confirmed the protective effect of adiponectin on NADPH oxidase activation and therefore, on ROS production. They also confirmed that this effect was promoted through the activation of AMP-protein activated kinase (AMPK) [254]. AMPK is a heterotrimeric serine/threonine protein kinase which is well recognized as a key regulator of cellular metabolism by maintaining intracellular energy homeostasis [255]. Its activity is highly linked to the change of ATP consumption. Upon activation, AMPK conserves cellular energy by down regulating proteins, fatty acid, and glycogen synthesis while it activates catabolic pathways by increasing lipid and glucose oxidation. In addition, AMPK induces mitogenesis and expression of antioxidant defense proteins [256]. The role of AMPK will be further discussed in the next chapter. More recently, Park's group has demonstrated that the expressions of adiponectin receptors were decreased at the early stage of CKD in patient with T2D [257]. Adiponectin acts on tissue through the activation of two receptors: AdipoR1 and R2. Both receptors are involved in adiponectin-stimulated activation of varied signal pathways such as AMPK or PPARγ. AdipoR1 and R2 are ubiquitously expressed. However, in kidney, AdipoR1 appears to be more expressed than AdipoR2 [258,259]. Several studies with specific deletion of AdipoR1 or AdipoR2 reported that AdipoR1 is the prominent receptor mediating adiponectin stimulation of AMPK while AdipoR2 deletion blocks adiponectin stimulation of PPARγ [260,261]. In Park's study, the use of AdipoRon, an orally active synthetic adiponectin receptor agonist, in *in vivo* and *in vitro* experimental model of diabetes-induced CKD significantly improved lipotoxicity and oxidative stress by activating AMPK [257][262]. Overall, the adiponectin/AMPK axis could play a

major role in preventing obesity-related renal inflammation and oxidative stress. As already mentioned, while anti-inflammatory cytokines are decreased, an increase in inflammatory cytokines is observed in obesity-induced metabolic alteration. Notably, MCP-1 was found to be increased as early as one week in kidney of mice fed a HFD, promoting the subsequent recruitment of macrophages and enhancement of pro-inflammatory factors such as TNF-α or even pro-fibrotic markers such as the Transforming Growth Factor (TGFβ) [120]. Interestingly, mice lacking MCP-1 have been shown to be protected against diabetes-induced CKD probably through the sustain expression of nephrin into podocytes that, in turn, maintain podocyte integrity [263]. Among other inflammatory cytokines, TNFα plays a pivotal role in the onset and development of the renal complications in obesity and diabetes [264]. Indeed, pharmacological inhibition of TNFα protected kidneys against oxidative damages and apoptosis [265]. This result was also observed in TNFα deficient mice fed a HFD and TNFα siRNA-treated primary proximal tubular cells [266]. In addition, within kidney, various factors such as angiotensin II or even advanced glycation stimulate its synthesis, promoting renal damages [267,268]. Therefore, it is worth to suggest that pro-inflammatory cytokines are greatly involved in the obesity-induced renal damages. Moreover, renal inflammation is often associated with increased oxidative stress and in the subsequent renal fibrosis [269]. Oxidative stress is caused by an imbalance between increased production of ROS and/or a reduced antioxidant activity. ROS induce cellular damages such as lipid peroxidation, DNA and protein adducts, promoting glomerular and tubular injury [270,271]. One of the major sources of vascular and renal ROS production is the Nox family, specially NOX1, NOX2, NOX4. Contribution of Nox family in obesity-induced glomerular and tubular injury has been widely highlighted. Notably, the role of NOX4 has been more specifically investigated. Jha *et al.* (2014) demonstrated in diabetic $ApoE^{-/-}$ mice that Nox4 deletion or treatment with Nox4 inhibitor prevented renal ROS production and prevented glomerular injury and albuminuria [272]. They also showed in human cultured podocytes that silencing NOX4 reduced ROS production and downregulated the expression of pro-inflammatory cytokines and pro-fibrotic markers. Finally, another hallmark of the progression of kidney injury is renal fibrosis that is marked by progressive tissue scarring leading to glomerulosclerosis and tubulointerstitial fibrosis [273]. In glomeruli, the hyperplasia of the mesangial cells has been described. In addition, an accumulation of the mesangial matrix is observed that reflects an activation of these cells. This activation results from the production of pro-inflammatory cytokines such as MCP-1 or growth factors such as TGF-β [274]. TGF-β, an important cytokine intimately involved in tissue fibrosis, has been found to be up-regulated in a variety of kidney diseases characterized by excess matrix deposition [275,276]. In particular, Sharma et al. previously demonstrated that

the chronic type 1 diabetic mouse and the db/db mouse overexpress TGF-β in the glomeruli [277][278]. Its expression was also increased in renal cortex of mice fed a HFD. This was associated with an overproduction of mesangial matrix components such as fibronectin, type I and IV collagen [279].

2.3.5 Renal abnormal lipid metabolism and ectopic lipid accumulation

2.3.5.1 Renal lipid uptake and ectopic lipid accumulations in obesity

As described in the previous chapter, obesity and HFD are associated with increased circulating lipids: increased TG and FFA, decreased HDL-C with HDL dysfunction and normal or slightly increased LDL-C with increased small dense LDL. Theses lipids will accumulates into non-adipose tissue; this phenomenon is called "ectopic lipid accumulation" and is associated to detrimental effects for the tissue [280]. Studies from experimental models and human samples showing ectopic lipid deposition in mesangial cells, podocytes, and tubular cells have emerged, suggesting therefore the role of lipotoxicity in the development of obesity-induced CKD [179,281–286]. In kidney, even though passive diffusion of FFA through the plasma membrane is possible, lipid intake results mostly from receptor-/transporter-mediated mechanisms involving the upregulation CD36, the Fatty Acid Transport Proteins (FATPs) and the fatty Acid-binding Protein (FABP). CD36 has been the most studied. CD36 is a receptor scavenger expressed in podocytes, mesangial cells, microvascular endothelial cells, interstitial macrophages and tubular cells (reviewed in [287]). Its renal expression is significantly increased during the progression of CKD in patient and in experimental mouse model. The deletion of CD36 in mice largely reduced fatty acid uptake and decreased ectopic renal lipid accumulation and prevented the progression of renal disease [288]. CD36 allow the intake of oxidized LDL, favoring the intracellular increase of cholesterol ester which therefore are stored into lipid droplets or metabolized into active metabolites that have been reported to activate PPARγ [289]. This leads in turn to a positive feedback by trans-activating CD36 gene promoter, promoting its expression. In podocytes, saturated FA particularly increase the CD36 expression which results in the increase in FFA uptake. This has been demonstrated to contribute to mitochondrial dysfunction, ROS production, podocyte-specific insulin resistance and even to the activation of the apoptotic pathway [240,290]. Ectopic lipid accumulations into mesangial cells have also been shown. Mesangial cells play a protective and supporting role of the glomerular tuft. Indeed, these cells are considered as a specialized form of microvascular pericyte in the glomerulus that notably support capillary loops, produce and maintain mesangial matrix, secrete growth factors and cytokine to communicate with each other glomerular cells and thanks to their contractile properties may regulate the glomerular capillary flow.

These cells have functions similar to those of scavenger macrophages. Thus, they also expressed CD36 that allow the bound and uptake of LDL which thereby increases the intracellular cholesterol ester [291][292]. In addition, they also express apoB and apoE and can hence accumulate TG via lipoprotein lipase [66] [67]. In obesity, these cells have been shown to take the form of lipid-laden spumous cells, losing their contractile function which results into the loss of the integrity of the glomerular tuft [68][69]. In tubular cells, predominantly in the proximal convoluted tubule (PCT), lipid deposition has now been well documented [179,281–286]. Increased lipid accumulations are correlated with impaired brush border and increased oxidative stress, showing evidence of tubular dysfunction. The primary role of PCT is the active reabsorption of filtered sodium. This process requires a large amount of ATP which is mostly provided through the mitochondrial β-oxidation of FFA. In PCT, FFA are mostly taken up via the CD36 and the FABP. Circulating FFA are complexed with carrier proteins (mostly albumin), and their uptake requires dissociation from carrier proteins mostly mediated by CD36. Declèves et al. particularly characterized the lipid accumulation in PTC of HFD mice [120,293]. Total cholesterol esters and phosphatidylcholine content in the kidney were elevated while the fatty acid and TG content was unchanged. Evidence of proximal tubule injury was clearly observed with the presence of enlarged clear vacuoles and multilaminar inclusions. The margins of these vacuoles/inclusions were positive for the endolysosomal marker, LAMP1, suggesting lysosome accumulation. Characterization of vesicles by special stains (Oil Red O, Nile Red, Luxol Fast Blue) and by electron microscopy revealed that this contained onion skin-like accumulation consistent with phospholipids (**Figure 12**).

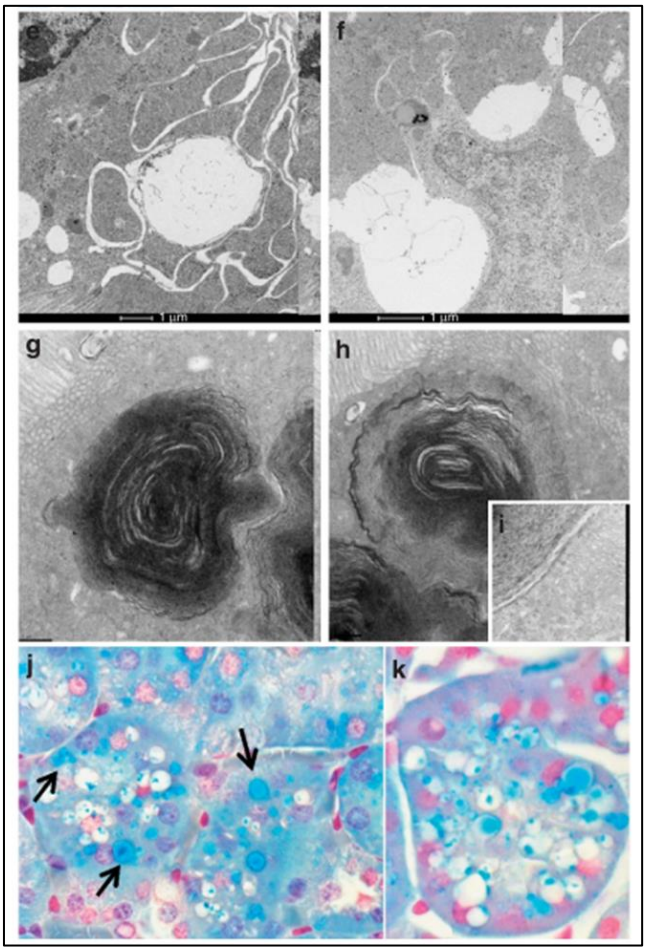

Figure 12 | Lipid storage in tubular cells in mice fed a high-fat diet (HFD). Representative photomicrograph of electron microscopy evaluation of ultrastructure of vacuoles in proximal tubules in mice treated with a HFD: presence of (e, f) enlarged clear vacuoles and (g, h) multilaminar inclusions (i: higher magnification). (j, k) Representative photomicrographs (original magnification X1000) illustrating phospholipid accumulation in vacuolated tubule with Luxol Fast Blue in HFD (arrow, vacuoles stained in blue) from [294].

2.3.5.2 Abnormal lipid metabolism in the kidney

FFA can be then used to supply energy. However, excess intracellular FFA content can lead to the accumulation of toxic metabolites (DAG or ceramide) that participate to cellular dysfunction, chronic inflammation and insulin resistance. Furthermore, a recent study has shown that the inhibition of mitochondrial FA oxidation induced increased intracellular lipid depositions, cellular dedifferentiation, and cell death in kidney [295]. Regarding renal lipid metabolism, many studies have focused on the implication of the sterol regulatory element-binding protein-1 (SREBP-1) and PPARγ [296–298]. Indeed, in addition to renal accumulation of TG and cholesterol, there is an increase in *de novo* lipogenesis within the kidney, resulting from an overexpression of the transcription

factor, SREBP-1, as shown by Levi's group [296–298]. Upon activation, SREBP participates to the regulation of its targeted genes involved in lipid synthesis such as acetyl coA carboxylase (ACC), fatty acid synthase (FAS) or steroyl CoA desaturase 1 (SCD 1). However, the same group demonstrated that transgenic mice overexpressing SREBP-1 presented an elevated renal TG content with glomerulosclerosis and proteinuria [296]. In contrast, SREBP-1c knockout mice fed a HFD diet were protected from renal lipid accumulation and glomerulosclerosis [299]. Similar to SREBP up-regulation, heterozygous PPARγ-deficient mice showed to be protected against HFD-induced obesity-induced kidney disease. Indeed, mice did not present renal lipid accumulation and were protected from albuminuria and glomerular and tubulointerstitial damages [300]. Similarly, using PPARα agonist such as fenofibrate in mice fed a HFD showed protective effect regarding renal lipid accumulation, ROS production and thus development of glomerulosclerosis [301]. Finally, AMPK has also been reported to play a critical role in regulating the chronic cellular response to lipid excess. Indeed, Declèves *et al.* established that HFD-induced kidney disease is characterized by renal hypertrophy, increased albuminuria and elevated markers of renal fibrosis and inflammation while these HFD-induced markers of inflammation, oxidative stress, and fibrosis were reversed by AMPK activation. In addition, the activity of ACC, the rate-limiting enzyme of fatty acid biosynthesis, and HMG-CoA reductase (HMGCR), the rate-limiting enzyme in cholesterol biosynthesis, were both altered, leading to lipid accumulation in the kidney. Therefore, the group highlighted for the first time the appearance of phospholipidosis in kidney upon a context of obesity [120,293]. Later, the phospholipid accumulation in the proximal tubules was associated with lysosomal dysfunction, stagnant autophagic flux, mitochondrial dysfunction and inflammasome activation. The lysosomal dysfunction in link with mitochondrial damages was further investigated by Yamamoto *et al.* [286]. In addition, an analysis of lipid species by quantitative mass spectrometry was performed to further determine the role of AMPK and to explore the connections between lipid metabolism and biochemical pathways. In that study, a dysregulation of eicosanoid synthesis and metabolism in the kidney with HFD and their amelioration with AMPK activation were demonstrated. These results sheds light on the mechanism behind HFD related toxicity and the eicosanoid pathways under the control of AMPK activation in the kidney. The role of AMPK in kidney physiology and obesity-related kidney disease will be further discussed in the next section.

2.3.6 Obesity-induced CKD and gut microbiota

Different studies have demonstrated that obesity induces gut microbiota alterations. As evidenced, the experimental gut microbiota transfer from obese mice to lean mice is associated to the development of metabolic syndrome phenotype in these mice [302]. The diet seems to be the major driver of the modified gut microbiota. Gut microbiota disturbance and activation of inflammation pathways have been linked to insulin resistance in diabetic and obese patients [303]. Particularly, obesity was associated to impairment of the intestinal barrier function as well as changes in the composition of the intestinal flora that might contribute to the development and progression of CKD [304]. The gastro-renal axis in obesity condition and the mechanisms involved in this process need further investigations. Indeed, the underlying mechanisms of these changes are still unclear and different hypotheses are discussed. Disturbance of gut microbiota in obesity may contribute to the leakage of inflammatory factors from the intestine (endotoxin), disrupting intestinal homeostasis and amplifying inflammation in CKD patients [304]. Another hypothesis is that the inflammation triggered by CKD and associated uremic molecules retention (such as phenols, indoles, and amines that may contribute to uremic toxicity) favor pathogen overgrowth (dysbiosis) in the gut [305]. Particularly, uremic toxins generated from bacteria in the gut have been linked to insulin resistance in obese animals [306]. Thus, it would be hypothesized that the combination of uremic toxins retention in CKD and dysbiosis-associated production of toxins may participate to the uremic molecules accumulation in obesity-induced CKD, which could contribute to the progression of metabolic syndrome as well as CKD. Interestingly, the uremic environment in CKD has also been associated to a sensing failure of AMPK in response to AMP increase [307]. Dietary restriction, drugs and other factors have the potential to beneficially modify the abundance and function of the microbiota in patients with CKD. High-fiber diets promote the growth of short-chain fatty acid (SCFA)-producing bacteria in the intestine and have been demonstrated in preclinical studies to be effective in treating the metabolic syndrome, obesity, and CKD [308]. Moreover, increased fiber intake is associated with decreased inflammation and all-cause mortality in patients with CKD [309]. Similarly, probiotics seem to ameliorate renal dysfunction [310]. Finally, whether there is a specific enterotype associated with CKD, how these changes are modulated by obesity, and whether obesity accelerates renal dysfunction in patients with CKD regardless of alterations in the microbiota requires further investigations. Similarly, we also need to confirm whether the dysbiosis of microbiota in patients with CKD can affect fat homeostasis and facilitate adipogenicity.

3 AMPK and metabolic disease-induced chronic kidney disease

3.1 Introduction

Progressive decline in renal function leads to chronic kidney disease (CKD) and, ultimately end-stage renal disease (ESRD) requiring dialysis or transplantation. CKD prevalence is estimated to be between 11 and 13% in the general population, becoming a public health problem with an enormous global economic burden [200,311]. Diabetic kidney disease remains the leading cause of ESRD in the developed world. CKD is associated with metabolic syndrome (MetS), a cluster of metabolic disorders, including hypertension, hyperlipidemia, hyperglycemia, and obesity [312]. MetS contributes to the appearance of albuminuria, the first sign of kidney disease in patients with diabetes [313–315]. Moreover, accumulating studies reported that obesity, even alone, is a significant risk factor of CKD [204,316,317]. The growing epidemic of obesity contributes to the increased prevalence of type II diabetes and its related kidney complications.[318] Obesity and diabetes-associated kidney disease are both associated with glomerulomegaly, hemodynamic changes, and increased albuminuria, as well as similar structural and functional changes in the kidney [319]. Although the lesions of obesity-induced kidney disease are slightly different to non-obese diabetic patients, it is difficult to discriminate the effects of obesity vs. the concomitant effects of hyperglycemia and insulin resistance in clinical studies as there is considerable overlap between diabetic and overweight/obese patients [318].

Adiposity and adipose tissue dysfunction, associated with insulin resistance, lead to the release of pro-inflammatory cytokines and free fatty acids (FA) in the circulation, as well as changes in the production of adipokines (leptin and adiponectin), which likely contribute to the pathogenesis of obesity and diabetes-induced kidney disease [320]. Obesity enhances the renin-angiotensin-aldosterone system (RAAS), leptin-induced activation of the sympathetic nervous system (SNS), tubular sodium reabsorption, and volume expansion in the kidney leading to hypertension [321]. Obesity-induced hypertension accelerates glomerular hyperfiltration, leading to obesity-related glomerulopathy characterized by glomerulomegaly with focal and segmental glomerulosclerosis lesions [216]. Meanwhile, systemic inflammation and dyslipidemia contribute to the initiation of oxidative stress and insulin resistance, contributing to renal fibrosis and low-grade inflammation (**Figure 13**) [322]. Finally, both obesity and diabetes-induced kidney disease are characterized by ectopic lipid depositions in the kidney and associated direct lipotoxicity both in rodents and humans [179,281–286].

Obesity and diabetes-related kidney diseases share not only physiological initiating events but also critical molecular mechanisms of renal cell injury. Studies have

demonstrated an essential role of AMP-activated protein kinase (AMPK) dysregulation in obesity and diabetes-associated kidney disease both in experimental and clinical models [262,279,323–326]. In several studies, AMPK activators attenuate diabetic nephropathy and improved high fat-induced kidney disease in mice [293,327–329]. However, therapeutic approaches to prevent or to treat kidney disease in patients with obesity and/or diabetes are not very specific to these altered pathways. The delay in the development of therapeutic strategies to modulate AMPK in obesity and diabetes-induced kidney disease is partially due to the complexity of the underlying physiological and molecular mechanisms. It this review, we discuss the physiological role of AMPK signaling within renal cells and its dysregulation in obesity and diabetes-related chronic kidney disease.

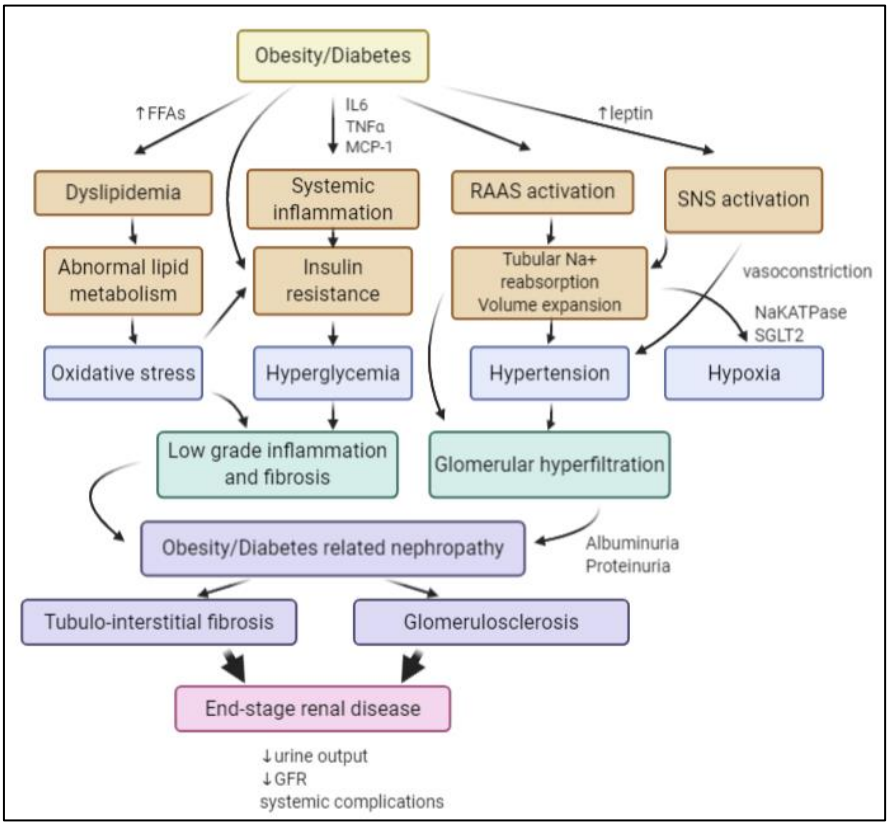

Figure 13 | Mechanisms involved in the pathogenesis of MetS-related kidney disease and consequent end-stage renal disease. Obesity and diabetes initiate systemic disturbances (orange boxes) including pro-inflammatory signals, dyslipidemia, the activation of the SNS and RAAS that contribute to intra-renal stresses (blue boxes) consecutive to abnormal lipid metabolism, insulin resistance, tubular reabsorption of sodium and hypertension and associated glomerular hyperfiltration with increased albuminuria and proteinuria. Renal oxidative stress and hyperglycemia lead to inflammation and fibrosis that contribute to the initiation and progression of obesity and diabetes related nephropathy. Consecutive tubule-interstitial fibrosis and glomerulosclerosis are associated to progressive decline in the GFR, loss of nephron and ultimately end-stage renal disease. IL-6, interleukin-6; TNFα, tumor necrosis factor-α; MCP-1, Monocyte chemoattractant protein-1; FFAs, free fatty acids; NaKATPase, sodium–potassium pump; SGLT2, sodium/glucose cotransporter 2; SNS, sympathetic nervous system; GFR, glomerular filtration rate.

3.2 AMPK: structure, renal expression, and function

AMPK is a heterotrimeric complex composed of 3 different subunits: α, β, and γ (**Figure 14**). The catabolic subunit α is present in two different isoforms α1 and α2. The β and γ subunits are the regulatory subunits. There are two β-subunits β1 and β2 and three γ subunits γ1, γ2, and γ3. Those multiple protein isoforms are encoded by seven different genes: PRKA1/2, PRKAB1/2, and PRKAG1/2/3. The expression of AMPK subunits is tissue-specific and seems to vary in response to stress, suggesting differential functions of each isoform, which is not well understood yet. The α subunit contains a kinase domain phosphorylated by upstream kinases on Thr172, an auto-inhibitory domain (AID), and a βγ binding domain, essential for complex formation. The AMPKβ contains a carbohydrate-binding molecule (CBM) that allows AMPK to bind to glycogen and an αγ binding domain. The β subunit is implicated in the re-localization of AMPK to the lysosome with glucose starvation and to mitochondrial membranes to achieve its function in mitophagy [330]. The structural characteristic of AMPKγ is the four tandem repeats termed cystathionine β-synthase (CBS) motifs that bind adenine nucleotides. The binding of AMP rather than ADP or ATP to the AMPKγ subunit leads to the activation of AMPK [256].

AMPK is highly expressed in renal cells. Few studies describe the expression of specific AMPK subunit isoforms in the kidney, as most of the time, all AMPK isoforms are expressed. AMPK is also often studied in total kidney lysates, which makes it difficult to have very relevant data regarding subunits expression in the whole kidney. However, it is evident that specific cell populations in the kidney differentially express AMPK isoforms due to their specific functions and metabolism. According to The Human Protein Atlas (HPA), AMPK is mostly expressed in the tubules. AMPK is mostly expressed in cortical tubular epithelial cells, notably on apical surfaces of distal tubules in mice, as demonstrated with immunostaining for Thr172 Phospho-AMPKα [294,331]. The α2 subunit is the predominant catalytic isoform. However, the α1 subunit is also detectable in the tubule but not detectable in the glomeruli. In HPA, the β1 and β2 isoforms are both expressed in the kidney, but Salatto *et al.* showed that human and rodent kidneys predominately express AMPK β1 [332]. The γ2 subunit is also expressed in the human kidney tissue according to the HPA. In the rat kidney, the α1 isoform is the most expressed, while both γ1 and γ2 are expressed at similar levels in the kidney [333]. Expression of γ3 is the most restricted to skeletal muscle and is not detected in the kidney.

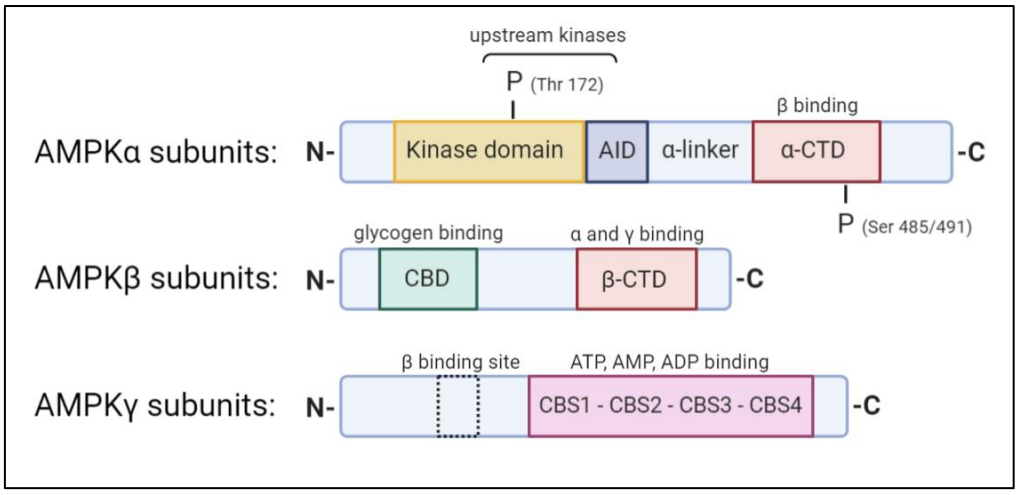

Figure 14 | Structure of the AMPK α, β and γ subunits. The different domains and specific sites of the α, β and γ subunits that constitute the AMPK heterotrimeric complex are represented with the crystal structure. The AMPKα subunits are composed of a serine/threonine kinase domain at the N-terminus phosphorylated by upstream kinases on the residue Thr172, directly followed by an autoinhibition domain (AID) that maintains the kinase domain inactive in the absence of AMP, and a C-terminus domain (α -CTD) that interacts with the β subunits. Phosphorylation of Ser 485/491 residues on the α -CTD negatively regulates AMPK. The AMPKβ subunits contain a glycogen-binding domain (CBD) and and a α and γ subunits interaction domain (β-CTD). The AMPKγ subunits present 4 β -synthase (CBS) domains (CBS1-4) binding ATP, AMP and ADP. Binding of AMP initiates the allosteric activation of AMPK and promotes phosphorylation of AMPK by upstream kinases.

An allosteric mechanism activates AMPK. When the AMP: ATP ratio is high during starvation, hypoxia, or exercise, AMP binds the regulatory γ subunit, stimulating AMPK activity through an allosteric activation. This AMP binding favors the phosphorylation of AMPK by upstream kinases on α subunits at specific Thr172 residues. Besides, AMP binding prevents dephosphorylation of AMPK by protein phosphatases, PP2A, and PP2C. The two central upstream kinases that phosphorylate AMPK are the serine-threonine liver kinase B1 (LKB1) and the calcium/calmodulin kinase kinase β (CAMKKβ). LKB1 activates AMPK in response to low energy states (e.g., exercise, starvation), while CAMKKβ is sensitive to increases in intracellular Ca^{2+}[256]. The transforming growth factor (TGF)-β-activated kinase-1 (TAK1) is also known to phosphorylate AMPK on Thr172 of the α subunit [334]. Other phosphorylation sites, particularly on Ser485/491 (equivalent rodent sequence is Ser487/491) are targeted by other kinases such as Akt through insulin-related signaling or PKA through c-AMP-related signaling pathways. However, these phosphorylations lead to negative regulation of AMPK by blocking its interaction with upstream kinases from phosphorylating T172 [335–337].

AMPK exhibits a dual function in cell metabolism. First, AMPK decreases ATP consumption by inhibiting anabolic pathways, including lipid synthesis, glycogen synthesis, and protein synthesis. Secondly, AMPK activates catabolic pathways by increasing lipid oxidation, glucose uptake, autophagy flux, and mitochondrial biogenesis. These pathways will be discussed in the context of their impact on obesity and diabetes and related kidney disease in the following sections. Energy sensing by AMPK is particularly relevant in renal cells because these cells are strongly dependent on the regulation of energy metabolism for tubular transport.

AMPK regulates the Na^+-K^+-ATPase (NKA), epithelial sodium channel (ENaC), the Na-K-Cl cotransporter (NKCC), Cystic fibrosis transmembrane conductance regulator (CFTR), and other ion transport proteins in the kidney [333]. AMPK plays an essential role in kidney homeostasis, as evidenced by AMPK knockdown studies. Kidney-specific deletion of both AMPKα subunits displayed salt and water wasting defects [338]. AMPKα2 KO mice and endothelium specific knockdown of AMPKα2 increase angiotensin-converting enzyme (ACE)-levels [339]. AMPK is also implicated in specific renal physiological processes such as ion transport, blood pressure control, and nitric oxide production. Tubular epithelial-specific deletion of LKB1, the primary upstream kinase of AMPK, was associated with de-differentiation of tubule epithelial cells, fibrosis, and inflammation, mediated by AMPK and its downstream metabolic effects [326]. On the other hand, uncontrolled sustained activation of AMPK in a Wolff-Parkinson-White Syndrome model led to a disastrous accumulation of glycogen in the kidney and subsequent impairment of renal function [340]. While these genetic studies of AMPK highlight the importance of an accurate regulation of AMPK activity in the kidney during physiological conditions, AMPK impairment in the kidney's response to metabolic stress initiates deleterious outcomes.

3.3 AMPK activity in obesity and diabetes-induced CKD

Type II diabetes, obesity, and MetS are all characterized by lipid accumulation and hyperglycemia, which is perceived by the cells as a nutrient excess. According to the classic view, the cells respond to this high-energy state by a decreased AMPK activity. However, the mechanisms by which AMPK is inhibited seem to implicate a myriad of cellular and molecular events directly or indirectly linked to metabolic disturbances in the whole body [341]. As previously mentioned, AMPK activation is strongly correlated to the AMP: ATP ratio during physiological conditions or adaptations such as exercise or starvation. In obesity and diabetes, additional mechanisms, independent of the AMP: ATP ratio, might also promote the reduced AMPK activity. With nutrient excess, the energy state of the cell favors an altered redox status with higher NADH production

through glycolysis [342]. This increase in NADPH, in turn, leads to reduced activity of Sirtuin 1 (SIRT1), an NAD^+ dependent deacetylase, that is a significant activator of LKB1, therefore favoring the dephosphorylated state of AMPK [343–345].

Increased levels of circulating hormones such as insulin and leptin in metabolic diseases downregulate AMPK by inducing inhibitory phosphorylation on different serine residues. For example, insulin decreases AMPK activity through phosphorylation on Ser485 and Ser 491 of AMPKα subunits by the Akt pathway. At the same time, leptin induces AMPK inhibition by p70S6 Kinase downstream of Akt [346,347]. Additionally, low adiponectin levels in obesity and type II diabetes could also decrease AMPK activation *via* its receptor, AdipoR1. Adiponectin KO mice have decreased AMPK activity while AMPK activity correlates with adiponectin levels in an obesity model [348]. In high-fat and high-sucrose diet models, tissue expression of adiponectin receptors was perturbed, highlighting a mechanism of adiponectin resistance in peripheral tissues that could also contribute to impaired AMPK activity [349,350]. More recently, the treatment of db/db mice with an activator of adiponectin, AdipoRon, showed the upregulation of phosphorylated AMPK in the kidney along with reduced inflammation and lipotoxicity [262]. Finally, obesity and diabetes are associated with inflammation and oxidative stress that are both recognized to inhibit AMPK [351]. The pro-inflammatory cytokine, TNFα, is known to suppress AMPK activity via the induction of PP2C in skeletal muscle *in vitro* and *in vivo*, suppressing fatty acid (FA) oxidation and promoting insulin resistance [352].

3.4 AMPK in renal transport

The kidneys function as regulatory organs by maintaining a constant volume and composition of the body fluids. This essential and vital role is permitted by tubular reabsorption and secretion thanks to polarized localization of various transport proteins in the apical and basolateral cellular membrane along the nephron. First, plasma is filtered into the glomeruli to produce the ultrafiltrate that will then undergo changes in composition along the nephron and ultimately form the final urine. The role of AMPK in ion transport has been described in earlier reviews [353,354]. However, little is known regarding the role of AMPK in renal transport in the setting of obesity and diabetes. Both obesity and insulin resistance are associated with significant changes in tubular transport leading to electrolyte disorders such as hypomagnesemia, hyper/hyponatremia, hyper/hypokalemia, and hyper/hypocalciuria [355,356]. The renal handling of glucose and amino acids is very complex relying on primary active transport that requires a direct energy input; secondary active transport utilizing an indirect energy input, and even carriers for facilitated diffusion. AMPK interferes with Na^+-handling, notably by

activating the primary transport, the NKA [357]. Xiao et al. demonstrated that the AMPK pathway is the principal regulator of NKA signaling as the hyperuricemia-induced renal tubular injury impairs NKA. Moreover, AMPK activation exerted protective effects regarding NKA-mediated mechanisms of tubular injury by regulating NKA expression and reducing lysosomal NKA degradation [358]. However, AMPK activation also downregulates the ENaC expression in the distal tubule [359,360] while it seems to enhance the stimulation of the NKCC that is responsible for sodium reabsorption in the thick ascending limb [361,362]. Nevertheless, the use of knockout mice for AMPK subunits demonstrated only a moderate role for AMPK in renal sodium handling, suggesting that AMPK might only play a secondary modulatory role [363]. Besides, AMPK downregulates many other renal transporters such as Na^+-coupled phosphate transporter NaPi-IIa or CFTR [364,365]. Therefore, reduced renal AMPK activity in metabolic diseases contributes to the salt and water imbalance in obesity or diabetes-related disease, although further investigations are still needed.

3.5 AMPK and renal lipid metabolism

Lipid homeostasis is regulated by the influx, the synthesis, catabolism, and the efflux of lipids. Diabetic nephropathy and obesity-induced CKD are both linked to renal lipid accumulation, and abnormal lipid metabolism (**Figure 15**) [284,300,366]. Activated AMPK induces the inhibitory phosphorylation of Acetyl-CoA Carboxylase (ACC), the rate-limiting step of FA synthesis, reducing the production of malonyl-CoA. Decreased malonyl-CoA promotes the activation of carnitine palmitoyltransferase-1 (CPT-1), allowing the entry of FA into the mitochondria for β-oxidation. Therefore, a direct consequence of AMPK dysfunction in the kidney is the increase of ACC activity, likely contributing to lipogenesis and, ultimately, to lipid accumulation. This fact was confirmed by AMPK dysregulation, and subsequent renal accumulation of cholesterol and triglycerides (TG) in mice fed a high-fat diet [298].

Sterol Regulatory Element-binding Proteins (SREBP) are implicated in fatty acid and cholesterol metabolism [296,297]. Specifically, SREBP-1 and -2 have increased expression in the context of obesity or diabetes. SREBP-1c knockout mice fed an HFD diet are protected from renal lipid accumulation [298]. However, transgenic mice overexpressing SREBP-1a demonstrate an elevated renal TG content with glomerulosclerosis and proteinuria [367]. Even though the AMPK activation was not probed, we may postulate a role of AMPK in SREBP pathways. Indeed, in recent studies, AMPK was found to be a direct upstream kinase of SREBP in the liver [368,369]. Activation of AMPK resulted in inhibition of SREBP1-c and attenuation of lipogenesis [370]. Another study about the effects of nifedipine, a calcium channel

blocker, demonstrated the accumulation of intrarenal lipids that was associated with decreased AMPK activity and overexpression of SREBP1/2 [371]. These studies confirm the role of AMPK dysregulation in renal lipid accumulation via the SREBP pathway. Other groups have also highlighted the increase of lipogenesis along with the decrease in lipolysis [284,300].

Kume *et al.* demonstrated an increase of renal TG content and marked neutral lipid accumulations in both glomeruli and tubular compartment with overexpression of the Peroxisome Proliferator-activated Receptor gamma (PPARγ), while heterozygous PPARγ mice were protected [300]. This study demonstrated decreased AMPK activity, but no link between AMPK and PPARγ was discussed. Interestingly, several independent studies have highlighted a cross-regulation of AMPK and PPARγ, suggesting an expanded regulation of lipid metabolism by AMPK [372–374].

On the other hand, high-fat diet-fed mice demonstrated decreased lipolysis and AMPK activity [294]. Cholesteryl esters and phosphatidyl contents but not TG were increased along with a significant increase of lipid droplets in proximal tubular cells (PTC). AICAR, a specific AMPK activator, prevented all these changes. In that study, AMPK activation in HFD mice also prevented cholesterol synthesis by the regulation of the rate-limiting cholesterol synthesis enzyme, the 3-hydroxy-3-methylglutaryl-CoA reductase (HMGCR) [284]. Other groups also confirmed lipid droplet accumulation in PTC [179,281–286]. Under physiological conditions, the primary role of PTC is the active reabsorption of filtered sodium. This process requires a large amount of ATP, which is mostly provided through the mitochondrial β-oxidation of FA. Inhibition of FA oxidation induced increased intracellular lipid depositions, cellular de-differentiation, and cell death in the kidney [375,376]. In PTC, FA can also be taken up via the fatty acid translocase (CD36) and the fatty acid-binding proteins (FABP). FA can then be used to supply energy. CD36 was shown to be upregulated in kidney biopsies of diabetic patients [287]. In the study with nifedipine, upregulation of CD36 in the kidney led to the inhibition of AMPK activity and subsequent lipotoxicity [371].

Excess intracellular FA content can lead to the accumulation of toxic lipid metabolites such as diacylglycerol (DAG) and ceramides. Both the DAG and ceramide are known to be involved in insulin resistance and inflammation. Both are endogenous activators of protein kinase C (PKC) and protein phosphatase 2A (PP2A) [377]. Moreover, the downregulation of AMPK activity through the PKC-dependent Ser487 phosphorylation has been demonstrated in human endothelial cells [378]. Using lipidomics, Declèves *et al.* demonstrated HFD-induced dysregulation of lipid metabolism and particularly eicosanoids, which are implicated in the inflammatory response in the kidney. Direct activation of AMPK with AICAR reduced arachidonic acid and docosahexaenoic acid-

derived metabolites in the kidney, thus improving the eicosanoid pathway and associated lipotoxicity [379]. Therefore, the altered lipid metabolism in the kidney characterized by an imbalance between FA accumulation and degradation seems to be primarily mediated by AMPK.

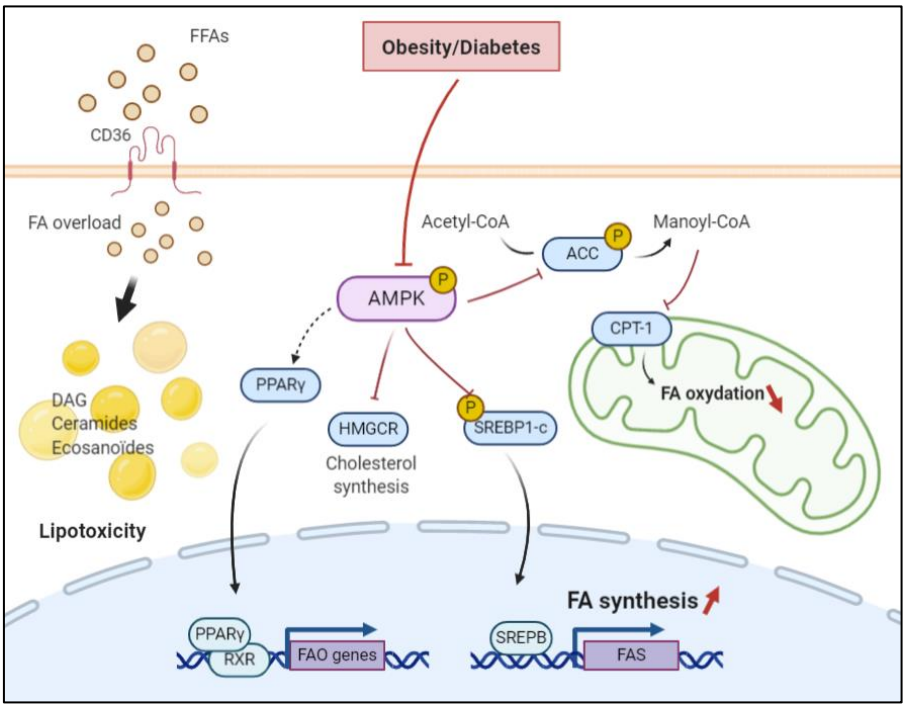

Figure 15 | Impaired regulation of lipid metabolism by AMPK in renal cell in obesity/diabetic context. Inhibition of AMPK and the increased FA overload lead to a decreased mitochondrial FA oxidation and an enhanced lipogenesis, initiating lipotoxicity in renal cells. Inhibitory phosphorylation of ACC by AMPK is abolished that consequently allows manoyl-CoA production, leading to inhibition CPT-1 activity and suppression of FA oxidation in mitochondria. HMGCR and SREBP1-c are enhanced and initiate cholesterol and FA synthesis that contributes to a general increase of lipogenesis that contributes to further lipid accumulation in renal cells. Excess FA content associated to impaired AMPK pathway and related lipid metabolism initiate ectopic lipid accumulation in renal cells, including deleterious lipid metabolites (DAG, ceramides and eicosanoids) that cause lipotoxicity. AMPK, AMP-activated protein kinase; ACC, Acetyl-CoA carboxylase; CPT1, Carnitine palmitoyltransferase I; PPARγ, Peroxisome proliferator-activated receptor γ; HMGCR, 3-hydroxy-3-methyl-glutaryl-coenzyme A reductase; RXR, retinoid X receptor; SREBP, Sterol regulatory element-binding proteins; FAS, fatty acid synthesis; FAO, fatty acid oxidation; DAG diacylglycerol; FFAs, free fatty acids. The arrow indicates whether the regulation is activating (black) or inhibitory (red). The dashed arrow indicates a potential regulation.

3.6 AMPK and renal glucose metabolism

In conditions with abundant glucose, AMPK was reported to promote glucose uptake and activation of glycolysis, as well as to promote GLUT4 gene expression in insulin-sensitive cells. Several studies have reported the role of AMPK in mediating glucose transport in podocytes as well as insulin resistance in diabetic nephropathy [380,381]. Indeed, podocytes display a complex cellular morphology that requires a sustained energy supply in order to maintain cytoskeletal remodeling. In podocytes, the mitochondrial abundance is low and anaerobic glycolysis represents the predominant energy source that makes them uniquely sensitive to insulin [382]. Although insulin-stimulated glucose uptake is mostly independent of AMPK, Rogacka *et al*. significantly demonstrated that AMPK activity is essential for insulin sensitivity in podocytes. Moreover, insulin resistance in podocytes cultured in high glucose medium was closely related to AMPK activity [380]. Using pharmacological and genetic approaches, they suggested the involvement of AMPK in PTEN (phosphatase and tensin homolog) regulation in cultured podocytes is disturbed in high glucose conditions leading to decreased insulin sensitivity. More recently, it has been shown that insulin mediates AMPK regulation through Transient Receptor Potential Canonical Channel 6 (TRPC6) activation[383]. TRPC6 is a nonselective Ca^{2+} channel protein that was recently implicated in the physiopathology of kidney diseases [384]. In diabetic nephropathy, TRPC6 is shown to be upregulated, suggesting a putative role of TRPC6 expression in the progression of diabetic nephropathy pathology. Wang et al. investigated the effect of TRPC6 KO on diabetic kidney disease in the Akita model of type I diabetes [385]. They surprisingly demonstrated a protective effect of TRPC6 downregulation on proteinuria and albuminuria. This role of TRPC6 is contrary to promoting the progression of glomerular impairment associated with insulin resistance *in vivo* and podocyte cultures.

Like AMPK, SIRT1 is a nutrient sensor in cells. AMPK and SIRT1 are reciprocally regulated and share common targets. The expression of SIRT1 is significantly reduced in animal models and diabetic patients. Moreover, podocyte-specific overexpression of SIRT1 led to improvements in glomerular and tubular injuries in diabetic mice [386]. AMPK activity is decreased when SIRT1 is downregulated in podocyte cultures. When SIRT1 is suppressed, the stimulation of AMPK by insulin was also suppressed, suggesting that the SIRT1/AMPK pathway is essential in podocytes for proper insulin response [387]. Both AMPK and SIRT1 promote autophagy flux in renal tissue, regulate mitochondrial homeostasis, and antioxidative defense. Shati *et al.* showed that the hypoglycemic and renoprotective effects of Salidroside are mediated by downstream activation of SIRT1 by AMPK [388].

3.7 AMPK and renal mitochondrial function and dysfunction

3.7.1 Mitochondrial biogenesis and dynamics

As already mentioned, the kidneys are very highly metabolic organs with high energy demand and, therefore, rich in mitochondria. Especially, PTCs have a high number of active transporters that require energy to reabsorb ions, glucose, or other nutrients. Maintaining the mitochondrial function is, therefore, essential to sustain the energy demand and kidney function. AMPK activity promotes mitochondrial homeostasis by regulating mitochondrial biogenesis and dynamics and by limiting reactive oxygen species (ROS) formation [256,389]. There is a very substantial body of evidence demonstrating the mitochondrial protection exerted by AMPK, notably through the activation of the peroxisome proliferator-activated receptor gamma co-activator 1-alpha (PGC-1α) [390–393]. PGC-1α is a transcriptional co-activator and the master regulator of mitochondrial biogenesis. Upon activation, it migrates to the nucleus and activates different transcription factors, including nuclear respiratory factor 1 and 2 (NRF-1 and -2), which in turn activate the expression of nuclear coded respiratory chain protein as well as the expression of Mitochondrial Transcription Factor A (Tfam), driving replication of mitochondrial DNA and transcription [394]. Under metabolic diseases-induced CKD, mitochondrial dysfunction has been well documented (reviewed in [395,396]) and is now considered as a critical player of the pathogenesis [397]. In this context, it makes sense to involve AMPK in mitochondrial dysfunction in diabetic- and obesity-induced CKD. Szeto et al. demonstrated that the use of SS-31, a mitochondrial-targeted antioxidant, in HFD mice preserved mitochondrial structure and led to the improvement of glomerular and tubular injuries. Interestingly, these effects were attributed to restored AMPK activity, suggesting that mitochondria integrity is essential to maintain AMPK phosphorylation [398]. Even in diabetic nephropathy, the restoration of AMPK activation *via* AICAR restored mitochondrial function and superoxide production, in association with PGC-α activation, leading to a reduction of kidney injury. In another study, treatment with chloroquine in an *in vitro* and *in vivo* diabetic environment enhanced AMPK phosphorylation and led to mitochondrial biogenesis but also an improved balance of mitochondrial fusion/fission proteins [399]. Considering mitochondrial dynamics, AMPK was recently demonstrated to be implicated [400]. Toyama et al. found a new AMPK target protein, the mitochondrial fission factor (MFF), which is the primary receptor for the dynamin-like protein (Drp1) involved in the mitochondrial fission mechanism. The authors showed that mitochondrial fragmentation was related to AMPK activation in human osteosarcoma cells. Later, the AMPK/MFF/Drp1 axis was also demonstrated in mesenchymal stromal cells. Renal mitochondrial fragmentation has been observed in *in vitro* and *in vivo* model of diabetic

nephropathy and was prevented by both AMPK activators, AICAR, and metformin. Interestingly, in that study, this improvement was correlated with AMPK-mediated activation of PGC-α and the consequent restoration of Drp1 and Mfn1 expression in tubular cells [401].

3.7.2 AMPK and oxidative stress

Oxidative stress plays a crucial role in the development and the progression of diabetic nephropathy and obesity (**Figure 16**). Because renal cells are metabolically very active and contain many mitochondria, they are highly vulnerable to ROS generation and, therefore, to oxidative damage [396]. Under physiological conditions, ROS are generated as standard products of aerobic metabolism, acting as intracellular signaling messengers. Therefore, ROS such as the superoxide radical ($O_2^{\bullet -}$) and hydroxyl radical (•OH) or even the non-radical hydrogen peroxide (H_2O_2) are continuously produced during cell metabolism and are eliminated by the antioxidant defenses that include superoxide dismutase (SOD), catalase, peroxidases and the glutathione system to prevent cellular protein damage or lipid peroxidation. However, under nutrient stress such as during chronic hyperglycemia or hyperlipidemia, over-production of ROS due to the disruption of the redox status occurs, leading to renal inflammation, fibrosis, and impairment of organ structure and function [316,402].

In the kidney, the primary source of ROS production is the mitochondria, due to a leakage from the mitochondrial electron-transport chain. Regarding AMPK and oxidative stress, it has been well established that AMPK activity plays a crucial role in maintaining redox homeostasis in the cells. AMPK is essential in the suppression of ROS and acts thus as an antioxidative stress defense. Different models have described a link between reduced AMPK activity and mitochondrial ROS (mtROS) [392,395–397]. Physiologically, mtROS promotes non-canonical activation of AMPK, triggering antioxidative responses through PGC1α activation and regulating mitochondria homeostasis by activation of the mitophagy process *via* AMPK mediated phosphorylation of ULK-1 [389]. Also, AMPK regulates gene expression of several antioxidative genes, including catalase, SOD2, UCP2, and SIRT3 [403]. Notably, it has been shown that cells lacking AMPKα or PGC1α present increased oxidative stress [389]. The cells lacking AMPK signaling cannot overcome ROS-induced damages and mitochondrial homeostasis disruption.

Under pathological conditions, the contribution of ROS to the development and the progression of kidney disease is controversial. For example, previously, Ruggiero et al. (2011) have highlighted in a model of HFD mice that the kidney, despite evidence of

renal oxidative stress, was able to maintain mitochondrial biogenesis and bioenergetics, suggesting an adaptive response to the free FA overload [214]. Still, Dugan *et al.* reported a reduced superoxide production associated with suppression of mitochondrial activity in the type I diabetic model [279]. The decreased mtROS was concomitant with a decreased AMPK activity and led to further inhibition of mitochondria in a feedback loop manner. Interestingly, AICAR treatment restored AMPK activity along with the mitochondrial superoxide production reversing the hallmarks of diabetic kidney disease such as glomerular matrix expansion and albuminuria [279]. Then, it has also been proposed by Sharma *et al.* that stimulation of mitochondrial function and superoxide production by AMPK agonists would be associated with better outcomes in the diabetic kidney [404]. However, it has been shown that AMPK activity could be inhibited by mtROS production through the SIRT1 pathway. Indeed, mtROS-mediated damages cause DNA breaks in the nucleus that require the activation of PARP (repair enzyme, poly adenosine diphosphate ribose polymerase), another NAD^+-dependent enzyme. Therefore, upon PARP activation, the pool of cellular NAD^+ is reduced, decreasing NAD^+ availability for SIRT1 that in turn reduced the phosphorylation of AMPK through LKB1 activation [405]. In conclusion, the direct link between AMPK and mtROS production has not been fully understood and will require further investigations in the context of diabetic- and obesity-induced CKD.

Another important source of ROS in renal cells is linked to NADPH oxidases (NOXs). NOX-derived ROS are involved in vascular oxidative stress and endothelial dysfunction in obesity. AMPK also plays a role in regulating the NOX system. NOX4 is the most abundant NOX isoform in the kidney and mostly generates H_2O_2 that also plays physiological roles in renal cells [406,407]. NOX4 is upregulated in both diabetic nephropathy and obesity-related CKD [408,409]. The downstream consequences of NOX4 activation in the kidney lead to increased inflammation and fibrosis. This process was described to be mostly dependent on AMPK signaling. Indeed, AMPK activation reduced NOX4 production and ROS, inhibiting NFκB, and reduced TGF-β-mediated fibrosis. He *et al.* demonstrated that in renal fibroblast cells, high glucose-induced ROS generation is mainly derived from NOX4 and not NOX1 and NOX2 and in a similar way in *db/db* mice. NOX4 activation led to the proliferation and activation of resident fibroblasts and, ultimately, renal fibrosis. Resveratrol treatment in *db/db* mice prevented NOX4 expression primarily due to increased AMPK activity [410]. Similarly, numerous recent studies highlighted the beneficial effects of antioxidants or other compounds against renal injuries implicating AMPK/NOX4/ROS [411–417]. Furthermore, two independent studies reported that Sestrin-2 mediated activation of AMPK led to the inhibition of ROS production, renal impairment in the hyperglycemic condition in podocytes, and NOX4 suppression in glomerular mesangial cells [418,419]. AMPK and

NOX4 dysregulation promote p53 and polyunsaturated fatty acids (PUFA), driving the pro-apoptotic pathway in podocytes and glomeruli of diabetic mice that were reduced by AICAR treatment [325]. In contrast, other studies have demonstrated NOX4 downregulation in the kidney, suggesting a protective role of NOX4 in the physiopathology of diabetic nephropathy [420]. Recently, Muñoz *et al.* demonstrated reduced endothelial NOX4 expression associated with decreased H_2O_2 generation and H_2O_2-mediated vasodilatation in obese rats [421].

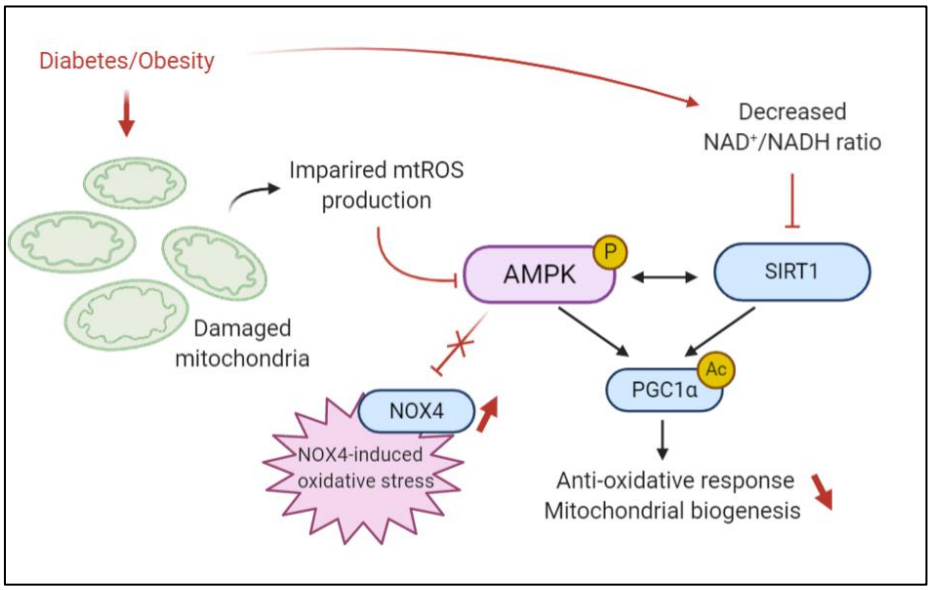

Figure 16 | Schematic representation of the proposed mechanism by which diabetes/obesity lead to decreased anti-oxidative response mediated by AMPK and enhanced oxidative stress in renal cell. Regulation of mitochondrial production of ROS is required for proper adaptation to metabolic stress. Diabetes and/or obesity results in impaired renal mitochondrial ROS, which is associated with decreased AMPK. AMPK inhibition and decreased SIRT1 activity lead to maladaptive anti-oxidative response through PGC1α activity suppression, notably decreasing mitochondrial biogenesis. Decreased AMPK also results in increased NOX4-dependent ROS production, further increasing oxidative stress in renal cells. The arrow indicates whether the regulation is activating (black) or inhibitory (red).

3.8 AMPK and the regulation of renal autophagy and mitophagy

Autophagy is a complex and highly regulated process of self-degradation of cellular components. In the kidney, basal autophagy flux is essential to maintain cellular homeostasis and, therefore, renal function. Kidney specific autophagy-deficient mice reveal evidence of damaged mitochondria, protein aggregates, endoplasmic reticulum stress, podocyte, and proximal tubular cell loss, and progressive impairment of renal function [422]. The role of AMPK in the regulation of the autophagy flux has been extensively investigated in liver, muscle, brain, or adipocytes, whereas only a few studies explore the role of AMPK in renal autophagy [423–426]. AMPK positively

regulates the autophagy process through phosphorylation of essential target proteins, mainly through the mechanistic target of rapamycin (mTOR) and the Unc-51 like autophagy activating kinase (ULK-1) [427]. Upon activation, AMPK inhibits mTOR and activates ULK-1, which, in turn, leads to an activation of autophagy [428]. The inhibition of mTOR by AMPK is either by direct phosphorylation or through phosphorylation of the Tuberous Sclerosis Complex 2 (TSC2) protein that then reduces mTOR activity [429]. Interestingly, the high basal level of autophagy observed in podocytes is mainly regulated by the AMPK/ULK-1 axis rather than mTOR pathway, suggesting that the activation of autophagy by AMPK might be cell-type dependent in kidneys [430]. Moreover, AMPK phosphorylates Raptor leading to a decrease in mTORC1 activity [431]; Finally, the ongoing partnership between AMPK and SIRT1 has also been accounted for in the activation of autophagy. AMPK activity leads to an increased intracellular pool of NAD^+ that allows the increase of SIRT1 activity. SIRT1 targets FOXO1 and FOXO3 in the nucleus and autophagy-related genes Atg5, Atg7, and Atg8, that positively regulate autophagy [432].

Obesity or diabetes can lead to impairment of autophagy flux in renal cells [433,434]. HFD/obesity-induced autophagy impairment has been described in rodent models and obese patients [286,435]. Yamamoto *et al.* described the stagnation of the autophagy flux as a novel mechanism of renal lipotoxicity in a model of mice fed an HFD. They significantly demonstrated that long term lipid overload was associated with impairments of the lysosomal system and to a consequent accumulation of phospholipids, probably of mitochondrial origin. This lipotoxicity was associated with a sustained mTOR activation, but they did not investigate the association with AMPK. Excessive fat also induces constitutive activation of mTORC1 that directly inhibits AMPK activity [436,437]. However, AMPK-mediated activation of autophagy has been shown to play a protective role against renal injury, particularly in AKI [438]. Regarding metabolic diseases-related CKD, Yamahara *et al.* demonstrated that obesity significantly suppressed autophagy in PTC of both mice and humans. Notably, they found that AMPK was implicated in FFA-albumin–induced autophagy in PTCs. In PTCs, AMPK downregulation was associated with decreased autophagy induction by albumin-binding FFA, suggesting that AMPK may be essential for maintaining proper autophagy flux. In obesity, activation of AMPK was not altered by FFA-albumin overload, but its activity failed to decrease the hyperactivation of the mTORC1 signal, leading to the obesity-mediated exacerbation of proteinuria-induced tubulointerstitial damage. Delayed activation of AMPK with fenofibrate was associated with subsequent autophagy activation in the kidney of HFD mice, supported by AMPK activation by AICAR [293,439]. Antioxidant drugs such as Berberine or Mangiferin were shown to

improve autophagy flux in diabetic nephropathy through the activation of AMPK [440–442].

There is no direct evidence of the role of AMPK in mitophagy pathways. However, activated ULK-1 translocates to damaged mitochondria and phosphorylates FUN14 domain containing 1 (FUNDC1) protein, which is considered as a critical player of mitophagy, allowing the formation of an autophagosome around damaged mitochondria [443]. Therefore, AMPK-induced ULK-1 activation may be a crucial mediator of mitophagy [444]. In the study of Yamamoto et al., the induction of the mitophagy pathway was demonstrated to protect PTC from mitochondrial dysfunction. Activation of AMPK with AICAR or Metformin led to an increase of autophagy flux and removal of damaged mitochondria in STZ-induced diabetic nephropathy [401]. Finally, AMPK has been recently found to be implicated in lipophagy, the autophagic degradation of lipid droplets (LDs). Lipophagy and lipolysis of LDs for intracellular lipid mobilization are preceded by the targeted autophagy of Perilipin2 (PLIN2). Indeed, PLIN2 must be removed from LDs to be released for the lysosome or lipolysis. This process is controlled by AMPK-dependent phosphorylation of PLIN2, suggesting a new pathway for the control of lipid metabolism by AMPK through the regulation of lipophagy [445].

The precise role of AMPK in the regulation of autophagy, mitophagy, or lipophagy in renal cells needs further investigation. However, AMPK dysregulation could inhibit autophagy and participates in the pathogenesis of obesity and diabetic CKD. AMPK activation may be a valuable way of restoring the autophagy process in metabolic diseases-induced CKD.

3.9 AMPK and Sirtuins

The sirtuins are members of the Class III deacetylase. So far, seven forms have been identified (Sirt1-7) [446]. Mainly SIRT1 and SIRT3 are induced by caloric restriction and have been connected to AMPK [447]. Interconnection between AMPK and SIRT1 has been demonstrated, especially the AMPK/SIRT1/PGC1α act as a crucial network to maintain mitochondrial homeostasis (already discussed in this review) [448,449]. However, studies highlighting an AMPK/SIRT3 axis in disease have emerged over these recent years. SIRT3 is an NAD^+-dependent deacetylase, mainly localized in mitochondria. Deacetylation accounts for a crucial mechanism to regulate the activity of many substrates involving in energy metabolism [450]. Accordingly, SIRT3 plays a significant role in mitochondrial homeostasis by the regulation of the mitochondrial respiratory chain and ATP production. SIRT3 promotes FAO through the deacetylation of long Chain Acyl-CoA Dehydrogenase (LCAD) [451] and also exerts an antioxidant activity by targeting the superoxide dismutase 2 (SOD2) and the isocitrate dehydrogenase (IDH2)[446,452]. More interestingly, the cytosolic form of SIRT3 has

been shown to activate LKB1, which in turn activates AMPK in primary cardiomyocytes [453]. Therefore, reduction in SIRT3 expression in a setting of obesity could, in part, explain the reduction in AMPK activity. Another evidence of the role of SIRT3 in AMPK activation is its involvement in the increase of cytosolic calcium level that involves the activation of CaMKKβ and so promotes the activation of AMPK. It is thus worth hypothesizing that the AMPK/SIRT3 axis plays a vital role in renal lipotoxicity.

The importance of SIRT3 in metabolic diseases has also been demonstrated in rodents and humans, showing a reduction in SIRT3 activity in these settings [454,455]. Also, mice deficient for SIRT3 and fed an HFD revealed an acceleration of MetS hallmarks [456]. SIRT3 restoration is beneficial in models of acute kidney injury (AKI) [457–459]. Indeed, maintaining SIRT3 activity was shown to prevent acute damages in renal tubular cells by maintaining the mitochondrial functional integrity and dynamics through the normalization of mitochondrial protein acetylation [457,459]. Morigi *et al*. (2015) even reported tin mice with cisplatin-induced AKI, tubular cell mitochondrial abnormalities were associated with decreased renal SIRT3 mRNA and protein expression while treatment with AICAR, an activator of AMPK, improved renal function through the restoration of SIRT3 expression and activity. That study also demonstrated the normalization of mitochondrial protein acetylation concomitantly with the upregulation of proximal tubular SIRT3 expression after AICAR treatment. This latter provides evidence of the capacity of AMPK activity to restore SIRT3 deacetylase activity. These recent data shed light on a putative new beneficial pathway, AMPK/SIRT3, to maintain cellular homeostasis through the improvement of mitochondrial functional integrity.

3.10 Conclusion and future directions

The downregulation of AMPK activity in obesity- and diabetes-induced CKD has been extensively reported in *in vivo* and *in vitro* experimental models and patients. Inhibition of AMPK activity in the kidney is the result of the systemic metabolic dysregulation as well as signaling factors mediated by other dysfunctional tissues and organs (called organ crosstalk) as well as by intra-renal disturbances. It is incredibly challenging to delineate the pleiotropic pathways regulated by AMPK and the potential impact of their dysregulation in renal cell function and metabolism. A better understanding of the AMPK pathway and the consequences of its dysregulation in metabolic-induced kidney diseases is thus essential to improve therapeutic strategies. Here, we presented a more comprehensive and exhaustive view of the experimental and clinical evidence supporting a central role of AMPK in the development and progression of diabetic- and obesity-induced CKD. In particular, we summarized relevant data regarding molecular mechanisms and critical targets related to AMPK in kidney tissue, in a context of

excessive energy supply. In the kidney, AMPK is essential to maintain ATP levels for high metabolic demand in renal cells. Mainly, the regulation of renal transport along the nephron is AMPK-dependent. Moreover, there is a body of evidence demonstrating that AMPK activation leads to the prevention of renal lipotoxicity and lipid accumulation by reducing FA synthase. In podocytes, AMPK is implicated in glucose metabolism and associated insulin resistance. Beyond its regulation of glucose and lipid metabolism as an energy sensor in the kidney, AMPK is a critical protein in the protection of mitochondrial damage by at least four mechanisms (**Figure 17**). 1) AMPK is strongly implicated in the regulation and the response to ROS production by altered mitochondria, thus preventing damage induced by mtROS; 2) activation of AMPK favors mitochondrial biogenesis to enhance metabolism by inducing AMPK/SIRT1/PGC1α pathway; 3) AMPK regulates mitochondrial dynamics and quality control, including mitochondrial fission/fusion; 4) AMPK activity initiates autophagy flux and selectively degrades unhealthy mitochondria. Therefore, inhibition of AMPK in kidney tissue is associated with poor outcomes and leads to lipotoxicity, insulin resistance, inflammation, fibrosis, and loss of renal function. Targeting AMPK in metabolic disease and/or associated renal injury thus represents an important therapeutic target [460].

During the last few years, the research has become very dynamic in order to extend classical knowledge regarding AMPK beyond energy sensing, and novel AMPK-related pathways and mechanisms have emerged in different models and pathologies. While *in vitro* studies of renal cells in the context of excess energy supply are helpful to investigate cellular and molecular mechanisms, they offer a reductive view of the complex regulation of AMPK in vivo that is dependent on many factors. However, in animal models of metabolic syndrome, diabetes, or obesity, it is worth noting that the use of *in vivo* AMPK activators demonstrates several unintended off-target effects in the dosage used. Also, it is not possible to assess the exclusive effects of these drugs on the kidney or specific renal cells. Therefore, more studies in genetic deletion or overexpression of AMPK models in a tissue or cell type-specific manner in the context of metabolic-related kidney disease are still needed to delineate the pleiotropic roles of AMPK presented in this review.

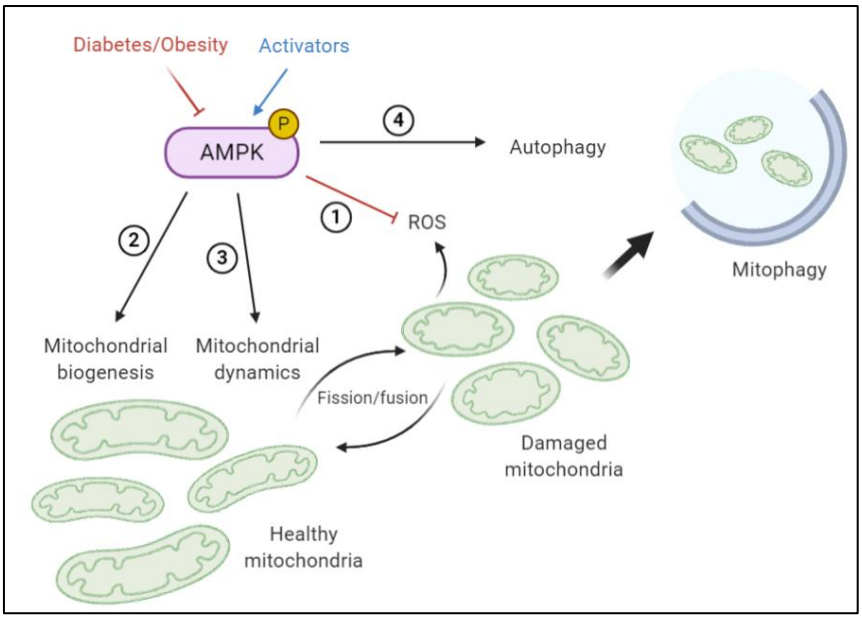

Figure 17 | Mechanisms by which AMPK regulates mitochondrial homeostasis in renal cell. Activation of AMPK in obesity and/or diabetic context leads to improved mitochondrial dysfunction and cellular metabolism by 1) decreasing oxidative stress (ROS) by inducing anti-oxidative stress defense 2) favoring mitochondrial biogenesis to increase mitochondrial density 3) participating in dynamic regulation of mitochondrial fission and fusion to separates healthy and damaged mitochondria in order to facilitate their degradation by mitophagy 4) promoting autophagy and ultimately regulating mitochondrial quality control by the initiation of mitophagy.

Objectives

4 Objectives

In the Western world, obesity is largely due to the combination of sedentary lifestyle, usually associated with a high caloric intake and a lack of exercise. Obesity leads to an excessive body fat linked to other metabolic disorders such as hypertension, insulin-resistance, hyperglycemia, and dyslipidemia as well as to lipid accumulation in non-adipose tissues. In the kidney, lipid accumulation leads to lipotoxicity, cellular dysfunction and CKD. Our group investigates the ectopic renal lipid accumulation and its consequences on cellular functions. In a previous study, we showed that lipid accumulation was mainly located into the proximal tubular cells**.** This lipid accumulation was associated with impaired brush border and increased oxidative stress, showing evidence of tubular dysfunction with perturbation in autophagy flux and mitochondrial function. These changes were observed along with a decreased activity of the central cellular energy sensor, AMPK. Interestingly, these pathological features were prevented by pharmacological AMPK activators. Nowadays, AMPK activators such as AICAR are still not demonstrated to have substantial effectiveness for clinical use. Moreover, current strategies to slow down the progression of obesity-induced CKD mostly rely on control of the body weight gain, hyperglycemia, hyperlipidemia, and blood pressure. However, the management of CKD is limited and inevitably leads to loss of renal function and associated physiological and metabolic disorders. Therefore, there is still a need for a better understanding of the cellular and molecular mechanisms underlying renal lipotoxicity in order to further highlight novel biomarkers that could serve as new therapeutic strategies. Therefore, our general aim was to extend the knowledge regarding the central role of AMPK on renal lipid accumulation after high caloric exposure and to develop new potential therapeutic approaches that could sustain its activity and hence prevent renal dysfunction through an exercise-based therapy. The different approaches of this PhD thesis will be divided this three successive sections (the specific aims will be described in each section):

1. First, the scientific approach of this work was to focus on exercise training intervention (a behavioral intervention). To assess the mechanistic cellular pathways in response to endurance exercise training (EET), we used a mice model fed a high fat diet (HFD). Indeed, HFD mice present characteristic features of obesity and metabolic syndrome and are widely recognized as a suitable model to study obesity-related disease *in vivo*. Moreover, we and others demonstrated that mice fed a HFD for at least 12 weeks developed CKD associated to obesity. Here, we applied a 8-week endurance exercise training on mice after 12 weeks on diet as a treatment for obesity-induced CKD. This will determine whether endurance ET can rescue metabolic and renal changes in obese mice through AMPK activation.

2. Interestingly, the first objective allows us to highlight the Sirtuin 3 (SIRT3), a mitochondrial NAD^+-dependent deacetylase, as a possible valuable player in the AMPK axis and potentially as a potential new biomarker or therapeutic target for obesity-induced CKD. Hence, the second objective of this work was to evaluate whether the overexpression of SIRT3 protect HFD mice from obesity-related CKD development.

3. In the last part, both *in vitro* and *in vivo* models of obesity were used to unravel the role of SIRT3 in regulating mitochondrial function and dynamics in a context of renal lipotoxicity. We particularly explored the cellular dysfunction resulting from the accumulation of lipids in the kidney through the sirtuin 3 (SIRT3)/AMPK axis in a setting of excess calories. In addition, the putative beneficial effects of the activation of SIRT3 by Nicotinamide Riboside, a NAD^+ precursor, were investigated.

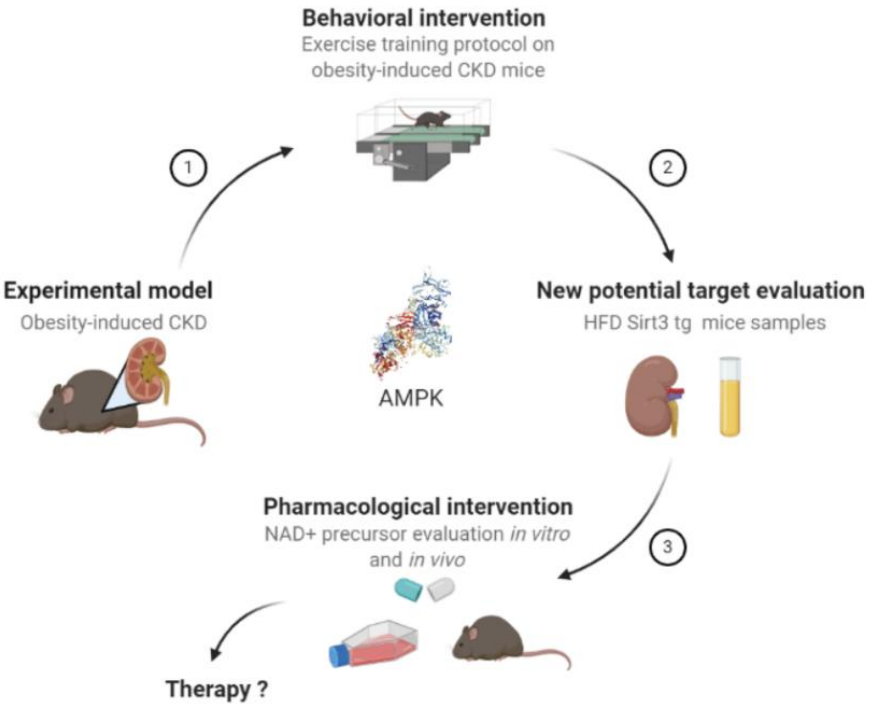

SECTION I

Specific aims

Obesity results in lipid accumulation in adipose tissue but also in non-adipose tissues. The pandemic of obesity is largely due to the combination of sedentary lifestyle, usually associated with a high caloric intake and the lack of exercise [280,461]. Excess lipid accumulation may lead to lipotoxicity and may be the major driver of cellular dysfunction in obesity. In the general population, obesity is the second most highly prognostic factor to predict ESRD [462]. Despite considerable efforts to prevent obesity-related metabolic diseases, there is still a lack of efficient therapeutic strategies, particularly for obesity-induced kidney disease. Specific drug treatments of complex diseases such as dyslipidemia, diabetes or hypertension exist, but our current potential to treat obesity by pharmacological compounds is limited [463]. Indeed, current anti-obesity drugs that aim to reduce food intake and so, weight reduction have been associated with chronic disorders and consequently to severe side effects when used for long periods of time. Moreover, weight regain after the end of the treatment is very common and represents the main limitation for clinical prospects for obesity-related diseases [464]. Regarding AMPK activators such as AICAR, it has not shown adequate and efficient therapeutic effects in clinical use (in term of specificity, bioavailability and pharmacokinetic) [465]. This highlights the urgent need for alternative therapeutic strategies. It is now well established that targeting the underlying molecular pathways that mediate the potential beneficial effects of behavioral interventions such as calorie restriction or exercise training may represent a safer alternative therapeutic approach for the treatment of chronic metabolic disorders.

Therefore, the scientific approach of this section aims to better understand the response of the kidney to endurance exercise training (EET) (a behavioral intervention) in the context of a HFD, with a particular focus on the AMPK activity. Moreover, potential new biomarkers that could be targeted with dietary compounds as an exercise mimetic to treat or prevent obesity-induced CKD will be investigated. Thereby, the potential therapeutic effect of an EET on a treadmill (Collab. Dr. Alexandra Tassin, Laboratory of Physiology and Respiratory Rehabilitation, UMONS) applied on obese mice presenting CKD was investigated.

In this section, different questions were asked, divided in three specific aims:

- To highlight the impact of EET in mice fed a High-Fat diet (HFD, 60% of total calories from fat) *versus* Low Fat Diet (LFD, 10% of total calories from fat) on key metabolic parameters: impact of EET in male mice will be tested after 12 weeks (8 weeks EET protocol) for a total of 20 weeks on HFD. This will determine whether EET can rescue metabolic changes in obese mice. Particularly, the effects of EET on key features of the metabolic syndrome were evaluated including body weight evolution, plasma lipid profile, insulinemia, glucose tolerance, hepatic steatosis and blood pressure.
- To investigate the impact of EET on the development of CKD in mice fed a HFD. The renal structural and functional changes in all experimental groups were investigated by measuring albuminuria and proteinuria, oxidative stress biomarkers, renal lipid content and morphological analysis of kidney sections.
- To investigate the mechanistic cellular pathways in response to EET in mice fed a HFD. Key underlying molecular pathways were highlighted in kidney tissue, focusing on AMPK regulation.

5 Exercise training in obesity-induced CKD

5.1 Introduction

In the general population, obesity is the second most highly predictive factor for end-stage renal disease, independently of diabetes and hypertension [204]. Central obesity is related to caloric excess promoting deleterious cellular responses in targeted organs. Obesity is mainly caused by a sedentary lifestyle commonly characterized by an excess consumption of ultra-processed food containing high amounts of saturated fat, and a lack of physical activity [466]. The prevalence of obesity is increasing worldwide and predictive projections suggest that nearly 50% of adults will be obese by 2030 [25,467]. The consequences of adiposity include the endocrine activity of the adipose tissue *via* the production of adipokines, leading to the development of inflammation, oxidative stress, activation of the renin-angiotensin-aldosterone system and increased insulin resistance in the kidney [468]. Clinical and experimental studies have also demonstrated obesity-related glomerulopathy, which is characterized by glomerulomegaly with thickening of the glomerular basement membrane, mesangial matrix expansion, hyperfiltration-related glomerular filtration barrier injury and ultimately focal glomerulosclerosis [216,366,469]. Furthermore, studies showing ectopic lipid depositions in the kidney have emerged, suggesting a role of fat accumulation in the development and progression of CKD [284,470–472]. Direct intrarenal effects of obesity involve lipid accumulation and impaired fatty acid β-oxidation (FAO) in kidney cells and tissue [295]. Renal proximal tubular cells (PTC) are metabolically very active, requiring a large amount of ATP which is mostly provided through the mitochondrial FAO. In a previous work, we demonstrated a robust accumulation of lipids within enlarged multilamellar inclusions (MLI) into the PTC along with impaired tubular function and increased oxidative stress in obese mice [284]. Yamamoto *et al*. also described the stagnation of the autophagy flux in PTC, associated with the impairment of the lysosomal system. These alterations likely contribute to albuminuria, a progressive decline in renal function and end-stage renal disease. Moreover, evidences of a dysregulation of AMPK activity in podocytes and proximal tubular cells in diabetic and obesity conditions have been demonstrated [473,474]. In addition, pharmacological AMPK activation has been shown to improve pathologic features of the disease [284]. AMPK is a ubiquitous heterotrimeric enzyme that is the master energy sensor in all eukaryotic cells and is abundantly expressed in kidneys [475]. It is a central mediator of energy homeostasis responsive to nutritional and metabolic stresses such as obesity [256]. AMPK also activates autophagy through phosphorylation of ULK-1 in renal cells

[430,435]. Therefore, inhibition of AMPK in kidney tissue is associated with poor outcomes.

Despite considerable efforts in the development of new therapeutic strategies, there is still a lack of effective treatment without strong side effects. Current pharmacotherapies that target food intake regulation have side effects (psychiatric and/or cardiovascular side effects) observed for long periods of use and may be associated to weight regain once the medication is stopped [476]. In addition, even though AMPK has been demonstrated to represent a key target for the treatment of metabolic diseases, indirect AMPK activators such as AICAR has been widely investigated during the last decade by our group an others but did not demonstrate an adequate and efficient therapeutic effects in clinical use [465]. The ongoing development of direct and specific AMPK activators thus represents an important pharmacological challenge [477]. This highlights the urgent need for alternative therapeutic strategies. Recently, the study of the effects of behavioral interventions as exercise training in obesity-related diseases has regained interest. Indeed, targeting key pathways that could mediate beneficial effects by exercise represent a safer alternative therapeutic approach for the treatment of chronic metabolic disorders. Exercise training has been shown to exert beneficial outcomes in managing obesity-associated diseases [478,479]. However, there is still a lack of knowledge about the underlying mechanisms. Moreover, the efficacy of exercise-based therapeutic approach in patients presenting CKD remains controversial, mainly due to the experiment biases of the clinical studies regarding exercise training in obese patients with CKD [480–483].

Here, we evaluated for the first time the potential therapeutic effect of a delayed exercise-based therapy on a treadmill in obesity-induced CKD mice model. We further investigated the regulation of AMPK pathway in response to the treatment.

5.2 Material and methods

5.2.1 Animals and diet

The study was conformed to APS's guiding principles in the Care and Use of Animals and was approved by the Animal Ethics Committee of the University of Mons. Experiments were performed on 8 weeks old C57Bl/6J male mice (Janvier Labs, Le Genest Saint-Isle, France) housed in cages with *ad libitum* access to water and food and were maintained at 35– 40 % relative humidity and a temperature of 20–23 °C in a 12:12 h light–dark cycle. Eight-weeks old male mice were randomized either to a low-fat diet (LFD – 10% of total calories from fat; D12450J, Research Diets, New Brunswick, NJ,

USA) or a high-fat diet (HFD – 60% of total calories from fat; D12492, Research Diets, New Brunswick, NJ, USA). Food intake and body weight were measured weekly during a 20 weeks exposure period. At week 13, LFD and HFD mice were randomized in either two additional groups submitted to an endurance exercise training (EET) for 8 weeks (LFDT and HFDT) or the untrained control groups (LFD and HFD) (*n=10* in each group). Mice fed a high-fat diet for 12 weeks were previously described to present obesity-related metabolic disturbance as well as characteristic features of obesity-induced CKD [294] and were used to evaluate exercise training protocol as a therapeutic strategy.

5.2.2 Exercise training protocol

After 12 weeks of the experimental protocol, trained groups (LFDT and HFDT) were exercised for a total of 8 weeks (5 days a week) as previously described in [484]. Briefly, mice were acclimated to a treadmill (Treadmill Control LE8700, Panlab apparatus®, Barcelona, Spain) at a speed of 3 m/min for 5 min and 9 m/min for 10 min during weeks 13 and 14. At the beginning of week 15, a maximal running velocity test was performed for each trained mice with a gradual speed increase of 1.2 m/min every 2 min until exhaustion (defined as a maximum of four electric stimulations in one minute). Then, the running velocity (Vmax) was set at 70 % of the maximal speed for each mice. As shown in Supplementary materials, the maximal running velocity (Vmax) was similar in both trained groups of mice, LFDT and HFDT respectively, indicating that ET had no impact on exercise performance in obese mice (**Figure S1**). Therefore, mice from LFDT and HFDT were trained with an equivalent running velocity (70% of the Vmax) throughout the EET protocol. The exercise duration started at 10 min/day and was increased by 10 min every weeks. Sedentary mice were not exposed to exercise training and stayed in their cages during exercise sessions.

5.2.3 Sample collection

Mice were euthanized after 20 weeks on diet. Blood sample was collected by intra-cardiac puncture and centrifuged at high speed for 20 min at 4˚C. Plasma was collected and stored at -80˚C until use. Liver, heart, and kidney were collected, weighted, and immediately processed for further analysis. Portions of tissues were snap-frozen in liquid nitrogen for RNA, protein extraction and lipid content quantification. Additional portions of tissues were fixed in Duboscq-Brazil solution for histological analysis.

5.2.4 Urine collection and measurement of urinary markers

At weeks 0, 12 and 20 of the protocol, mice were placed into metabolic cages for 24h-urine collection. A mouse Albuwell ELISA kit and a Creatinine Companion kit (Exocell, Philadelphia, USA) were used to determine the urinary albumin to creatinine level for each mice at the different timepoints. Total proteinuria was quantified using the Bradford binding assay as previously described [485]. As an index of oxidative stress, urine samples were also analyzed for hydrogen peroxide by Amplex red assay (Thermo Fisher Scientific, Waltham, USA) and for 8-hydroxy-2-deoxy Guanosine (8-OH-dG) by competitive ELISA (Gentaur, Kampenhout, Belgium) following the manufacturer's instructions and the data were normalized to the urinary creatinine from each mice.

5.2.5 Glucose tolerance test

After a 12h-overnight fast and 18h after the last exercise session, a glucose tolerance test (GTT) was performed at weeks 0, 12 and 20 of the experimental protocol. A dose of 2 g/kg body weight of D-glucose (Roth, Karlsruhe, Germany) was administered intraperitoneally. Blood samples were then obtained from the caudal vein, and the blood glucose level was measured at 0, 30, 60, and 120 min after glucose injection using a One Touch® Verio® glucometer (Zug, Switzerland).

5.2.6 Biochemical assays

ELISA. Plasma insulin level was determined by ELISA with the Rat/Mouse Insulin ELISA kit (Merck, Darmstadt, Germany). The homeostasis model assessment (HOMA) for insulin resistance index was determined using a calculator available from the Oxford Centre for Diabetes, Endocrinology and Metabolism. Plasma Adiponectin concentration was measured according to the manufacturer's instructions (Adiponectin: MRP300, R&D Systems, Minneapolis, MN, USA). Plasma TNFα concentration was measured according to the manufacturer's instructions (TNF alpha (mouse) ELISA kit; Gentaur, Kampenhout, Belgium).

Plasma lipid levels. Colorimetric enzymatic tests were performed to measure plasma triglycerides (TG) and cholesterol levels (Diasys, Diagnostic System, Holzheim, Germany) and plasma non-esterified fatty acids (NEFA) level (Wako Pure Chemical Industries, Ltd, Japan) following to the manufacturer's instructions.

Kidney and liver lipid levels. 90 mg of frozen kidney or liver tissue were prepared as described in [293]. Briefly, renal tissues were homogenized in a dounce homogenizer (Tenbroeck, Kimble/Kontes Glass Co, Vineland, USA) at 4°C with nitrogen-sparged acid methanol:[0.2N HCl/0.2M NaCl] (4:1 mix) solution. For the first extraction phase, chloroform was added followed by a 30 second vortex to denature and extract proteins. The second extraction phase was performed by adding chloroform/water (2.5:3) to the mix. The samples were centrifuged at 16 000g for 10 min at 4°C to separate the phases. The lower phase (chloroform) containing lipids was used for measurement of total triglycerides and cholesterol (Diasys, Diagnostic System, Holzheim, Germany) according to the manufacturer's instructions. NEFA level was measured in the same phase using a colorimetric enzymatic test according to the manufacturer's instructions (Wako Pure Chemical Industries, Ltd, Japan).

5.2.7 Morphological analysis

Paraffin-embedded kidney sections were stained with Periodic Acid Schiff (PAS), Hemalun, and Luxol fast blue for morphological analysis. Morphometry of kidney sections was carried out as previously reported [120]. The glomerular area, mesangial matrix expansion and nuclei count were determined by randomly analyzing 25 glomeruli in the outer cortex in each kidney section using ImageJ based on [486]. In addition, a semi-quantitative single-blind analysis was performed to evaluate the frequency of vacuolated tubular cells in renal cortex using an additional lens engrave with a square grid inserted in one of microscope eyepieces. For each paraffin section, 10 square fields (0.084 mm^2/field) were analyzed at x400 magnification. In order to evaluate tubule-interstitial fibrosis, paraffin-embedded kidney sections were stained with picrosirius red (collagen I and III deposits). Ten randomly selected area of each kidney section were then analyzed with imageJ to measure the percentage of positive area. Paraffin-embedded liver sections were stained with hematoxylin and eosin and steatosis was graded as described by Ryu *et al.*, 2015 [487].

5.2.8 Immunohistochemistry

Paraffin-embedded kidney sections were dewaxed and rehydrated followed by a microwave pre-treatment in 1 mM EDTA buffer to unmask antigens present in the renal tissue. Endogenous peroxidase activity was removed by incubation with 3% H2O2 for 10 min and blockade with 10% normal goat serum. Sections were incubated with primary antibody against LAMP-1 (Abcam) overnight at 4°C. After rinsing in TBS, slides were exposed for 30 min with SignalStain® Boost IHC Detection Reagent (Cell signaling) and bound peroxidase activity was detected with the DAB kit (DAKO,

Belgium). Counterstaining was performed with hemalun and Luxol fast blue. For each section, 10 square fields (0.084 mm2/field) were observed at x400 magnification in the renal cortex. The randomly selected area of each kidney section were then analyzed with imageJ software. The relative area occupied by the positive staining was expressed as a percentage.

5.2.9 Quantitative real-time PCR.

Snap-frozen kidney tissues were homogenized, and total RNA was then extracted with Trizol (Sigma-Aldrich, Saint-Louis, MO, USA) and treated with DNAse (Promega, Madison, WI, USA). Then, total RNA concentration was measured using NanoDrop (NanoDrop 1000, Thermo Scientific, Waltham, MA, USA) and 2 µg of total RNA were used for reverse transcription using MLV reverse transcriptase (Promega) following manufacturer's instructions. Real-time quantitative PCR was performed in order to quantify mRNA level of *Col I*, *Col III*, *TGFβ*, *MCP-1*, *IL1β*, *TNFα*, *IL6*, *ACC*, *CPT-1*, *FAS* and *18S* as a housekeeping gene (see **Table S1**). Quantitative PCR amplification of a triplicate for each gene was performed using the SYBR Green Master Mix (Roche, Basel, Switzerland). Relative gene expressions were calculated using the $2^{-\Delta\Delta CT}$ method.

5.2.10 Western Blot analysis

Frozen kidney tissues were homogenized in Cell Lysis Buffer (Cell Signaling, Danvers, MA, USA) with phosphatase and protease inhibitor cocktail (Thermo Fisher Scientific, Waltham, MA, USA) at 4°C. Samples were subsequently centrifuged at 14 000g for 15 min at 4°C and supernatants were collected. Protein concentrations were quantified by Pierce BCA assay kit (Thermo Fisher). Next 40µg of total lysate were separated on Tris-Glycine 12% or Tris-acetate 3-8% (for high-molecular weight proteins) gels and transferred onto nitrocellulose membranes. The relative amounts of LMW, MMW and HMW Admer in plasma were determined using a non-denaturing PAGE-SDS as described in [484]. Membranes were blocked with 5% BSA for 1 h and primary antibodies against: phospho-ACC and ACC (Cell Signaling), phosphor-LKB1 and LKBA (Cell Signaling) phospho-AMPK and AMPK (Cell Signaling), CPT-1 (Abcam), Adiponectin (Abcam), Beclin-1 (Cell Signaling), p62 (Cell Signaling), phospho-ULK1 (Ser555) and ULK1 (Cell Signaling) and β-actin (Thermo Fisher) were applied in 5% BSA overnight at 4°C. Finally, membranes were incubated with secondary antibodies (Li-Cor Biosciences, Lincoln, NE, USA) in 1% BSA for 1h. Proteins were visualized using the Odyssey Infrared Imager (Li-Cor Biosciences). The fluorescence was quantified using the imaging software Odyssey V3.0 from the Odyssey Infrared Imager (Li-Cor Biosciences).

5.2.11 Statistical analysis

Results are presented as mean values ± SEM. The level for statistical significance was defined as $p < 0.05$. Analyses were carried out using Prism GraphPad Software version 6 (San Diego, CA, USA). Differences between data groups were evaluated for significance using independent *t-test* of data, one-way or two-way ANOVA and Newman–Keuls *post hoc* tests for multiple comparisons.

5.3 Results

5.3.1 Delayed endurance exercise training limits calorie intake and prevents body and tissue weight gain in HFD mice.

The body weight and the calorie intake along the protocol as well as tissue weights at week 20 were measured in mice fed a LFD or a HFD. The associated effects of a delayed EET treatment on these parameters were also determined. As observed in **Figure 1B**, a significant increase in body weight was observed from week 5 in HFD groups compared to LFD groups. This increase was maintained throughout the experimental protocol in HFD-fed mice compared with LFD-fed mice. This increase was observed along with a higher calorie intake in HFD mice that was significantly increased since the first week of the protocol, compared to LFD (**Figure 1D**). After the beginning of EET protocol (week 12), HFDT mice showed a stabilization of the body weight. The BW of HFDT mice was significantly lower as soon as 2 weeks of EET compared to untrained HFD mice (**Figure 1B**). The **Figure 1C** presents the percentage of body weight gain in HFD and HFDT from the beginning of EET. The linear regression analysis demonstrated that the slope of HFD was highly significant ($p<0.0001$) but not in HFDT ($p=0.2397$) compared with zero. This results were associated to a decrease in calorie intake at week 20 in HFDT mice compared to HFD (**Figure 1D**). The **Figure 1E** presents the changes in kidney, liver and heart weights of mice fed a LFD or a HFD with or without EET at the end of the protocol. As shown, the weights of kidneys and heart were higher in mice fed a HFD compared to mice fed a LFD but not in HFDT mice. Interestingly, the important hypertrophy of the liver observed in mice fed a HFD was significantly prevented by the EET.

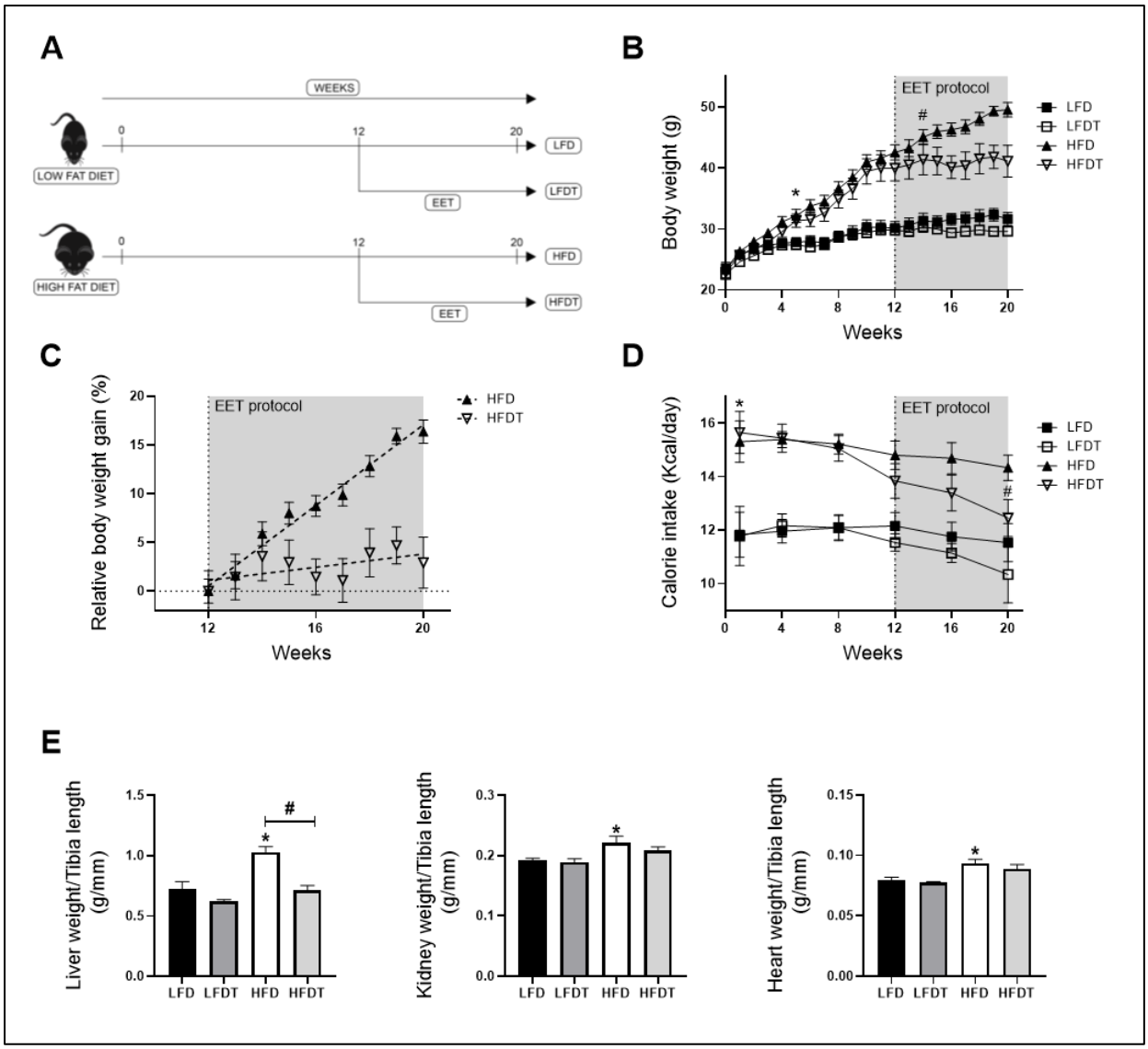

Figure 1. Delayed EET prevents body weight gain and organ hypertrophy induced by HFD in mice. A. Schematic representation of experimental design. Obesity in mice was induced with 12 weeks on high-fat diet (HFD). Control mice were fed with a low-fat diet (LFD). Mice were subsequently divided in sedentary or trained groups on a treadmill for 8 additional weeks (LFD, LFDT, HFD, HFDT). **B.** Body weight evolution throughout the experimental protocol (20 weeks). Statistical analyses were performed by two-way ANOVA followed by Newman–Keuls *post hoc* test. **C.** Relative body weight gain in HFD vs HFDT mice during EET protocol normalized with body weight at week 12. The slope was determined with simple linear regression analysis. n=10 in each group. **D.** Calorie intake evolution throughout the experimental protocol. Number of calories consumed per day calculated for each mouse at different time-point (at week 1, 4, 8, 12, 16 and 20 of the experimental protocol). Statistical analyses were performed by two-way ANOVA followed by Newman–Keuls *post hoc* test. **E.** Organ weights at week 20. Statistical analyses were performed by one-way ANOVA followed by Newman–Keuls *post hoc* test. Data are presented as means ± SEM.* $P \leq 0.05$ *versus* LFD $^{\#}$ $P \leq 0.05$ *versus* HFD. *n=10* in each group.

5.3.2 Delayed EET improves obesity-related metabolic disorders in HFD mice.

HFD feeding in mice is known to induce glucose intolerance, insulin resistance, dyslipidemia and hepatic steatosis. We further characterized the effects of EET on obesity-related disorders in HFD mice. To determine the impact of delayed EET on glucose tolerance, glucose tolerance tests (GTT's) were performed at week 0, before EET (12 weeks) (**Figure S2**) and at the end of the experimental protocol (20 weeks) (**figure 2A**). At week 20, the AUC for HFD fed mice was significantly higher than for LFD groups. However, an improvement of glucose tolerance by EET was demonstrated, as observed by the significant decrease of AUC in HFDT mice compared to the HFD mice (**Figure 2A**). Consistently, these changes were associated to a significantly higher level of plasma insulin in HFD mice that was decreased by EET in HFDT (**Figure 2B**). Insulin resistance in HFD mice was confirmed by the calculation of the HOMA-IR index (**Figure 2C**). Serum levels of adiponectin also correlates with insulin sensitivity in obesity and diabetes [488]. Despite we have not found any changes in the total plasma adiponectin levels in the experimental groups, we evaluated the S_A index (defined as the HMW/(HMW + LMW) ratio of adiponectin multimers in plasma) that was reported as a more relevant indicator of insulin sensitivity [489]. The results demonstrated a reduction of the S_A index in HFD mice (**Figure S3**) indicating an decreased HMW forms in favour of the LMW multimers as demonstrated by Pierard et al., 2016 [484]. This change was particularly reversed following exercise in HFD mice. The plasma levels of cholesterol, triglycerides and NEFA were also measured after EET treatment (**Figure 2D**). As illustrated, HFD induced a significant elevation of plasma NEFA and cholesterol levels, whereas these increases were counteracted by EET in HFDT mice. Interestingly, there was no change in TG level. Dyslipidaemia commonly leads to hepatic steatosis in HFD mice and is associated to the metabolic syndrome consequences. Thus, the liver steatosis score and TG content within the liver tissue were evaluated as a marker of non-adipose tissue ectopic lipid accumulation. As illustrated in **Figure 2E**, histopathologic analyses of liver from HFD mice showed the presence of macrovesicular steatosis (large fat droplets), compared with the LFD groups. This was correlated with the steatosis score evaluation (**Figure 2E**). In contrast, hepatic steatosis was drastically reduced by EET in HFDT mice. Similarly, hepatic TG accumulation in HFD mice was prevented by the EET .The results thus indicate that a delayed EET protocol applied on obese mice induces a substantial improvement of the metabolic syndrome features and obesity-related disorders. Lastly, we recorded blood pressure during the last week of the protocol. We measured the systolic, diastolic, and mean blood pressure. As shown in **Table S2**, no significant difference was observed in the different experimental groups for each of these measurements.

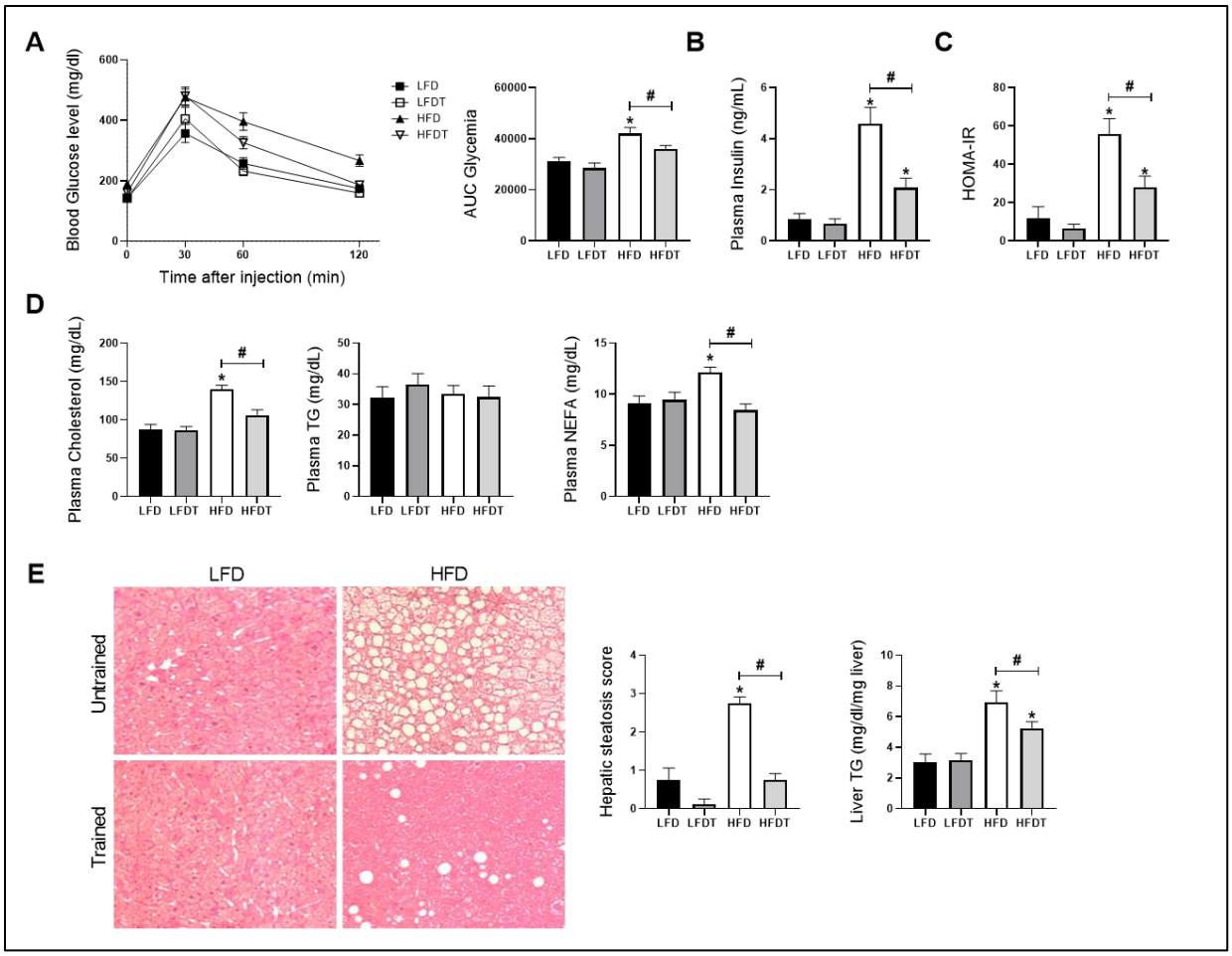

Figure 2. Delayed EET improves obesity-induced metabolic disorders and hepatic steatosis in HFD mice. A. Glucose tolerance test at week 20. Fasted mice were submitted to an intraperitoneal injection of glucose (2 g/ kg b.w.). Glycemia was measured before (0) and 30, 60 and 120 min after injection. Histogram represents the area under the curve (AUC) of glycemia from 0 to 120 min. **B.** Plasma insulin level at week 20. **C.** HOMA-IR index calculation. **D.** Plasma levels of cholesterol, triglycerides (TG) and non-esterified fatty acids (NEFA) at week 20. **E.** Representative photomicrograph (original magnification ×400) of H&E staining illustrating hepatic steatosis from liver sections from mice on LFD, LFDT, HFD and HFDT at week 20 of the experimental protocol, steatosis scoring by semi-quantitative analyses of lipid accumulation and quantitative analysis of triglycerides (TG) in the liver tissue. Statistical analyses were performed by one-way ANOVA followed by Newman- Keuls *post hoc* test. Data are presented as means ± SEM. * $P \leq 0.05$ versus LFD $^{\#}$ $P \leq 0.05$ versus HFD. *n=10* in each group. .

5.3.3 Delayed EET improves obesity-related glomerulopathy and renal function.

In order to characterize the effects of delayed EET protocol on the pathogenesis of obesity-induced chronic kidney disease, we first evaluated glomerular impairments and renal function. The morphological analysis of glomeruli revealed that mice fed a HFD without EET developed a significant increase of glomerular area along with a dense Periodic-Acid-Schiff (PAS)-positive matrix in the mesangium as well as an increase in nuclei number (**Figure 3A-D)**. This glomerular expansion was prevented by EET in HFD mice. To further determine the effect of a delayed EET on renal function in obese mice, urinary albumin to creatinine ratio (UACR) and total proteinuria were investigated (**Figure 3E**). After 12 weeks on diet (before EET), both groups of HFD-fed mice presented a significant higher UACR compared to the groups of LFD-fed mice. In contrast, at week 20 (after EET intervention), the UACR in HFDT mice was significantly lower than in HFD mice, demonstrating a decreased albuminuria . The same patterns were found for urinary protein level (**Figure 3F**). Indeed, mice fed a HFD presented a significant increase in total proteinuria while this increase was prevented by with EET. These results demonstrate that EET protocol is beneficial to counteract the progression of obesity-related glomerulopathy and associated renal dysfunction in obese mice.

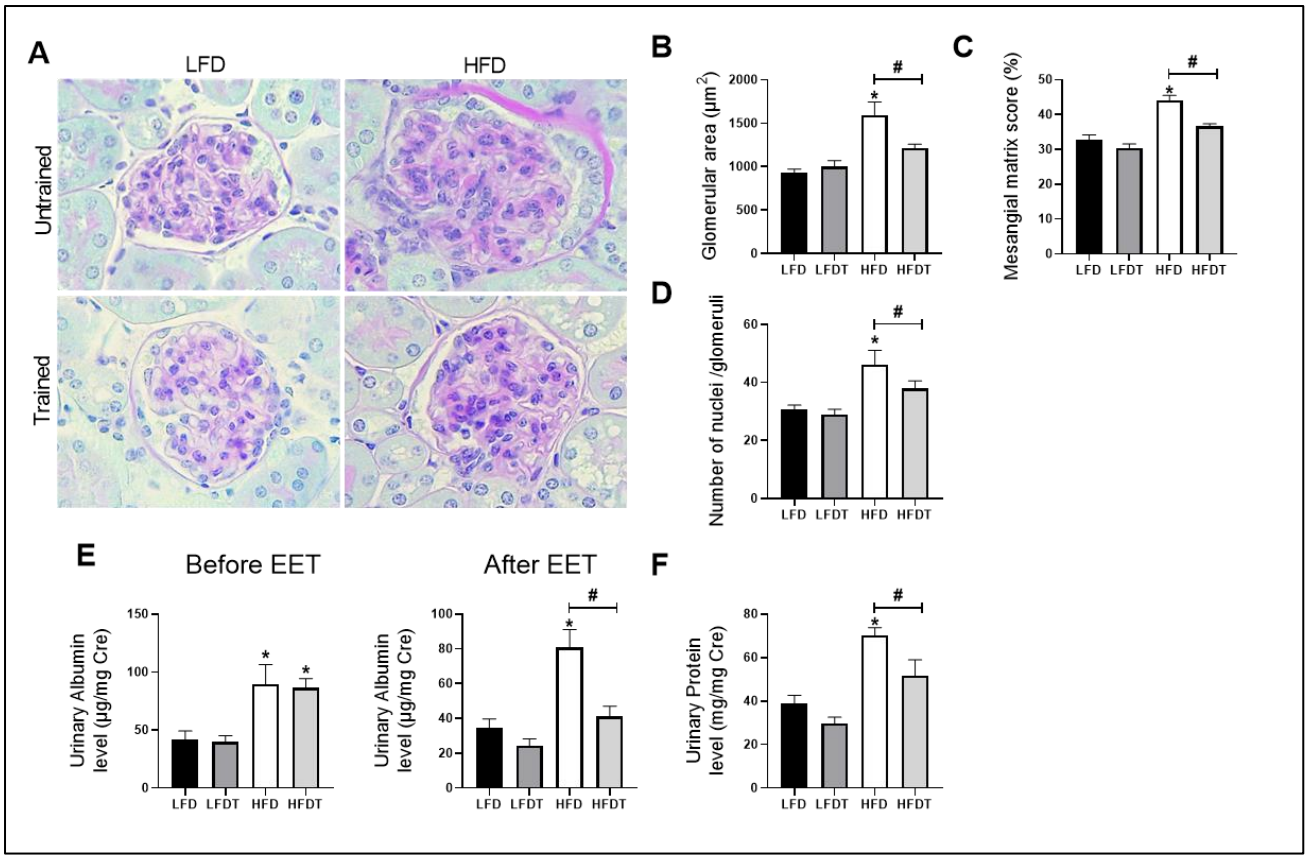

Figure 3. Effects of a delayed EET on renal function and glomerular histology in mice on LFD or HFD. **A**. Representative photomicrographs (original magnification × 400) of PAS staining illustrating glomerular structure from renal cortex sections from mice on LFD, LFDT, HFD and HFDT. **B**. Glomerular area. The glomerular tuft area was averaged from 15 glomeruli per kidney section, using one kidney section per animal. **C**. Mesangial matrix area percentage of total glomerular area. **D**. Nuclei count. **E**. Quantitative measurement of urinary albumin to creatinine ratio (UACR) at week 12 (before EET protocol) and at week 20 (after EET protocol) from mice on LFD, LFDT, HFD and HFDT. **F.** Quantitative analysis of urinary total protein to creatinine ratio at week 20. Statistical analyses were performed by one-way ANOVA followed by Newman–Keuls *post hoc* test. * $P \leq 0.05$ *versus* LFD $^{\#}$ $P \leq 0.05$ *versus* HFD. Data are presented as means ± SEM. *n=10* in each group.

5.3.4 Delayed EET ameliorates renal fibrosis, inflammation and oxidative stress.

Obesity-induced chronic kidney disease is also characterized by an increased tubulo-interstitial fibrosis, inflammation and oxidative stress in HFD mice. To decipher the impact of EET on these key characteristics of the pathological progression, collagen I and III depositions were studied by morphometric analysis in Sirius red-stained renal sections as an index of the fibrotic response. As illustrated in **Figure 4A,** collagen accumulated in the interstitium of HFD mice. This observation was confirmed by the quantitative analysis of Sirius Red positive staining (**Figure 4B**). EET treatment significantly reduced collagen I and III deposition. Candidate genes expression involved in renal fibrosis (TGF-β1, collagen type 1 and III) and inflammation (TNFα, IL-1β, IL-6 and MCP-1) were also measured by real-time qPCR. As observed in **Figure 4E**, renal mRNA levels of the pro-fibrotic markers were all significantly decreased with EET in mice fed a HFD as well as for the pro-inflammatory markers in HFD mice. These changes were prevented by EET. The plasma TNFα concentration for systemic inflammation was also evaluated and the data reported an increased concentration of this pro-inflammatory cytokine in HFD mice that was significantly reduced with exercise. As markers of oxidative stress, the urinary hydrogen peroxide and 8-hydroxy-2'-deoxyguanosine (8-OHdG) levels were measured at week 20. These markers were both significantly higher in HFD mice compared to LFD mice (**Figure 4C,D**). The increase in urine hydrogen peroxide and 8-OHdG were also prevented by EET. The results demonstrate that EET reduces renal injuries by decreasing oxidative stress, fibrosis and inflammation in obese mice.

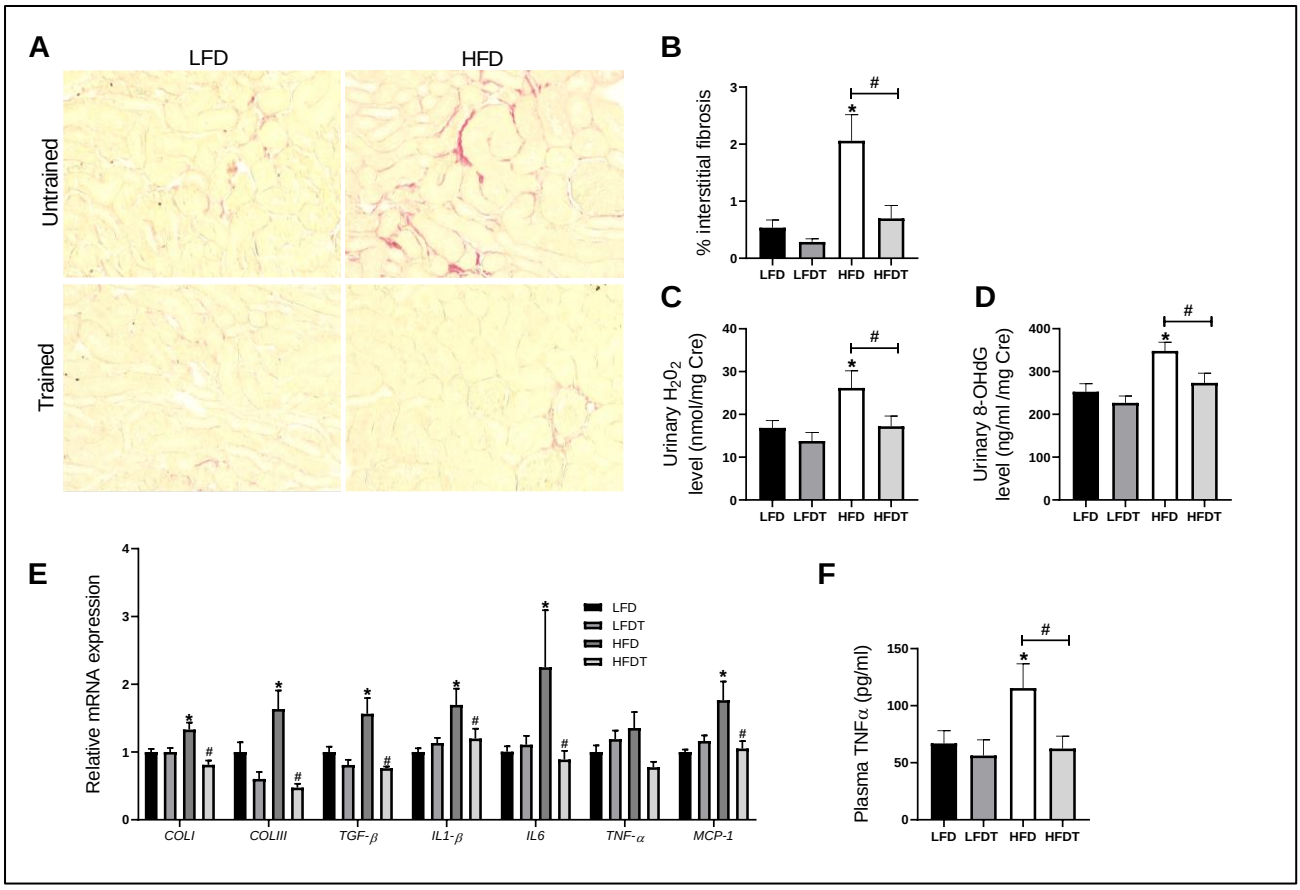

Figure 4. Effects of delayed EET on tubulointerstitial fibrosis, oxidative stress and inflammation from mice on LFD or HFD. A. Representative photomicrographs (original magnification ×400) of Sirius Red staining illustrating tubulointerstitial fibrosis in renal cortex. *n=10* in each group. **B.** Quantitative analysis of the mean percentage of positive staining for Sirius red staining. *n=10* in each group. **C.** Quantitative analysis of urinary H_2O_2 to creatinine ratio at week 20. *n=10* in each group. **D**. Quantitative analysis of urinary 8-OHdG to creatinine ratio at week 20. *n=10* in each group. **E.** Real-time quantitative qPCR for type I collagen (COLI), type III collagen (COLIII), transforming growth factor β (TGFβ), interleukin 1β (IL1β), tumor necrosis factor α (TNFα), interleukin 6 (IL6) and monocyte chemoattractant protein 1 (MCP1). mRNA expressions were performed on kidney tissue from LFD, LFDT, HFD and HFDT mice normalized against 18S. *n=6* in each group. **F**. TNFα plasmatic level. The TNFαconcentration was measured using indirect ELISA. *n=8* in each group Statistical analyses were performed by one-way ANOVA followed by Newman–Keuls *post hoc* test. * $P \leq 0.05$ *versus* LFD $^{\#}P \leq 0.05$ *versus* HFD. Data are presented as mean ± SEM. *n=10* in each group.

5.3.5 Delayed EET reduces renal ectopic lipid accumulations.

The ectopic lipid deposition in the kidney is a key feature of obesity-induced chronic kidney disease which is associated to renal lipotoxicity. We further characterized the effect of delayed EET on tubular lipid accumulation in mice fed a LFD or HFD. As described before by Declèves *et al*. (2014), vacuolated tubular cells were observed in HFD groups (**Figure 5A**; black arrows). These tubular alterations in proximal tubules were specifically found in the renal cortex. The quantitative analysis revealed that mice fed a HFD showed a strong increase in vacuolated tubules that was significantly reduced with EET (**Figure 5B**). Moreover, as illustrated in **Figure 5C**, cholesterol, TG and NEFA renal tissue content were also measured at week 20. Data demonstrated a significant increase in TG in HFD group that was prevented by EET. While there was no change in cholesterol content, the level of NEFA was decreased with EET in both the LFDT and the HFDT groups. Thus, EET treatment is associated to a reduced lipid accumulation in the renal tissue in obese mice.

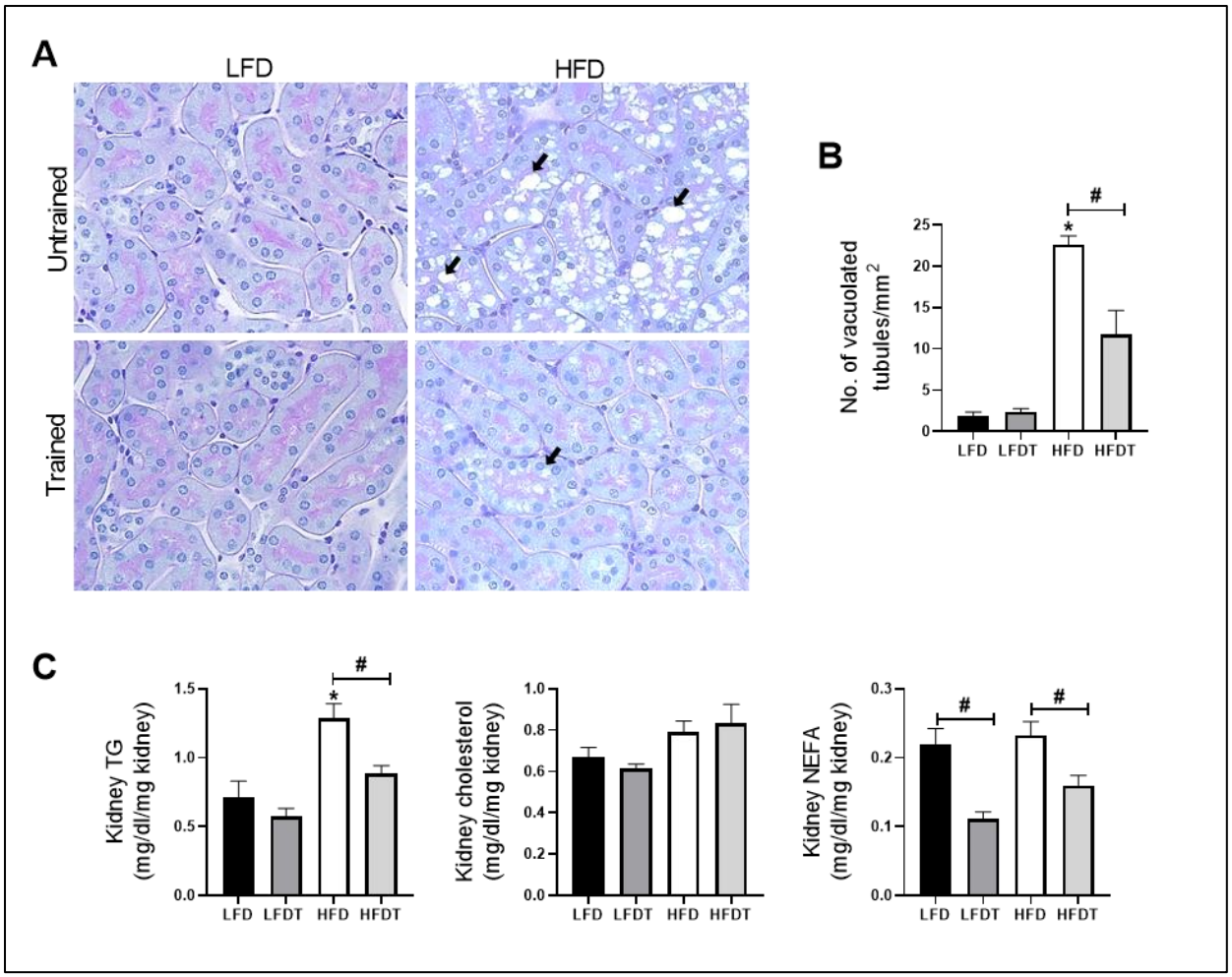

Figure 5. Delayed EET reduces ectopic lipid accumulation in renal tissue induced by HFD in mice. **A.** Representative photomicrographs (original magnification ×400) of PAS staining illustrating vacuolated proximal convoluted tubular cells from renal cortex sections from mice on LFD, LFDT, HFD and HFDT at week 20. **B**. Quantitative analysis of number of vacuolated tubules per mm^2. **C.** Quantitative analysis of cholesterol, triglycerides (TG) and non-esterified fatty acids (NEFA) in renal tissue. Statistical analyses were performed by one-way ANOVA followed by Newman–Keuls *post hoc* test. * $P \leq 0.05$ *versus* LFD $^{\#}$ $P \leq 0.05$ *versus* HFD. Data are presented as means ± SEM. *n=10* in each group.

5.3.6 Delayed EET enhances AMPK activity in renal tissue of obese mice.

AMPK pathway dysregulation plays an important role in obesity-associated renal cell dysfunction. To better characterize the effect of a delayed EET on AMPK activity in obese mice, phosphorylation of AMPK and its main downstream target, the acetyl-CoA carboxylase (ACC) as well as the main AMPK upstream kinase the liver kinase B1 (LKB1) were measured by Western blot (**Figure 6**). As illustrated in **Figure 6B**, p-LKB1 protein level wad significantly decreased in HFD mice compared to the control that was prevented by exercise. Moreover, total LKB1 protein level did not change between experimental groups while p-LKB1 to LKB1 ratio was increased in HFDT mice compared to sedentary HFD. Mice fed a HFD exhibited a significant decrease in p-AMPK protein level, whereas EET treatment prevented this reduction. Total AMPK protein level was similar in each group while AMPK activity (p-AMPK to AMPK ratio) was increased in HFDT mice (**Figure 6C**). Since AMPK inhibits fatty acid synthesis and promotes fatty acid oxidation by phosphorylation of ACC, p-ACC and ACC protein level were also determined (**Figure 6D**). Consistently, protein level of phospho-ACC was reduced along with the decreased of AMPK activity in HFD group and was significantly increased with EET. Interestingly, total ACC protein level was decreased in both HFD and HFDT groups, participating in the significant increase of the p-ACC to ACC ratio in HFDT compared to LFD. We also investigated the protein level of CPT-1 but its expression was not regulated by HFD or EET (**Figure 6E**). Furthermore, the lipolysis and lipogenic markers mRNA expression were not affected by any treatment (**Table S3**).

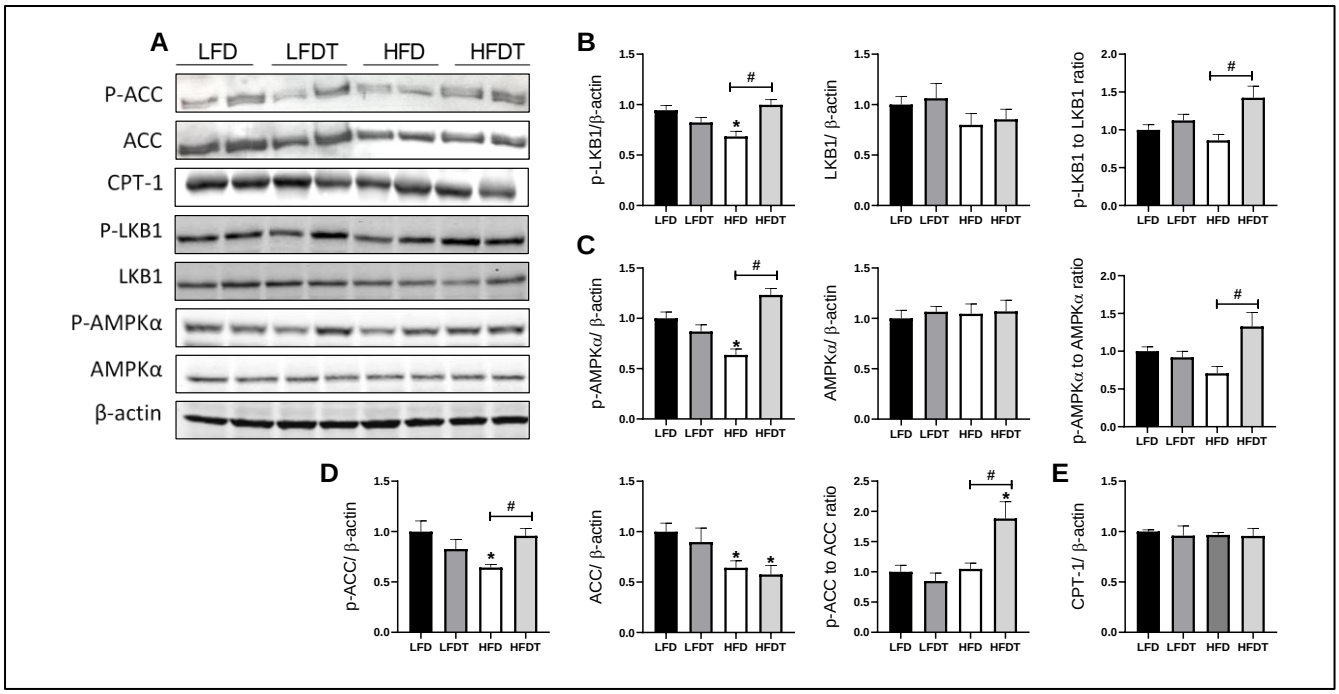

Figure 6. Delayed EET restores AMPK activity in the kidney of HFD mice. A. Western Blot analysis of phosphor-LKB1, LKB1, phospho-AMPK, AMPK, phospho-ACC, ACC and CPT-1 in kidney tissue from mice on LFD, LFDT, HFD and HFDT at week 20. **B**. Relative densitometry of the immunoblots representing respectively phospho-LKB1 protein level normalized with β-actin, LKB1 protein level normalized with β-actin and phospho-LKB1 to LKB1 ratio. **C**. Relative densitometry of the immunoblots representing respectively phospho-AMPK protein level normalized with β-actin, AMPK protein level normalized with β-actin and phospho-AMPK to AMPK ratio. **D.** Relative densitometry of the immunoblots representing respectively phospho-ACC protein level normalized with β-actin, ACC protein level normalized with β-actin and phospho-ACC to ACC ratio. **E.** Relative densitometry of the immunoblots representing CPT-1 protein level normalized with β-actin. Statistical analyses were performed by one-way ANOVA followed by Newman–Keuls *post hoc* test. Data are presented as means ± SEM. * $P \leq 0.05$ *versus* LFD # $P \leq 0.05$ *versus* HFD. *n=6-8* in each group.

5.3.7 Delayed EET improves autophagy flux in obese mice by AMPK-mediated ULK1 activation.

Cellular lipid accumulation and decreased AMPK activity were also associated to an impairment of the autophagy flux. Under physiological conditions, intracellular lipid storages are regulated by autophagy process that plays a major role to prevent the deleterious effects of a lipid overload on cellular function. AMPK regulates autophagy by phosphorylating ULK-1 that mediates the initiation of autophagy. Thus, we first evaluated p-ULK1 (Ser 555) protein level in response to HFD and EET treatment. Consistently, p-ULK1 was found to be decreased in HFD mice while EET increased p-ULK1 in HFDT compared to HFD (**Figure 7B**). This result was corroborated with the evaluation of the autophagy marker Beclin-1, p62 for autophagy flux and LAMP-1, a specific marker of lysosomes. Indeed, western blot analyses revealed that mice fed a HFD exhibited a significant increase in p62 protein level but not with EET (**Figure 7C**). p62 is a substrate of autophagy that is degraded during this cellular process. An accumulation of p62 in HFD mice revealed a stagnant autophagy process that is normalized by EET in obese mice. Beclin-1 acts during the initiation stage of autophagy by mediating the formation of double-membrane structure that envelops cytoplasmic material to form the autophagosome. The protein level of Beclin-1 was significantly reduced in HFD and was shown to be restored by EET treatment (**Figure 7D**). Lastly, we demonstrated by immunohistochemistry an increased positive staining for LAMP-1 in the margins of the lipid vacuoles in proximal tubules that was significantly reduced by EET in HFDT group (**Figure 7 E**). These data indicate that EET enhances autophagy flux in renal tissue of obese mice possibly by AMPK-mediated phosphorylation of ULK1, ameliorating the progression of obesity-induced CKD.

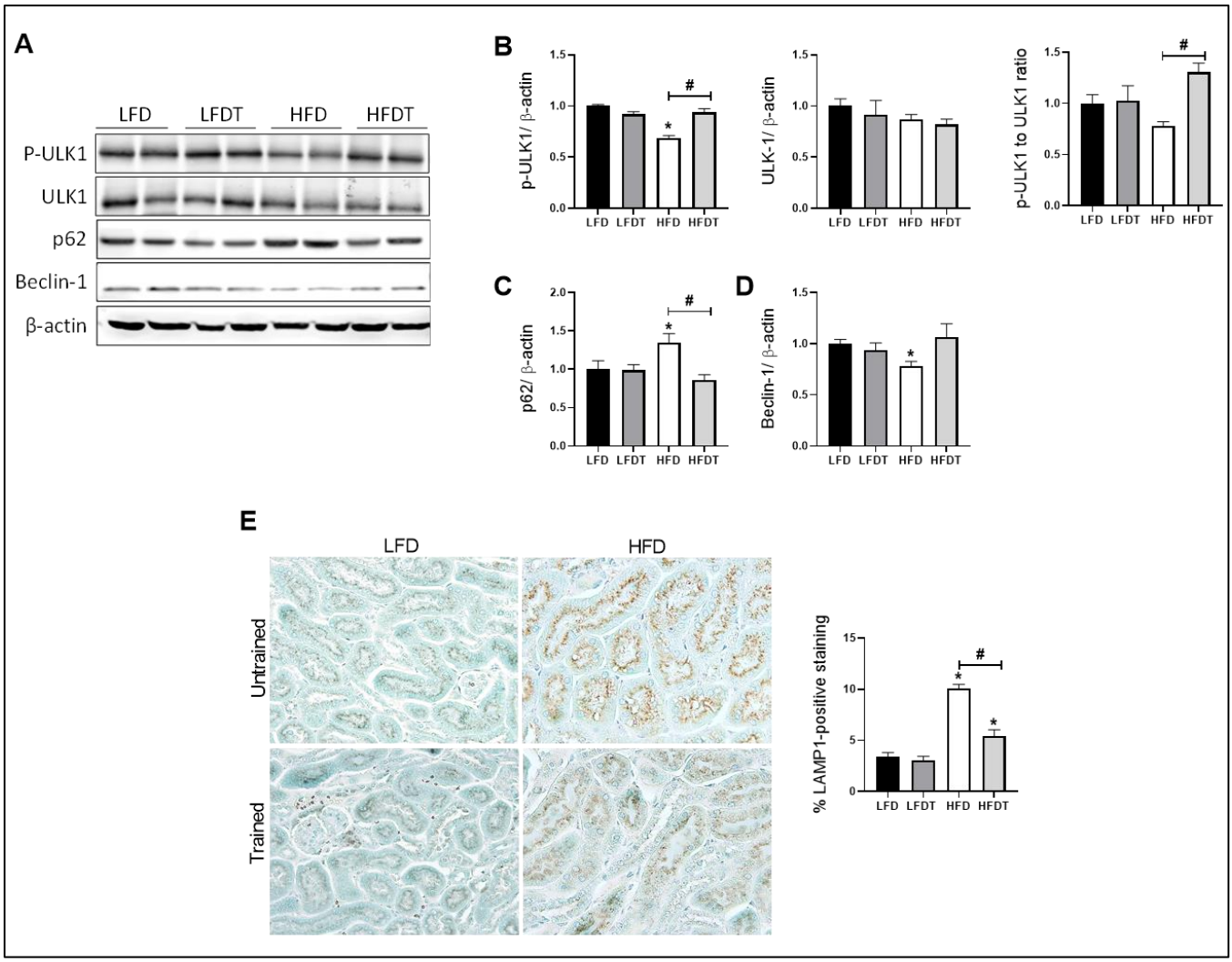

Figure 7. Effects of a delayed EET on autophagy and lysosomal markers in the kidney from mice on LFD or HFD. A. Western Blot analysis of phospho-ULK-1 (Ser 555), ULK-1, p62 and Beclin-1 in kidney tissue from mice LFD, LFDT, HFD and HFDT. **B**. Relative densitometry of the immunoblots representing respectively phosphor-ULK1 (Ser 555) protein level normalized with β-actin, ULK-1 protein level normalized with β-actin and Phospho-ULK1 (Ser 555) to ULK-1 ratio. **C.** Relative densitometry of the immunoblots representing p62 protein level normalized with β-actin. **D**. Relative densitometry of the immunoblots representing Beclin-1 protein level normalized with β-actin. **E.** Representative photomicrograph (original magnification ×400) showing lysosomal-associated membrane protein 1 (LAMP1)–positive staining on intracellular vacuoles and related quantitative analysis of LAMP1-positive staining**.** Statistical analyses were performed by one-way ANOVA followed by Newman–Keuls post hoc test. Data are presented as means ± SEM. * $P \leq 0.05$ versus LFD # $P \leq 0.05$ versus HFD. *n=6-8* in each group.

5.4 Discussion

Endurance exercise training (EET) is now considered as an interesting therapeutic strategy for managing obesity-related disorders. Emerging studies have demonstrated that EET is an effective strategy to prevent insulin resistance, hepatic steatosis and cardiovascular diseases [490,491]. The expected impact of exercise training treatment in obese patients is in reducing or maintaining body weight. Interestingly, EET has been shown to present beneficial effects without weight loss, suggesting independent effects of EET on obesity-related disorders [492,493]. Particularly, a redistribution of body fat along with a reduced ectopic lipid accumulation and a reduction of inflammation in tissues have been revealed with exercise [494]. Despite evidence that exercise training may improve obesity related disorders, there is still a lack of knowledge about the underlying cellular and molecular mechanisms. Moreover, in the most experimental studies in obese rodents, animals were concomitantly exposed to EET and HFD, employing therefore EET in a prevention setting and not as a treatment.

In contrast, here, the potential beneficial impact of EET was investigated as a therapeutic strategy on obese mice. Indeed, mice were fed a HFD for 12 weeks to achieve a significant level of metabolic and biochemical changes associated to obesity including fat mass accumulation, glucose intolerance, insulin resistance, hepatic steatosis, ectopic lipid accumulations and associated chronic kidney disease (CKD) [474,495,496]. Thereafter, EET was applied for 8 additional weeks. After 20 weeks on diet, mice exposed to HFD presented the hallmarks of obesity-related disorders including insulin resistance, glucose intolerance and hyperlipidemia (NEFA and cholesterol). Hepatic steatosis also appeared in HFD mice as demonstrated with histological analysis and TG quantification. Several studies have already demonstrated that exercise training prevented obesity-associated disorders, including diabetes and hepatic steatosis [497–499]. Interestingly, in our model, delayed EET treatment in HFD mice also improved most of the metabolic changes. First, insulin resistance that was demonstrated in the HFD mice was reversed by EET along with the improvement of glucose metabolism in HFD trained mice, as supported by HOMA-IR calculation and GTTs. The decreased insulinemia could be attributed to a lower secretion of insulin required to maintain glucose level, suggesting a better insulin sensitivity. The exercise-induced changes in insulin sensitivity have been already extensively reported [500]. During exercise, glucose uptake is stimulated by skeletal muscle contraction. This occurs as a result of GLUT4 translocation to the muscle cell membrane [500]. Moreover, chronic exercise enhances insulin sensitivity largely due to activation of AMPK, a master regulator of glucose metabolism in the muscle [501]. The effects of exercise training on insulin resistance were also confirmed by the evaluation of adiponectin multimers distribution.

As demonstrated by the S_A index, exercise training was associated to amelioration of the multimers distribution in favor of the HMW forms that are the most biologically active forms of adiponectin regarding glucose homeostasis [502]. EET also reduced dyslipidemia and drastically decreased intra-hepatic fat contents, consequently reversing HFD-related hepatic steatosis. During exercise, skeletal muscle contraction induces production of variety of molecules called myokines that mediate beneficial responses in other organs. Experimental studies suggest that both IL-6 and Irisin might be involved in muscle/liver crosstalk mediating improvement of hepatic steatosis. In the liver, EET induces AMPK activity with an enhanced mitochondrial function which lead to a decreased lipogenesis and an increased lipid oxidation. Hepatic AMPK activation also promotes autophagy induction *via* phosphorylation of ULK-1. As a result, excess lipids are eliminated by lysosomes leading to decreased ectopic lipid accumulations in the liver [503–505]. Furthermore, high blood pressure is another important component of the metabolic syndrome and exercise training is a recognized strategy for the prevention and treatment of hypertension [506,507]. However, in Bruder-Nascimento *et al*., mice fed a HFD for 24 weeks did not present any change in arterial blood pressure [508]. Similarly, we did not observed in our experimental model any significant difference of the systolic, diastolic or mean arterial blood pressure between LFD and HFD groups neither between trained and untrained groups suggesting that EET has no effect on blood pressure in our experimental conditions.

Even though EET mediates improvement in key features of obesity in humans and animal models, its effects on renal function and metabolism in obesity are not well reported so far. In the general population, obesity is the second most highly prognostic factor to predict end-stage renal disease. However, the underlying mechanisms are complex and include physiological and metabolic aspects. Adiposity could directly impact the kidneys *via* the pro-inflammatory environment mediated by adipokines produced by adipose tissue but also oxidative stress, activation of the renin-angiotensin-aldosterone system and IR [468]. These changes lead to characteristic features of obesity-induced kidney injury including the development of glomerulomegaly and ectopic lipid accumulation in the kidney, leading to the renal lipotoxicity. Exercise training has been proposed to be included in renal care at any step of CKD progression [509]. A recent study has even showed that concomitant cafeteria diet exposure and EET prevented lipid depositions in the kidney in mice [510]. To further explore the adaptation of a “fatty kidney” to EET, we evaluated the effect of an EET protocol to a HFD-induced CKD mice model. We demonstrated that EET treatment improved key parameters of obesity-induced CKD, as evidenced by improvement of renal function as well as morphological alterations. Notably, increased proteinuria and albuminuria which reflect

both glomerular and tubular impairments are established predictors of CKD progression [511]. Here, we demonstrated that EET reduced glomerular impairment by reducing mesangial matrix expansion and thus glomerulomegaly. At a tubular level, ectopic lipid depositions in the kidney were markedly decreased, leading to better outcomes regarding CKD progression. Consistently, we demonstrated that EET was associated to reduced interstitial fibrosis, renal inflammation and oxidative stress.

Accumulating studies have demonstrated reduction of AMPK activity in caloric excess conditions [341,512]. Activity of AMPK was reduced in kidneys of diabetic mice and humans [279]. In several studies, pharmacological AMPK activators (5-aminoimidazole-4-carboxamide ribonucleoside, Metformin, Resveratrol, Fenofibrate and AdipoRon) attenuated diabetic nephropathy and obesity-induced CKD [262,293,513–515]. Consistent with the previous studies, our results showed a decrease in AMPK activity in kidney tissue following HFD as well as the decreased phosphorylation of its main target ACC as well as its main upstream kinase LKB1, indicating inhibition of the AMPK pathway. Interestingly, we demonstrated that EET restored the activity of AMPK in obese mice, suggesting a critical role of AMPK regulation in the beneficial effects of EET in obesity-induced CKD. AMPK plays essential roles in glucose and lipid metabolism, cell survival, growth, and inflammation. AMPK also exerts a key role in mitochondria homeostasis and has been revealed to regulate autophagy in mammalian cells. Obesity induces AMPK dysregulation by multiple mechanisms independently of the AMP:ATP ratio (reviewed in [516]) including insulin resistance, inflammation, decreased adiponectin, oxidative stress and decreased activity of AMPK upstream kinase. Here, we particularly highlighted the beneficial effects of exercise training on these parameters that may reduce the detrimental intra-renal environment leading to AMPK dysregulation in favor of a proper AMPK signaling. Under physiological conditions, autophagy is critical for the maintenance of renal function and homeostasis [517]. Autophagy is a complex and highly regulated cellular degradation pathway, well conserved among eukaryotes that has been intensely documented in many pathological conditions [427]. Both obesity and HFD negatively regulates autophagy in the kidney [518]. In a setting of renal lipid overload, Yamamoto *et al*. (2016) and our work have demonstrated the impairment of autophagy in proximal tubular cells (PTC) [286,293]. Here, we also highlighted a beneficial role of EET associated with activation of AMPK in preventing impairment of autophagy in PTC and lipid accumulation in these cells. Chronic EET was shown to induce autophagy *in vivo* in various tissues including muscles, liver, adipose tissue and pancreas [519]. In this study, we investigated whether EET treatment could lead to a restored autophagy flux in renal tissue in an obesity context. We demonstrated that EET

regulated autophagy markers by decreasing p62 in obese trained mice and increasing Beclin-1 protein level. Activation of the autophagic flux leads to a decline in p62 level because of its degradation during the process and, contrarily, an accumulation of p62 reflects a stagnant autophagic flux [520]. Moreover, HFD also inhibits autophagy by reducing autophagosome/lysosome fusion [286]. Here, we described an increased lysosomal marker LAMP-1 that was reduced by EET in renal tissue of obese mice. Finally, we demonstrated the AMPK-mediated phosphorylation of ULK-1, an autophagy inducer, by EET in HFD mice. Thus, our data confirmed disturbance of autophagy by HFD and indicated the potential induction of autophagy process by EET *via* AMPK activation, leading to improvement of renal cell homeostasis. Since autophagy is a highly dynamic process, further investigations are needed to delineate the precise molecular mechanisms of exercise-induced autophagy in the kidney and the particular role of AMPK in this process. Particularly, the use of ULK-1 knockout mice would be an interesting mechanistical strategy in order to confirm the role of AMPK-dependent autophagy in response to exercise in renal tissue. Finally, how skeletal muscle communication can prevent or suppress kidney injury is particularly emerging and has not been strongly investigated yet, particularly regarding muscle-kidney cross-talk during exercise. A recent work has nicely demonstrated that the Irisin, an exerkine, ameliorated tubule cell damage and renal fibrosis in CKD model [521]. Interestingly, inhibition of AMPK by a specific inhibitor reduced the effects of Irisin in myocytes and hepatocytes, suggesting that Irisin could be implicated in AMPK pathway regulation [522]. However, the particular effects of Irisin on AMPK regulation in the kidney is still unexplored and needs further investigations.

5.5 Conclusion

Based on our data, exercise training can be considered as an interesting strategy for the management of obesity-induced CKD. Kidney function was improved through reducing albuminuria, glomerular hypertrophy, inflammation, oxidative stress and fibrosis as well as attenuating intra-renal fat content. We demonstrated that these beneficial effects implicate restored AMPK activity and autophagy induction in renal tissue (**Figure 8**). Exercise training may thus represent an interesting non-pharmacological alternative strategy for AMPK activation in obesity-induced CKD.

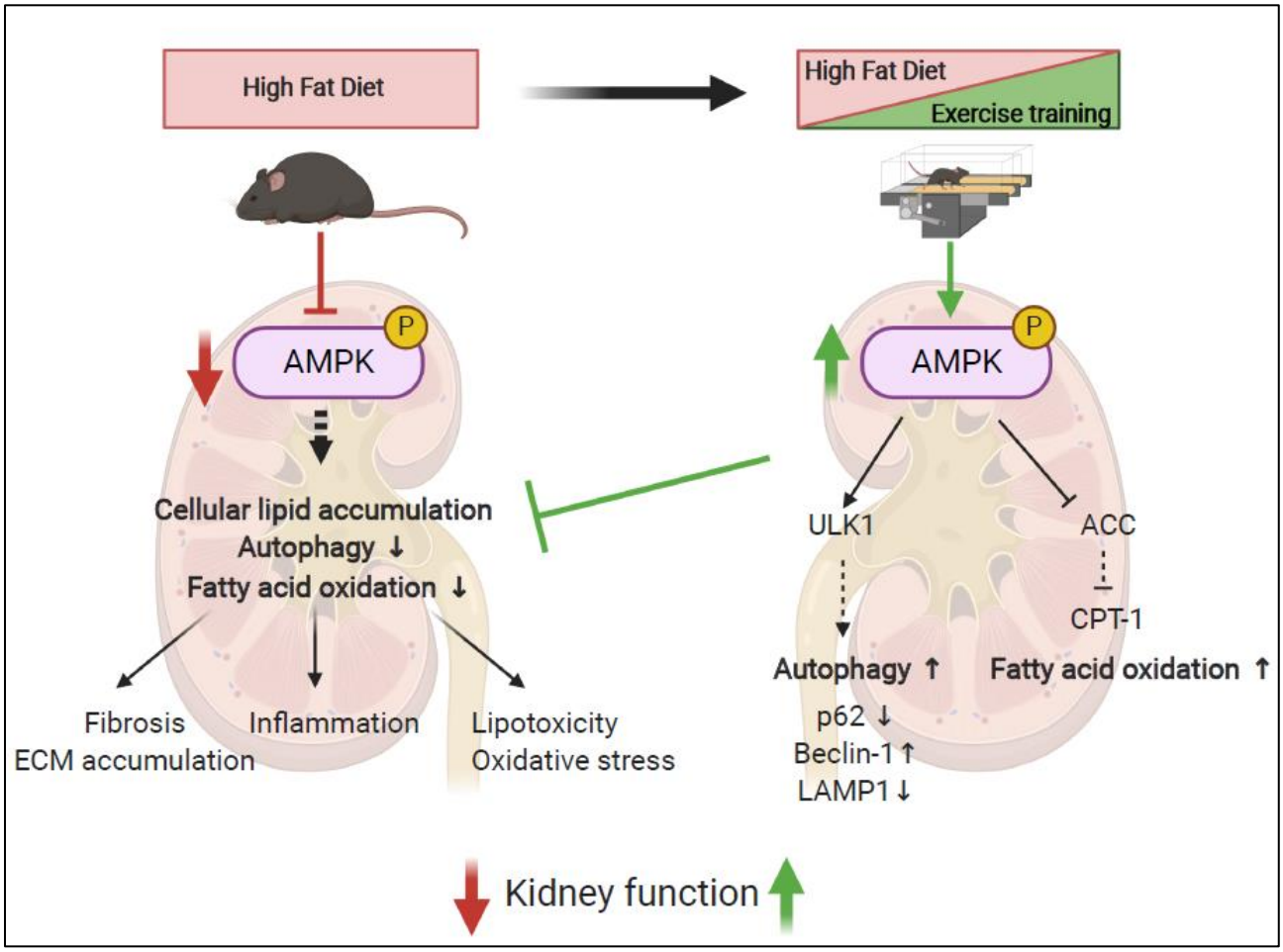

Figure 8. Schematical representation of the effects of HFD and EET on the underlying molecular mechanisms of obesity-induced CKD in mice. Created with Biorender.com.

SECTION II

Specific Aims

The next step of the PhD project was to investigate new potential biomarkers for obesity-induced CKD. Particularly, we focused on SIRT3, a mitochondrial NAD^+-dependent deacetylase. Indeed, in our EET experimental study, we tested its renal expression (data unshown in section I) in the different experimental groups (LFD, LFDT, HFD, and HFDT). As illustrated below in **Figure 1**, its protein expression was significantly decreased in mice fed a HFD while EET appeared to prevent this change.

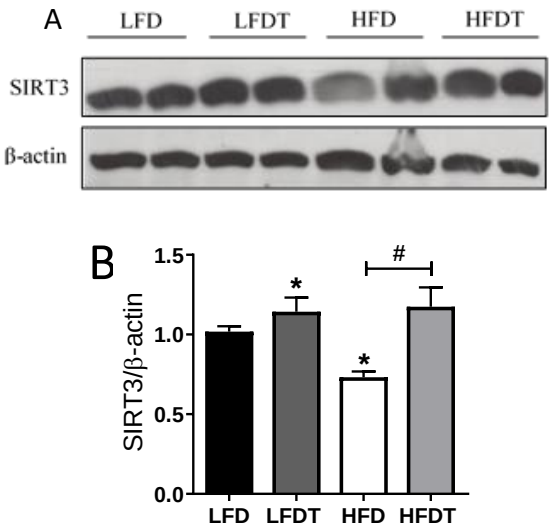

Figure 1. Effects of diet and EET on SIRT3 protein level. **A**. Western Blot analysis of SIRT3 and β-actin from total kidney protein extracts. **B**. Quantitative densitometry of the immunoblot. Statistical analyses were performed by One-way ANOVA followed by Newman-Keuls. *$p \leq 0.05$ vs LFD, # $p \leq 0.05$ vs HFD. Mean ± SEM. n=8

6 SIRT3 as a new biomarker and therapeutic target for obesity-induced chronic kidney disease.

6.1 Background

SIRT3 is a NAD^+-dependent deacetylase belonging to the Sirtuin family which is mainly localized in mitochondria but also in cytoplasm. Deacetylation accounts for a crucial mechanism to regulate the activity of many substrates involving in energy metabolism [450]. Accordingly, SIRT3 plays a major role in mitochondria homeostasis by the regulation of mitochondrial respiratory chain and ATP production. SIRT3 promotes FA β-oxidation through LCAD [451] and also exerts an antioxidant activity by targeting the SOD2 and the isocitrate dehydrogenase (IDH2) [446,452]. Interestingly, it has been reported that exercise training affects the expression and/or activity of Sirtuins. Particularly, studies have investigated the regulation of SIRT1 and SIRT3 in response to different types of exercise in skeletal muscle. Researchers demonstrated that acute exercise (a single load of exercise) resulted in the activation of SIRT1, while long term exercise training was related to an increase of genic and proteic SIRT3 expression, associated to enhanced synthesis of NAD^+ in healthy individuals [523,524]. More generally, SIRT3 expression is promoted in response to metabolic stresses such as caloric restriction, exercise or fasting. Kincaid *et al.* have proposed a positive feedback mechanism by which cellular stress activates SIRT3 and results in neuroprotection during aging or obesity (see **Figure 2**) [525]. Indeed, cytosolic form of SIRT3 has been shown to activate LKB1, which in turn activates AMPK in primary cardiomyocytes [453]. Therefore, reduction in SIRT3 expression in a setting of obesity could in part explain the reduction in AMPK activity. Another evidence of the role of SIRT3 in AMPK activation is its involvement in the increase of cytosolic calcium level that involves the activation of CaMKKβ and so, promotes the activation of AMPK [526].

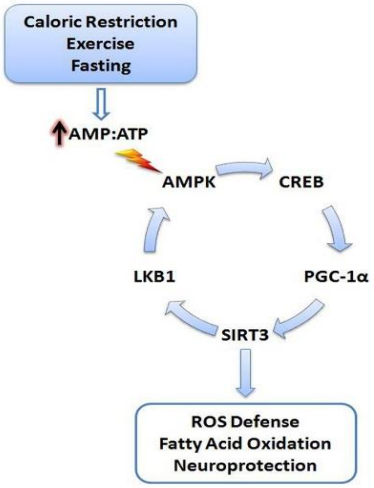

Figure 2. **Cellular stress activates SIRT3**. Energy deficits resulting from calorie restriction, exercise, and fasting cause the cellular AMP:ATP ratio to increase. Increased levels of AMP trigger activation of AMPK, initiating a signaling cascade promoting SIRT3 expression. SIRT3 promotes activation of antioxidant systems, FA oxidation, and neuroprotection. A positive feedback mechanism is also initiated via the deacetylation and activation of LKB1 by SIRT3, further promoting activation of AMPK. **AMPK**, AMP-activated protein kinase; **CREB**, cyclic AMP response element-binding protein; **PGC-1*α***, peroxisome proliferator-activated receptor gamma coactivator 1-alpha; **LKB1**, liver kinase B1; **AMP**, adenosine-5′-monophosphate; **ATP**, adenosine-5′-triphosphate. From [525].

In a context of obesity, it has been shown that beneficial impacts of ET were associated to SIRT3 regulation in cognitive dysfunction, heart failure and liver disease [527]. Despite most of evidence of exercise-induced expression of SIRT3 were studied in obese animal models, studies have observed an increased expression of SIRT3 in the muscle of obese adolescent after aerobic [528,529]. Particularly, the importance of SIRT3 in metabolic diseases has been demonstrated in rodents and humans, showing a reduction in SIRT3 activity in this setting [454][455]. In humans, it has even been shown that a single nucleotide polymorphism in the SIRT3 gene is associated with increased risk to develop a metabolic syndrome [455]. In addition, mice deficient for SIRT3 and fed a HFD revealed an acceleration of metabolic syndrome hallmarks [530]. In the kidney, most of the studies were performed in models of acute kidney injury (AKI). In those, the beneficial effect of restoring SIRT3 activity was always highlighted [457,458]. Indeed, maintaining SIRT3 activity was shown to prevent acute damages in renal tubular cells by maintaining the mitochondrial functional integrity and dynamics through the normalization of mitochondrial protein acetylation. Finally, it is important to highlight that SIRT3 activity is dependent on the availability of its co substrate NAD^+, and consequently on the $[NAD^+]$/[NADH] ratio while this ratio was reported to be lower in metabolic disease [459]. Since PTC are metabolically very active cells, requiring a large amount of ATP [531], mitochondrial function and integrity are therefore essential to the metabolism of these cells. As described in the introduction and shown in the section I of the result section, the beneficial role of AMPK in preventing impairment of macroautophagy in PTC and therefore, preventing lipid accumulation in these cells has been already demonstrated. Therefore, considering the emerging evidence of SIRT3 activation, its importance in metabolic disease and its close relation with AMPK regulation, it is worth to hypostatize that AMPK/SIRT3axis plays an important role in renal lipotoxicity. However, SIRT3 expression and activity has never been investigated in obesity-induced CKD.

In this regard, the objective of this second part was to investigate the implication of SIRT3 in a context of obesity-induced CKD. In this section, mice overexpressing SIRT3 were employed (Collab. Prof. Thierry Arnould, Laboratory of Biochemistry and Cell Biology (URBC), UNamur). Moreover, assuming that SIRT3 may be linked to AMPK activity in renal tissue, AMPK activity was also investigated.

6.2 Methods

6.2.1 Animals

Male C57BL/6 WT and SIRT3$^{+/+}$ transgenic mice were assigned either to a LFD or a HFD for 20 weeks (**Figure 3**). At the end of the experimental protocol, urine and kidney samples were collected.

Figure 3. experimental design

6.2.2 Histological analysis

Paraffin-embedded kidney sections were stained with Periodic Acid Schiff (PAS), Hemalun, and Luxol fast blue to assess morphological alterations. Morphometry of kidney sections was carried out as previously reported [120]. The frequency of tubules containing vacuolated cells was evaluated by a semi-quantitative basis by adapting a single-blind analysis. To standardize the evaluation procedure, an additional lens engrave with a square grid was inserted in one of microscope eyepieces. For each paraffin section, 10 square fields (0.084 mm2/field) were observed at x400 magnification.

6.2.3 Kidney function

At the end of the experimental protocol, mice were placed into metabolic cages for 24h-urine collection. Urine were subsequently stored at -20°C until analyses were performed. The urinary albumin and creatinine levels were measured with a mouse Albuwell ELISA kit and a Creatinine Companion kit (Exocell, Philadelphia, PA, USA). Total proteinuria was quantified by the Bradford binding assay as previously described [485]. As an index of oxidative stress, urine samples were also analyzed for hydrogen peroxide by Amplex red assay (Thermo Fisher Scientific, Waltham, MA, USA). All values of urinary markers were normalized to the urinary creatinine concentration.

6.2.4 Western blot analysis

Frozen kidney tissues were homogenized in Cell Lysis Buffer (Cell Signaling, Danvers, MA, USA) with phosphatase and protease inhibitor cocktail (Thermo Fisher Scientific, Waltham, MA, USA) at 4°C. Samples were subsequently centrifuged at 14 000g for 15 min at 4°C and supernatants were collected. Protein concentrations were quantified by Pierce BCA assay kit (Thermo Fisher). Next 40µg of total lysate were separated on Tris-Glycine 12% gels and transferred onto nitrocellulose membranes. Membranes were blocked with 5% BSA for 1 h and primary antibodies against: phospho-AMPK and AMPK (Cell Signaling) were applied in 5% BSA overnight at 4°C. Finally, membranes were incubated with secondary antibodies (Li-Cor Biosciences, Lincoln, NE, USA) in 1% BSA for 1h. Proteins were visualized using the Odyssey Infrared Imager (Li-Cor Biosciences). The fluorescence was quantified using the imaging software Odyssey V3.0 from the Odyssey Infrared Imager (Li-Cor Biosciences).

6.2.5 RT-qPCR analysis

Frozen kidney tissues were homogenized, and total RNA was then extracted with Trizol (Sigma-Aldrich, Saint-Louis, MO, USA) and treated with DNAse (Promega, Madison, WI, USA). Total RNA concentration was measured by NanoDrop (NanoDrop 1000, Thermo Scientific, Waltham, MA, USA). Transcript-specific primers were generated based on mouse sequences from GenBank. NCBI Primer Blast was used to ensure specificity of primers for each target. All pairs of primers were analyzed for dissociation curves and melting temperatures. Real-time quantitative PCR was performed in order to quantify mRNA level of Col I, TGFβ, IL1β-6, MCP-1, TNFα, SOD1, SOD2, Nrf2, HO-1 and 18S as a housekeeping gene (see **Table 1**). Briefly, 2 µg of total RNA were used for reverse transcription using MLV reverse transcriptase (Promega) during 1h at 70°C. Quantitative PCR amplification was performed using the SYBR Green Master Mix (Roche, Basel, Switzerland) and the Prism 7300 Real-Time PCR Detection System (Applied Biosystems, CA, USA). Mean fold changes were calculated by averaging the triplicate measurement for each gene. Relative gene expressions were calculated using the $2^{-\Delta\Delta CT}$ method.

Table 1.

Gene		Primer Sequences (5'-3')
COLI	Fw	CTTGCCCCATTCATTTGTCT
	Rv	GCAGGTTCACCTACTCTGTTCT
TGFβ	Fw	TGGAGCAACATGTGGAACTC
	Rv	GTCAGCAGCCGGTTACCA
TNFα	Fw	TACTGAACTTCGGGGTGATTGGTCC
	Rv	CAGCCTTGTCCCTTGAAGAGAACC
IL6	Fw	GCTACCAAACTGGATATAATCAGGA
	Rv	CCAGGTAGCTATGGTACTCCAGAA
MCP-1	Fw	CTTCTGGGCCTGCTGTTCA
	Rv	CCAGCCTACTCATTGGGATCA
SOD1	Fw	AAGGCCGTGTGCGTGCTGAA
	Rv	CAGGTCTCCAACATGCCTCT
SOD2	Fw	TGCTCTAATCAGGACCCATTG
	Rv	GTAGTAAGCGTGCTCCCACAC
Nrf2	Fw	AGGCATCTTGTTTGGGAATGTG
	Rv	CTTTAGCTAGCGACAGAAGGAC
HO-1	Fw	GAAGGGTCAGGTGTCCAGAG
	Rv	CCAGGTAGCGGGTATATGCGT
18S	Fw	CGCCGCTAGAGGTGAAATTCT
	Rv	CGAACCTCCGACTTTCGTTCT

6.2.6 Statistical analysis

Results are presented as mean values ± SEM. The level for statistical significance was defined as $p < 0.05$. Analyses were carried out using Prism GraphPad Software version 6 (San Diego, CA, USA). Differences between data groups were evaluated using one-way ANOVA followed by Newman–Keuls *post hoc* tests for multiple comparisons.

6.3 Results

6.3.1 SIRT3 overexpression prevents ectopic lipid accumulation in PTC of mice fed a HFD

We first analysed the ectopic lipid accumulation in proximal tubules of wild-type LFD, HFD and SIRT3 Tg mice. As illustrated in **Figure 4. A**, HFD mice present a strong accumulation of intracellular lipid droplets in proximal tubular cells in comparison to LFD mice. This lipid accumulation was markedly decreased in SIRT3 Tg HFD where only a few numbers of vacuolated proximal tubules was observed. The quantification of vacuolated tubules in renal cortex of each group confirmed a significant increase of ectopic lipid accumulation in HFD mice compared to LFD control that was significantly decreased in SIRT3 Tg HFD mice compared to HFD wild type mice (**Figure 4. B**).

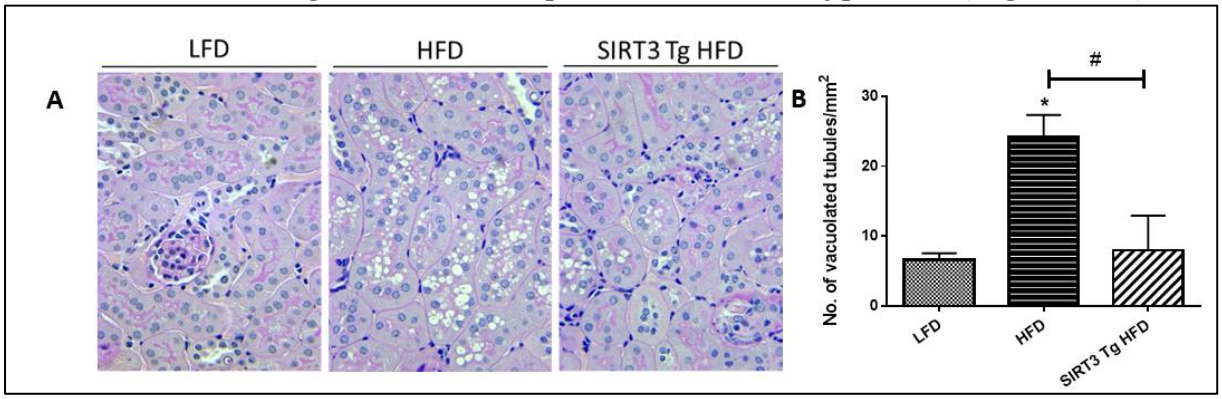

Figure 4. Overexpression of SIRT3 prevents ectopic lipid accumulation in PTC in HFD mice. **A**. Representative photomicrographs (200X) illustrating vacuolated proximal convoluted tubular cells (arrow). **B**. Quantitative analysis of the number of vacuolated tubules per mm^2. Statistical analyses were performed by One-way ANOVA followed by Newman-Keuls. *p≤0.05 vs LFD, # p≤0.05 vs HFD. Mean ± SEM. n=6

6.3.2 SIRT3 overexpression improves renal dysfunction of HFD-induced CKD

Regarding kidney function, the urinary albumin and total protein concentration was determined in urinary sample collected after 20 weeks on diet. Urinary albumin and protein levels of each animal were normalized with the corresponding urinary creatinine level. The data showed a significant increase of both urinary albumin to creatinine ratio and protein to creatinine ratio in HFD mice compared to the control that was significantly decreased in SIRT3 Tg HFD mice compared to WT HFD mice (**Figure 5**). Finally, urinary H_2O_2 concentrations followed the same pattern.

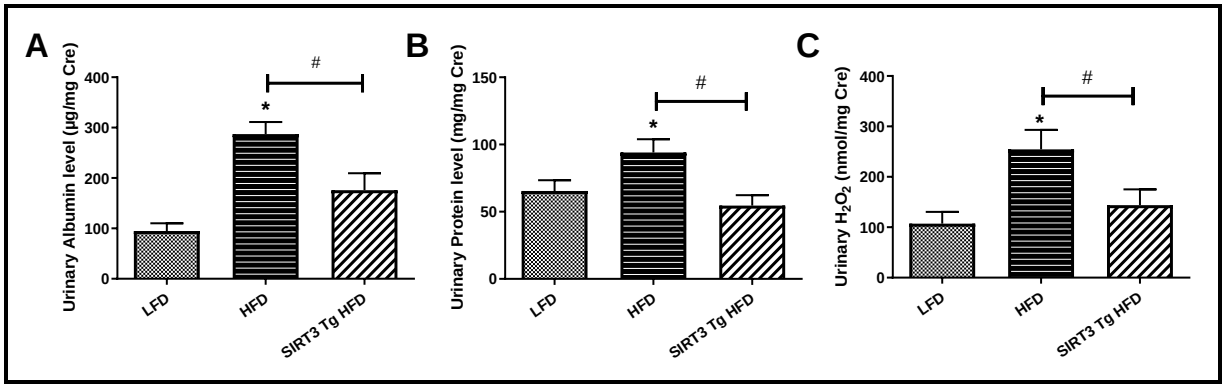

Figure 5. Overexpression of SIRT3 prevents (**A**) the increase in albuminuria, (**B**) in total proteinuria and (**C**) urinary H_2O_2 levels in HFD mice. Statistical analyses were performed by one-way ANOVA followed by Newman-Keuls. *p≤0.05 vs LFD, # p≤0.05 vs HFD. Mean ± SEM. n=6

6.3.3 SIRT3 overexpression is linked to an activation of AMPK in mice fed a HFD

We further investigated the AMPK activity in renal tissue of LFD, HFD and SIRT3 Tg HFD mice. Phosphorylated-AMPK (P-AMPK) and total AMPK protein levels were analyzed by western blot and quantified by densitometry of the immunoblot for each experimental group. The AMPK activity was represented as the ratio of phospho-AMPK over total AMPK (P-AMPK/AMPK). In **Figure 6**, we observed the expected decrease in AMPK activity in renal tissue of HFD mice compared to LFD control mice. AMPK activity of SIRT3 Tg HFD mice was shown to be normalized and significantly increased compared to HFD wild-type mice.

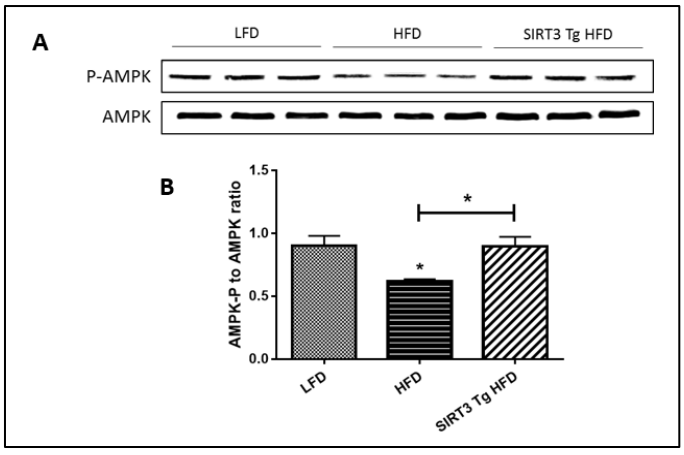

Figure 6. Overexpression of SIRT3 prevents the decrease in AMPK activity in HFD mice. **A**. Western blot analysis on total kidney protein extracts for phospho-AMPK and total AMPK. **B**. Quantitative densitometry of the immunoblot. Statistical analyses were performed by one-way ANOVA followed by Newman-Keuls *p≤0.05 vs LFD, #p≤0.05 vs HFD. Mean ± SEM. n=6

6.3.4 SIRT3 overexpression reduces fibrosis, inflammation and oxidative stress in renal tissue of mice fed a HFD

The **Table 2.** presents candidate genes expression involved in renal fibrosis (TGF-β, collagen type 1), inflammation (TNFα, MCP-1, IL-6) and oxidative stress (SOD1, SOD2, Nrf2, NOX1, NOX2, HO-1) measured by real-time qPCR. Regarding pro-fibrotic and pro-inflammatory markers, renal mRNA levels of COL I and MCP-1 were particularly increased with HFD in comparison to the LFD exposure. SIRT3 overexpression in HFD mice prevented these changes as evidenced by the significant decreased observed in SIRT3 Tg HFD mice compared to WT HFD mice. Moreover, mRNA expression of oxidative markers including SOD2, NOX1 and HO-1 were found to be significantly decreased in HFD mice but not in SIRT3 Tg HFD mice in comparison to the LFD control mice.

	LFD	**HFD**	**SIRT3 Tg HFD**
Profibrotic markers			
COL I	1,000 ±0,0764	**1,617±0,1634***	**1,178±0,1391#**
TGFβ	1,000 ±0,0796	1,486 ±0,1169	1,166 ±0,0743
Proinflammatory markers			
TNFα	1,000 ±0,1874	1,894 ±0,5410	1,336±0,1578
IL-6	1,000 ±0,0938	3,220±1,6350	1,602±0,3649
MCP-1	1,000 ±0,0613	**2,411±0,4571***	**1,376±0,3015#**
Antioxidant markers			
SOD1	1,000 ±0,1193	0,728±0,0897	0,957±0,0826
SOD2	1,000 ±0,0685	**0,850±0,0268***	**1,118±0,0793#**
Nrf-2	1,000 ±0,2363	0,813±0,1221	**1,377±0,1357#**
HO-1	1,000 ±0,1423	**0,630±0,1559***	**1,239±0,1466#**

Table 2. Effects of overexpression of SIRT3 on renal gene expression in mice fed a LFD or HFD. Real-time quantitative qPCR for type I collagen (COLI), transforming growth factor β (TGFβ),), tumor necrosis factor α (TNFα) and interleukin 6 (IL6), Monocyte chemoattractant protein-1 (MCP-1), Superoxide dismutase 1 (SOD1), Superoxide dismutase 2 (SOD2), Nuclear factor (erythroid-derived 2)-like 2 (Nrf2) and Heme oxygenase-1 (HO-1). mRNA expression was performed on kidney tissue from LFD, HFD and SIRT3 Tg HFD mice normalized against 18S Statistical analyses were performed by one-way ANOVA followed by Newman-Keuls *p≤0.05 vs LFD, #p≤0.05 vs HFD. Mean ± SEM. n=6

6.4 Discussion

In this section, we characterized the effect of systemic SIRT3 overexpression in kidney of obese mice, particularly regarding obesity-induced CKD hallmarks. Here, we demonstrated a protective effect of SIRT3 overexpression in HFD-related CKD. First, our results confirmed the expected ectopic lipid accumulation in proximal tubular cells associated to an impairment of renal function, decreased AMPK activity and renal inflammation and fibrosis in HFD fed mice. Our present findings reveal that SIRT3 plays a protective role in ectopic lipid accumulation in proximal tubular cells and in impairment of renal function. Moreover, markers of inflammation and fibrosis were also improved with SIRT3 overexpression. In addition, antioxidant factors were more expressed in SIRT3 Tg HFD mice compared to WT HFD mice. The *SOD2* gene codes for the mitochondrial superoxide dismutase 2 (SOD2), which is an antioxidant protecting cells and mitochondria against ROS by catalysing the dismutation of superoxide radicals in mitochondria by converting anion superoxide into hydrogen peroxide and oxygen [532]. It is important to note that SOD2 is one of the main targets of SIRT3, which lead to activation of SOD2 by deacetylation. However, the post-translational modifications of SOD2 were not investigated in this study. Our data were consistent with other studies demonstrating the protective role of SIRT3 activation in renal disease [533]. Most of the kidney disease models have focused on AKI but very recently, Locatelli *et al.* demonstrated a decreased expression of SIRT3 and SIRT6 but not SIRT1 in renal tissue of *Ob/Ob* mice presenting type II diabetes-induced CKD. They particularly showed that the activation of SIRT3 by honokiol (an antioxidant extracted from the seed cones of the Magnolia) treatment attenuated albuminuria, ameliorated glomerular structural damages with reduction in podocyte injury [534]. Indeed, SIRT3 activation preserved mitochondrial function through especially the activation of SOD2 and associated anti-oxidative defences.

Surprisingly, we demonstrated that SIRT3 overexpression in mice was associated to AMPK activity, suggesting a possible SIRT3/AMPK regulation. We previously described the role of AMPK as a key player of obesity-induced CKD. So, it is not surprising that protection of HFD mice conferred by overexpression of SIRT3 was associated to AMPK activation in renal tissue. The SIRT3/AMPK pathway has particularly emerged in the literature over the past few years [535–537]. Even if the cross-regulation of SIRT3 and AMPK has not been investigated in details like the AMPK/SIRT1 cross-regulation, our results suggest an activation of AMPK *via* SIRT3 that corroborate previous studies presenting SIRT3-dependant AMPK activation through LKB1 activation [538]. However, the specific crosstalk between AMPK and SIRT3 in our model needs further investigations.

Furthermore, this preliminary study presents some limitations. Indeed, the overexpression of SIRT3 is induced in all tissues. Therefore, it is not possible to discriminate the specific effect of SIRT3 overexpression on intra-renal outcomes. It is thus possible that the improvements of renal injuries were a consequence of a systemic effect of SIRT3 activity. Moreover, the SIRT3 Tg LFD control group is lacking, which makes difficult to confirm the overexpression of SIRT3 in control mice (**Supplemental data 2**) and to characterize the consequences of SIRT3 overexpression alone without other factors. However, regarding our translational perspectives, this study presents a proof of concept of the implication of SIRT3 as a potential player of the obesity-induced CKD. Consequently, we will further determine, in the next section, whether activation of SIRT3, with a natural compound, the Nicotinamide Riboside, may improve obesity-related kidney impairments.

6.5 Conclusion

Here, we demonstrated for the first time the decreased expression and function of SIRT3 in obesity-induced CKD. Based on these preliminary results, SIRT3 represent a biomarker of renal damages in response to a HFD in mice. Overexpression of SIRT3 prevented the renal alterations observed in HFD mice and may therefore be a potential key target to improve altered lipid metabolism in HFD-induced CKD. Finally, SIRT3 overexpression was associated to the activation of AMPK that needs further investigations.

SECTION III

Specific aims

In this section, the goal was to determine the effects of the pharmacological activation of SIRT3 by a NAD^+ precursor supplementation – the Nicotinamide Riboside (NR) - in our experimental *in vivo* model as well as in an *in vitro* model of PTC exposed to palmitic acid (Prof. Thierry Arnould, Laboratory of Biochemistry and Cell Biology (URBC), UNamur). This section is thus divided in two specific parts:

- To assess the effects of NR in PA-induced mitochondrial dysfunction and lipotoxicity in PTC culture (immortalized human kidney cells - HK-2 cells). We first evaluated the effects of PA-treated cells on lipid accumulation, viability, metabolic activity and AMPK activity in order to determine the relevant concentration of PA to mimic obesity-induced lipotoxicity *in vitro*. Next, we characterized the mitochondrial dysfunction in HK2 cells treated with 300 µM of PA and we further evaluated the potential beneficial effects of NR to improve mitochondrial homeostasis ad lipotoxicity.
- To demonstrate the putative beneficial effect of the activation of SIRT3 by NR in in vivo obese model: WT male mice were fed either LFD or a HFD during 20 weeks treated or not with early (at the beginning of the specific diet) or late (starting at week 12) supplementation with NR in the diet (400 mg/kg/day – as described in [539]). The experimental investigations were the same than described in the first section. Moreover, our particular interest was to determine the acetylation status, SIRT3 and AMPK expression and activity in mitochondrial or cytosolic fractions from kidney tissue.

7 Targeting SIRT3 with Nicotinamide Riboside in obesity-induced CKD

7.1 Background

As already described, SIRT3 plays a role in the mitochondrial function and the cellular metabolism. Moreover, based on our preliminary study on mice overexpressing SIRT3 (section II) SIRT3 appeared as a target of interest in obesity-induced CKD [446,457,533]. The SIRT3 activity relies on the NAD+/NADH ratio. Therefore, a reduction of the ration induces a reduction of SIRT3 activity. However, in obesity, it has been demonstrated that the ratio is reduced [530,540]. Recently, several studies have found that NR, a natural dietary supplement and precursor of NAD^+, enhances SIRT3 activity by increasing the NAD^+/NADH ratio [540,541].

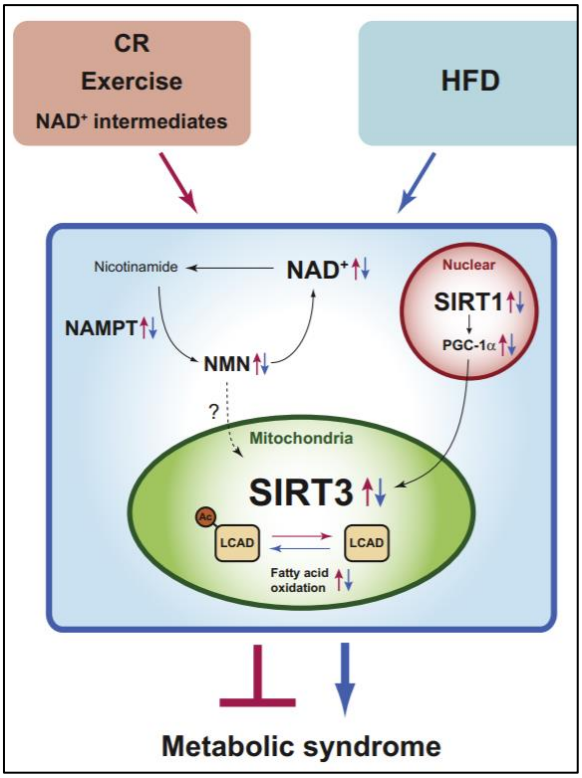

Figure 1. Therapeutic Potential of Mitochondrial SIRT3 for Metabolic Syndrome. High-fat diet (HFD) feeding suppresses SIRT3 activity and NAMPT-mediated NAD+ biosynthesis, contributing to the pathogenesis of metabolic syndrome (blue arrows). SIRT3 activation is expected to protect against metabolic syndrome by deacetylating key mitochondrial enzymes such as long-chain acyl-CoA dehydrogenase (LCAD). Calorie restriction (CR), exercise, and key NAD+ intermediates are likely able to enhance SIRT3 dosage/activity (red arrows). Here, we expect to increase SIRT3 with NR supplementation. From [542]

7.1.1 NAD: its function in cellular metabolism and energy production

The nicotinamide adenine dinucleotide (NAD) is a critical co-substrate and metabolic co-factor required by every living cell to support cellular energy production, as well as cellular repair and defense processes, and regulating metabolism and longevity [541]. NAD^+ is composed of two nucleotides linked together by phosphate groups, the nicotinamide (NAM), a form of vitamin B_3 and an adenine nucleobase (**Figure 2**). An additional phosphate group added to the ribose of the adenine nucleobase by a NAD kinase forms the nicotinamide adenine dinucleotide phosphate ($NADP^+$). $NADP^+$ especially plays an essential role as a cofactor for the rate-limiting step of the pentose-phosphate pathway. NAD^+ is a redox molecule and exists in an oxidized or reduced form, NAD^+ and NADH, respectively.

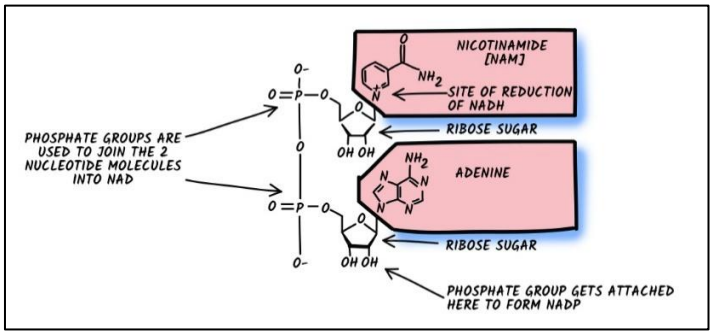

Figure 2. NAD structure. Nicotinamide-containing Nucleotide (top) and Adenine-Containing Nucleotide (bottom). From Neurohacker collective®.

NAD^+ is synthetized by the cells from different sources. First, NAD^+ can be synthetized via three independent pathways, from dietary sources (**Figure 3**): **1**) by the *de novo* synthesis (DNS) pathway, from the essential amino acid tryptophan. The major dietary source of NAD^+ is the nicotinic acid, a form of niacin (i.e., vitamin B3) that can be transformed by indoleamine 2,3-dioxygenase (IDO) or tryptophan 2,3-dioxygenase (TDO). However, DNS pathway has been mostly described in the liver and macrophages [342]; **2**) by the classical Preiss-Handler pathway. This pathway uses dietary nicotinic acid and the enzyme nicotinic acid phosphoribosyltransferase (NAPRT) to generate the nicotinic acid mononucleotide (NAMN), which is then transformed into nicotinic acid adenine dinucleotide (NAAD) by NAMN transferase (NMNAT). The process is completed by the transformation of NAAD into NAD^+ by NAD^+ synthase (NADS). **3**) By the NAD^+ salvage pathway, that recycles nicotinamide produced as a byproduct by NAD^+-consuming enzymes (or directly from dietary source): sirtuins, PARPs, and the cADPR synthases (CD38 and CD157). Initially, NAMPT recycles nicotinamide into NMN, which is then converted into NAD^+ via the different NMNATs [543,544].

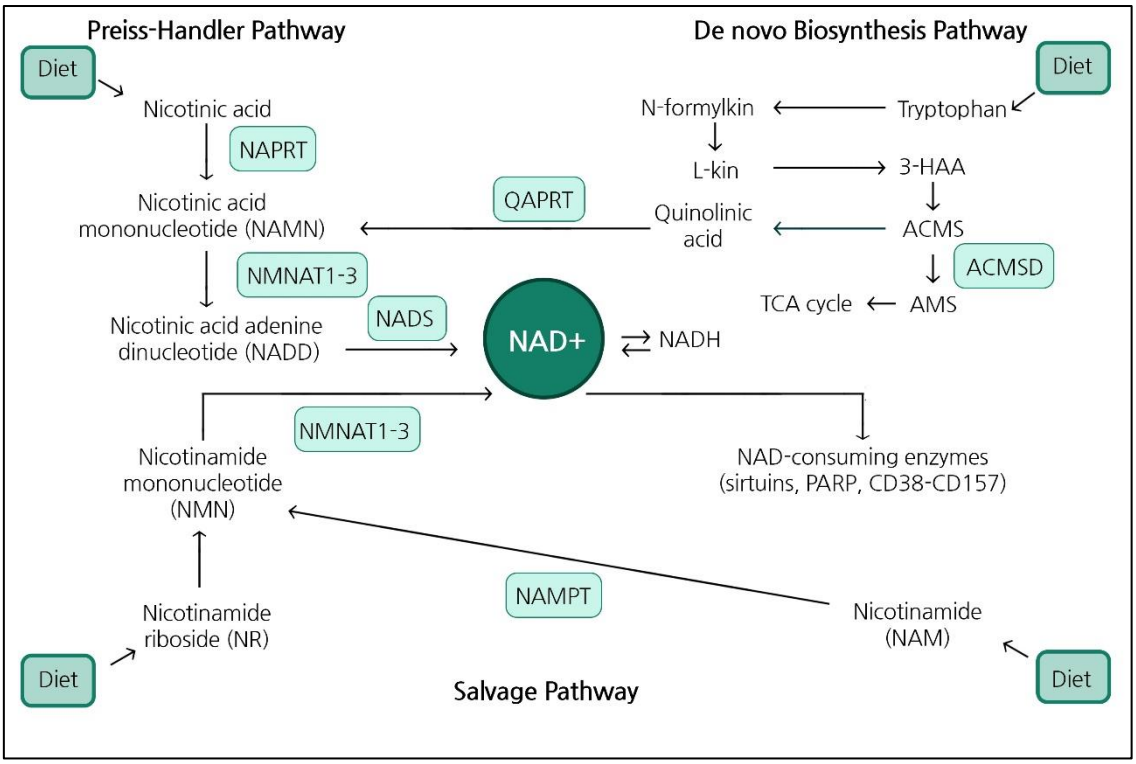

Figure 3. NAD+ biosynthetic pathways. Adapted from [543]

As a redox molecule, NAD^+ is a coenzyme for redox reactions involved in cellular and mitochondrial metabolism. NAD^+ is converted in NADH and reversely to carry out energy and to promote the production of ATP. However, NAD is mainly maintained in its oxidized state, NAD^+, into the cells. Metabolic processes involving NAD^+ include glycolysis, the tricarboxylic acid (TCA) cycle, β-oxidation, alcohol metabolism, lactate oxidation and during the oxidative decarboxylation of pyruvate. The reduced form, NADH, delivers electrons to the electron transport chain for oxidative phosphorylation. NADH also acts as a cofactor for desaturases, enzymes involved in the synthesis of unsaturated fatty acids [545]. Beyond its role as a coenzyme in redox reactions, NAD^+ is known to be a co-substrate for NAD-consuming enzymes, including three main classes of enzymes [546]: (1) poly-ADP-ribose polymerases (PARPs), (2) Sirtuin deacetylases (Sirtuins) and (3) cluster of differentiation 38 (CD38) (**Figure 4**).

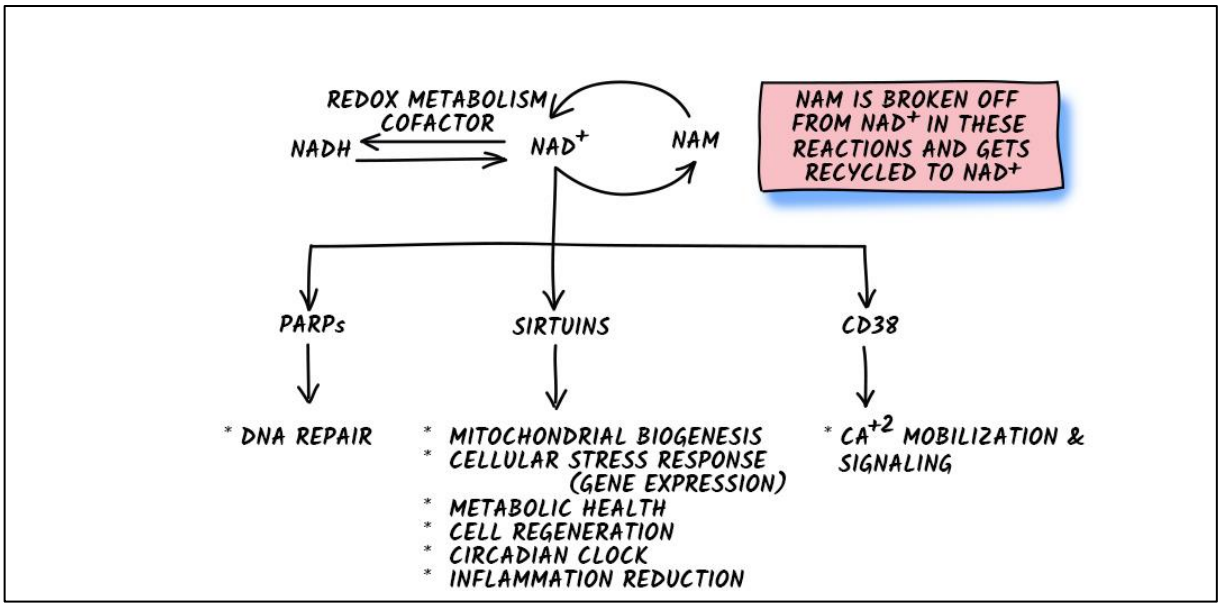

Figure 4.

The PARP protein family has a central role in DNA repair [547]. Activated PARP1 and PARP2 catalyze the transfer of multiple ADP-ribose moieties from NAD^+ to protein acceptors, generating long poly(ADP-ribose) (PAR) chains at sites of DNA damage, leading to NAD^+ hydrolysis into NAM [548]. Sirtuins deacetylate their substrate by using NAD^+ as a co-substrate, generating the deacylated substrate and NAM. As previously mentioned, Sirtuins modulate cellular metabolism through the regulation of proteins including histones, transcription factors and co-activators (p53, NF-κB, PPARγ co-activator 1α (PGC1α) and FOXO1) and signaling regulators of metabolism, including protein kinase A, AMPK and mTOR [549]. CD38 is mainly found in immune cells and can use NAD^+ to create the signaling molecule cyclic ADP-ribose, essential for the regulation of intracellular Ca^{2+} [550][551]. On the basis of their K_m values, SIRT1 and SIRT3 are higher more dependent on NAD^+ availability compared to other Sirtuins. Moreover, the K_m of PARPs and CD38 are far below the physiological range of NAD^+ and are the main consumers of NAD^+ in cells. Thus, decreased NAD^+ might be less rate limiting than for SIRT1 and SIRT3 [552].

7.1.2 NAD^+ level in diseases

Regarding the importance of NAD(H) in ATP production and the NAD^+-dependent enzymes for cell signaling and homeostasis, maintaining a high NAD+ to NADH ratio is essential for proper cellular processes. Indeed, it is widely acquired that NAD^+/NADH ratio has a critical role in health and diseases. A decline in NAD^+/NADH balance level has been associated with a wide variety of chronic diseases as well as aging and age-related diseases. Particularly, it has been demonstrated that levels decline with obesity

and diabetes in multiple murine tissues, including the adipose tissue, skeletal muscles, liver, and hypothalamus [342,553–555]. The underlying mechanisms by which NAD^+ is decreased in obesity is not fully elucidated but recent studies have demonstrated a decreased in the mRNA/protein expression of rate-limiting enzyme of NAD biosynthesis NAMPT, at least in adipose tissue and in the liver [556]. Interestingly, Nampt gene transcription has been reported to be controlled by AMPK [557,558]. Regarding kidney disease, most of the NAD^+ research reported to date has used models of AKI [559]. Studies has particularly described an accelerated consumption of NAD^+ by tubular PARP and a defective *de novo* NAD^+ biosynthesis, leading to fall in renal NAD^+ levels and decreased FA oxidation [559,560]. Interestingly, one study on Zucker diabetic fatty rats demonstrated CD38 overexpression may be related to a reduction in the NAD^+/NADH ratio in the diabetic kidney that enhanced mitochondrial oxidative stress in the diabetic kidney mediated by the reduction of SIRT3 activity [561]. In preclinical settings, various strategies to increase NAD^+ levels have shown beneficial effects, particularly with NAD^+ precursors. These compounds are specific smaller molecules and are metabolized by the cells to produce NAD^+. The administration of NAD^+ precursors are now been considered promising for the treatment of multiple diseases [562].

7.1.3 Nicotinamide Riboside: an interesting NAD^+ precursor to enhanced SIRT3 activity

The NR is a type of vitamin B3 found in cow's milk and yeast-containing food products such as beer [563]. NR is converted to NAD^+ via the NR kinase (NRK) pathway and the nicotinamide (NAM) salvage pathway [564,565]. In mice and humans, NR has been shown to be more efficient in boosting NAD^+ than NA or NAM [566]. Several studies have shown that NR supplementation increases NAD^+ level, enhances mitochondrial biogenesis and oxidative metabolism, protects against neurodegenerative disorders and age-related physiological decline in mammals [554,567,568].In the study of Canto *et al*., it was demonstrated that 400 mg/kg/J NR treatment in HFD mice for 10 weeks increased plasma and intracellular NAD^+ in muscle, brown adipose tissue dans liver as well as activated SIRT3 activity [541]. However, the particular effects of NR supplementation for obesity-associated abnormalities is still poorly investigated.

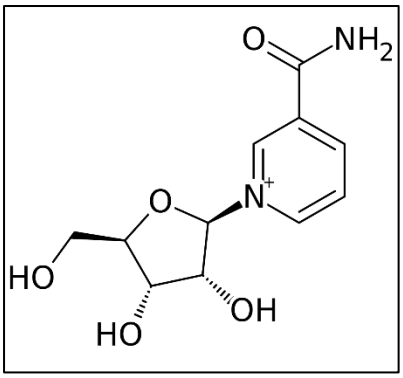

Figure 5. Chemical structure of Nicotinamide Riboside

7.2 Aim of the study

Here, the NR, a NAD+ precursor, will be used to maintain SIRT3 deacetylase activity both in *in vitro* and *in vivo* models of renal lipid overload. Particularly, we will characterize mitochondrial (mt) function and dynamics in a context of renal lipotoxicity.

7.3 Materials and Methods

7.3.1 *In vitro* study

7.3.1.1 Cell culture

HK-2 cells (Human Kidney 2, ATCC® CRL-2190™, Belgium), immortalized epithelial proximal tubular cells were cultivated in DMEM/F12 (ThermoFisher) supplemented with 10% fetal bovine serum (FBS, Gibco), 1000 U/L penicillin, 100ug/mL streptomycin in an atmosphere containing 5% CO2 at 37 °C. Cells were treated with 300 µM of palmitic acid (PA) or 300 µM of BSA for 24h with or without 1 mM of Nicotinamide Riboside (NR) (Niagen, ChromaDex, Irvine, CA).

7.3.1.2 Viability assay

Cell number was assessed indirectly by staining with crystal violet dye, as described in [569]. Briefly, cells were seeded in 96-well plates at a density of 4000 cells/well in complete DMEM/F12 medium for 18h. Cells were then exposed to treatments for 24h as described before. Medium was removed, cells were gently rinsed with phosphate-buffered saline (PBS), fixed with 1% glutaraldehyde/PBS for 15 minutes and stained with 0.1% crystal violet (weight/vol in double distilled H2O) for 30 minutes. Cells were washed under running tap water for 15 minutes and subsequently lysed with 0.2% Triton

X-100 (vol/vol in double distilled H2O). The absorbance was measured at 550 nm and blank wells containing medium alone were used for background subtraction.

7.3.1.3 MTT assay

Metabolic activity of the cells was assessed by MTT colorimetric assay. HK-2 cells were seeded in a 96-well plate at a density of 10000 cells/well in complete DMEM/F12 medium for 18h. Cells were then exposed to treatments for 24h as described before. Then, cells were incubated with MTT (50 µg/well) for 2 h. The supernatant was removed and 100 µl dimethylsulfoxide was subsequently added to each well. After shaking the plate, the absorbances of each well at 570 nm were measured and blank wells were used for background subtraction.

7.3.1.4 Measurement of oxygen consumption rate and metabolic profiling

OCR in HK-2 was measured with XFp Extracellular Flux Analyzers (Agilent Seahorse Biosciences) in collaboration with Prof. Olivier Devuyst, University of Zurich. After treatment, the cells were incubated with XF-Base Medium (non-buffered RPMI 1640 containing either 2 mM L-glutamine, 1 mM sodium pyruvate, and 10 mM glucose, pH 7.4). Three measurements were assessed under basal conditions and upon addition of 2 µM Oligomycin (Oligo), 0.5 µM FCCP, and 1 µM Rotenone (ROT)/Antimycin A (ANT). All the reagents were provided by XFp Cell Mito Stress Test Kit (Agilent Seahorse Biosciences). OCR measurements were normalized to the numbers of cells (TC10TM automated cell counter, Bio-Rad). After incubation in a non-CO2 incubator at 28.5 °C for 20 min, the metabolic measurements were analyzed in live. One measurement cycle consisted of a brief wait period to acclimate the plate, 2 min mix, 1 min wait, and 2 min data acquisition. Three measurement cycles were performed to establish the average value for each biological replicate.

7.3.1.5 Measurement of lipid droplets content

Lipid uptake was observed by BODIPY 493/503 lipid probe (Invitrogen, D3922). To evaluate the lipid droplet content, cells were washed 3 times with PBS and incubated with 1 µM of BODIPY diluted in HBSS for 15 min at 37°C. To visualize nuclei, 3,75 µg/mL of Hoechst 33342 (Miltenyi Biotec) were used at the same time. Then, cells were washed 3 times with PBS and immediately examined under a confocal microscope (Olympus IX81). Analysis of lipid droplet content and size was performed using the

Lipid Droplets Tool in ImageJ. Quantifications of number of lipid droplets obtained from five randomly selected field per condition, with each containing 20-30 cells.

7.3.1.6 NAD^+/NADH ratio assessment

NAD+ levels were measured using the NAD/NADH-Glo Assay Kit (Promega) following manufacturer's instructions. Briefly, cells were seeded in 96-well plate at a density of 10000 cells/well in complete DMEM/F12 medium for 18h. Cells were then exposed to treatments for 24h as described before. Then, cells were washed in PBS and lysed with DTAB solution (dodecyltrimethylammonium bromide). Each well was divided in to lysed cell samples to measure NAD^+ and NADH separately. To measure NAD^+, 0.4N HCl were added and cell lysates were heated at 60°C for 15 minutes. Samples were incubated at room temperature for 10 minutes and Trizma® base solution was added to each well of acid-treated samples. To measure NADH, cell lysates were heated at 60°C for 15 minutes. Samples were incubated at room temperature for 10 minutes and HCl/Trizma® solution was added to each well of base-treated samples. Finally, after adding the detection reagent (reductase, reductase substrate, NAD Cycling enzyme and NAD cycling substrate to form NAD/NADH-Glo™), luminescence were recorded using a luminometer.

7.3.1.7 Detection of mitochondrial ROS

Mitochondrial superoxide generation was detected using MitoSOX (ThermoFisher), a red fluorescent dye localized to mitochondria. Once it enters the mitochondria, MitoSOX is specifically oxidized by superoxide and exhibits red fluorescence. MitoSOX (5 μM) were used according to the manufacturer's instructions and treated cells were examined under a confocal microscope (Olympus IX81) and fluorescence intensity of each cell was analyzed with ImageJ. Hoechst 33342 (Miltenyi Biotec) were used to visualize nuclei. Quantifications of mean fluorescence intensity obtained from five randomly selected field per condition, with each containing 20-30 cells.

7.3.1.8 Lipid peroxidation assay

The detection of lipid peroxidation in live cells was performed using the Image-iT™ Lipid Peroxidation (ThermoFisher). This reagent localizes to lipid membranes throughout live cells and upon oxidation by lipid hydroperoxides, fluorescence from live cells shifts from red to green, providing a ratiometric indication of lipid peroxidation. Cells were treated as previously described and incubated with Image-iT™ Lipid

Peroxidation (10nM) following manufacturer's instruction. Treated cells were examined under a fluorescence microscope (Nikon Eclipse 80i) and fluorescence intensity of each cell was analyzed with ImageJ. Hoechst 33342 (Miltenyi Biotec) were used to visualize nuclei. Quantifications of mean fluorescence intensity obtained from five randomly selected field per condition, with each containing 20-30 cells.

7.3.1.9 Western blot

HK-2 was collected and then proteins form each sample were extracted using RIPA buffer (Tris 25mM, NaCl 150mM, Igepal 1%, SDS 0.1%, DTT 1mM, protease inhibitors). Protein concentrations were quantified by Pierce BCA assay kit (Thermo Fisher) and then thirty micrograms of total lysate were separated by SDS-PAGE 12% and transferred onto nitrocellulose membranes. Following blocking step, the membrane was incubated with the primary antibody against phospho-AMPK and SIRT3 (Cell Signaling Technology) overnight at 4°C. After incubation with fluorescent secondary antibody (IRDye® 800CW Donkey anti-Rabbit, Licor) diluted in Odyssey Blocking Buffer PBS-0.1 % Tween20 for 1 hour at room temperature, proteins were visualized and quantified using the Odyssey® imaging system (LICOR, USA).

7.3.1.10 Statistical analysis

Results are presented as mean values ± SEM. The level for statistical significance was defined as $p < 0.05$. Analyses were carried out using Prism GraphPad Software version 6 (San Diego, CA, USA). Differences between data groups were evaluated using one-way ANOVA followed by Newman–Keuls *post hoc* tests for multiple comparisons.

7.3.2 *In vivo* study

7.3.2.1 Experimental model

Eight-week old C57Bl/6 male mice were used. All animal procedures were approved by the Institutional Animal Care and Use Committee of the University of Namur. Mice were fed a LFD (10% of total calories from fat) or a HFD (D12492, Research Diets, New Brunswick, NJ) supplemented or not with 400 mg/kg/J of NR (from week 0 or week 12) for 20 weeks (**Figure 6**). Mice were placed in metabolic cages for 24-h urine collection at baseline and at the end of the protocol while the body weight and the blood glucose will be also measured at those time points. After 20 weeks, mice were euthanized and blood samples were collected while kidneys were dissected into cortex,

outer medullary and inner medulla. Then, each renal area will be either snap-frozen in liquid nitrogen for further analysis. An additional portion was fixed in 4% PAF for histological analysis. A kidney portion of cortex was freshly processed for mitochondrial isolation with the Mitochondria Isolation Kit for Tissue (ThermoFisher), following manufacturer's instructions. Morphological analyzes, glucose tolerance test, biochemical assays and immunoblots were performed as described in the section I.

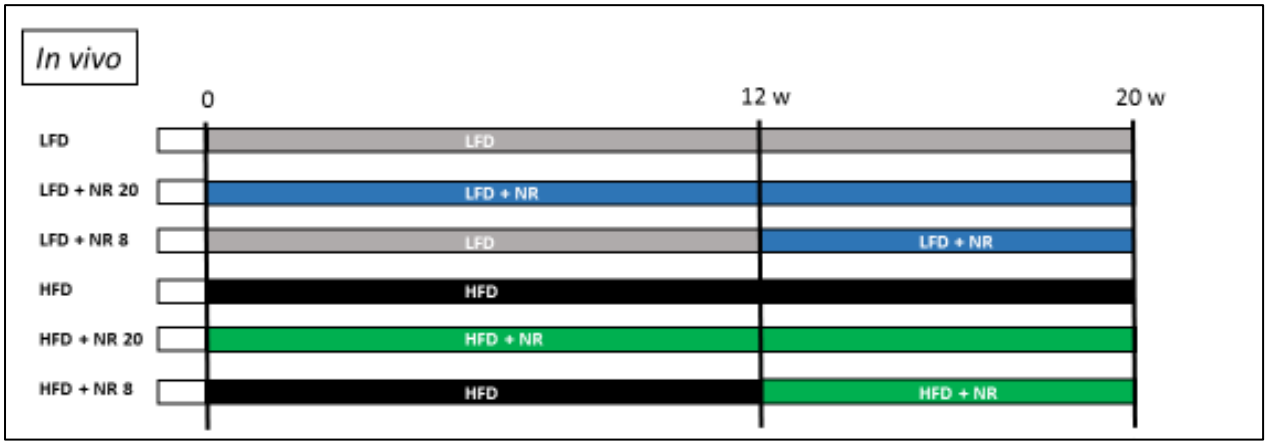

Figure 6. Experimental design of the *in vivo* study.

7.4 Results

For the *in vitro* experiments, we first assessed different concentrations of palmitic acid (PA) in HK-2 cells in order to confirm renal tubular cell impaired metabolism and ectopic lipid accumulation. Therefore, HK-2 cells were treated with a range from 50 to 700 µM of PA for 24h (**Supplemental Data 3**). As observed in **Supplemental data 3A**, no significant difference was observed for cell viability at any concentration used. However, the cell metabolic activity was found to be decreased from 300 µM of PA exposure (**Supplemental Data 3B**). This change was associated to a steadily dose-dependent decreased AMPK activity along with increased PA concentration (**Supplemental Data 3C**). Moreover, we assessed the lipid accumulation in HK-2 cells with PA. As shown in Supplemental **Supplemental Data 3D**, an increased positive staining for Oil Red O and BODIPY was present in HK-2 treated with PA, which confirms the accumulation of neutral lipids in HK-2 cells. We further analyzed the number and size of these lipid droplets in cells treated with 300 or 500µM of PA (**Supplemental Data 4**). The data showed an increased lipid droplet number and size in PA-treated cell compared to untreated cells. Moreover, this increase was higher in 500 µM than in 300 µM PA-treated cells, suggesting a dose-dependent accumulation of neutral lipids in PA-treated HK-2. Thus, regarding our data and previous studies, we decided to use a 300µM concentration of PA for the following experiments.

7.4.1 NR enhances NAD^+ to NADH ratio in renal tubular cells and activates AMPK/SIRT3 expression and activity

First, we wondered how PA treatment would affect $NAD^{+/}$NADH ratio in HK-2 cells. We analyzed the ability of NR to increase intracellular $NAD^{+/}$NADH ratio *in vitro* and potentially to activate SIRT3 *in vitro*. The results illustrate that PA exposure led to a decreased NAD^+/NADH ratio and that NR treatment was a valid tool to boost NAD^+ levels in renal tubular cells (**Figure 7**). Indeed, the NAD^+/NADH ratio was significantly increased with NR both in BSA (control) and PA-treated cells. Next, we analyzed whether NR may increase SIRT3 expression as well as AMPK activity in PA-treated HK-2. Interestingly, SIRT3 expression was found to be decreased with PA, which is consistent with the *in vivo* results illustrated in the last section (**Figure 7**). Moreover, NR (0.5 and 1 mM) tends to reverse decreased expression of SIRT3 as well as to enhance AMPK activity, which confirms our hypothesis.

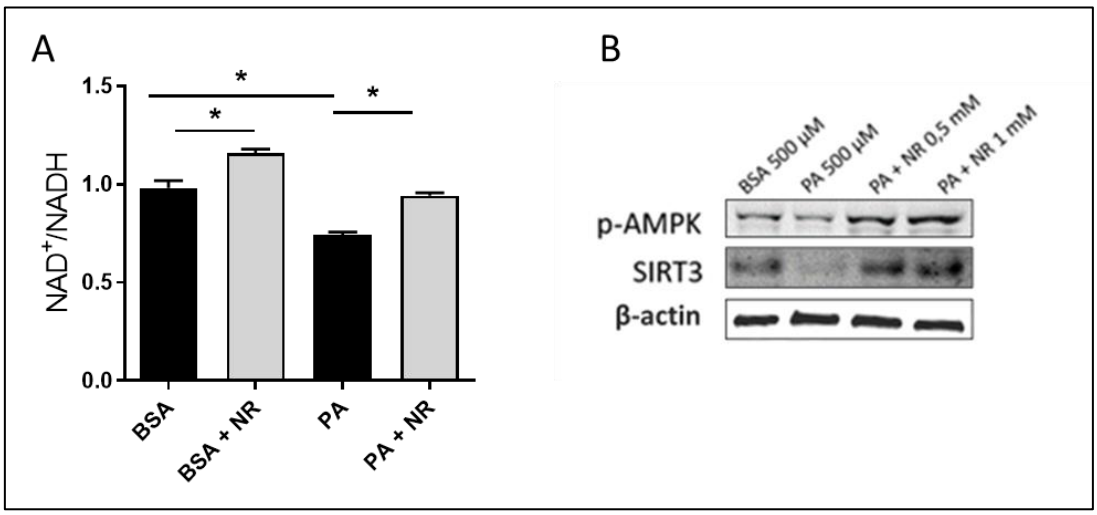

Figure 7. NR enhances NAD^+ to NADH ratio in HK2 and activates AMPK/SIRT3 in PA-treated HK-2 cells. A. The NAD+/NADH concentration was measured using the NAD/NADH-Glo Assay Kit in HK2 treated with BSA 300 µM, PA 300 µM with or without NR 1 mM. Data were normalized to the control BSA. Data are Mean ± SEM. One-way ANOVA followed by Newman Keuls post-hoc analysis. n=3 independent experiments. **B**. Representative immunoblots of P-AMPK and SIRT3 and the corresponding β-actin in cell lysates of HK2 treated with BSA 300 µM, PA 300 µM with or without NR 0.5 and 1 mM.

7.4.2 NR reduces lipid droplet accumulation in PA-treated renal tubular cells.

After confirming that NR is a consistent approach to increased NAD^+ and SIRT3 expression along with AMPK activation, we examined the effect of NR treatment on PA-induced accumulation of lipids in HK-2 cells. As presented in **Figure 8A**, BODIPY staining was increased with PA treatment as shown by the increased green dots around the nucleus of the cells. The number and size of lipid droplets were then quantified using ImageJ. The data showed a remarkable decreased in lipid droplet accumulation (number and size) in PA-treated cells with NR compared to PA alone (**Figure 8B; C**). This demonstrates a preventive role of NR in neutral lipid accumulation induced by PA in renal tubular cells.

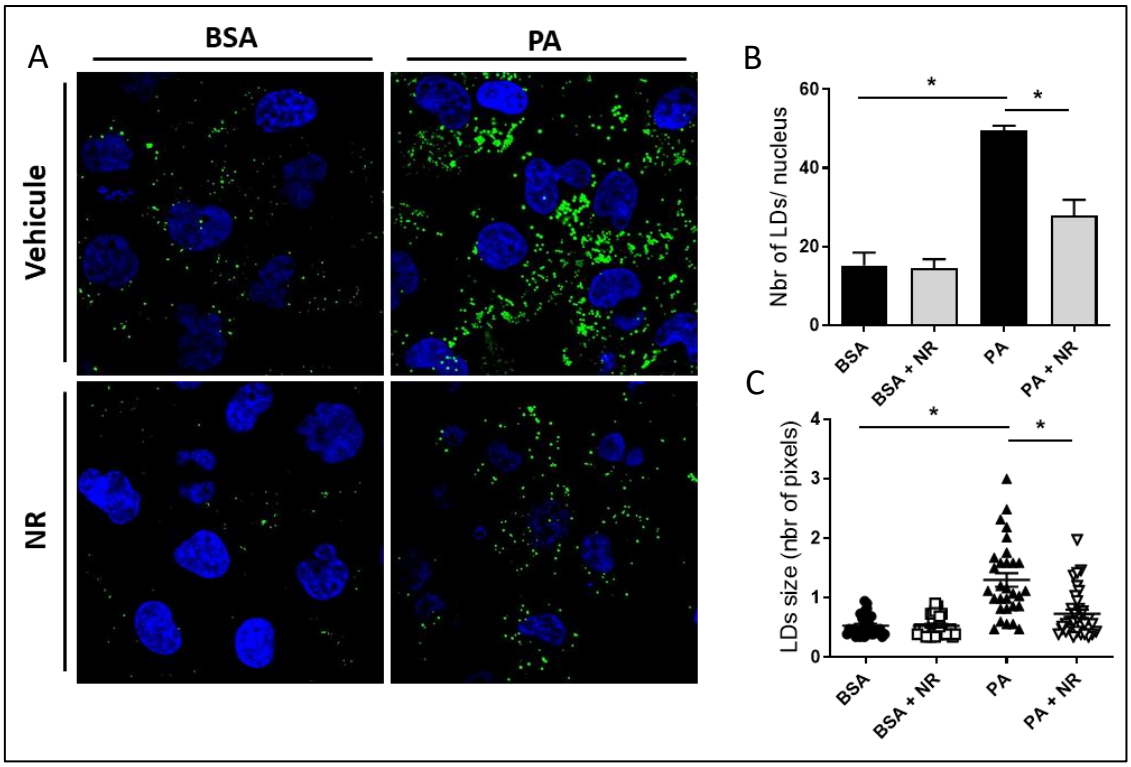

Figure 8. NR prevents PA-induced lipid droplets accumulation in HK-2 cells A. Confocal analysis of BODIPY 493/503 staining (green) to visualize lipid droplets structures in HK2 treated with BSA 300 µM, PA 300 µM with or without NR 1 mM. Nuclei were counterstained with Hoechst Dye (blue). **B**. Quantifications of number of lipid droplets obtained from five randomly selected field per condition, with each containing 20-30 cells, normalized with the number of nuclei. n=3. **C**. Quantifications of changes in the average size of lipid droplets in HK2 cells (n=30 cells from 3 independent replicates). Each point represents the average size of lipid droplets in a cell. Data are Mean ± SEM. One-way ANOVA followed by Newman Keuls post-hoc analysis.

7.4.3 NR prevents mitochondrial ROS production induced by PA in renal tubular cells.

ROS are short-lived oxygen-containing molecules that are highly reactive and can promote oxidative stress. They are the byproducts of aerobic respiration, and primarily arise from the mitochondria; excessive ROS production can cause damage to the mitochondria. In this study, we found that PA promoted mitochondrial ROS production in HK-2 cells by using the MitoSOX molecular probe. As demonstrated in **Figure 9B**, PA condition is associated to an increased MitoSOX fluorescence intensity as compared to BSA. However, this increased mitochondrial superoxide production was alleviated in PA+NR compared to PA alone. This allows us to suggest that NR in implicated in anti-oxidative response or improvement of mitochondrial dysfunction in PA-associated lipotoxicity in renal cells. To confirm the impact of NR on oxidative damages, the lipid peroxidation was then measured.

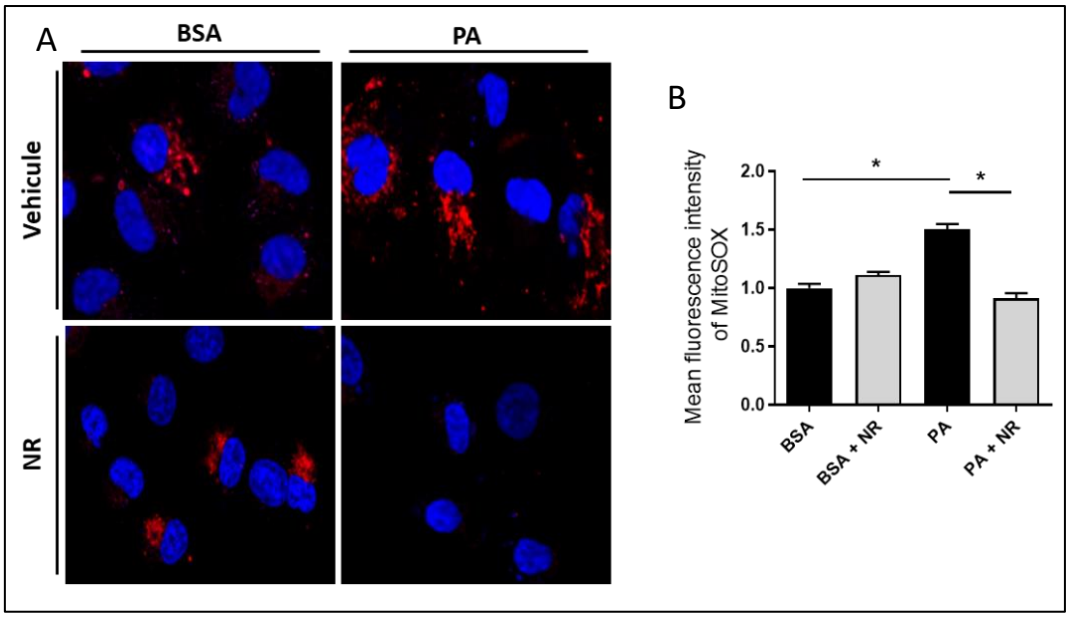

Figure 9. NR prevents PA-induced mitochondrial ROS in HK-2 cells A. Confocal analysis of MitoSOX staining in HK2 treated with BSA 300 µM, PA 300 µM with or without NR 1 mM. Nuclei were counterstained with Hoechst Dye (blue). **B**. Quantifications of mean fluorescence intensity obtained from five randomly selected field per condition, with each containing 20-30 cells, normalized with the number of nuclei. n=3 biological replicates. Data are Mean ± SEM. One-way ANOVA followed by Newman Keuls post-hoc analysis.

7.4.4 NR suppresses the induction of lipid peroxidation induced by PA in renal tubular cells.

To highlight the peroxidation of lipids in response to oxidative stress induced by lipotoxicity in HK-2, we used a lipid peroxidation sensor that shifts from red to green upon oxidation by lipid hydroperoxides. As demonstrated in **Figure 10**, the green to red ratio was increased in PA condition corresponding to an induction of lipid peroxidation by PA treatment of renal cells, possibly due to the production of ROS by mitochondria as demonstrated just before. Moreover, accordingly to the previous result, NR treatment also prevented lipid peroxidation in PA-treated HK2 cells. Thus, these results demonstrate that NR not only inhibits mitochondrial superoxide but also improved a key consequence on oxidative stress, the peroxidation of lipids.

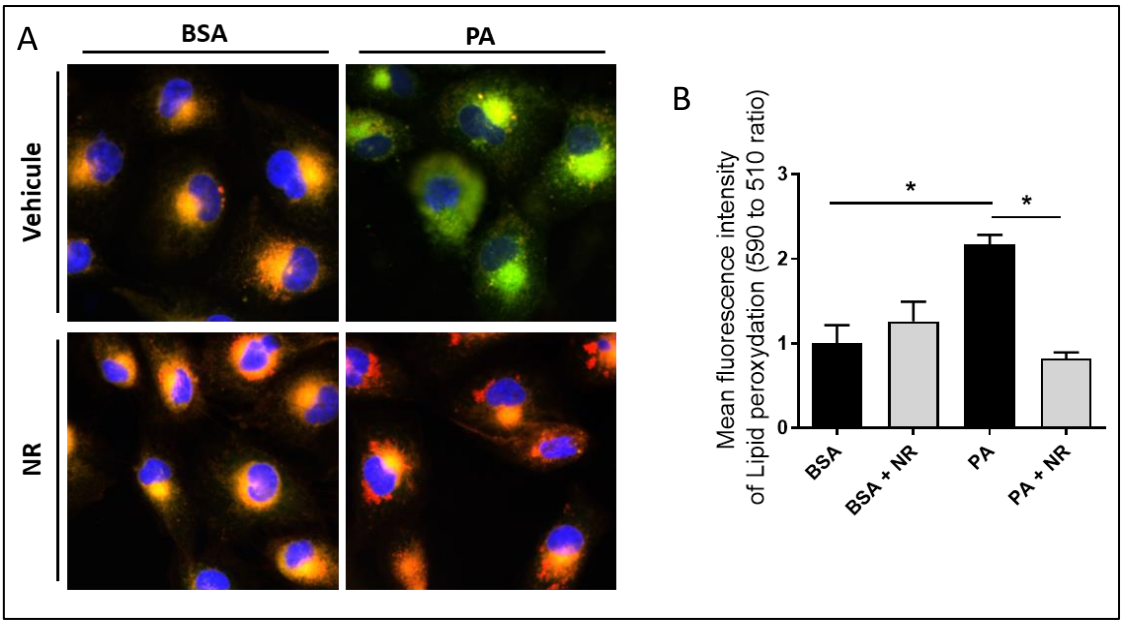

Figure 10. NR prevents PA-induced lipid peroxidation in HK-2 cells A. Confocal analysis of lipid peroxidation staining in HK2 treated with BSA 300 µM, PA 300 µM with or without NR 1 mM. Nuclei were counterstained with Hoechst Dye (blue). **B**. Quantifications of mean fluorescence intensity obtained from five randomly selected field per condition, with each containing 20-30 cells, normalized with the number of nuclei. the ratios of the signal from 590 to 510 channels were used to quantify lipid peroxidation in cells. Data normalized to the control BSA. *n=3* biological replicates. Data are Mean ± SEM. One-way ANOVA followed by Newman Keuls post-hoc analysis.

7.4.5 NR enhances mitochondrial function in proximal tubular cells exposed to PA.

Seahorse metabolic flux analyses measuring oxygen consumption rate (OCR) confirmed impaired mitochondrial bioenergetics in PA-treated cells, as evidenced by a significant reduction in the baseline respiration, ATP turnover and total respiratory capacity (**Figure 11**). The basal respiration represents the energetic demand of the cell under baseline conditions. The decrease in oxygen consumption rate upon injection of the ATP synthase inhibitor oligomycin represents the portion of basal respiration that was being used to drive ATP production. The proton leak represents the remaining basal respiration not coupled to ATP production. The maximal oxygen consumption rate attained by adding the uncoupler FCCP. FCCP mimics a physiological "energy demand" by stimulating the respiratory chain to operate at maximum capacity, which causes rapid oxidation of substrates (sugars, fats, and amino acids) to meet this metabolic challenge. The results demonstrate a decreased in basal respiration, ATP production and maximal respiration in HK-2 cells exposed to PA. Importantly, NR treatment improved all parameters suggesting that NR improves function and homeostasis of mitochondrial network in PA condition.

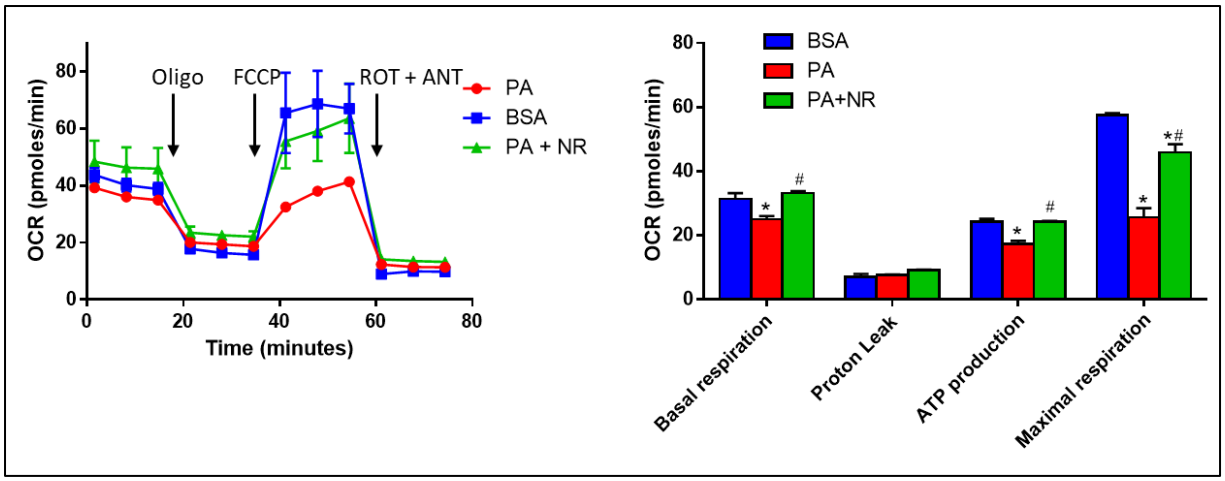

Figure 11. NR prevents mitochondrial dysfunction in PA-exposed HK2. Oxygen consumption rate (OCR) and individual parameters for basal respiration, ATP production, proton leak, and maximal respiration in HK2 treated with BSA 300 µM, PA 300 µM or PA 300 µM + NR 1 mM. Oxygen consumption rates (OCRs) were measured under basal level and after the sequential addition of oligomycin (Oligo, 1 µM), FCCP (0.5 µM), and Rotenone (ROT; 1 µM) + Antimycin A (ANT; 1 µM); *n = 3* independent experiments. Data are Mean ± SEM. One-way ANOVA followed by Newman Keuls post-hoc analysis.

7.4.6 NR supplementation does not impact body weight but decreases organ weight when used concomitantly with HFD.

Here, we investigated the effect of NR supplementation in food in mice fed a LFD or HFD for 20 weeks. The NR was administrated either concomitantly with the diet (LFD NR20 and LFD NR20) or as a delayed treatment for the last 8 weeks of the protocol (LFD NR8 and HFD NR8). We followed the body weight gain of each experimental group throughout the protocol. As observed in **Figure 12A**, a significant increase in body weight was observed from week 8 in HFD-fed mice compared to LFD-fed mice. This increase was maintained throughout the experimental protocol in HFD groups compared with LFD groups (**Figure 12**). However, no significant difference was observed with NR supplementation for each diet-matched group. The **Figure 12B** presents the changes in kidney, liver and heart weights of mice fed a LFD or a HFD with or without NR supplementation at the end of the protocol. As shown, the weights of kidneys and the liver were higher in mice fed a HFD compared to mice fed a LFD. Moreover, concomitant NR supplementation prevented this change as evidence by the significant decreased observed in HFD NR20 group compared to the HFD group. In contrast, no difference was observed in mice treated for the last 8 weeks.

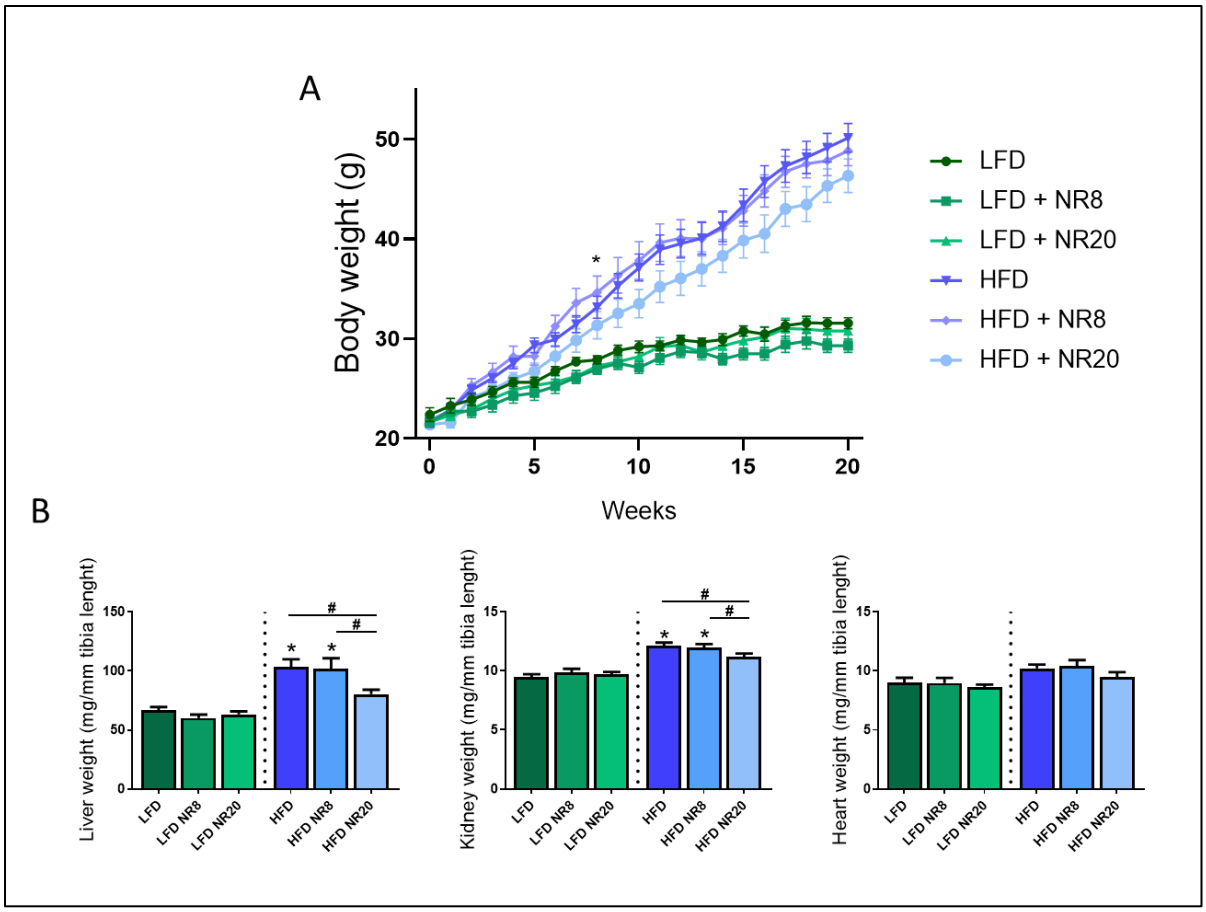

Figure 12. Effects of NR supplementation on body and organ weight gain mice fed a LFD or HFD. A. Body weight evolution. B. Organ weights at week 20. Statistical analyses were performed by two-way ANOVA followed by Newman–Keuls *post hoc* test. Data are presented as means ± SEM.* $P \leq 0.05$ *versus* LFD $^{\#}$ $P \leq 0.05$ *versus* HFD. *n=10* in each group.

7.4.7 NR supplementation does not improve glucose tolerance, hyperglycemia and insulin resistance in obese mice.

As previously described in the last chapters, mice fed a HFD for 20 weeks develop glucose intolerance, hyperglycemia, and hyperinsulinemia. The glycemia and insulinemia was significantly higher in all HFD groups compared to LFD groups with no change with concomitant or delayed NR supplementation. Moreover, a glucose tolerance test (GTT) was performed at the end of the experimental protocol (20 weeks) (**Figure 13**). The data confirmed the development of a glucose intolerance in all HFD groups compared to LFD controls. NR did not improve these parameters. Altogether, these results demonstrate that NR has no influence on impaired glucose metabolism in obese mice.

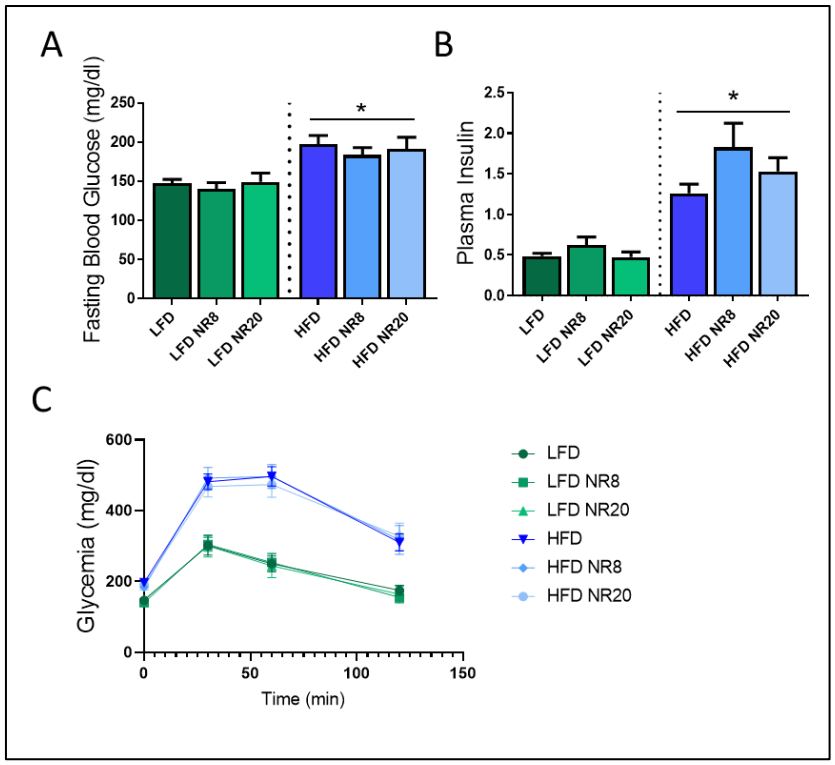

Figure 13. Effects of NR supplementation on glucose tolerance and insulin resistance in mice fed a LFD or HFD. Fasted mice were submitted to an intraperitoneal injection of glucose (2 g/ kg b.w.). Glycemia was measured before (0) and 30, 60 and 120 min after injection. **A. Fasted blood glucose at week 20. B. Plasma insulin level at week 20. C.** Glucose tolerance test (GTT) at week 20. Statistical analyses were performed by one-way ANOVA followed by Newman- Keuls *post hoc* test. Data are presented as means ± SEM. * $P \leq 0.05$ versus LFD # $P \leq 0.05$ versus HFD. *n=10* in each group.

7.4.8 NR supplementation does not improve hepatic steatosis in obese mice but reduces fibrosis

The **Figure 14** presents histological investigations of the liver from mice fed a LFD and a HFD with or without concomitant or delayed NR supplementation. As already described in the section I, HFD mice showed characteristic features of hepatic steatosis as evidenced by the presence of large lipid droplet accumulation in hepatocytes (**Figure 14A**). NR supplementation in HFD did not improved hepatic lipid accumulation. However, in the liver tissue of HFD mice treated with NR for 20 weeks, the accumulation of macrovesicular lipids seemed to be decreased, taking place for microvesicular lipid accumulation (high number of small lipid droplets). Surprisingly, a moderate accumulation of hepatocellular lipids was found in the LFD mice groups treated with NR either for the last 8 weeks or the 20 weeks of the protocol. On the other end, the hepatic fibrosis was investigated using Sirius red staining. As demonstrated in **Figure 14D**, HFD liver present an increased percentage of fibrosis compared to the LFD control. Liver fibrosis was prevented by NR supplementation in HFD mice. Moreover, LFD mice treated with NR did not shown any further fibrosis compared to the LFD without treatment.

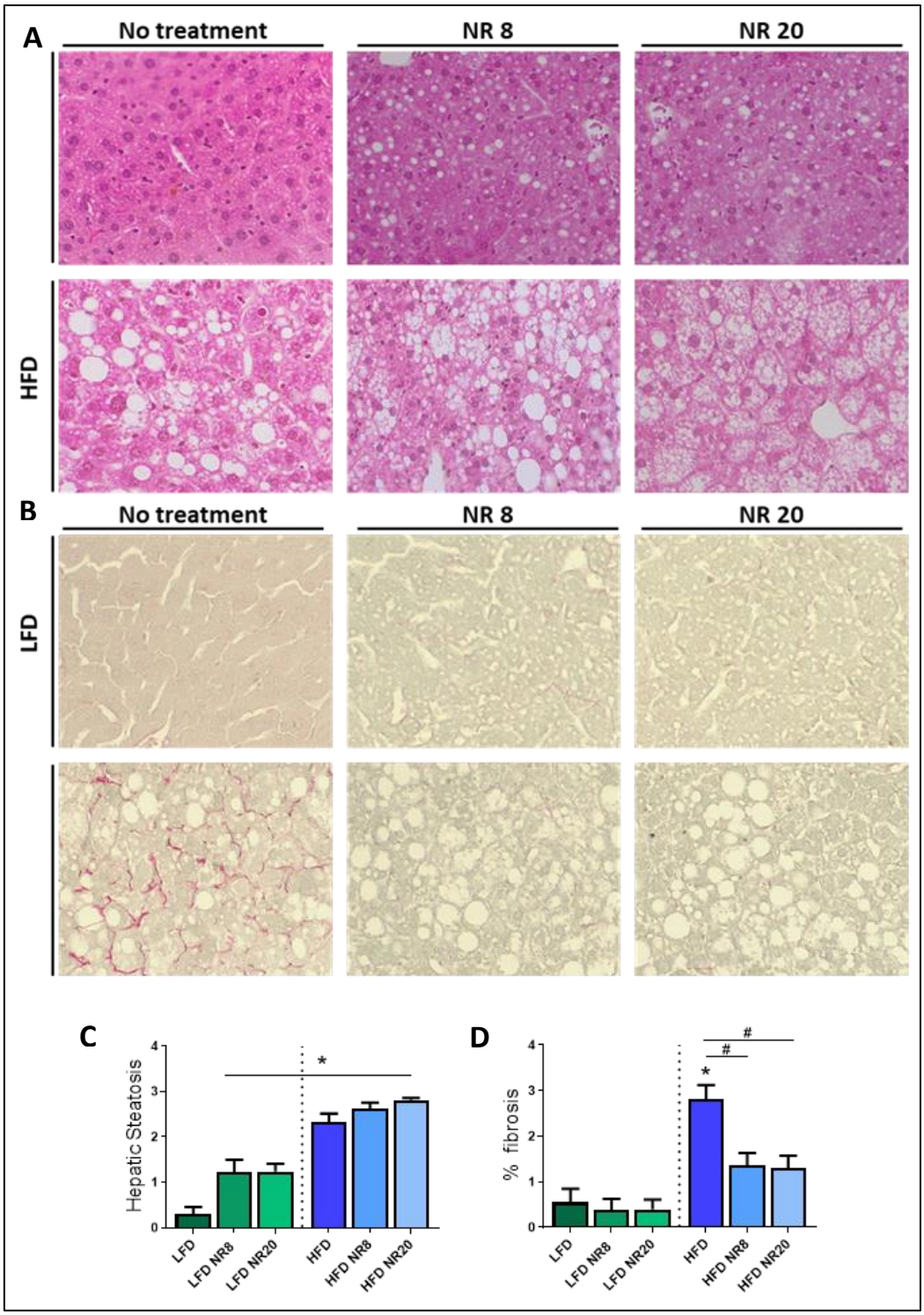

Figure 14. Effects of NR supplementation on hepatic steatosis and fibrosis in mice fed a LFD or a HFD. **A** Representative photomicrograph (original magnification ×400) of H&E staining illustrating hepatic steatosis from liver sections at week 20 of the experimental protocol. **B.** Representative photomicrographs (original magnification ×400) of Sirius red staining illustrating hepatic fibrosis. **C**. Steatosis scoring by semi-quantitative analyses of lipid accumulation. **D**. Quantitative analysis of the mean percentage of positive staining for Sirius red staining. Statistical analyses were performed by one-way ANOVA followed by Newman–Keuls *post hoc* test. * $P \leq 0.05$ *versus* LFD $^{\#}$ $P \leq 0.05$ *versus* HFD. Data are presented as means ± SEM. *n=10* in each group.

7.4.9 NR supplementation ameliorates glomerular hypertrophy but slightly improves kidney function in obese mice

As observed in **Figure 15**, HFD mice developed glomerular hypertrophy associated to impairments of renal function, which corroborate our previous results (section I). Indeed, glomerular area was increased in HFD mice in comparison with the LFD control (**Figure 15B**). However, the increased mesangial matrix expansion observed in HFD group did not reach a significant difference in HFD mice treated with NR (**Figure 15C**). Interestingly, albuminuria was found to be slightly improved in HFD mice supplemented with NR for the last 8 weeks of the protocol but the data did not reached the signification (p=0,0645). (**Figure 15D**). However, no significant difference was found between LFD and HFD mice treated with NR.

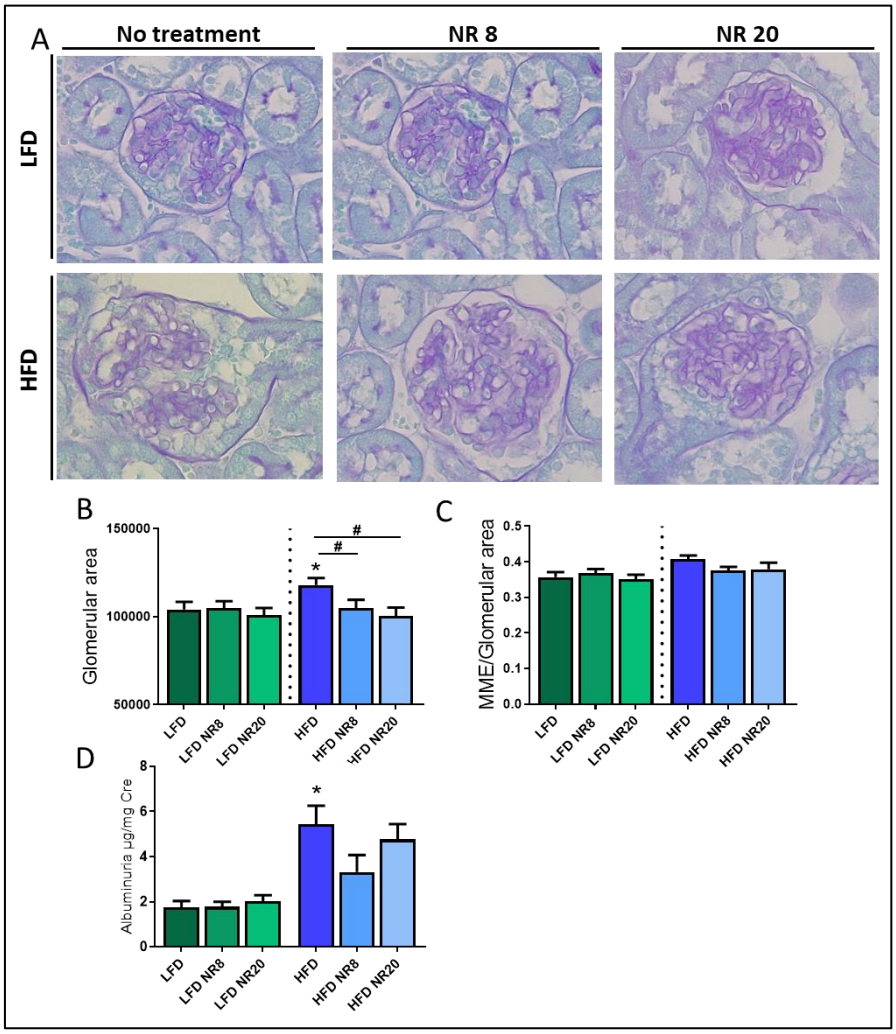

Figure 15. Effects NR supplementation on renal function and glomerular histology in mice on LFD or HFD. **A**. Representative photomicrographs (original magnification × 400) of PAS staining illustrating glomerular structure from renal cortex sections from mice et week 20. **B**. glomerular area. The glomerular tuft area was averaged from 15 glomeruli per kidney section, using one kidney section per animal. **C**. Mesangial matrix area percentage of total glomerular area. **E.** Quantitative measurement of urinary albumin to creatinine ratio (UACR) at week 20. Statistical analyses were performed by one-way ANOVA followed by Newman–Keuls *post hoc* test. * $P \leq 0.05$ *versus* LFD $^{\#}$ $P \leq 0.05$ *versus* HFD. Data are presented as means ± SEM. *n=10* in each group.

7.4.10 NR supplementation does not reduce tubular lipid deposition in obese mice

We further investigated the renal ectopic lipid depositions in proximal tubule. We particularly confirmed the consistent lipid droplets accumulation in proximal tubule of HFD mice (**Figure 16**). NR treatment was surprisingly associated to an increased number of vacuolated tubules in HFD mice but also in LFD mice in the group treated with NR for 20 weeks.

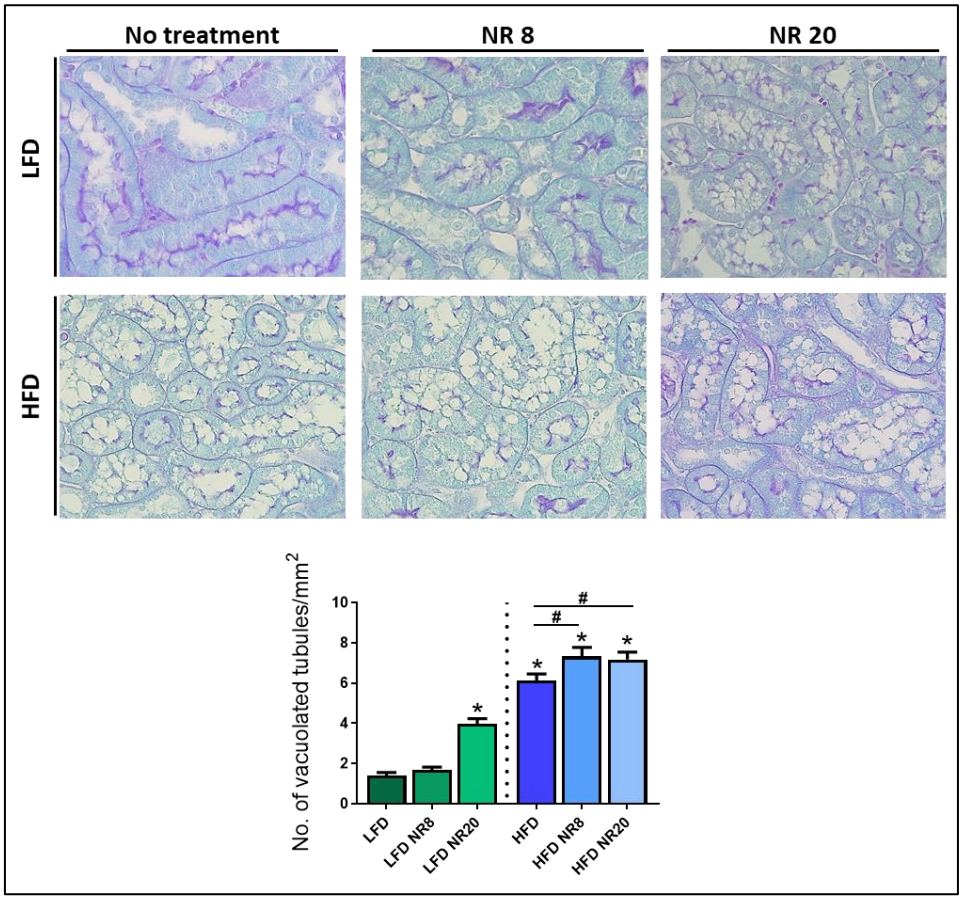

Figure 16. Effects NR supplementation on tubular lipid content from mice on LFD or HFD. A. Representative photomicrographs (original magnification ×400) of PAS staining illustrating vacuolated proximal convoluted tubular cells from renal cortex sections from mice at week 20. **B**. Quantitative analysis of number of vacuolated tubules per mm^2. Statistical analyses were performed by one-way ANOVA followed by Newman–Keuls *post hoc* test. * $P \leq 0.05$ *versus* LFD $^{\#}$ $P \leq 0.05$ *versus* HFD. Data are presented as means ± SEM. *n=10* in each group.

7.4.11 NR supplementation enhances SIRT3 activity in renal tissue of obese mice.

In order to confirm SIRT3 activation by NR supplementation in experimental mice, we analyzed the acetylation profile of lysine and the protein level of acetylated SOD2, one of the main targets of SIRT3, in mitochondrial enriched fraction of renal cortex. HFD mice appeared to present an increased acetylation of lysines (**Figure 17A; B**) but this change did not reach the signification (p=0,0872). However, HFD in mice induced a remarkable increased in acetylated-SOD2, as we expected, suggesting a decreased SIRT3 activity in mitochondria (**Figure 17A; C**). Moreover, NR treatment in mice fed a HFD significantly reduced the acetylation of SOD2 confirming the induction of deacetylation of SOD2 by SIRT3 in response to NR in renal tissue of obese mice. These results need to be replicates in order to confirm the statistical analysis.

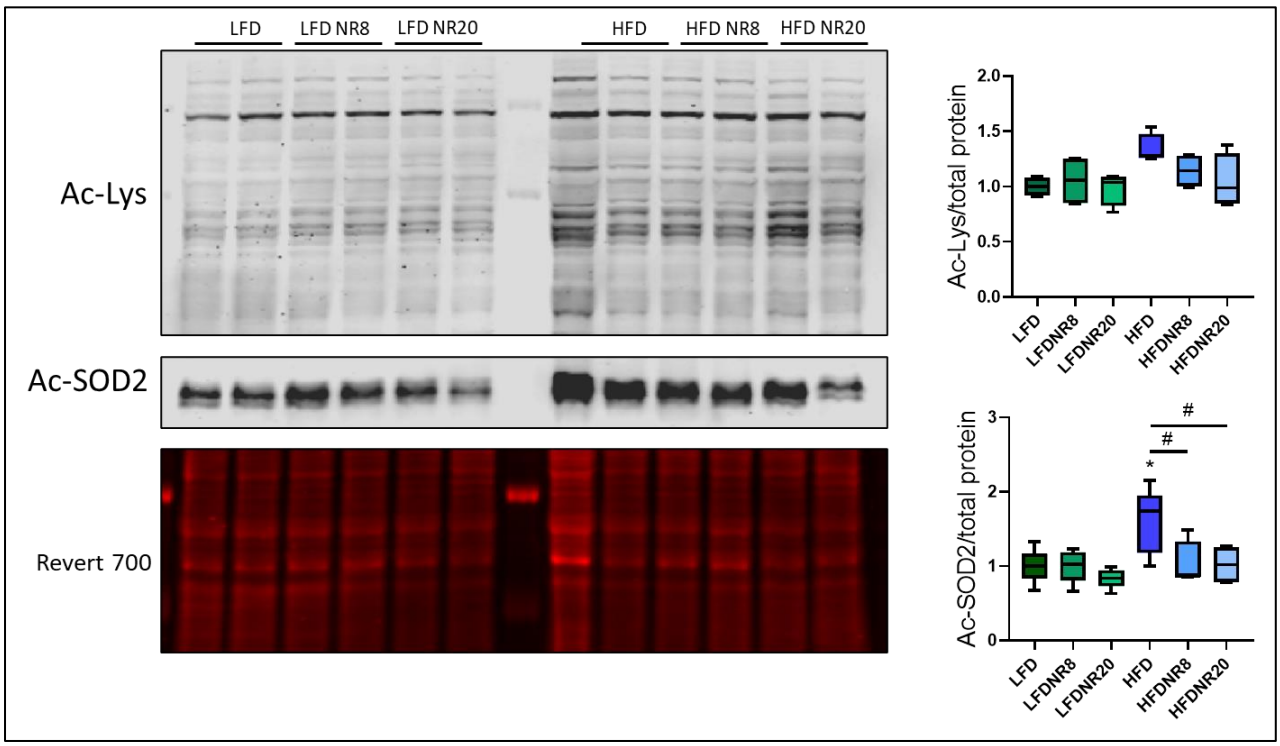

Figure 17. Effects NR supplementation on mitochondrial Lysine acetylation and SOD2 acetylation in renal tissue from mice on LFD or HFD. A. Western Blot analysis in mitochondria-enriched fractions of Ac-Lysine and Ac-SOD2 K68 (Cell signaling antibodies) in mitochondrial fraction of the renal tissue from mice at week 20. **B-C**. Relative densitometry of the immunoblots representing respectively Ac-Lys protein level normalized with total protein (Revert 700) and Ac-SOD2 K68 protein level normalized with total protein (Revert 700). Statistical analyses were performed by one-way ANOVA followed by Newman–Keuls *post hoc* test. Data are presented as Boxes min to max. * $P \leq 0.05$ versus LFD # $P \leq 0.05$ versus HFD. *n=4-6* in each group.

7.4.12 NR supplementation normalizes AMPK activity in obese mice

We further investigated the effects of NR supplementation on AMPK activity in mice fed a HFD. In line with our previous results, AMPK activity was decreased in response to 20 weeks of HFD (**Figure 18**). Indeed, AMPK activity in HFD mice was significantly decreased compared to the LFD control. Contrarily, HFD mice treated with NR did not present any significant difference compared to the LFD control, suggesting that NR supplementation prevented or enhanced AMPK activity in obese mice. However, no significant difference was observed between HFD treated mice and HFD mice without treatment. These results need to be replicates in order to confirm the statistical analysis.

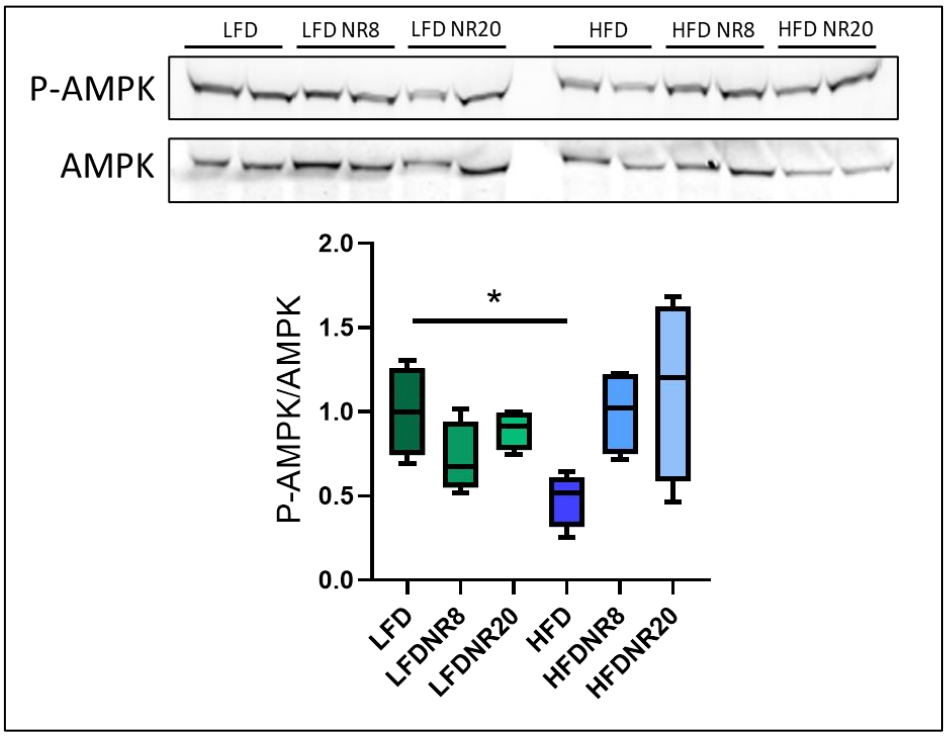

Figure 18. Effects of NR supplementation on AMPK activity in LFD or HFD mice. A. Western blot analysis on total kidney protein extracts for phospho-AMPK and total AMPK. **B**. Quantitative densitometry of the immunoblot. Statistical analyses were performed by one-way ANOVA followed by Newman-Keuls *p≤0.05 vs LFD, #p≤0.05 vs HFD. . Data are presented as Boxes min to max. *n=4*

7.5 Discussion

Based on our previous results regarding the potential role of SIRT3 in the pathogenesis of obesity-induced CKD, we decided to explore the cellular dysfunction resulting from the accumulation of lipids in the kidney through the SIRT3/AMPK axis in our *in vitro* and *in vivo* experimental conditions. Here, the putative beneficial effect of the activation of SIRT3 by Nicotinamide Riboside, a NAD^+ precursor, was explored.

In vitro study

First, we characterized the effects of NR on HK-2 cells. Cells were exposed to PA to mimic obesity *in vitro.* PA is the most abundant saturated FFA in the Western diet. Exposition with PA is widely used to investigate lipotoxicity on specific cell cultures. Its negative effects on cells include insulin resistance, atrophy, differentiation defects, apoptosis and increase of ROS along with mitochondrial dysfunction [184,570]. NR treatment was used to prevent lipotoxicity and mitochondrial dysfunction by activation of SIRT3/AMPK axis. First, we demonstrated that NAD^+/NADH ratio was significantly decreased in PA-treated HK-2 cells. As expected, treatment with NR prevented this reduction and even greatly increased the ratio in control condition. Thanks to this result, we may assume that NR is well metabolized into our cell culture conditions. As already mentioned, SIRT3 is a NAD+-dependent deacetylase, thus relying on NAD^+ to maintain an optimal activity. Similar decrease in NAD+ level in lipotoxicity context has been already highlighted in primary human hepatocytes and in hippocampal neurons [571,572]. In these studies, SIRT3 activity and expression were decreased. Here, as expected, NR treatment significantly upregulated SIRT3 protein level in HK-2 cells exposed to PA. Indeed, it was shown that NR upregulated SIRT3 in other cell types such as hepatocytes [573]. This upregulation may suggest that SIRT3 play a role in NR-mediated effects. The mitochondrial SIRT3 is likely to be particularly responsive to pharmacologically administered NR, since NR preferentially increases mitochondrial NAD^+ levels [541]. SIRT3 expression is notably regulated by PGC1-α that could explain its upregulation as it is the case for SIRT1. In hepatocytes, NR was associated to the upregulation of PGC1-α, thus leading to the upregulation of SIRT3 [573,574]. Moreover, AMPK activity was found to be increased with NR treatment. This is in agreement with our hypothesis regarding the SIRT3/AMPK axis. However, it is not unlikely that this could be an indirect effect of NR on AMPK activity, independent of SIRT3. However, we showed that the upregulation of SIRT3 expression and increased AMPK activity were associated to a decreased accumulation of lipid droplets with NR treatment in renal cells exposed to PA. This was also demonstrated in a model of alcoholic hepatic steatosis as well as in adipocytes [575]. Similarly, in another study, Zhang *et al* showed that SIRT3 activation led to an induction of the macroautophagy of lipid droplets through AMPK-mediated ULK-1 activation in adipocytes [576].

However, here, even though a decrease in lipid droplets was demonstrated, further investigations are needed to delineate the cellular mechanisms underlying these changes.

In our study, the increased lipid droplets in PA-treated cells was associated to an increase in mitochondrial superoxide, suggesting mitochondrial injury or reduction of anti-oxidative defense. Other groups have previously studied the effects of PA on ROS production in podocytes [577,578]. They showed an increased ROS production, associated to mitochondrial dysfunction and impairment of mitophagy. Here, the treatment with NR was associated to protection against oxidative stress. SIRT3 is known to be implicated in the regulation of oxidative stress by deacetylation of substrates involved in both ROS production and detoxification [579]. These results were then corroborated by the characterization of mitochondrial function using respirometry. Indeed, PA was associated to a decreased global mitochondrial function, particularly regarding the basal respiration of mitochondria and production of ATP that could lead to detrimental effects for renal cells as there are rich in mitochondria and highly ATP-dependent for their function. Interestingly, NR treatment abolished PA-induced mitochondrial dysfunction in the HK-2 cells. This result goes along with the increased NAD^+/NADH ratio in NR-treated cells. Administration of NAD^+ precursor, nicotinamide mononucleotide (NMN), has already shown to improve mitochondrial bioenergetics in brain tissue [580]. In that study, the beneficial effect was dependent of SIRT3. Finally, another hallmark of lipotoxicity is the lipid peroxidation which corresponds to the oxidative degradation of lipids by ROS. Lipid peroxidation may affect cellular membranes, lipoproteins, and other molecules that contain lipids by impairing membrane integrity. In line with the enhanced ROS production, lipid peroxidation was also increased in PA-treated renal cells. As we expected, NR prevented this change suggesting the reduction of detrimental effects of ROS in renal cells exposed to PA. Indeed, SIRT3 controls the mitochondrial oxidative pathways and consequently the rate of ROS production [581]. SIRT3-mediated deacetylation activates enzymes responsible for reducing ROS in protective action against oxidative stress such as SOD2. SIRT3 also promotes the tricarboxylic acid cycle and electron transport chain function by regulating the complex I, thus in turn lead to an enhanced mitochondrial bioenergetic [582,583].

In summary, the *in vitro* data demonstrated beneficial effects of NR in reducing mitochondrial impairment and associated ROS damages by enhancing SIRT3 expression and AMPK activity.

More investigations in our model must be performed to better highlight the precise role of SIRT3 in lipotoxicity-induced cellular damages. Moreover, here, we were not able to prove a direct link between SIRT3 and AMPK, even though upregulation of SIRT3

expression was concomitant to increased AMPK activity. Gain and loss of function experiments will be very useful in order to characterize the implication of each factor in NR-induced effects.

In vivo study

The next step was to investigate the SIRT3 gain of function in the HFD mice model that we previously described in section I and II. Here, NR was used as a preventive therapy (long-term administration of NR for 20 weeks) or as a treatment (for the last 8 weeks of the protocol- similar to the protocol with exercise training, section I). Indeed, Canto *et al* nicely demonstrated that 400 mg/kg/J NR treatment in HFD mice for 10 weeks increased plasma and intracellular NAD^+ in muscle, brown adipose tissue dans liver as well as increased SIRT3 activity [541]. However, the particular effects of NR supplementation for obesity-associated abnormalities is still poorly investigated.

First, we studied the effects of chronic exposition to NR in HFD mice on metabolic parameters. As already reported, NR had no effect on glucose metabolism as described by Canto *et al*. However, while NR supplementation had no major effect on body weight, chronic supplementation with NR for 20 weeks reduced liver and kidney weight, suggesting a potential metabolic effect of NR, especially regarding liver steatosis. Unexpectedly, HFD mice with NR presented similar hepatic steatosis than the one found in HFD mice without treatment, excepted for HFD mice treated with NR for 20 weeks where we noticed more microvesicular steatosis compared to the other HFD groups. More surprisingly, NR in the control LFD was associated to an increased lipid deposition, suggesting that NR may enhances lipogenesis or decrease lipolysis in hepatocytes. In contrast, NR was associated to beneficial effects regarding liver fibrosis as attested by collagen deposition that was markedly reduced in HFD mice treated with NR. Very recently, Pham *et al.* reported the effects of NR supplementation for 20 weeks (at the same dose than our study) on hepatic steatosis in mice fed a high-fat/high-sucrose/high-cholesterol diet [584]. Interestingly, they showed that NR markedly reduced collagen accumulation in the liver but not lipid accumulation as we also observed in our study, suggesting that the protective effect of NR on liver fibrosis was independent of changes in liver steatosis. Unfortunately, they did not present the corresponding control mice treated with NR. Here, the particular impact of NR on lipid accumulation in the liver needs further investigations, particularly on the nature of lipids and the potential association with lipotoxicity. Also, intracellular NAD^+ increase by NR supplementation would lead to an activation of NAD^+ dependent enzymes, mostly SIRT1 and SIRT3 as previously demonstrated by Canto *et al*. However, since NAD^+ acts also as a cofactor for metabolic pathways, a chronic NR treatment may induce an increase in the NAD^+/NADH ratio that results in more NAD^+ availability for glycolysis

as well as in an increased NAD^+/NADH ratio in mitochondria that could lead to a decrease in electron transfer to Complex I as suggested by Song *et al* [585]. Therefore, long term exposure with NAD^+ could thus reduce metabolic flexibility by sustaining a high NAD^+/NADH ratio that is normally tightly regulated by the cells to adapt their metabolism.

Next, we demonstrated for the very first time the ability of NR to activate SIRT3 in mitochondrial fraction of renal cortex as evidenced by the decreased acetylation of SOD2. SOD2 becomes hyperacetylated due to a decline in activity of the mitochondrial deacetylase SIRT3. Reduced SIRT3 activity and SOD2 hyperacetylation contribute to oxidative stress and associated mitochondrial dysfunction [586]. In our experimental model, HFD mice presented SOD2 hyperacetylation in renal tissue that was abolished by NR supplementation. Further investigations on oxidative stress and mitochondrial markers will give us precious data on the downstream effects of SIRT3 activation in renal tissue. We also described the effects of NR on kidney function, glomerular and tubular injuries. The results did not demonstrate a valuable effect of NR supplementation in HFD mice regarding characteristic features of obesity-induced kidney injury. Indeed, despite the glomerular area was found to be decreased in HFD mice treated with NR for 20 weeks, the albuminuria was not strongly affected. Moreover, NR supplementation was associated to a small but significant increase in ectopic lipid accumulation in tubular cells in line with the results found in the liver. Also, chronic treatment with NR during 20 weeks was associated to an increased lipid depositions in control mice, suggesting the NR is implicated in further accumulation of lipids in renal tissue, as we also shown in liver tissue. This may also suggest that NR may impact the lipogenesis and/or lipolysis in PTC.

Overall, despite we demonstrated that NR supplementation effectively activates SIRT3 in renal tissue of obese mice associated to a stronger AMPK activity, the renal impacts were mitigated. Moreover, our results highlighted an increased ectopic lipid deposition in liver and kidney, probably by an alternative mechanism independent of SIRT3 and AMPK activity. We suspect that NR supplementation leading to NAD^+ increase in tissues may reduce metabolic flexibility of tissue during long-term exposure. The renal and liver impact of NR should be further explored as number of clinical trials on NAD+ precursors like the Nicotinamide riboside (NR) and the nicotinamide mononucleotide (NMN) are ongoing [ABOUTNAD (https://www.aboutnad. com/human-clinical-trials)]. A more complete understanding of the effects of these compounds would lead to invaluable data regarding long term use of NAD^+ precursors in human.

DISCUSSION

8 General discussion

The increased prevalence and incidence of obesity and associated metabolic syndrome have constantly increased worldwide during the last decades as never seen in human history. According to the previsions, this phenomenon will continue to grow to dramatic levels in the future (60% of the population would become obese by 2050 in Europa). This tendency for which emerging countries were spared until now, seems to extend to all countries because of the westernization and globalization. The increased number of overweight people around the world is mainly due to poor eating habits and a marked decrease in physical activity. Diets rich in sugars, animal products and *trans*-fat are important risk factors for non-communicable diseases, such as CVD, diabetes and various types of cancer. Moreover, obesity prevalence among children and teenagers is also importantly increasing and it is still poorly known what the consequences during their adulthood will be. Thus, obesity epidemic represents an important health and scientific challenge to prevent and/or treat obesity-related diseases. Indeed, obesity has been associated to metabolic disturbances that contribute or initiate multiple pathologies, representing an important health care issue and an economic burden. Despite the scientific research have shown growing interest in the understanding of obesity-associated diseases and the discovery of potential therapeutic strategies, there is an evident lack of knowledge regarding the emerging plethora of the health consequences of obesity.

This present PhD thesis was dedicated to the study of the renal consequences of obesity and the new perspectives in obesity-induced CKD healthcare. A robust accumulation of lipids within enlarged multilaminar inclusions into the proximal tubules along with an impaired tubular function, increased oxidative stress as well as mitochondrial dysfunction in obese mice were demonstrated by our group and others. In addition, we previously showed that AMPK plays a critical role in regulating the chronic cellular response to lipid excess. AMPK is a major sensor of energy in cells. It has been widely demonstrated that AMPK pathway is dysregulated in the liver and in muscle tissue during obesity. Despite its role as an energy sensor, the implication of AMPK in mitochondrial dysfunction and mitophagy as well as in lipophagy has been particularly highlighted during the last years. Consequently, AMPK has been proposed as a key therapeutic target for obesity-related diseases. Most of the studies have shown interesting beneficial impacts of AMPK activation to counteract obesity-related health problems as CVD or non-alcoholic fatty liver disease. However, little is known about the precise implication of AMPK in obesity-induced CKD, particularly in regulating autophagy and mitochondrial function in renal cells.

Limitations of the actual therapeutic strategies

It might be worth to remind that the current diagnosis of obesity relies on a formula that uses height and weight and thus, not by a specific biomarker. Current management of obesity is based on lifestyle modifications (weight loss by dietary modification and/or physical activity), drug therapies or surgical interventions. Current pharmacotherapies that target food intake regulation present side effects (psychiatric and/or cardiovascular side effects) observed for long periods of use and may be associated to weight regain once the medication is stopped [476]. In addition, even though AMPK has been demonstrated to represent a key target for the treatment of metabolic diseases, indirect AMPK activators such as AICAR has been widely investigated during the last decade by our group an others but did not demonstrate adequate and efficient therapeutic effects in clinical use. The ongoing development of direct and specific AMPK activators thus represents an important pharmacological challenge (discussed below) [477]. This highlights the urgent need for alternative therapeutic strategies. Recently, the study of the underlying effects of behavioral interventions as exercise training in obesity-related diseases has regained interest. Indeed, targeting the pathways that mediate the potential beneficial effects of exercise represent a safer alternative therapeutic approach for the treatment of chronic metabolic disorders. The main objective of this PhD project was thus to highlight directly applicable therapeutic strategies for the clinical management of obesity-induced CKD based on pre-clinical investigations.

Exercise-based therapy for obesity-induced CKD

Exercise training has been shown to exert beneficial outcomes in managing obesity-associated diseases. However, there is still a lack of knowledge about the underlying mechanisms. Moreover, the effectiveness of exercise-based therapeutic approach in patients presenting CKD remains controversial, mainly due to the experimental biases of the clinical studies regarding exercise training in obese patients with CKD. In the first part of the PhD thesis, we investigated the potential therapeutic effect of an EET protocol on a treadmill in obesity-induced CKD mice model. We demonstrated that EET was associated with strong metabolic improvement without weight loss in obese mice, as already reported in the literature [494]. However, only a few studies highlighted the beneficial effects of EET in long-term HFD mice model, and particularly as a delayed treatment. The originality of the study is that we particularly followed the metabolic parameters along the protocol (glucose tolerance tests, body weight, food intake, albuminuria) and that we demonstrated the potential restorative effects of EET on metabolic disturbances induced by a HFD, particularly for glucose tolerance and hepatic steatosis. Moreover, we demonstrated that delayed EET also prevented obesity-induced CKD hallmarks. Particularly, kidney function was improved along with a decreased

obesity-related glomerulopathy. Interestingly, ectopic lipid accumulations in PTC were strongly decreased with exercise. Thus, the decreased lipid depositions in the kidney and the liver suggests a particular effect of EET on the ectopic lipid accumulations in non-adipose tissues which is one of the main risk factor for obesity-associated tissues impairments [47]. This result was associated with a decreased tubulo-interstitial fibrosis along with reduced oxidative stress an inflammation in renal tissue. Finally, we highlighted that EET renal effects were associated to the activation of the AMPK pathway, leading to the restauration of the autophagy flux in renal tissue. However, autophagy involves dynamic and complicated processes that needs specific controls to alleviate the "static measurement" of basal autophagy . Thus, further studies are still needed to delineate the effects of EET on autophagy flux and its regulation by AMPK. Particularly, we propose an interesting model of primary proximal tubular cells to study the autophagy regulation *in vitro* (**see annex 1**).

The underlying effects of exercise training: exercise-induced organ communication

Exercise is known to stimulate muscle oxidative capacity and lipid oxidation. The main determinant of these metabolic effects is the increased mitochondrial oxidative capacity. The underlying molecular pathways involved in exercise-induced response in skeletal muscle cells include PGC1-α, PPARβ (transcription factors) and AMPK (metabolic sensor) [587]. Particularly, PGC1-α muscle-specific transgenic mice exhibit a similar phenotype to that of endurance trained animals regarding exercise-induced mRNA responses [588]. While ET drastically increases metabolic demand in the whole body, this metabolic demand varies depending on the exercise type, intensity and duration. Therefore, the adaptation to exercise to sustain muscle contraction not only impact muscle tissue but also other organs, highlighting the importance of inter-organ communication during exercise. Indeed, the beneficial effects of exercise training have been firstly attributed to body weight loss or body weight control, increased cardiorespiratory fitness and the maintenance of muscle mass. It is now well recognized that the important organ cross-talk during exercise for metabolic adaptation in response to this "stress" strongly explains the protection from lifestyle-induced diseases or many other pathologies by this cell-to-cell and organ-to-organ communication [589]. Despite skeletal muscle is the main communicator during exercise by its endocrine and/or paracrine function, other tissues such as the liver and the adipose tissue produce and secrete molecules in response to exercise, participating in inter-organ communication and exercise-induced effects in tissues that are not particularly recruited (metabolically) during exercise such as the brain or the kidney [590].

The molecules that are produced and released by muscle tissue are called myokines. These molecules are characterized by being produced and secreted by muscle cells and by inducing biological function in an endocrine or paracrine manner. Recently, the contraction-induced myokines, which means produced during exercise, are called "exerkines" [591]. These are either specifically produced during exercise or enhanced following muscle contraction. IL6 is particularly released by myocytes at high levels following exercise. Plasma concentration of IL-6 may increase up to 100-fold after a single boot of acute exercise session, suggesting the importance of this cytokine as an exercise-induced factor [592]. The biological effects of muscle derived-IL-6 is to contribute to the maintenance of glucose homeostasis during exercise as well as to mediate lipolysis in adipose tissue. Moreover, IL-6 also inhibits the effects of pro-inflammatory cytokines such as TNF-α [593]. IL-6 production during exercise is followed by anti-inflammatory cytokines release such as IL-10, suggesting that IL-6 may participate to the anti-inflammatory effects of exercise [593]. In AKI models, IL-6 levels in renal tissue were shown to be elevated following kidney injury [594]. However, IL-6 KO mice presented more severe AKI compared to wild-type controls, suggesting that IL-6 may be essential to control AKI-induced impairment of the kidney, particularly regarding inflammation response [594,595]. Miyagi *et al.* particularly demonstrated that aerobic exercise training in cisplatin-induced AKI in mice was associated to a lower inflammatory response in renal tissue, with less TNFα and IL-10 expression in the kidney and serum [596]. In the same study, they observed an increase of IL-6 and HO-1 expression in the kidney, indicating that chronic aerobic exercise was able to attenuate inflammation by IL-6 and HO-1 production. Moreover, stimulation of IL-6 signaling significantly improved renal damage and preserved renal function by enhancing anti-oxidative stress defense in AKI [594]. Finally, IL-6 signaling in ischemia-reperfusion model was found to be important in promoting repair process [597]. Contrarily, in our model, we described a decrease of IL-6, MCP-1 and IL-1β mRNA, suggesting that EET was associated to a decreased inflammatory response in renal tissue. However, compared to AKI, obesity-induced CKD is characterized by a low-grade inflammation and the consequent enhanced IL-6 expression as well as other cytokines in renal tissue in favor of the disease progression. Here, we thus demonstrated that EET was associated to amelioration of the inflammatory response in the kidney. However, the circulating cytokines such as IL-6 in response to exercise were not evaluated and the precise role of inflammatory environment needs further investigations. Interestingly, pharmacological activation of AMPK was associated to a decreased IL-6 production stimulated by inflammation by suppressing phosphorylation of signal transducer and activator of transcription 3 (STAT3) in the liver and adipose tissue [598]. Furthermore, IL-6 signaling in response to exercise has been associated to AMPK activation in the

muscle [599]. Another important interleukin that act as a myokine in response to exercise is IL-15 [600]. Interestingly, treatment with high doses of IL-15 results in metabolic adaptations such as improved insulin sensitivity and whole-body fatty acid oxidation and protection from high-fat-diet-induced obesity and insulin resistance, suggesting the beneficial endocrine function of IL-15 [601]. Moreover, circulating irisin, a proteolytic cleavage product of FNDC5 in skeletal muscles, is particularly increased during exercise-induced activities [602]. Irisin can act in an autocrine/paracrine manner, and when released into circulation, acts as an endocrine hormone, mediating peripheral activity. Irisin has been demonstrated to counteract insulin resistance by increasing sensitivity of the insulin receptor in skeletal muscle and heart, to improve hepatic glucose and lipid metabolism and browning of white adipose tissue through MAPK signaling but other irisin-dependent alternative pathway are currently discussed in the literature, particularly regarding a potential link with AMPK pathway [603].

These examples of the few already known myokines only represent the tip of the iceberg as "myokinome" studies have suggested that more than 300 molecules are potentially secreted by muscle tissue during exercise and this is also underestimated because many molecules communicate from the muscle to other tissues by extracellular vesicles (EVs) which include proteins, metabolites and microRNA [589]. Moreover, the liver has also a key role in inter-tissue communication during exercise. Indeed, liver tissue secretes a wide variety of molecules (more than 2500) including hepatokines and some are particularly enhanced during or after exercise [604]. The most important is probably the Fibroblast growth factor-21 (FGF21) that is particularly released by the liver following exercise [605].

Muscle-kidney crosstalk and exercise

Despite CKD is well recognized to participate in muscle wasting, the muscle-kidney crosstalk has not been strongly investigated yet, particularly regarding exercise-induced communication. Indeed, how skeletal muscle communication can prevent or suppress kidney injury is particularly emerging and not well described. However, a recent work used muscle specific PGC1-α transgenic mice to evaluate the effect on different CKD models in mice [521]. Their results suggest that muscle-kidney crosstalk ameliorates tubule cell damage and renal fibrosis. Interestingly, this study showed that myokines and particularly irisin were implicated in the muscle-induced kidney improvements. Treatment of CKD mice with recombinant irisin was notably associated to the inhibition of the TGFβ pathway and reduced renal fibrosis.

Based on the idea that exercise training has shown beneficial outcomes in pre-dialysis patients in different studies, Hanatani *et al.* investigated the effects of skeletal muscle growth *per se* on kidney diseases [606]. To do so, the authors used a muscle specific

transgenic mice overexpressing Akt1 that promotes the growth of functional skeletal muscle in order to study the muscle-kidney crosstalk in a model of renal injury induced by unilateral ureteral obstruction (UUO). Akt1 transgenic mice displayed attenuation of renal fibrosis and tubular injuries after UUO, a decreased renal cell apoptosis and reduced inflammatory cell infiltration into injured kidneys. A cytokine array using muscle tissue demonstrated that the expression of many cytokines was upregulated in Akt1 TG mice compared with WT mice, including not only renoprotective cytokines (e.g., IL-2 and IL-10) but also those that potentially have adverse effects (e.g., TNF-α). In another recent study in UUO model, Dojuksan treatment (a herbal decoction) in mice with UUO increased PGC1α and FNDC5 expression, enhanced irisin release, and attenuated kidney inflammation and fibrosis [607]. Interestingly, inhibition of AMPK by a specific inhibitor reduced the effects of irisin in myocytes and hepatocytes, suggesting that irisin could be implicated in AMPK pathway regulation [522]. In perspective with our data regarding the physiological effects of EET on kidney injury, it could be hypothesized that the beneficial effects of EET could be explained by the muscle-kidney crosstalk.

Limitations of the study

In our study, we demonstrated that delayed exercise was associated with improvement of obesity-induced CKD in mice. The exercise-induced effects were associated to improvement of AMPK-mediated FAO and autophagy. However, this study presents some limitations.

Firstly, it is worth to mention that despite we demonstrated beneficial effects of exercise training regarding obesity-induced CKD, the direct intra-renal effects of EET or the indirect effects on exercise-induced communication on the kidney is still not clear. Indeed, as we described that EET improved AMPK pathway in renal tissue, as demonstrated in other tissues such as the muscle, liver and adipose tissue, the question is how AMPK is improved in response to EET in the kidney. The kidney is not particularly recruited during exercise, suggesting that the underlying effects of EET is at least partly a consequence of muscle-kidney crosstalk, as discussed earlier. Moreover, EET improved obesity-induced metabolic disorders such as glucose intolerance, dyslipidemia and insulin resistance which are the leading cause of ectopic lipid accumulation in the kidney, mitochondrial dysfunction, and the consequent AMPK pathway dysregulation. Indeed, AMPK inhibition occurs in renal cells in response to a plethora of mechanisms including a reduced sirtuin activity, decreased adiponectin signaling, elevated circulating leptin and insulin, renal tissue inflammation and oxidative stress or CKD-associated acidosis and uremic metabolites. We could thus hypothesize that AMPK activity would benefit from EET indirect effects on these

parameters, leading to increased FAO and autophagy flux and the consequent reduced lipotoxicitiy. Furthermore, adipose tissue also exerts cross-communication with the kidney. During obesity, adipose tissue dysfunction is related to the development of chronic inflammation which participates to oxidative stress, inflammation, and fibrosis in the kidney [608]. Exercise training has been shown to improve adipocyte glucose and insulin sensitivity, β-oxidation, and mitochondrial biogenesis by activating AMPK and PGC1-α [609]. This, in turn, mediates attenuation of metabolic stress, reduction of systemic inflammation and modulation of macrophages phenotypes. The decreased inflammatory environment, FFA release and enhanced adiponectin production with exercise are known to increase FAO and to reduce ectopic lipid accumulations in skeletal muscle and in the liver [610]. In our experimental conditions, we particularly described a decreased inflammation and fibrosis in renal tissue that could be a direct or indirect consequence of adipose tissue-mediated communication and improved inflammatory environment.

Another limitation of this study is the molecular pathways that we investigated in renal tissue as well as the systemic effects of exercise in obesity condition were mostly descriptive and needs further mechanistic investigations in order to delineate the effects of exercise on the "fatty kidney". First, we must remind that cellular metabolic adaptation is highly dynamic, particularly in response to stress such as exercise in skeletal muscle. For example, exercise training-induced muscle contraction does not constitutively activate AMPK in skeletal muscle, but its activity is dependent on the type of exercise, duration and only occurs until energy recovery. This is also true for the exercise-induced short-term effects in other peripheral tissues. Despite exercise is also associated to long-term outcomes in targeted tissues, the analysis of the pathways are quite different during, right after or after exercise sessions. Here, we investigated the effects of exercise 48h after the last session of the 8-weeks EET protocol to highlight the long-term effects of exercise. Thus, all the parameters such as systemic markers or intra-renal pathways represent the exercise-induced long-term regulation of these parameters, which implies that AMPK activity or autophagy flux markers represent the basal regulation of these metabolic and cellular markers. Moreover, the regulation of FAO, AMPK activity or autophagy is also dependent on the nutritional status of the animals before euthanasia (meaning starved or fed) which is also the case for the kidney metabolism. All of these parameters may influence the collection, analysis and interpretation of the data. This is particularly important for the evaluation of the autophagy flux in experimental models. Indeed, the evaluation of the dynamic process of autophagy flux by the evaluation of specific markers such as p62 or LC3 I to LC3 II conversion could lead to misinterpretation of the autophagy flux status. For example, the increased basal protein level of p62 could be either a consequence of an increased

autophagy flux though an increased targeting of the cargo or a stagnant autophagy flux thought a downstream blockade of the autophagosome-lysosome fusion, mediating the accumulation of non-degraded p62 protein. Thus, specific controls are necessary to evaluate the efficacy of autophagy flux in specific conditions such as autophagy inducers (rapamycin or starvation) or genetic and/or pharmacological autophagy inhibition (e.g. chloroquine or ATG gene deletion) [520]. In our study, we hypothesized that exercise training was associated to an improvement of autophagy in renal tissue based on our data regarding autophagy and lysosomal markers and the previous studies. Indeed, it was previously described that a high fat diet was associated to an impairment of the autophagy flux in renal tissue. Yamamoto *et al*. nicely demonstrated that HFD induces lysosomal dysfunction with impairment in acidification leading to autophagy flux stagnation, accumulation of enlarged lysosomes and autophagosomes and accumulation of p62 and LAMP-1 in renal tissue [286]. These data corroborate our results regarding the accumulation of p62 and lysosomal markers in the kidney that were improved following EET.

Lastly, in our experimental conditions, we applied an 8-weeks exercise training protocol to mice that are known to present obesity-induced CKD (after 12 weeks on diet) as a therapeutic strategy. However, whether the beneficial effects of EET are preventative or restorative is not easy to demonstrate. Indeed, in our study, we compared sedentary CKD mice with exercised CKD mice after 20 weeks on diet and not the progression of CKD on these animals before (at 12 weeks) and after (at 20 weeks) EET. However, the data regarding the follow-up of glycemia and glucose tolerance clearly describe an improvement of obesity-related disorders with exercise suggesting that EET protocol is associated to amelioration of insulin resistance in obese mice without weight loss. CKD is defined as an irreversible and progressive disease. Therefore, we cannot exclude that our results regarding delayed EET in mice are related to a prevention of the progression of the disease when compared to sedentary control. It would be valuable to add a 12-weeks control to evaluate the restorative effect of exercise training on obesity-induced CKD features.

SIRT3 is new interesting therapeutic target for obesity-induced chronic kidney disease

The next step of the PhD project was to investigate new potential biomarkers or targets that were highlighted in the first part of the PhD project. Particularly, we focused on SIRT3, a mitochondrial NAD^+-dependent deacetylase, that we demonstrated to be decreased with HFD while its expression was enhanced with ET in kidney tissue. Indeed, SIRT3 has been found to be strongly implicated in renal diseases, particularly on acute kidney injury. However, its impact on chronic kidney diseases remained poorly investigated. Moreover, SIRT3 plays an important role in exercised-based therapy

underlying mechanisms. Here, we demonstrated for the first time that SIRT3 is decreased in renal tissue of HFD mice, suggesting a potential implication of SIRT3 in obesity-induced CKD. As we did not know whether decreased SIRT3 is a key driver of the pathology or a consequence of mitochondrial dysfunction in the kidney of obese mice, we investigated SIRT3 overexpression in our experimental model to test our hypothesis. Interestingly, HFD SIRT3 transgenic mice were found to be protected from renal dysfunction compared with wild type mice. Particularly, renal ectopic lipid accumulations were decreased with SIRT3 overexpression. These contributed to sustain our hypothesis regarding the implication of SIRT3 in renal lipotoxicity and especially to demonstrate a new potential therapeutic target for obesity-induced CKD. Interestingly, AMPK activity was restored with SIRT3 overexpression in HFD mice. As the cross-link between AMPK and SIRT3 is emerging in the literature, we suggested that SIRT3 activation is an interesting way to restore AMPK activity and to mediate beneficial renal outcomes.

The evaluation of the therapeutic potential of Nicotinamide Riboside for obesity-induced CKD

As we proposed that targeting the underlying molecular pathways that mediate the beneficial effects of exercise training is an interesting therapeutic approach, we decided to use a pharmacological compounds that enhances Sirtuin activity and that could be directly applicable in human care. The NR, an NAD^+ precursor, is a natural compound and dietary supplement that has been demonstrated to effectively activate SIRT3. Thus, we investigated the effects of NR treatment in *in vitro* and *in vivo* models of obesity. As discussed above, exercise-induced muscle contraction and subsequent release of myokines such as irisin is induced through PGC1-α. Indeed, exercise training induce an energetic stress in skeletal muscle by consumption of ATP and other substrates like NADH. Consequently, the increased AMP and NAD^+ concentration, in turn, activates AMPK and Sirtuin proteins such as SIRT1. AMPK and SIRT1 respectively phosphorylates and deacetylates target proteins and promote oxidative remodeling in muscle. NAD^+-dependent deacetylation by SIRT1 activates PGC1-α, promoting its transcriptional factor activity on mitochondrial and metabolic-related genes. Thus, we may hypothesize that NAD^+-boosting compounds such as NR could induce exercise-mimicking effects through SIRT1 activation in the muscle. Moreover, exercise was also associated to SIRT3 increased activity in skeletal muscle, leading to AMPK activation and consequent PGC1-α induction [524]. In line with previous studies, NAD^+ increase with NR in renal cell culture led to an enhanced mitochondrial function that prevented PA-induced oxidative damages. Our *in vivo* study demonstrated that NR supplementation effectively led to SIRT3 activation in renal tissue as previously showed in the muscle and the liver by others. However, the effects of NR on metabolic

alterations induced by obesity and renal injury were not prevented or ameliorated by NR. More surprisingly, NR treatment was associated to further lipid depositions in the liver and the kidney. This highlights potential adverse effects of enhancing NAD^+ content in tissues by a NAD^+ precursor. Further studies are still needed to better characterize the impacts of NR *in vivo* as no relevant data are available yet. Indeed, the question is what are the pathways implicated in the increase of lipids in response to NR treatments, what is the nature of lipids that accumulate in the tissues, is these lipid droplet accumulations are associated to lipotoxicity, is this independent on SIRT3 activation? We particularly aim to investigate the lipid profile within these tissues by lipidomics to better characterize potential effects of long-term NAD^+ supplementation on cellular metabolism. Interestingly, a very recent study has demonstrated that dihydronicotinamide riboside (NHR; which is converted to NR and thus, NAD^+) was associated to detrimental consequences for hepatocytes (HepG3) [611]. Indeed, NHR exposure was associated to changes in NAD(P)H and GSH/GSSG pools, leading to a redox imbalance. Thus, NHR induced a metabolic dysregulation and the consequent mitochondrial respiration impairment. These data further suggest the potential adverse effects of NAD^+ supplementation in regards with the metabolic fate of the cells (on redox potential and/or metabolic flexibility), independent from the role of NAD^+ as a co-substrate for NAD-dependent enzymes. This needs to be further evaluated *in vivo* in long-term study regarding the number of current clinical trials for NAD^+-boost molecules.

What role for AMPK?

As discussed in our review on AMPK (*Introduction*), the downregulation of AMPK activity in obesity-induced CKD has been extensively reported by our group and others. Due to the pleiotropic pathways regulated by AMPK beyond the regulation of metabolic pathways, its decreased activity may lead to renal cell dysfunction, associated with lipotoxicity, insulin resistance, inflammation, fibrosis, and loss of renal function. Moreover, targeting AMPK directly or indirectly in renal injury represents an important therapeutic strategy. However, whether AMPK downregulation is a key driver of the cellular dysfunction or a downstream effect of other pathways is still unknown. Moreover, there is still a lack of drug therapy targeting AMPK in an effective way. Here, we demonstrated that AMPK activity was constantly enhanced in our different therapeutic approaches. Particularly, AMPK activation in response to endurance exercise training in obese mice led to an improved kidney function and decreased kidney injuries, associated to an enhanced autophagy flux. Indeed, AMPK activation leads to the prevention of renal lipotoxicity by inhibiting fatty acid synthesis, and enhancing FA oxidation. AMPK is also recognized to play an important role in the protection of mitochondrial function and mitochondrial homeostasis. AMPK activity initiates

autophagy flux and selectively degrades unhealthy mitochondria. Finally, a role of AMPK in the degradation of lipid droplets by selective macroautophagy (lipophagy) is emerging in the literature. Interestingly, we demonstrated that overexpression of SIRT3 allowed the activation of AMPK in HFD mice, leading to protection from obesity-induced kidney injury and ectopic lipid accumulation. We suggest that targeting AMPK by enhancing SIRT3 activity would be an interesting therapeutic strategy as the AMPK/SIRT3 axis has a strong potential as regulators of the general metabolism of the cell as well as mitochondrial homeostasis. Moreover, the cross-regulation between AMPK and SIRT3 has been recently highlighted. However, despite activation of SIRT3 by NR enhanced AMPK activity both *in vitro* and in *vivo*, as we hypothesized, the downstream effects on renal impairment were contrasted. We assume a deleterious effect of the sustained NAD^+/NADH ratio regarding metabolic pathway or redox potential, independently of SIRT3/AMPK axis. This hypothesis needs further investigations.

Targeting AMPK and SIRT3: future therapeutic strategy for kidney disease

The emerging insights suggesting that targeting renal metabolism impairments including mitochondrial dysfunction, lipid metabolism or autophagy process would have a potential therapeutic benefit in obesity-induced CKD were corroborated by our different approaches. These therapeutic strategies must be complementary but different from the effects of renin-angiotensin blockers. The drug development and the evaluation of these compounds represent an important therapeutic challenge, particularly in order to mimic lifestyle interventions, as demonstrated in this work for exercise training. Indeed, multiple tissues and organ systems are affected by exercise, initiating diverse homeostatic responses that implicate a high number of mediators and a multiplicity and complexity of adaptations as well as an integrative physiology, as discussed above. Thus, it is highly unrealistic that any drug or combination of compounds would ever reproduce exercise phenotype. Another issue is that drugs that maintain a "metabolic overdrive" for a long period of time in multiple tissues could have potentially deleterious health consequence as discussed by Weihrauch and Handschin [612]. This hypothesis was further partially confirmed by our experimental study on the effect of a sustained NAD^+ boost molecule (NR) treatment in mice. However, it is not pointless to better understand, along with behavioral intervention studies, what are the major drivers of the disease and to target master regulators in specific molecules in a specific tissue to alleviate the possible off-target and potential side effects associated to the expected benefice of the therapy. Moreover, a partial activation of specific exercise pathways could be a necessary approach in patients with a compromised exercise tolerance or a reduced ability to train. These drugs or dietary supplements should be combined with physical activity or should help patients to improve resistance to exercise and to gain

more health benefice from exercise. In this context, in addition to the well-studied AMPK agonist AICAR that showed beneficial effects on obesity and diabetes-related complications, new small molecules that directly activate AMPK are investigating. This strategy appears to be particularly relevant as Kikuchi *et al.* presented data supporting that AMPK was decreased in CKD model despite a high AMP:ATP ratio, suggesting that AMPK activity is not strongly dependent on energy depletion and highlighting the limitation of AMP analog use [307]. In this study, the use of the β-1 selective compound A-769662, which bypasses the AMP sensing mechanism was associated with an improvement of fibrosis and energy status in the kidney of CKD mice. In another study, a pan-AMPK activator, MK-8722 led to prevention of fibrosis and decreased lipotoxicity in renal cell in diabetic nephropathy [328]. Olivier *et al*. also suggested the potential therapeutic opportunity to target specific isoforms or specific heterotrimers of AMPK in order to directly target AMPK in a tissue or cell-specific way [477]. Moreover, SIRT3-specific drugs for use in order to strictly activate SIRT3-dependant metabolism are emerging and could represent another interesting therapeutic strategy and could help to better evaluate the role of SIRT3 in obesity-induced CKD [613].

As discussed before, we demonstrated that EET was associated to improvement of obesity-induced CKD as well as the underlying mechanisms of the long-term adapted renal metabolism. The future direction of these results would logically be the understanding of the muscle-kidney crosstalk during exercise and the dynamic of renal molecular pathways in response to exercise. To do so, the evaluation of the muscle secretome during or just after exercise and the relation with AMPK activity in renal tissue could expand our understanding of exercise-induced effects in the kidney. Particularly, irisin has been demonstrated to be particularly increased in model of PGC1-α muscle-specific transgenic mice and to prevent different kidney injuries. The effect of this specific exerkine on renal cells and the relation with AMPK activity needs to be evaluated *in vitro* and *in vivo*. To answer the question about the direct communication between the muscle tissue and the kidney, the muscle secretome during exercise could be applied to primary cell culture of PTC (see section 10.) cultivated with palmitic acid. Moreover, the use of kidney-specific or tubule-specific AMPK KO animals will allow us to clearly state the role of AMPK in the kidney in response to HFD and exercise. Indeed, are the beneficial effects of exercise training on CKD-dependent on AMPK pathway regulation is still an open question. The decreased AMPK activity in renal tissue following HFD has been extensively demonstrated in the literature but its role as the major driver of the renal cell metabolism impairment and lipotoxicity or a downstream consequence of mitochondrial dysfunction is still controversial. However, AMPK knockout mice deficient for the AMPK-β1 subunit fed a normal diet showed tubular vacuolation and lipid accumulation in proximal tubular cells suggesting that

AMPK dysfunction in HFD mice may participate to this phenomena that needs to be confirmed by the use of AMPK KO models [614]. Moreover, kidney is comprised of heterogenous cell types with different metabolic activities and there is still a few data regarding the expression of AMPK isoforms (see introduction; section 3.2), the regulation of AMPK activity, and the consequence of AMPK activation (physiologically or pharmacologically) in these different cell types. Moreover, as we demonstrated a potential AMPK-dependent autophagy regulation *via* ULK-1, we hypothesize that AMPK could also play an important role in autophagy dysregulation in obesity-induced CKD. Thus, the regulation of autophagy process in the kidney in renal lipotoxicity could be further studied in details by the use of specific controls for autophagy as discussed before as well as the use of AMPK KO mice and direct AMPK activators.

CONCLUSION

9 Conclusion

Obesity and associated disorders have become a major medical concern since the beginning of the century. Particularly, population aging, the growing increase of obesity and type II diabetes could considerably intensify incidence and prevalence of chronic kidney disease (CKD) across the Western world and beyond. Thus, a better understanding of the physiopathology of obesity-induced CKD and the effects of behavioral and/or pharmacological therapeutic strategies is required. In this work, we aimed to better delineate the effects of exercise-based therapy and the potential of an exercise mimetic on the regulation of AMP-activated protein kinase in models of renal lipotoxicity. The past studies have remarkedly presented AMPK dysregulation as a main driver of the physio-pathological progression in the kidney and pharmacological AMPK activation (directly or indirectly) was constantly associated to beneficial outcomes. However, traditional AMPK activators such as AICAR or Metformin present a limited clinical use, particularly for kidney disease. In this context, the effects of a delayed endurance exercise training were particularly investigated in high-fat diet-fed mice presenting CKD. We better described the restorative effects of a delayed exercise training on obesity-induced impairments such as glucose tolerance, insulin resistance or dyslipidemia and hepatic steatosis. These data were concordant with clinical studies in obese patients demonstrating the translational relevance of our experimental model. We further demonstrated for the very first time the beneficial effects of a delayed exercise on inflammation, fibrosis and oxidative stress intra-renal environment. Particularly, ectopic lipid accumulations in proximal tubule were decreased with exercise, associated to an improved AMPK pathway, as previously demonstrated with AICAR treatment in the same experimental model. The regulation of signaling pathways by AMPK in response to a high fat diet and/or exercise requires further investigations and mechanistic studies to further confirm the role of AMPK activity in obesity-induced CKD and in treatment response. Our results could also suggest a muscle-kidney communication mediated by myokines, stimulating research into improving communication between the kidneys and other organs for progressive kidney diseases. The recent studies have particularly highlighted that the identification of cellular targets activated by exercise may lead to the development of therapeutic strategies that could mimic systemic and central effects of exercise, called “exercise mimetics”. This pharmacological-based therapeutic strategy mostly includes AMPK, NAD^+-dependent SIRT1/3, PPARα/γ or PGC1-α activators. Based on our data regarding exercise training and transgenic mice, the potential of SIRT3 as an interesting therapeutic target in order to improve AMPK pathway was highlighted. Thus, we evaluated the effects a dietary intervention with NAD^+ supplementation (with nicotinamide riboside; NR). NR treatment was associated to an improved AMPK activity, mitochondrial function and a reduced ectopic lipid

accumulation in renal cells. However, long-term treatment with NR in obesity-induced mice model highlighted potential deleterious effects of this drug induced by a metabolic overdrive for a sustained period as evidenced by an increased lipid accumulation in the kidney and the liver, despite an activation of SIRT3 in the renal tissue. Thus, the therapeutic potential of exercise mimetics such as NR may present limitations that are not enough considered in the current research. Indeed, the exercise-induced adaptation are episodic in term of metabolic overload, organs communication, and direct short-term effects, followed by adequate recovery for substrates, muscle repair and regeneration for optimal adaptation. The optimal dose required to maintain activation/repression of targeted signaling pathways and the optimal response to obtain in a specific tissue is thus particularly challenging, as further demonstrated by this present work. When considering the physical health problems that limit the ability to be physically active of obese or CKD patients, the underlying effects of exercise training for kidney diseases stay a very interesting area of research with a great therapeutic potential. Furthermore, a better understanding of the role of the master metabolic regulator AMPK and the appropriate path to target the AMPK pathway remains essential in future investigations.

Annexes

Supplemental Data 1

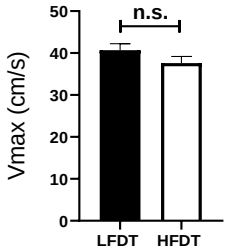

Figure S1. Effects of endurance exercise training on running velocity. Representation of maximal running velocity performance after 14 weeks on diet. *t-test*. Data are presented as means ± SEM. *ns* = non-significant. *n=10* in each group.

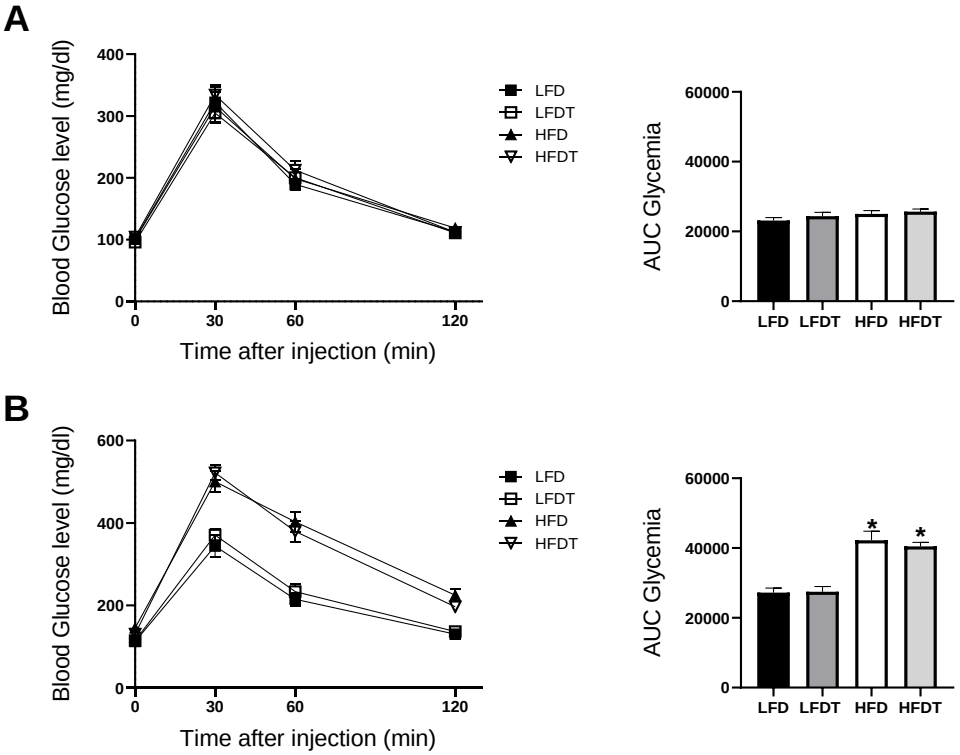

Figure S2. Effects of LFD and HFD on glucose tolerance in mice. Glucose tolerance test at week 0 (**A**) and week 12 (**B**). Fasted mice were submitted to an intraperitoneal injection of glucose (2 g/ kg b.w.). Glycemia was measured before (0) and 30, 60 and 120 min after injection. Histogram represents the area under the curve (AUC) of glycemia from 0 to 120 min.

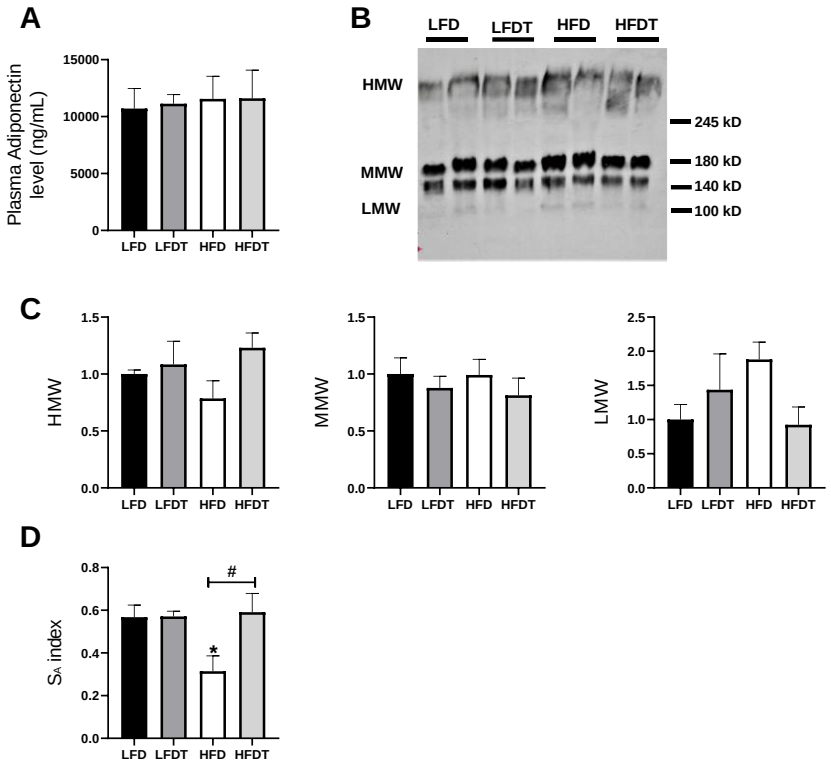

Figure S3. Total plasma adiponectin and adiponectin multimers distribution analysis at week 20. A. Ad plasmatic level. The total plasma Ad concentration was measured using indirect ELISA. **B**. Representative immunoblots of Adiponectin multimers expression in plasma sample. **C**. Relative densitometry of the immunoblots representing respectively HMW (High Molecular Weight), MMW (Medium Molecular Weight) and LMW (Low Molecular Weight) multimers of Adiponectin normalized with total Adiponectin protein level. **D**. S_A index was calculated as the ratio HMW/(HMW + LMW). Data are presented as means ± SEM. * $P \leq 0.05$ versus LFD $^{\#}$ $P \leq 0.05$ versus HFD. *n=6-8* in each group.

Table S1. Primer sequences for RT-qPCR analysis of mRNA expression

Gene		**Primer Sequences (5'-3')**
COLI	Fw	CTTGCCCCATTCATTTGTCT
	Rv	GCAGGTTCACCTACTCTGTTCT
COLIII	Fw	TGAGTCGAATTGGGGAGAAT
	Rv	TCCCCTGGAATCTGTGAATC
TGFβ	Fw	TGGAGCAACATGTGGAACTC
	Rv	GTCAGCAGCCGGTTACCA
MCP-1	Fw	CTTCTGGGCCTGCTGTTCA
	Rv	CCAGCCTACTCATTGGGATCA
IL1β	Fw	AGTTGACGGACCCCAAAAG
	Rv	AGCTGGATGCTCTCATCAGG
TNFα	Fw	TACTGAACTTCGGGGTGATTGGTCC
	Rv	CAGCCTTGTCCCTTGAAGAGAACC
IL6	Fw	GCTACCAAACTGGATATAATCAGGA
	Rv	CCAGGTAGCTATGGTACTCCAGAA
ACC (Acaca)	Fw	ATGGGCGGAATGGTCTCTTTC
	Rv	TGGGGACCTTGTCTTCATCAT
FAS (FASN)	Fw	GGAGGTGGTGATAGCCGGTAT
	Rv	TGGGTAATCCATAGAGCCCAG
CPT-1 (CPT1a)	Fw	CTCCGCCTGAGCCATGAAG
	Rv	CACCAGTGATGATGCCATTCT
18S	Fw	CGCCGCTAGAGGTGAAATTCT
	Rv	CGAACCTCCGACTTTCGTTCT

Table S2. Effects of delayed EET on systolic, diastolic and mean blood pressure in mice fed a LFD, LFDT or HFD and HDFT. Measurement were performed during the last week of the experimental protocol (week 20). Systemic, diastolic and mean blood pressures were measured using a non-invasive CODA tail-cuff blood pressure occlusion system (Kent Scientific, Torrington, USA). During the week 20, measurements were taken for each animal that were acclimatized for a 1-hour period before experiments into restraining chambers. The animals were placed onto a preheated pad maintained at 30°C in a designed quiet area and blood pressure measurements were initiated when tail temperature reached 30°C (measured using an infrared sensor) and recorded at least 5 times. Mice were acclimated for at least 3 consecutive days before baseline blood pressure measurements. No statistical difference was found by One-way ANOVA analysis. *n=5* in each group.

	LFD	**LFDT**	**HFD**	**HFDT**
Systolic blood pressure *(mmHg)*	128,6 ± 10,99	138,0 ± 4,988	119,5 ± 10,86	119,3 ± 5,850
Diastolic blood pressure *(mmHg)*	106,8 ± 10,60	117,6 ± 2,584	96,33 ± 8,750	101,7 ± 6,035
Mean blood pressure *(mmHg)*	117,7 ± 10,78	127,8 ± 3,763	107,9 ± 9,768	110,5 ± 5,570

Table S3. Effects of delayed EET on renal gene expression in mice fed a LFD, a LFDT, a HFD and a HFDT. Real-time quantitative qPCR for Acetyl-CoA carboxylase (ACC), Fatty acid synthase (FAS) and Carnitine palmitoyltransferase I (CPT1). mRNA expressions were performed on kidney tissue from LFD, LFDT, HFD and HFDT mice normalized against 18S. Statistical analyses were performed by one-way ANOVA followed by Newman–Keuls post hoc test. Data are presented as means ± SEM. * $P \leq 0.05$ versus LFD $^{\#}$ $P \leq 0.05$ versus HFD. *n=6* in each group.

	LFD	**LFDT**	**HFD**	**HFDT**
Lipid metabolism markers				
ACC	1,000 ± 0,0918	0,9636 ± 0,1356	1,067 ± 0,1404	1,028 ± 0,0796
FAS	1,000 ± 0,0265	1,023 ± 0,1480	1,218 ± 0,2496	1,112 ± 0,1884
CPT-1	1,000 ± 0,0326	0,9017 ± 0,1308	0,8483 ± 0,1201	1,222 ± 0,2337

Supplemental Data 2

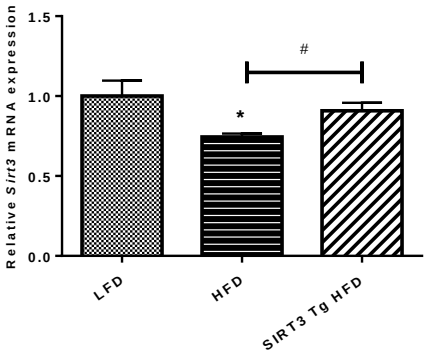

Supplemental Data 3

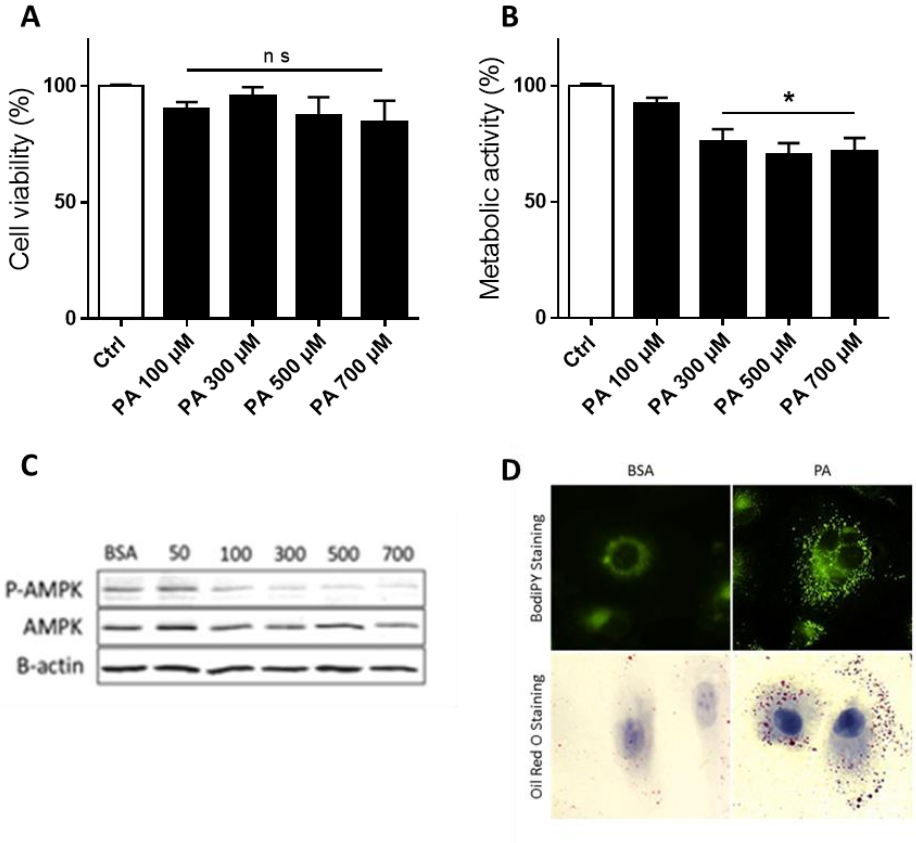

Supplemental Data 3. Effects of PA treatment on HK-2 cells. **A.** Evaluation of HK-2 cells viability for control 100, 300, 500 and 700 µM of PA treatment after 24h. n=3 **B**. Metabolic activity of HK-2 cells determined with the MTT test for control 100, 300, 500 and 700 µM of PA treatment after 24h. n=3 **C.** P-AMPK, AMPK and b-actin immunoblots for 50, 100, 300, 500 and 700 µM of PA treatment *vs* BSA 300 µM after 24h. **D.** BodiPY staining and Oil Red O staining showing lipid droplet accumulation in HK-2 cells treated with PA 500 µM *vs* BSA 500µM for 24h. Data are Mean ± SEM. One-way ANOVA followed by Newman Keuls post-hoc analysis.

Supplemental Data 4

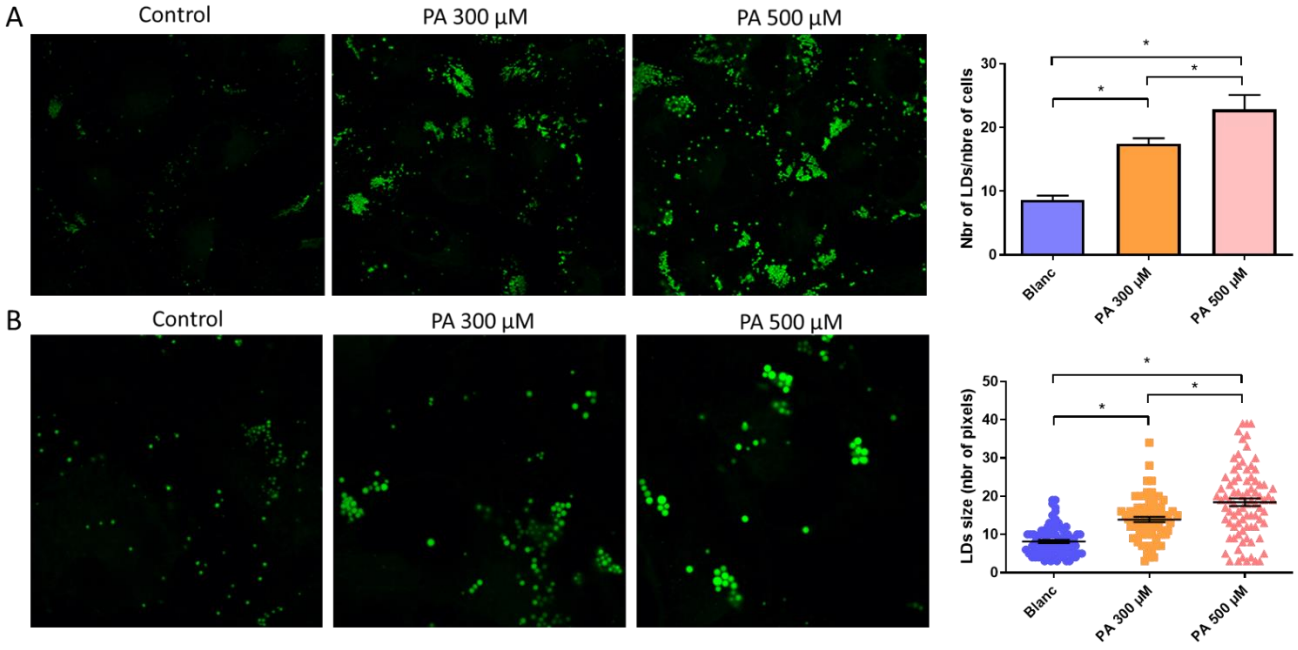

Supplemental Data 4. A-B. Confocal analysis of BODIPY 493/503 staining (green) to visualize lipid droplets structures in HK2 treated with PA 300 and 500 µM. **A**. Quantifications of number of lipid droplets obtained from five randomly selected field per condition, with each containing 20-30 cells, normalized with the number of nuclei. (400X) n=3. **B**. Quantifications of changes in the average size of lipid droplets in HK2 cells. Each point represents the average size of lipid droplets in a cell. (600X). Data are Mean ± SEM. One-way ANOVA followed by Newman Keuls post-hoc analysis.

10 Development of an *ex-vivo* and *in vitro* model of proximal tubular cells for the characterization of autophagy flux after lipid overload.

As previously mentioned, abnormal renal accumulation of lipids may be considered as a cause of renal impairments. We and other have demonstrated the significant increase of lipid droplets into proximal tubular cells in mice fed a HFD [120,285,293,295]. This change was concomitant with the loss of brush borders of these cells, the increase in oxidative stress and to the loss of kidney function. We also established that HFD-induced kidney disease is characterized by renal hypertrophy, increased albuminuria and elevated markers of renal fibrosis and inflammation [120,293]. In addition, evidence of proximal tubule injury was clearly observed with the presence of enlarged clear vacuoles and multilaminar inclusions. The margins of these vacuoles/inclusions were positive for the endolysosomal marker, LAMP1, suggesting lysosome accumulation. Characterization of vesicles by special stains (Oil Red O, Nile Red, Luxol Fast Blue) and by EM revealed that this contained onion skin-like accumulation consistent with phospholipids [293]. Indeed, similar ultra-structural abnormalities had already been observed in the proximal tubular cells of rodents and humans exposed to aminoglycosides demonstrating an accumulation of phospholipids in lysosomes [615,616]. However, the underlying cellular mechanisms were unknown. Recent studies have pointed out the importance of autophagy in physiological and pathological processes. In particular, autophagy is involved in reducing the number of lipid droplets by the degradation of the lysosome *via* a process called lipophagy. However, the mechanisms of lipophagy are not well understood in terms of its initiation and regulation [617,618].
As shown in section I, we have been able to demonstrate a reduction in the number of lipid inclusions within proximal tubular cells in obese mice undergoing exercise training, suggesting the potential involvement of autophagy in this phenomenon. It should also be noted that the accumulation of lipid droplets has been demonstrated in obese patients [285,293]. In addition, although lysosomal dysfunction coupled with a disturbance in lipid metabolism in the kidney has been experimentally validated by other researchers, all underlying molecular mechanisms are not yet known [286]. Therefore, it is necessary to develop an optimal experimental model to deeper study the lipophagy process in the context of renal lipotoxicicty.

Relevance of *in vivo* and *in vitro* model. Even though the *in vivo* approach to study the metabolic diseases such as obesity remains necessary or even essential, the investigation of specific biological questions is sometimes more difficult to study in an entire organ composed of different cell types. For example, the lipotoxicity into PTC appears as major. It is therefore more relevant to study these cells isolated from the rest of the organ. Therefore, many groups use immortalized cells such as HK-2 (human proximal tubular cells). The use of these *in vitro* cells is a good model, providing relevant data but has also some limitations. For example, these cells might present a modified cell program or no longer have specific expression of the markers defining their native phenotype. These aspects must therefore be

considered in the interpretations of the results and especially in the translational relevance of the results with the *in vivo* model. In addition, the immortalization of cell lines profoundly affects their phenotype and how it responds to their environment. In this regard, the use of primary cells directly isolated from the targeted organ is a better model. Indeed, these cells maintain their phenotype *in vitro,* giving the opportunity to better characterize precise molecular and cellular mechanisms. In addition, numerous studies have shown the value of the use of primary PTC in the study of diabetic nephropathy [619].
Hence, one of the objectives of my PhD was to develop a technique of isolation of PTC from kidneys of lean and obese mice to characterize the molecular mechanisms involved in PTC impairment in a context of caloric overload. In addition, we sought to develop an *in vitro* model of primary cells from these isolated cells to evaluate the regulation of autophagy in PTC.

1. **Isolation of PTC from mice based on a technique developed by Legouis et al. (2015)** (Collab. Prof. C. Chatziantoniou, INSERM, Hôpital Tenon, Paris, France)

The technique relies on the use of a mechanical dissociation of the organ based on magnetic microbeads coupled with a specific antibody of targeted cells (GentleMACS dissociator, Miltenyi Biotec) [620].

Methods

Control male C57Bl/6J mice were used to develop the technique of PTC isolation. First step, after euthanasia with Ketamine/Xylazine, kidney wass rapidly harvested, decapsulated and immerged in 1mL of sterile dissociation buffer (PBS 1×0.5% bovine serum albumin, and 2mM EDTA) at 4°C. Then, kidney was roughly chopped with a surgical blade. The solution obtained was transferred into GentleMACS C-tubes. Specific set program of the GentleMACS dissociator were used to maintain cell integrity. Next, the solution obtained was filtered through a 30-µm sieve and rinsed with 4mL of dissociation buffer. After centrifugation at 500g for 10 minutes, the supernatant was removed, and cell pellet was resuspended in dissociating buffer. The second step consisted to isolate the PTC by magnetic activated cell sorting (MACS) by positive selection using the CD133 (prominin-1) cell isolation kit and the MACS separator (Miltenyi Biotec) as described in [620]. Briefly, cells were labelled with conjugated CD133 microbeads antibody. The magnetically labelled target cells were depleted by retaining them on a MACS column in the magnetic field of a magnet, while unlabeled cells passed through the column.

Flow cytometry

In order to assess the purity of isolated PTC, cells were harvested and directly resuspended in FACS Buffer (PBS 1% PenStrep 2% Fetal Bovine Serum) with Hoechst Dye (Miltenyi) 1:100 for 30 minutes in the dark at room temperature. Next, cells were washed with FACS Buffer and incubated with prominin-1 APC antibody (Miltenyi) 1:50 for 30 min at 4°C. Cells were washed

and fixed in PBS PFA 2% (paraformaldehyde) for 15 min at room temperature. Cells were finally washed and resuspended in FACS Buffer before being acquired on a FACSCantoll (BD Biosciences) and analysed on FlowJo software (Treestar).

Western Blot

The proteins extracted from total kidney were run on 4-12% polyacrylamide gels and transferred onto nitrocellulose membrane. The anti-promonin-1 (CD133, Biorbyt) was used. Detection was performed with SuperSignal™ West Femto Maximum Sensitivity Substrate kit (ThermoScientific).

Result

Isolations of PTC were performed on control lean mice. As illustrated in Figure 1, to confirm that PTC isolation worked, flow cytometry was carrying out. Before the PTC isolation, only 11% of prominin 1-positive cells were obtained in analysed solution. However, after isolation, around 82% of positive cells were present in the analysed solution (**Figure 1A**). To validate flow cytometry results, a western blot analysis was performed (**Figure 1B**). As observed, in the enriched solution, there was a signal for prominin-1 whereas no signal was present in the negative fraction solution (**Figure 1B**).

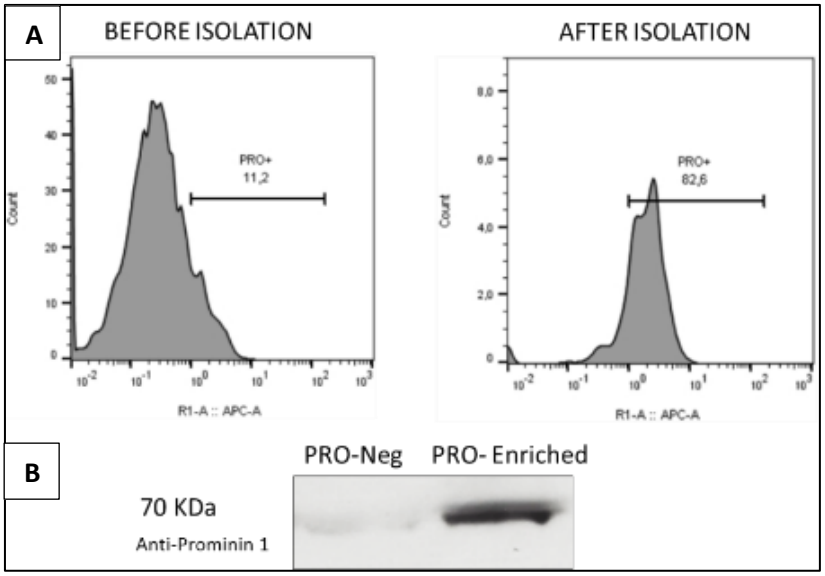

Figure 1. A. Flow cytometry analysis before and after of promonin-positive PT cells. B. Western blot analysis of enriched (promonin+) fraction and negative fraction.

Finally, isolated cells were used to test primary cell culture. After 8 days in culture, cells from the negative fraction were obviously morphologically different than cells from positive fraction. Positive cells presented a more cubic phenotype and were grouped together (**Figure 2**) while negative cells were dispersed and presented cytoplasmic extensions.

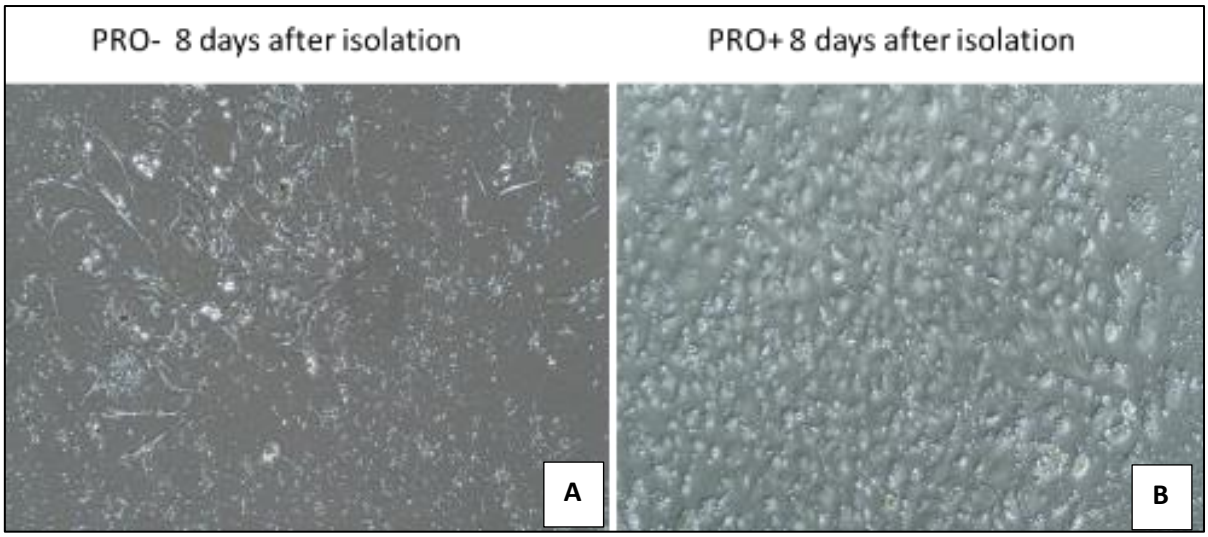

Figure 2. Representative photomicrograph (x10) showing primary cell culture from negative (A) and positive (B) fractions.

Conclusion

The protocol developed by Legouis *et al.* allowed us to effectively isolate prominin positive cell population from the whole kidney. We were able to perform a primary culture of positive cells *in vitro* as we demonstrated tubular cell-like phenotype after 8 days of culture. However, the yield obtained from positive cells in culture was very low and time-consuming, making difficult to perform relevant experiments with this method. Moreover, we were not able to reproduce this methods multiple times as the cells showed a particularly slow growth in culture, ultimately leading to cell death. Finally, the direct *ex-vivo* analysis of isolated cells represent a more interesting methods for the analysis of isolated proximal tubule fraction but our major concern is that prominin is expressed in the brush border that is impaired with HFD in the S1 and S2 segment of the proximal tubule. Thus, we assume that the S3 segment would be better isolated than the S1 and S2, introducing an experimental bias for further analysis. Thus, we decided to assess another approach developed by Devuyst's group.

2. **Isolation of PTC developed in Devuyst O. group** (Collab. Prof. Olivier Devuyst, Laboratory of Mechanisms of inherited kidney disorders, UZH)

This approach is a more simple method to establish primary cultures of kidney proximal tubule cells described by Terryn *et al.* 2006 [621].

Methods

Renal cortex from control male C57Bl/6J mice were dissected in ice-cold a dissection solution (HBSS with in mmol/l: 10 glucose, 5 glycine, 1 alanine, 15 HEPES, pH 7.4 and osmolality 325 mosmol/kgH2O) and sliced into piece. The fragments were transferred to collagenase solution at 37°C and digested for 30 min. After digestion, the supernatant was sieved through two nylon sieves (pore size 250 µm and 80 µm). The proximal tubules (PTs) remained in the 80-µm sieve and were resuspended in warm DS (37°C) containing BSA 1%. The PTs were then centrifuged for 5 min at 170 g, washed, and then resuspended into the appropriate amount of culture medium. The PT fragments were seeded onto collagen-coated plates for 48 h. The medium was then replaced every 2 days. After 7 days, cell cultures were organized as a confluent monolayer.

Results

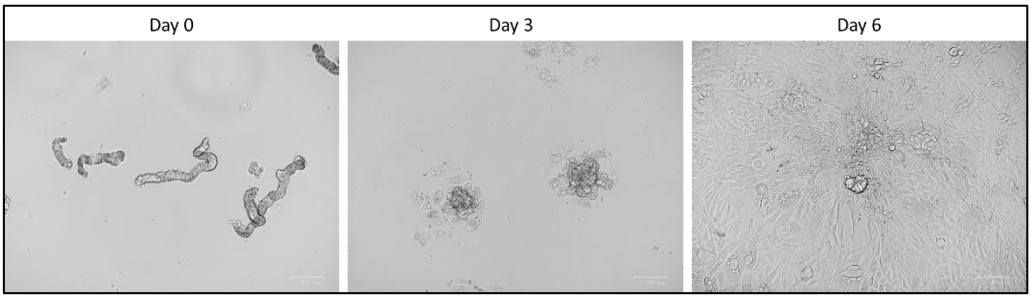

Figure 3. Representative photomicrograph (x10) showing isolated proximal tubule directly after isolation (day 0), after 3 and 5 days of culture.

In the **Figure 3**, we present representative photomicrographs of isolated proximal tubules just after isolation (day 0), 3 days after isolation and 6 days after isolation. As shown at day 0, the proximal tubule structures are present in the medium without contamination with glomeruli. At 3 days, cellular outgrowth was observed at the open ends of the tubular fragments. After 6 days, islands of cellular outgrowth became progressively larger to form a confluent monolayer of polygonal cells. We further tested different concentrations of PA and BSA as we used for HK-2 cells in the section III. The viability of the cells was dramatically impaired as demonstrated in **Figure 4A; B**. Thus, we decided to use lower concentration of PA and BSA that were not toxic for PTC (**Figure 4C; D**). Next, we analyzed whether these concentrations of PA were able to induce lipid droplets accumulations in PTC. As shown in **Figure 5**, LDs accumulation was enhanced in 50 µM of PA-treated cells as demonstrated by an increased BodiPY staining. Finally, an albumin (BSA) uptake in PTC was performed following incubation with

different concentrations of PA (**Figure 6**). We showed that PTC exposed to 50 µM of PA present a decreased uptake of BSA as evidenced by the decreased BSA^+ puncta compared to other concentrations.

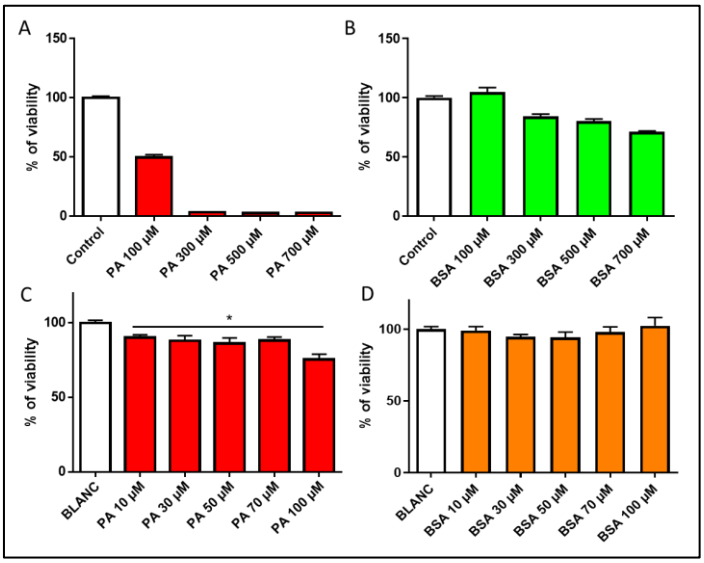

Figure 4. Effects of PA treatment on primary PTC cells. Evaluation of PTC viability for control 100, 300, 500 and 700 µM of PA or BSA treatment after 24h. *Experimental procedure described in section III.*

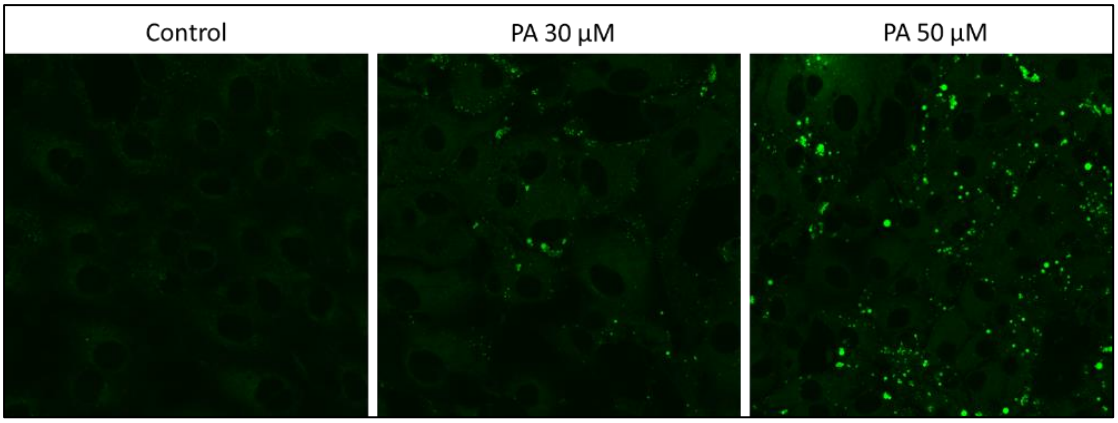

Figure 5. Confocal analysis of BODIPY 493/503 staining (green) to visualize lipid droplets structures in PTC treated with PA 30 and 50 µM for 24h. *Experimental procedure described in section III.*

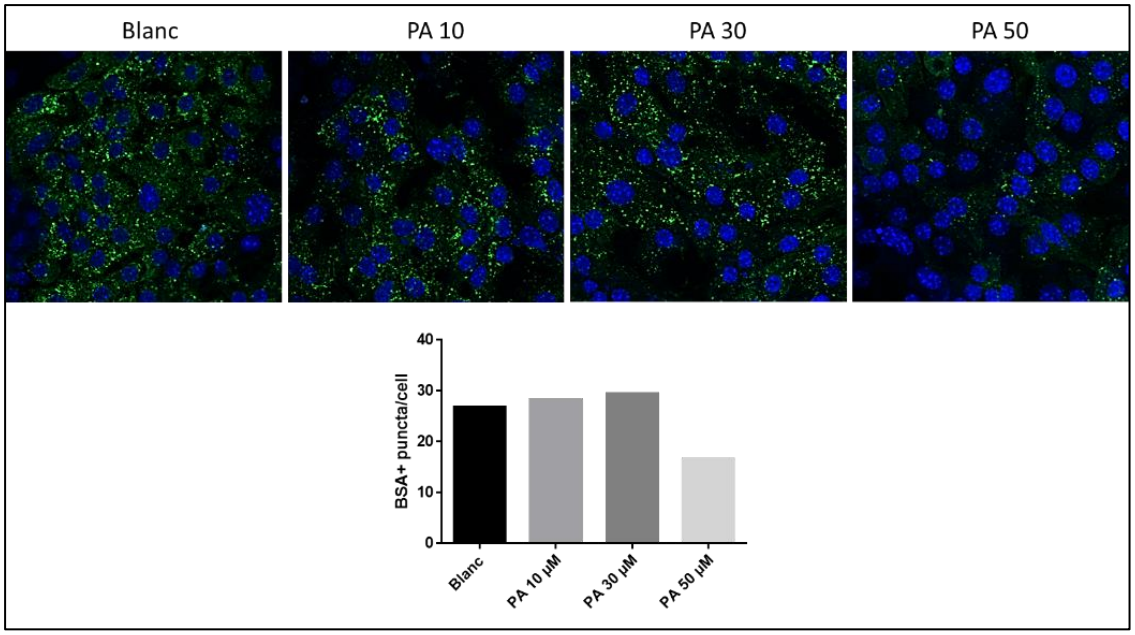

Figure 6. Albumin (BSA) uptake evaluation in PTC. After being exposed to PA 10, 30 or 50 µM, the cells were loaded with fluorescent Al647-BSA (50 µg ml−1 for 15 min at 37 °C) and imaged by confocal microscopy. Then, quantification of numbers of Al647-BSA+ structures was performed using ImageJ (normalized by the number of nuclei).

Conclusion

Here, we present a valuable model of mouse primary proximal tubular cells in culture for the study of PA-induced impairments of PTC function. Despite our first experimental approach failed to give us expected biological materials, we next switched to a simpler methods based on sieve isolation of proximal structures. This allowed us to demonstrate a suitable model of PA-induced lipid droplet accumulations in PTC along with an impaired cellular function, as demonstrated by BSA-uptake dysfunction. This model would be interesting to study the autophagic pathway in response to PA treatment *in vitro*.

REFERENCES

11 Bibliography

1. Sikaris KA. The clinical biochemistry of obesity. Clin Biochem Rev. 2004 Aug;25(3):165–81.
2. Obesity: preventing and managing the global epidemic. Report of a WHO consultation. Vol. 894, World Health Organization technical report series. Switzerland; 2000.
3. Wharton S, Lau DCW, Vallis M, Sharma AM, Biertho L, Campbell-Scherer D, et al. Obesity in adults: a clinical practice guideline. C Can Med Assoc J = J l'Association medicale Can. 2020 Aug;192(31):E875–91.
4. Ross R, Neeland IJ, Yamashita S, Shai I, Seidell J, Magni P, et al. Waist circumference as a vital sign in clinical practice: a Consensus Statement from the IAS and ICCR Working Group on Visceral Obesity. Nat Rev Endocrinol. 2020 Mar;16(3):177–89.
5. Ness-Abramof R, Apovian CM. Waist circumference measurement in clinical practice. Nutr Clin Pract Off Publ Am Soc Parenter Enter Nutr. 2008;23(4):397–404.
6. Russo C, Sera F, Jin Z, Palmieri V, Homma S, Rundek T, et al. Abdominal adiposity, general obesity, and subclinical systolic dysfunction in the elderly: A population-based cohort study. Eur J Heart Fail. 2016 May;18(5):537–44.
7. Ping Z, Pei X, Xia P, Chen Y, Guo R, Hu C, et al. Anthropometric indices as surrogates for estimating abdominal visceral and subcutaneous adipose tissue: A meta-analysis with 16,129 participants. Diabetes Res Clin Pract. 2018 Sep;143:310–9.
8. Shah R V, Murthy VL, Abbasi SA, Blankstein R, Kwong RY, Goldfine AB, et al. Visceral adiposity and the risk of metabolic syndrome across body mass index: the MESA Study. JACC Cardiovasc Imaging. 2014 Dec;7(12):1221–35.
9. Han TS, Lean ME. A clinical perspective of obesity, metabolic syndrome and cardiovascular disease. JRSM Cardiovasc Dis [Internet]. 2016;5:204800401663337. Available from: http://journals.sagepub.com/doi/10.1177/2048004016633371
10. Fang H, Berg E, Cheng X, Shen W. How to best assess abdominal obesity. Curr Opin Clin Nutr Metab Care. 2018 Sep;21(5):360–5.
11. Nimptsch K, Konigorski S, Pischon T. Diagnosis of obesity and use of obesity biomarkers in science and clinical medicine. Metabolism. 2019 Mar;92:61–70.
12. Onesi SO, Ignatius UE. Metabolic syndrome: Performance of five different diagnostic criterias. Indian J Endocrinol Metab. 2014 Jul;18(4):496–501.
13. Hill JO, Wyatt HR, Peters JC. The Importance of Energy Balance. Eur Endocrinol. 2013 Aug;9(2):111–5.
14. Hill JO, Wyatt HR, Peters JC. Energy balance and obesity. Circulation. 2012 Jul;126(1):126–32.
15. Hall KD, Heymsfield SB, Kemnitz JW, Klein S, Schoeller DA, Speakman JR. Energy balance and its components: implications for body weight regulation. Am J Clin Nutr. 2012 Apr;95(4):989–94.
16. Obri A, Claret M. The role of epigenetics in hypothalamic energy balance control: implications for obesity. Cell Stress. 2019 Jun;3(7):208–20.
17. Bell EA, Rolls BJ. Energy density of foods affects energy intake across multiple levels of fat content in lean and obese women. Am J Clin Nutr. 2001 Jun;73(6):1010–8.
18. Stelmach-Mardas M, Rodacki T, Dobrowolska-Iwanek J, Brzozowska A, Walkowiak J, Wojtanowska-Krosniak A, et al. Link between Food Energy Density and Body Weight Changes in Obese Adults. Nutrients. 2016 Apr;8(4):229.
19. Roberts SB, McCrory MA, Saltzman E. The influence of dietary composition on energy intake and body weight. J Am Coll Nutr. 2002 Apr;21(2):140S-145S.
20. Brand-Miller JC, Holt SHA, Pawlak DB, McMillan J. Glycemic index and obesity. Am J Clin Nutr.

2002 Jul;76(1):281S-5S.

21. Kim D-Y, Kim SH, Lim H. Association between dietary carbohydrate quality and the prevalence of obesity and hypertension. J Hum Nutr Diet Off J Br Diet Assoc. 2018 Oct;31(5):587–96.

22. Heymsfield SB, Pietrobelli A. Individual differences in apparent energy digestibility are larger than generally recognized. Vol. 94, The American journal of clinical nutrition. United States; 2011. p. 1650–1.

23. Hruby A, Hu FB. The Epidemiology of Obesity: A Big Picture. Pharmacoeconomics. 2015 Jul;33(7):673–89.

24. González-Muniesa P, Mártinez-González M-A, Hu FB, Després J-P, Matsuzawa Y, Loos RJF, et al. Obesity. Nat Rev Dis Prim. 2017 Jun;3:17034.

25. Blüher M. Obesity: global epidemiology and pathogenesis. Nat Rev Endocrinol. 2019;15(5):288–98.

26. Farooqi IS, O'Rahilly S. Monogenic obesity in humans. Annu Rev Med. 2005;56:443–58.

27. Huvenne H, Dubern B, Clément K, Poitou C. Rare Genetic Forms of Obesity: Clinical Approach and Current Treatments in 2016. Obes Facts. 2016;9(3):158–73.

28. Locke AE, Kahali B, Berndt SI, Justice AE, Pers TH, Day FR, et al. Genetic studies of body mass index yield new insights for obesity biology. Nature. 2015 Feb;518(7538):197–206.

29. Hinney A, Nguyen TT, Scherag A, Friedel S, Brönner G, Müller TD, et al. Genome wide association (GWA) study for early onset extreme obesity supports the role of fat mass and obesity associated gene (FTO) variants. PLoS One. 2007 Dec;2(12):e1361.

30. Winkler TW, Justice AE, Graff M, Barata L, Feitosa MF, Chu S, et al. The Influence of Age and Sex on Genetic Associations with Adult Body Size and Shape: A Large-Scale Genome-Wide Interaction Study. PLoS Genet. 2015 Oct;11(10):e1005378.

31. Maffeis C, Morandi A. Effect of Maternal Obesity on Foetal Growth and Metabolic Health of the Offspring. Obes Facts. 2017;10(2):112–7.

32. Nogues P, Dos Santos E, Jammes H, Berveiller P, Arnould L, Vialard F, et al. Maternal obesity influences expression and DNA methylation of the adiponectin and leptin systems in human third-trimester placenta. Clin Epigenetics. 2019 Feb;11(1):20.

33. Dunford AR, Sangster JM. Maternal and paternal periconceptional nutrition as an indicator of offspring metabolic syndrome risk in later life through epigenetic imprinting: A systematic review. Diabetes Metab Syndr. 2017 Dec;11 Suppl 2:S655–62.

34. Wahl S, Drong A, Lehne B, Loh M, Scott WR, Kunze S, et al. Epigenome-wide association study of body mass index, and the adverse outcomes of adiposity. Nature. 2017 Jan;541(7635):81–6.

35. Frank AP, De Souza Santos R, Palmer BF, Clegg DJ. Determinants of body fat distribution in humans may provide insight about obesity-related health risks. J Lipid Res. 2019;60(10):1710–9.

36. Power ML, Schulkin J. Sex differences in fat storage, fat metabolism, and the health risks from obesity: possible evolutionary origins. Br J Nutr. 2008 May;99(5):931–40.

37. Karastergiou K, Smith SR, Greenberg AS, Fried SK. Sex differences in human adipose tissues - the biology of pear shape. Biol Sex Differ. 2012 May;3(1):13.

38. Aras Ş, Üstünsoy S, Armutçu F. Indices of Central and Peripheral Obesity; Anthropometric Measurements and Laboratory Parameters of Metabolic Syndrome and Thyroid Function. Balkan Med J. 2015 Oct;32(4):414–20.

39. Fuente-Martín E, Argente-Arizón P, Ros P, Argente J, Chowen JA. Sex differences in adipose tissue: It is not only a question of quantity and distribution. Adipocyte. 2013 Jul;2(3):128–34.

40. Kennedy A, Gettys TW, Watson P, Wallace P, Ganaway E, Pan Q, et al. The metabolic significance of leptin in humans: gender-based differences in relationship to adiposity, insulin sensitivity, and energy expenditure. J Clin Endocrinol Metab. 1997 Apr;82(4):1293–300.

41. Nickelson KJ, Stromsdorfer KL, Pickering RT, Liu T-W, Ortinau LC, Keating AF, et al. A comparison of inflammatory and oxidative stress markers in adipose tissue from weight-matched obese male and female mice. Exp Diabetes Res. 2012;2012:859395.

42. Newell-Fugate AE. The role of sex steroids in white adipose tissue adipocyte function. Reproduction. 2017 Apr;153(4):R133–49.

43. Chooi YC, Ding C, Magkos F. The epidemiology of obesity. Metabolism. 2019 Mar;92:6–10.

44. Finkelstein EA, Khavjou OA, Thompson H, Trogdon JG, Pan L, Sherry B, et al. Obesity and severe obesity forecasts through 2030. Am J Prev Med. 2012 Jun;42(6):563–70.

45. Kanter R, Caballero B. Global gender disparities in obesity: a review. Adv Nutr. 2012 Jul;3(4):491–8.

46. Swinburn BA, Sacks G, Hall KD, McPherson K, Finegood DT, Moodie ML, et al. The global obesity pandemic: shaped by global drivers and local environments. Lancet (London, England). 2011 Aug;378(9793):804–14.

47. Longo M, Zatterale F, Naderi J, Parrillo L, Formisano P, Raciti GA, et al. Adipose Tissue Dysfunction as Determinant of Obesity-Associated Metabolic Complications. Int J Mol Sci. 2019 May;20(9).

48. Stern JH, Rutkowski JM, Scherer PE. Adiponectin, Leptin, and Fatty Acids in the Maintenance of Metabolic Homeostasis through Adipose Tissue Crosstalk. Cell Metab. 2016 May;23(5):770–84.

49. Townsend K, Tseng Y-H. Brown adipose tissue: Recent insights into development, metabolic function and therapeutic potential. Adipocyte. 2012 Jan;1(1):13–24.

50. Mulya A, Kirwan JP. Brown and Beige Adipose Tissue: Therapy for Obesity and Its Comorbidities? Endocrinol Metab Clin North Am. 2016 Sep;45(3):605–21.

51. Ikeda K, Maretich P, Kajimura S. The Common and Distinct Features of Brown and Beige Adipocytes. Trends Endocrinol Metab. 2018 Mar;29(3):191–200.

52. Onal G, Kutlu O, Gozuacik D, Dokmeci Emre S. Lipid Droplets in Health and Disease. Lipids Health Dis. 2017 Jun;16(1):128.

53. Jo J, Gavrilova O, Pack S, Jou W, Mullen S, Sumner AE, et al. Hypertrophy and/or Hyperplasia: Dynamics of Adipose Tissue Growth. PLoS Comput Biol. 2009 Mar;5(3):e1000324.

54. Konige M, Wang H, Sztalryd C. Role of adipose specific lipid droplet proteins in maintaining whole body energy homeostasis. Biochim Biophys Acta. 2014 Mar;1842(3):393–401.

55. Czech MP, Tencerova M, Pedersen DJ, Aouadi M. Insulin signalling mechanisms for triacylglycerol storage. Diabetologia. 2013 May;56(5):949–64.

56. Boutens L, Stienstra R. Adipose tissue macrophages: going off track during obesity. Diabetologia. 2016 May;59(5):879–94.

57. Hill AA, Reid Bolus W, Hasty AH. A decade of progress in adipose tissue macrophage biology. Immunol Rev. 2014 Nov;262(1):134–52.

58. Thomas D, Apovian C. Macrophage functions in lean and obese adipose tissue. Metabolism. 2017 Jul;72:120–43.

59. Coelho M, Oliveira T, Fernandes R. Biochemistry of adipose tissue: an endocrine organ. Arch Med Sci. 2013 Apr;9(2):191–200.

60. Romacho T, Elsen M, Röhrborn D, Eckel J. Adipose tissue and its role in organ crosstalk. Acta Physiol (Oxf). 2014 Apr;210(4):733–53.

61. Gorska E, Popko K, Stelmaszczyk-Emmel A, Ciepiela O, Kucharska A, Wasik M. Leptin receptors. Eur J Med Res. 2010 Nov;15 Suppl 2(Suppl 2):50–4.

62. Montez JM, Soukas A, Asilmaz E, Fayzikhodjaeva G, Fantuzzi G, Friedman JM. Acute leptin deficiency, leptin resistance, and the physiologic response to leptin withdrawal. Proc Natl Acad Sci U S A. 2005 Feb;102(7):2537–42.

63. Geerling JJ, Boon MR, Kooijman S, Parlevliet ET, Havekes LM, Romijn JA, et al. Sympathetic nervous system control of triglyceride metabolism: novel concepts derived from recent studies. J Lipid Res. 2014 Feb;55(2):180–9.

64. Flier JS. Leptin expression and action: new experimental paradigms. Proc Natl Acad Sci U S A. 1997 Apr;94(9):4242–5.

65. Zhang F, Chen Y, Heiman M, Dimarchi R. Leptin: structure, function and biology. Vitam Horm. 2005;71:345–72.

66. Tartaglia LA, Dembski M, Weng X, Deng N, Culpepper J, Devos R, et al. Identification and expression cloning of a leptin receptor, OB-R. Cell. 1995 Dec;83(7):1263–71.

67. Frederich RC, Hamann A, Anderson S, Löllmann B, Lowell BB, Flier JS. Leptin levels reflect body lipid content in mice: evidence for diet-induced resistance to leptin action. Nat Med. 1995 Dec;1(12):1311–4.

68. Leon-Cabrera S, Solís-Lozano L, Suárez-Álvarez K, González-Chávez A, Béjar YL, Robles-Díaz G, et al. Hyperleptinemia is associated with parameters of low-grade systemic inflammation and metabolic dysfunction in obese human beings. Front Integr Neurosci. 2013;7:62.

69. Koch CE, Lowe C, Pretz D, Steger J, Williams LM, Tups A. High-fat diet induces leptin resistance in leptin-deficient mice. J Neuroendocrinol. 2014 Feb;26(2):58–67.

70. Lin S, Thomas TC, Storlien LH, Huang XF. Development of high fat diet-induced obesity and leptin resistance in C57Bl/6J mice. Int J Obes Relat Metab Disord J Int Assoc Study Obes. 2000 May;24(5):639–46.

71. Ravussin Y, LeDuc CA, Watanabe K, Mueller BR, Skowronski A, Rosenbaum M, et al. Effects of chronic leptin infusion on subsequent body weight and composition in mice: Can body weight set point be reset? Mol Metab. 2014 Jul;3(4):432–40.

72. Izquierdo AG, Crujeiras AB, Casanueva FF, Carreira MC. Leptin, Obesity, and Leptin Resistance: Where Are We 25 Years Later? Nutrients. 2019 Nov;11(11).

73. Banks WA, Farrell CL. Impaired transport of leptin across the blood-brain barrier in obesity is acquired and reversible. Am J Physiol Endocrinol Metab. 2003 Jul;285(1):E10-5.

74. Zhang X, Zhang G, Zhang H, Karin M, Bai H, Cai D. Hypothalamic IKKbeta/NF-kappaB and ER stress link overnutrition to energy imbalance and obesity. Cell. 2008 Oct;135(1):61–73.

75. Thaler JP, Yi C-X, Schur EA, Guyenet SJ, Hwang BH, Dietrich MO, et al. Obesity is associated with hypothalamic injury in rodents and humans. J Clin Invest. 2012 Jan;122(1):153–62.

76. De Souza CT, Araujo EP, Bordin S, Ashimine R, Zollner RL, Boschero AC, et al. Consumption of a fat-rich diet activates a proinflammatory response and induces insulin resistance in the hypothalamus. Endocrinology. 2005 Oct;146(10):4192–9.

77. Milanski M, Degasperi G, Coope A, Morari J, Denis R, Cintra DE, et al. Saturated fatty acids produce an inflammatory response predominantly through the activation of TLR4 signaling in hypothalamus: implications for the pathogenesis of obesity. J Neurosci. 2009 Jan;29(2):359–70.

78. Kleinridders A, Schenten D, Könner AC, Belgardt BF, Mauer J, Okamura T, et al. MyD88 signaling in the CNS is required for development of fatty acid-induced leptin resistance and diet-induced obesity. Cell Metab. 2009 Oct;10(4):249–59.

79. Mazor R, Friedmann-Morvinski D, Alsaigh T, Kleifeld O, Kistler EB, Rousso-Noori L, et al. Cleavage of the leptin receptor by matrix metalloproteinase-2 promotes leptin resistance and obesity in mice. Sci Transl Med. 2018 Aug;10(455).

80. van Andel M, Drent ML, van Herwaarden AE, Ackermans MT, Heijboer AC. A method comparison of total and HMW adiponectin: HMW/total adiponectin ratio varies versus total adiponectin, independent of clinical condition. Clin Chim Acta. 2017 Feb;465:30–3.

81. Barr VA, Malide D, Zarnowski MJ, Taylor SI, Cushman SW. Insulin stimulates both leptin secretion and production by rat white adipose tissue. Endocrinology. 1997 Oct;138(10):4463–72.

82. Bogan JS, Lodish HF. Two compartments for insulin-stimulated exocytosis in 3T3-L1 adipocytes defined by endogenous ACRP30 and GLUT4. J Cell Biol. 1999 Aug;146(3):609–20.

83. Gariballa S, Alkaabi J, Yasin J, Al Essa A. Total adiponectin in overweight and obese subjects and its response to visceral fat loss. BMC Endocr Disord. 2019 Jun;19(1):55.

84. Asterholm IW, Scherer PE. Enhanced metabolic flexibility associated with elevated adiponectin levels. Am J Pathol. 2010 Mar;176(3):1364–76.

85. Almabrouk TAM, White AD, Ugusman AB, Skiba DS, Katwan OJ, Alganga H, et al. High Fat Diet Attenuates the Anticontractile Activity of Aortic PVAT via a Mechanism Involving AMPK and Reduced Adiponectin Secretion. Front Physiol. 2018;9:51.

86. De Rosa A, Monaco ML, Capasso M, Forestieri P, Pilone V, Nardelli C, et al. Adiponectin oligomers as potential indicators of adipose tissue improvement in obese subjects. Eur J Endocrinol. 2013 Jul;169(1):37–43.

87. Kaser S, Tatarczyk T, Stadlmayr A, Ciardi C, Ress C, Tschoner A, et al. Effect of obesity and insulin sensitivity on adiponectin isoform distribution. Eur J Clin Invest. 2008 Nov;38(11):827–34.

88. He Y, Lu L, Wei X, Jin D, Qian T, Yu A, et al. The multimerization and secretion of adiponectin are regulated by TNF-alpha. Endocrine. 2016 Mar;51(3):456–68.

89. Engin A. Adiponectin-Resistance in Obesity. Adv Exp Med Biol. 2017;960:415–41.

90. Rasouli N, Kern PA. Adipocytokines and the metabolic complications of obesity. J Clin Endocrinol Metab. 2008 Nov;93(11 Suppl 1):S64-73.

91. Yoshimura T, Robinson EA, Tanaka S, Appella E, Kuratsu J, Leonard EJ. Purification and amino acid analysis of two human glioma-derived monocyte chemoattractants. J Exp Med. 1989 Apr;169(4):1449–59.

92. Takahashi K, Mizuarai S, Araki H, Mashiko S, Ishihara A, Kanatani A, et al. Adiposity elevates plasma MCP-1 levels leading to the increased CD11b-positive monocytes in mice. J Biol Chem. 2003 Nov;278(47):46654–60.

93. Xu H, Barnes GT, Yang Q, Tan G, Yang D, Chou CJ, et al. Chronic inflammation in fat plays a crucial role in the development of obesity-related insulin resistance. J Clin Invest. 2003 Dec;112(12):1821–30.

94. Weisberg SP, McCann D, Desai M, Rosenbaum M, Leibel RL, Ferrante AWJ. Obesity is associated with macrophage accumulation in adipose tissue. J Clin Invest. 2003 Dec;112(12):1796–808.

95. Sartipy P, Loskutoff DJ. Monocyte chemoattractant protein 1 in obesity and insulin resistance. Proc Natl Acad Sci U S A. 2003 Jun;100(12):7265–70.

96. Kanda H, Tateya S, Tamori Y, Kotani K, Hiasa K, Kitazawa R, et al. MCP-1 contributes to macrophage infiltration into adipose tissue, insulin resistance, and hepatic steatosis in obesity. J Clin Invest. 2006 Jun;116(6):1494–505.

97. Tanaka T, Narazaki M, Kishimoto T. IL-6 in inflammation, immunity, and disease. Cold Spring Harb Perspect Biol. 2014 Sep;6(10):a016295.

98. Eder K, Baffy N, Falus A, Fulop AK. The major inflammatory mediator interleukin-6 and obesity. Inflamm Res Off J Eur Histamine Res Soc . [et al]. 2009 Nov;58(11):727–36.

99. Kern L, Mittenbühler MJ, Vesting AJ, Ostermann AL, Wunderlich CM, Wunderlich FT. Obesity-Induced TNFα and IL-6 Signaling: The Missing Link between Obesity and Inflammation-Driven Liver and Colorectal Cancers. Cancers (Basel). 2018 Dec;11(1).

100. Han MS, White A, Perry RJ, Camporez J-P, Hidalgo J, Shulman GI, et al. Regulation of adipose tissue inflammation by interleukin 6. Proc Natl Acad Sci U S A. 2020 Feb;117(6):2751–60.

101. Hotamisligil GS, Shargill NS, Spiegelman BM. Adipose expression of tumor necrosis factor-alpha: direct role in obesity-linked insulin resistance. Science. 1993 Jan;259(5091):87–91.

102. Hotamisligil GS, Arner P, Caro JF, Atkinson RL, Spiegelman BM. Increased adipose tissue expression

of tumor necrosis factor-alpha in human obesity and insulin resistance. J Clin Invest. 1995 May;95(5):2409–15.

103. Liu Y, Lu X, Li X, Du P, Qin G. High-fat diet triggers obesity-related early infiltration of macrophages into adipose tissue and transient reduction of blood monocyte count. Mol Immunol. 2020 Jan;117:139–46.

104. Ziccardi P, Nappo F, Giugliano G, Esposito K, Marfella R, Cioffi M, et al. Reduction of inflammatory cytokine concentrations and improvement of endothelial functions in obese women after weight loss over one year. Circulation. 2002 Feb;105(7):804–9.

105. Liang H, Yin B, Zhang H, Zhang S, Zeng Q, Wang J, et al. Blockade of tumor necrosis factor (TNF) receptor type 1-mediated TNF-alpha signaling protected Wistar rats from diet-induced obesity and insulin resistance. Endocrinology. 2008 Jun;149(6):2943–51.

106. Kaddai V, Jager J, Gonzalez T, Najem-Lendom R, Bonnafous S, Tran A, et al. Involvement of TNF-alpha in abnormal adipocyte and muscle sortilin expression in obese mice and humans. Diabetologia. 2009 May;52(5):932–40.

107. Green A, Dobias SB, Walters DJ, Brasier AR. Tumor necrosis factor increases the rate of lipolysis in primary cultures of adipocytes without altering levels of hormone-sensitive lipase. Endocrinology. 1994 Jun;134(6):2581–8.

108. Ruan H, Miles PDG, Ladd CM, Ross K, Golub TR, Olefsky JM, et al. Profiling gene transcription in vivo reveals adipose tissue as an immediate target of tumor necrosis factor-alpha: implications for insulin resistance. Diabetes. 2002 Nov;51(11):3176–88.

109. Moreno-Indias I, Tinahones FJ. Impaired adipose tissue expandability and lipogenic capacities as ones of the main causes of metabolic disorders. J Diabetes Res. 2015;2015:970375.

110. Jones JEC, Rabhi N, Orofino J, Gamini R, Perissi V, Vernochet C, et al. The Adipocyte Acquires a Fibroblast-Like Transcriptional Signature in Response to a High Fat Diet. Sci Rep. 2020 Feb;10(1):2380.

111. Choe SS, Huh JY, Hwang IJ, Kim JI, Kim JB. Adipose Tissue Remodeling: Its Role in Energy Metabolism and Metabolic Disorders. Front Endocrinol (Lausanne). 2016;7:30.

112. Gustafson B, Gogg S, Hedjazifar S, Jenndahl L, Hammarstedt A, Smith U. Inflammation and impaired adipogenesis in hypertrophic obesity in man. Am J Physiol Endocrinol Metab. 2009 Nov;297(5):E999–1003.

113. Gustafson B, Nerstedt A, Smith U. Reduced subcutaneous adipogenesis in human hypertrophic obesity is linked to senescent precursor cells. Nat Commun. 2019 Jun;10(1):2757.

114. Spalding KL, Arner E, Westermark PO, Bernard S, Buchholz BA, Bergmann O, et al. Dynamics of fat cell turnover in humans. Nature. 2008 Jun;453(7196):783–7.

115. Wang QA, Tao C, Gupta RK, Scherer PE. Tracking adipogenesis during white adipose tissue development, expansion and regeneration. Nat Med. 2013 Oct;19(10):1338–44.

116. Hammarstedt A, Gogg S, Hedjazifar S, Nerstedt A, Smith U. Impaired Adipogenesis and Dysfunctional Adipose Tissue in Human Hypertrophic Obesity. Physiol Rev. 2018 Oct;98(4):1911–41.

117. Unger RH, Clark GO, Scherer PE, Orci L. Lipid homeostasis, lipotoxicity and the metabolic syndrome. Biochim Biophys Acta. 2010 Mar;1801(3):209–14.

118. Ferrara D, Montecucco F, Dallegri F, Carbone F. Impact of different ectopic fat depots on cardiovascular and metabolic diseases. J Cell Physiol. 2019 Dec;234(12):21630–41.

119. Johannsen DL, Conley KE, Bajpeyi S, Punyanitya M, Gallagher D, Zhang Z, et al. Ectopic lipid accumulation and reduced glucose tolerance in elderly adults are accompanied by altered skeletal muscle mitochondrial activity. J Clin Endocrinol Metab. 2012 Jan;97(1):242–50.

120. Declèves A-E, Mathew A V, Cunard R, Sharma K. AMPK mediates the initiation of kidney disease induced by a high-fat diet. J Am Soc Nephrol. 2011 Oct;22(10):1846–55.

121. Guilherme A, Virbasius J V, Puri V, Czech MP. Adipocyte dysfunctions linking obesity to insulin resistance and type 2 diabetes. Nat Rev Mol Cell Biol. 2008 May;9(5):367–77.

122. Saponaro C, Gaggini M, Carli F, Gastaldelli A. The Subtle Balance between Lipolysis and Lipogenesis: A Critical Point in Metabolic Homeostasis. Nutrients. 2015 Nov;7(11):9453–74.

123. Johnson AR, Milner JJ, Makowski L. The inflammation highway: metabolism accelerates inflammatory traffic in obesity. Immunol Rev. 2012 Sep;249(1):218–38.

124. Halberg N, Khan T, Trujillo ME, Wernstedt-Asterholm I, Attie AD, Sherwani S, et al. Hypoxia-inducible factor 1alpha induces fibrosis and insulin resistance in white adipose tissue. Mol Cell Biol. 2009 Aug;29(16):4467–83.

125. Jiang C, Qu A, Matsubara T, Chanturiya T, Jou W, Gavrilova O, et al. Disruption of hypoxia-inducible factor 1 in adipocytes improves insulin sensitivity and decreases adiposity in high-fat diet-fed mice. Diabetes. 2011 Oct;60(10):2484–95.

126. Collaboration GBMIM, Di Angelantonio E, Bhupathiraju S, Wormser D, Gao P, Kaptoge S, et al. Body-mass index and all-cause mortality: individual-participant-data meta-analysis of 239 prospective studies in four continents. Lancet (London, England). 2016 Aug;388(10046):776–86.

127. Kyrou I, Randeva HS, Tsigos C, Kaltsas G, Weickert MO. Clinical Problems Caused by Obesity. In: Feingold KR, Anawalt B, Boyce A, Chrousos G, de Herder WW, Dungan K, et al., editors. South Dartmouth (MA); 2000.

128. Chatterjee S, Khunti K, Davies MJ. Type 2 diabetes. Lancet (London, England). 2017 Jun;389(10085):2239–51.

129. Hocking S, Samocha-Bonet D, Milner K-L, Greenfield JR, Chisholm DJ. Adiposity and insulin resistance in humans: the role of the different tissue and cellular lipid depots. Endocr Rev. 2013 Aug;34(4):463–500.

130. Knowler WC, Barrett-Connor E, Fowler SE, Hamman RF, Lachin JM, Walker EA, et al. Reduction in the incidence of type 2 diabetes with lifestyle intervention or metformin. N Engl J Med. 2002 Feb;346(6):393–403.

131. Perreault L, Kahn SE, Christophi CA, Knowler WC, Hamman RF. Regression from pre-diabetes to normal glucose regulation in the diabetes prevention program. Diabetes Care. 2009 Sep;32(9):1583–8.

132. Weiss EP, Racette SB, Villareal DT, Fontana L, Steger-May K, Schechtman KB, et al. Improvements in glucose tolerance and insulin action induced by increasing energy expenditure or decreasing energy intake: a randomized controlled trial. Am J Clin Nutr. 2006 Nov;84(5):1033–42.

133. Tuomilehto J, Lindström J, Eriksson JG, Valle TT, Hämäläinen H, Ilanne-Parikka P, et al. Prevention of type 2 diabetes mellitus by changes in lifestyle among subjects with impaired glucose tolerance. N Engl J Med. 2001 May;344(18):1343–50.

134. Bastien M, Poirier P, Lemieux I, Després J-P. Overview of epidemiology and contribution of obesity to cardiovascular disease. Prog Cardiovasc Dis. 2014;56(4):369–81.

135. Krittanawong C, Tunhasiriwet A, Wang Z, Zhang H, Prokop LJ, Chirapongsathorn S, et al. Meta-Analysis Comparing Frequency of Overweight Versus Normal Weight in Patients With New-Onset Heart Failure. Am J Cardiol. 2018 Apr;121(7):836–43.

136. Kragelund C, Hassager C, Hildebrandt P, Torp-Pedersen C, Køber L. Impact of obesity on long-term prognosis following acute myocardial infarction. Int J Cardiol. 2005 Jan;98(1):123–31.

137. Koliaki C, Liatis S, Kokkinos A. Obesity and cardiovascular disease: revisiting an old relationship. Metabolism. 2019 Mar;92:98–107.

138. Rocha VZ, Libby P. Obesity, inflammation, and atherosclerosis. Nat Rev Cardiol. 2009 Jun;6(6):399–409.

139. Freitas WRJ, Oliveira LVF, Perez EA, Ilias EJ, Lottenberg CP, Silva AS, et al. Systemic Inflammation in Severe Obese Patients Undergoing Surgery for Obesity and Weight-Related Diseases. Obes Surg. 2018 Jul;28(7):1931–42.

140. Berg AH, Scherer PE. Adipose tissue, inflammation, and cardiovascular disease. Circ Res. 2005 May;96(9):939–49.

141. Shoelson SE, Lee J, Goldfine AB. Inflammation and insulin resistance. J Clin Invest. 2006 Jul;116(7):1793–801.

142. Stienstra R, van Diepen JA, Tack CJ, Zaki MH, van de Veerdonk FL, Perera D, et al. Inflammasome is a central player in the induction of obesity and insulin resistance. Proc Natl Acad Sci U S A. 2011 Sep;108(37):15324–9.

143. Duan Y, Zeng L, Zheng C, Song B, Li F, Kong X, et al. Inflammatory Links Between High Fat Diets and Diseases. Front Immunol. 2018;9:2649.

144. Declèves A-E, Sharma K. Novel targets of antifibrotic and anti-inflammatory treatment in CKD. Nat Rev Nephrol. 2014 May;10(5):257–67.

145. Poret JM, Souza-Smith F, Marcell SJ, Gaudet DA, Tzeng TH, Braymer HD, et al. High fat diet consumption differentially affects adipose tissue inflammation and adipocyte size in obesity-prone and obesity-resistant rats. Int J Obes (Lond). 2018 Mar;42(3):535–41.

146. Engin A. The Pathogenesis of Obesity-Associated Adipose Tissue Inflammation. Adv Exp Med Biol. 2017;960:221–45.

147. Cai D, Yuan M, Frantz DF, Melendez PA, Hansen L, Lee J, et al. Local and systemic insulin resistance resulting from hepatic activation of IKK-beta and NF-kappaB. Nat Med. 2005 Feb;11(2):183–90.

148. Nakamura T, Furuhashi M, Li P, Cao H, Tuncman G, Sonenberg N, et al. Double-stranded RNA-dependent protein kinase links pathogen sensing with stress and metabolic homeostasis. Cell. 2010 Feb;140(3):338–48.

149. Hirosumi J, Tuncman G, Chang L, Görgün CZ, Uysal KT, Maeda K, et al. A central role for JNK in obesity and insulin resistance. Nature. 2002 Nov;420(6913):333–6.

150. Yung JHM, Giacca A. Role of c-Jun N-terminal Kinase (JNK) in Obesity and Type 2 Diabetes. Cells. 2020 Mar;9(3).

151. Könner AC, Brüning JC. Toll-like receptors: linking inflammation to metabolism. Trends Endocrinol Metab. 2011 Jan;22(1):16–23.

152. Han MS, Jung DY, Morel C, Lakhani SA, Kim JK, Flavell RA, et al. JNK expression by macrophages promotes obesity-induced insulin resistance and inflammation. Science. 2013 Jan;339(6116):218–22.

153. Singh R, Wang Y, Xiang Y, Tanaka KE, Gaarde WA, Czaja MJ. Differential effects of JNK1 and JNK2 inhibition on murine steatohepatitis and insulin resistance. Hepatology. 2009 Jan;49(1):87–96.

154. Sabio G, Kennedy NJ, Cavanagh-Kyros J, Jung DY, Ko HJ, Ong H, et al. Role of muscle c-Jun NH2-terminal kinase 1 in obesity-induced insulin resistance. Mol Cell Biol. 2010 Jan;30(1):106–15.

155. Solinas G, Becattini B. JNK at the crossroad of obesity, insulin resistance, and cell stress response. Mol Metab. 2017 Feb;6(2):174–84.

156. Ying W, Fu W, Lee YS, Olefsky JM. The role of macrophages in obesity-associated islet inflammation and β-cell abnormalities. Nat Rev Endocrinol. 2020 Feb;16(2):81–90.

157. Saltiel AR, Olefsky JM. Inflammatory mechanisms linking obesity and metabolic disease. J Clin Invest. 2017 Jan;127(1):1–4.

158. Kammoun HL, Kraakman MJ, Febbraio MA. Adipose tissue inflammation in glucose metabolism. Rev Endocr Metab Disord. 2014 Mar;15(1):31–44.

159. Jornayvaz FR, Shulman GI. Diacylglycerol activation of protein kinase Cε and hepatic insulin resistance. Cell Metab. 2012 May;15(5):574–84.

160. Chavez JA, Summers SA. A ceramide-centric view of insulin resistance. Cell Metab. 2012 May;15(5):585–94.

161. Samuel VT, Petersen KF, Shulman GI. Lipid-induced insulin resistance: unravelling the mechanism.

Lancet (London, England). 2010 Jun;375(9733):2267–77.

162. Phillips DI, Caddy S, Ilic V, Fielding BA, Frayn KN, Borthwick AC, et al. Intramuscular triglyceride and muscle insulin sensitivity: evidence for a relationship in nondiabetic subjects. Metabolism. 1996 Aug;45(8):947–50.

163. Hegarty BD, Cooney GJ, Kraegen EW, Furler SM. Increased efficiency of fatty acid uptake contributes to lipid accumulation in skeletal muscle of high fat-fed insulin-resistant rats. Diabetes. 2002 May;51(5):1477–84.

164. Guebre-Egziabher F, Alix PM, Koppe L, Pelletier CC, Kalbacher E, Fouque D, et al. Ectopic lipid accumulation: A potential cause for metabolic disturbances and a contributor to the alteration of kidney function. Biochimie [Internet]. 2013;95(11):1971–9. Available from: http://dx.doi.org/10.1016/j.biochi.2013.07.017

165. Dubé JJ, Amati F, Toledo FGS, Stefanovic-Racic M, Rossi A, Coen P, et al. Effects of weight loss and exercise on insulin resistance, and intramyocellular triacylglycerol, diacylglycerol and ceramide. Diabetologia. 2011 May;54(5):1147–56.

166. Fu X, Zhu M, Zhang S, Foretz M, Viollet B, Du M. Obesity Impairs Skeletal Muscle Regeneration Through Inhibition of AMPK. Diabetes. 2016 Jan;65(1):188–200.

167. Nguyen M-H, Cheng M, Koh TJ. Impaired muscle regeneration in ob/ob and db/db mice. ScientificWorldJournal. 2011 Jul;11:1525–35.

168. Vanni E, Marengo A, Mezzabotta L, Bugianesi E. Systemic Complications of Nonalcoholic Fatty Liver Disease: When the Liver Is Not an Innocent Bystander. Semin Liver Dis. 2015 Aug;35(3):236–49.

169. Tarantino G, Citro V, Capone D. Nonalcoholic Fatty Liver Disease: A Challenge from Mechanisms to Therapy. J Clin Med. 2019 Dec;9(1).

170. Wang J, He W, Tsai P-J, Chen P-H, Ye M, Guo J, et al. Mutual interaction between endoplasmic reticulum and mitochondria in nonalcoholic fatty liver disease. Lipids Health Dis. 2020 Apr;19(1):72.

171. Nyman K, Granér M, Pentikäinen MO, Lundbom J, Hakkarainen A, Sirén R, et al. Cardiac steatosis and left ventricular function in men with metabolic syndrome. J Cardiovasc Magn Reson Off J Soc Cardiovasc Magn Reson. 2013 Nov;15(1):103.

172. van der Zijl NJ, Goossens GH, Moors CCM, van Raalte DH, Muskiet MHA, Pouwels PJW, et al. Ectopic fat storage in the pancreas, liver, and abdominal fat depots: impact on β-cell function in individuals with impaired glucose metabolism. J Clin Endocrinol Metab. 2011 Feb;96(2):459–67.

173. Fonseca SG, Gromada J, Urano F. Endoplasmic reticulum stress and pancreatic β-cell death. Trends Endocrinol Metab. 2011 Jul;22(7):266–74.

174. Sarparanta J, García-Macia M, Singh R. Autophagy and Mitochondria in Obesity and Type 2 Diabetes. Curr Diabetes Rev. 2017;13(4):352–69.

175. Liang W, Menke AL, Driessen A, Koek GH, Lindeman JH, Stoop R, et al. Establishment of a general NAFLD scoring system for rodent models and comparison to human liver pathology. PLoS One. 2014;9(12):e115922.

176. Glatz JFC, Angin Y, Steinbusch LKM, Schwenk RW, Luiken JJFP. CD36 as a target to prevent cardiac lipotoxicity and insulin resistance. Prostaglandins Leukot Essent Fatty Acids. 2013 Jan;88(1):71–7.

177. Angin Y, Steinbusch LKM, Simons PJ, Greulich S, Hoebers NTH, Douma K, et al. CD36 inhibition prevents lipid accumulation and contractile dysfunction in rat cardiomyocytes. Biochem J. 2012 Nov;448(1):43–53.

178. Wilson CG, Tran JL, Erion DM, Vera NB, Febbraio M, Weiss EJ. Hepatocyte-Specific Disruption of CD36 Attenuates Fatty Liver and Improves Insulin Sensitivity in HFD-Fed Mice. Endocrinology. 2016 Feb;157(2):570–85.

179. Zhao J, Rui H-L, Yang M, Sun L-J, Dong H-R, Cheng H. CD36-Mediated Lipid Accumulation and Activation of NLRP3 Inflammasome Lead to Podocyte Injury in Obesity-Related Glomerulopathy. Mediators Inflamm. 2019;2019:3172647.

180. Corpeleijn E, Pelsers MMAL, Soenen S, Mensink M, Bouwman FG, Kooi ME, et al. Insulin acutely upregulates protein expression of the fatty acid transporter CD36 in human skeletal muscle in vivo. J Physiol Pharmacol an Off J Polish Physiol Soc. 2008 Mar;59(1):77–83.

181. Bechmann LP, Gieseler RK, Sowa J-P, Kahraman A, Erhard J, Wedemeyer I, et al. Apoptosis is associated with CD36/fatty acid translocase upregulation in non-alcoholic steatohepatitis. Liver Int Off J Int Assoc Study Liver. 2010 Jul;30(6):850–9.

182. Fu D, Lu J, Yang S. Oleic/Palmitate Induces Apoptosis in Human Articular Chondrocytes via Upregulation of NOX4 Expression and ROS Production. Ann Clin Lab Sci. 2016 Jul;46(4):353–9.

183. Schönfeld P, Wojtczak L. Fatty acids as modulators of the cellular production of reactive oxygen species. Free Radic Biol Med. 2008 Aug;45(3):231–41.

184. Ly LD, Xu S, Choi S-K, Ha C-M, Thoudam T, Cha S-K, et al. Oxidative stress and calcium dysregulation by palmitate in type 2 diabetes. Exp Mol Med. 2017 Feb;49(2):e291.

185. Rial E, Rodríguez-Sánchez L, Gallardo-Vara E, Zaragoza P, Moyano E, González-Barroso MM. Lipotoxicity, fatty acid uncoupling and mitochondrial carrier function. Biochim Biophys Acta. 2010;1797(6–7):800–6.

186. Bosma M, Dapito DH, Drosatos-Tampakaki Z, Huiping-Son N, Huang L-S, Kersten S, et al. Sequestration of fatty acids in triglycerides prevents endoplasmic reticulum stress in an in vitro model of cardiomyocyte lipotoxicity. Biochim Biophys Acta. 2014 Dec;1841(12):1648–55.

187. Aon MA, Bhatt N, Cortassa SC. Mitochondrial and cellular mechanisms for managing lipid excess. Front Physiol. 2014;5:282.

188. Lee S-J, Zhang J, Choi AMK, Kim HP. Mitochondrial dysfunction induces formation of lipid droplets as a generalized response to stress. Oxid Med Cell Longev. 2013;2013:327167.

189. Jarc E, Petan T. Lipid Droplets and the Management of Cellular Stress. Yale J Biol Med. 2019 Sep;92(3):435–52.

190. Liu L, Trent CM, Fang X, Son N-H, Jiang H, Blaner WS, et al. Cardiomyocyte-specific loss of diacylglycerol acyltransferase 1 (DGAT1) reproduces the abnormalities in lipids found in severe heart failure. J Biol Chem. 2014 Oct;289(43):29881–91.

191. Global, regional, and national life expectancy, all-cause mortality, and cause-specific mortality for 249 causes of death, 1980-2015: a systematic analysis for the Global Burden of Disease Study 2015. Lancet (London, England). 2016 Oct;388(10053):1459–544.

192. Chawla LS, Bellomo R, Bihorac A, Goldstein SL, Siew ED, Bagshaw SM, et al. Acute kidney disease and renal recovery: consensus report of the Acute Disease Quality Initiative (ADQI) 16 Workgroup. Nat Rev Nephrol. 2017 Apr;13(4):241–57.

193. Lewington AJP, Cerdá J, Mehta RL. Raising awareness of acute kidney injury: a global perspective of a silent killer. Kidney Int. 2013 Sep;84(3):457–67.

194. Lameire NH, Bagga A, Cruz D, De Maeseneer J, Endre Z, Kellum JA, et al. Acute kidney injury: an increasing global concern. Lancet (London, England). 2013 Jul;382(9887):170–9.

195. Case J, Khan S, Khalid R, Khan A. Epidemiology of acute kidney injury in the intensive care unit. Crit Care Res Pract. 2013;2013:479730.

196. Ronco C, Bellomo R, Kellum JA. Acute kidney injury. Lancet (London, England). 2019 Nov;394(10212):1949–64.

197. Koza Y. Acute kidney injury: current concepts and new insights. J Inj Violence Res. 2016 Jan;8(1):58–62.

198. Makris K, Spanou L. Acute Kidney Injury: Definition, Pathophysiology and Clinical Phenotypes. Clin Biochem Rev. 2016 May;37(2):85–98.

199. Kellum JA, Lameire N. Diagnosis, evaluation, and management of acute kidney injury: a KDIGO summary (Part 1). Crit Care. 2013 Feb;17(1):204.

200. Hill NR, Fatoba ST, Oke JL, Hirst JA, O'Callaghan CA, Lasserson DS, et al. Global Prevalence of Chronic Kidney Disease - A Systematic Review and Meta-Analysis. PLoS One. 2016;11(7):e0158765.

201. Inker LA, Astor BC, Fox CH, Isakova T, Lash JP, Peralta CA, et al. KDOQI US commentary on the 2012 KDIGO clinical practice guideline for the evaluation and management of CKD. Am J kidney Dis Off J Natl Kidney Found. 2014 May;63(5):713–35.

202. Liyanage T, Ninomiya T, Jha V, Neal B, Patrice HM, Okpechi I, et al. Worldwide access to treatment for end-stage kidney disease: a systematic review. Lancet (London, England). 2015 May;385(9981):1975–82.

203. Jha V, Garcia-Garcia G, Iseki K, Li Z, Naicker S, Plattner B, et al. Chronic kidney disease: global dimension and perspectives. Lancet (London, England). 2013 Jul;382(9888):260–72.

204. Garofalo C, Borrelli S, Minutolo R, Chiodini P, De Nicola L, Conte G. A systematic review and meta-analysis suggests obesity predicts onset of chronic kidney disease in the general population. Kidney Int. 2017 May;91(5):1224–35.

205. Lu JL, Kalantar-Zadeh K, Ma JZ, Quarles LD, Kovesdy CP. Association of body mass index with outcomes in patients with CKD. J Am Soc Nephrol. 2014 Sep;25(9):2088–96.

206. Laville M. Conséquences rénales de l'obésite. 2011;7:80–5.

207. González E, Gutiérrez E, Morales E, Hernández E, Andres A, Bello I, et al. Factors influencing the progression of renal damage in patients with unilateral renal agenesis and remnant kidney. Kidney Int. 2005 Jul;68(1):263–70.

208. Tsujimoto T, Sairenchi T, Iso H, Irie F, Yamagishi K, Watanabe H, et al. The dose-response relationship between body mass index and the risk of incident stage ≥3 chronic kidney disease in a general japanese population: the Ibaraki prefectural health study (IPHS). J Epidemiol. 2014;24(6):444–51.

209. Elsayed EF, Sarnak MJ, Tighiouart H, Griffith JL, Kurth T, Salem DN, et al. Waist-to-hip ratio, body mass index, and subsequent kidney disease and death. Am J kidney Dis Off J Natl Kidney Found. 2008 Jul;52(1):29–38.

210. Blüher M. The distinction of metabolically "healthy" from "unhealthy" obese individuals. Curr Opin Lipidol. 2010 Feb;21(1):38–43.

211. Goumenos DS, Kawar B, El Nahas M, Conti S, Wagner B, Spyropoulos C, et al. Early histological changes in the kidney of people with morbid obesity. Nephrol Dial Transplant Off Publ Eur Dial Transpl Assoc - Eur Ren Assoc. 2009 Dec;24(12):3732–8.

212. Mathew A V, Okada S, Sharma K. Obesity related kidney disease. Curr Diabetes Rev. 2011 Jan;7(1):41–9.

213. Ritz E, Koleganova N, Piecha G. Is there an obesity-metabolic syndrome related glomerulopathy? Curr Opin Nephrol Hypertens. 2011 Jan;20(1):44–9.

214. Ruggiero C, Ehrenshaft M, Cleland E, Stadler K. High-fat diet induces an initial adaptation of mitochondrial bioenergetics in the kidney despite evident oxidative stress and mitochondrial ROS production. Am J Physiol Endocrinol Metab. 2011 Jun;300(6):E1047-58.

215. Chagnac A, Weinstein T, Korzets A, Ramadan E, Hirsch J, Gafter U. Glomerular hemodynamics in severe obesity.

216. D'Agati VD, Chagnac A, de Vries APJ, Levi M, Porrini E, Herman-Edelstein M, et al. Obesity-related glomerulopathy: clinical and pathologic characteristics and pathogenesis. Nat Rev Nephrol. 2016 Aug;12(8):453–71.

217. Krikken JA, Lely AT, Bakker SJL, Navis G. The effect of a shift in sodium intake on renal hemodynamics is determined by body mass index in healthy young men. Kidney Int. 2007 Feb;71(3):260–5.

218. Tomaszewski M, Charchar FJ, Maric C, McClure J, Crawford L, Grzeszczak W, et al. Glomerular hyperfiltration: a new marker of metabolic risk. Kidney Int. 2007 Apr;71(8):816–21.

219. Kriz W, Lemley K V. A potential role for mechanical forces in the detachment of podocytes and the progression of CKD. J Am Soc Nephrol. 2015 Feb;26(2):258–69.

220. Endlich N, Endlich K. The challenge and response of podocytes to glomerular hypertension. Semin Nephrol. 2012 Jul;32(4):327–41.

221. Nagata M, Kriz W. Glomerular damage after uninephrectomy in young rats. II. Mechanical stress on podocytes as a pathway to sclerosis. Kidney Int. 1992 Jul;42(1):148–60.

222. Nishizono R, Kikuchi M, Wang SQ, Chowdhury M, Nair V, Hartman J, et al. FSGS as an Adaptive Response to Growth-Induced Podocyte Stress. J Am Soc Nephrol. 2017 Oct;28(10):2931–45.

223. Griffin KA, Kramer H, Bidani AK. Adverse renal consequences of obesity. Am J Physiol Renal Physiol. 2008 Apr;294(4):F685-96.

224. Hall JE, do Carmo JM, da Silva AA, Wang Z, Hall ME. Obesity-induced hypertension: interaction of neurohumoral and renal mechanisms. Circ Res. 2015 Mar;116(6):991–1006.

225. Davy KP, Orr JS. Sympathetic nervous system behavior in human obesity. Neurosci Biobehav Rev. 2009 Feb;33(2):116–24.

226. Esler M, Straznicky N, Eikelis N, Masuo K, Lambert G, Lambert E. Mechanisms of sympathetic activation in obesity-related hypertension. Hypertens (Dallas, Tex 1979). 2006 Nov;48(5):787–96.

227. Nasrallah MP, Ziyadeh FN. Overview of the physiology and pathophysiology of leptin with special emphasis on its role in the kidney. Semin Nephrol. 2013 Jan;33(1):54–65.

228. Shek EW, Brands MW, Hall JE. Chronic leptin infusion increases arterial pressure. Hypertens (Dallas, Tex 1979). 1998 Jan;31(1 Pt 2):409–14.

229. Schelling P, Fischer H, Ganten D. Angiotensin and cell growth: a link to cardiovascular hypertrophy? Vol. 9, Journal of hypertension. England; 1991. p. 3–15.

230. Warnholtz A, Nickenig G, Schulz E, Macharzina R, Bräsen JH, Skatchkov M, et al. Increased NADH-oxidase-mediated superoxide production in the early stages of atherosclerosis: evidence for involvement of the renin-angiotensin system. Circulation. 1999 Apr;99(15):2027–33.

231. Jaimes EA, Galceran JM, Raij L. Angiotensin II induces superoxide anion production by mesangial cells. Kidney Int. 1998 Sep;54(3):775–84.

232. Mezzano SA, Ruiz-Ortega M, Egido J. Angiotensin II and renal fibrosis. Hypertens (Dallas, Tex 1979). 2001 Sep;38(3 Pt 2):635–8.

233. Ketteler M, Noble NA, Border WA. Transforming growth factor-beta and angiotensin II: the missing link from glomerular hyperfiltration to glomerulosclerosis? Annu Rev Physiol. 1995;57:279–95.

234. Leehey DJ, Singh AK, Alavi N, Singh R. Role of angiotensin II in diabetic nephropathy. Kidney Int Suppl. 2000 Sep;77:S93-8.

235. Thethi T, Kamiyama M, Kobori H. The link between the renin-angiotensin-aldosterone system and renal injury in obesity and the metabolic syndrome. Curr Hypertens Rep. 2012 Apr;14(2):160–9.

236. Toke A, Meyer TW. Hemodynamic effects of angiotensin II in the kidney. Contrib Nephrol. 2001;(135):34–46.

237. Kennedy CR, Burns KD. Angiotensin II as a mediator of renal tubular transport. Contrib Nephrol. 2001;(135):47–62.

238. Rüster C, Wolf G. The role of the renin-angiotensin-aldosterone system in obesity-related renal diseases. Semin Nephrol. 2013 Jan;33(1):44–53.

239. Abrass CK, Raugi GJ, Gabourel LS, Lovett DH. Insulin and insulin-like growth factor I binding to cultured rat glomerular mesangial cells. Endocrinology. 1988 Nov;123(5):2432–9.

240. Welsh GI, Hale LJ, Eremina V, Jeansson M, Maezawa Y, Lennon R, et al. Insulin signaling to the glomerular podocyte is critical for normal kidney function. Cell Metab. 2010 Oct;12(4):329–40.

241. Weinbaum S, Duan Y, Satlin LM, Wang T, Weinstein AM. Mechanotransduction in the renal tubule. Am J Physiol Renal Physiol. 2010 Dec;299(6):F1220-36.

242. Vallon V, Thomson SC. Renal function in diabetic disease models: the tubular system in the pathophysiology of the diabetic kidney. Annu Rev Physiol. 2012;74:351–75.

243. Heerspink HJL, Perkins BA, Fitchett DH, Husain M, Cherney DZI. Sodium Glucose Cotransporter 2 Inhibitors in the Treatment of Diabetes Mellitus: Cardiovascular and Kidney Effects, Potential Mechanisms, and Clinical Applications. Circulation. 2016 Sep;134(10):752–72.

244. Chen J-K, Nagai K, Chen J, Plieth D, Hino M, Xu J, et al. Phosphatidylinositol 3-kinase signaling determines kidney size. J Clin Invest. 2015 Jun;125(6):2429–44.

245. Hall JE, do Carmo JM, da Silva AA, Wang Z, Hall ME. Obesity, kidney dysfunction and hypertension: mechanistic links. Nat Rev Nephrol. 2019 Jun;15(6):367–85.

246. Tonneijck L, Muskiet MHA, Smits MM, van Bommel EJ, Heerspink HJL, van Raalte DH, et al. Glomerular Hyperfiltration in Diabetes: Mechanisms, Clinical Significance, and Treatment. J Am Soc Nephrol. 2017 Apr;28(4):1023–39.

247. Lane JT. Microalbuminuria as a marker of cardiovascular and renal risk in type 2 diabetes mellitus: a temporal perspective. Am J Physiol Renal Physiol. 2004 Mar;286(3):F442-50.

248. Pagtalunan ME, Miller PL, Jumping-Eagle S, Nelson RG, Myers BD, Rennke HG, et al. Podocyte loss and progressive glomerular injury in type II diabetes. J Clin Invest. 1997 Jan;99(2):342–8.

249. Chagnac A, Zingerman B, Rozen-Zvi B, Herman-Edelstein M. Consequences of Glomerular Hyperfiltration: The Role of Physical Forces in the Pathogenesis of Chronic Kidney Disease in Diabetes and Obesity. Nephron. 2019;143(1):38–42.

250. Unamuno X, Gómez-Ambrosi J, Rodríguez A, Becerril S, Frühbeck G, Catalán V. Adipokine dysregulation and adipose tissue inflammation in human obesity. Eur J Clin Invest. 2018 Sep;48(9):e12997.

251. Adamczak M, Wiecek A. The adipose tissue as an endocrine organ. Semin Nephrol. 2013 Jan;33(1):2–13.

252. Navarro-Díaz M, Serra A, López D, Granada M, Bayés B, Romero R. Obesity, inflammation, and kidney disease. Kidney Int Suppl. 2008 Dec;(111):S15-8.

253. Sharma K, Ramachandrarao S, Qiu G, Usui HK, Zhu Y, Dunn SR, et al. Adiponectin regulates albuminuria and podocyte function in mice. J Clin Invest. 2008 May;118(5):1645–56.

254. Fang F, Liu GC, Kim C, Yassa R, Zhou J, Scholey JW. Adiponectin attenuates angiotensin II-induced oxidative stress in renal tubular cells through AMPK and cAMP-Epac signal transduction pathways. Am J Physiol Renal Physiol. 2013 Jun;304(11):F1366-74.

255. Garcia D, Shaw RJ. AMPK: Mechanisms of Cellular Energy Sensing and Restoration of Metabolic Balance. Mol Cell. 2017 Jun;66(6):789–800.

256. Herzig S, Shaw RJ. AMPK: guardian of metabolism and mitochondrial homeostasis. Nat Rev Mol Cell Biol [Internet]. 2017; Available from: http://www.nature.com/doifinder/10.1038/nrm.2017.95

257. Kim Y, Lim JH, Kim MY, Kim EN, Yoon HE, Shin SJ, et al. The Adiponectin Receptor Agonist AdipoRon Ameliorates Diabetic Nephropathy in a Model of Type 2 Diabetes. J Am Soc Nephrol. 2018 Apr;29(4):1108–27.

258. Yamauchi T, Kamon J, Ito Y, Tsuchida A, Yokomizo T, Kita S, et al. Cloning of adiponectin receptors that mediate antidiabetic metabolic effects. Nature. 2003 Jun;423(6941):762–9.

259. Perri A, Vizza D, Lofaro D, Gigliotti P, Leone F, Brunelli E, et al. Adiponectin is expressed and secreted by renal tubular epithelial cells. J Nephrol. 2013;26(6):1049–54.

260. Kadowaki T, Yamauchi T, Kubota N. The physiological and pathophysiological role of adiponectin and adiponectin receptors in the peripheral tissues and CNS. FEBS Lett. 2008 Jan;582(1):74–80.

261. Iwabu M, Yamauchi T, Okada-Iwabu M, Sato K, Nakagawa T, Funata M, et al. Adiponectin and AdipoR1 regulate PGC-1alpha and mitochondria by Ca(2+) and AMPK/SIRT1. Nature. 2010 Apr;464(7293):1313–9.

262. Choi SR, Lim JH, Kim MY, Kim EN, Kim Y, Choi BS, et al. Adiponectin receptor agonist AdipoRon decreased ceramide, and lipotoxicity, and ameliorated diabetic nephropathy. Metabolism. 2018 Aug;85:348–60.

263. Tarabra E, Giunti S, Barutta F, Salvidio G, Burt D, Deferrari G, et al. Effect of the monocyte chemoattractant protein-1/CC chemokine receptor 2 system on nephrin expression in streptozotocin-treated mice and human cultured podocytes. Diabetes. 2009 Sep;58(9):2109–18.

264. Uysal KT, Wiesbrock SM, Hotamisligil GS. Functional analysis of tumor necrosis factor (TNF) receptors in TNF-alpha-mediated insulin resistance in genetic obesity. Endocrinology. 1998 Dec;139(12):4832–8.

265. Zhu X, Jiang S, Hu N, Luo F, Dong H, Kang Y-M, et al. Tumour necrosis factor-α inhibition with lenalidomide alleviates tissue oxidative injury and apoptosis in ob/ob obese mice. Clin Exp Pharmacol Physiol. 2014 Jul;41(7):489–501.

266. Wang H, Li J, Gai Z, Kullak-Ublick GA, Liu Z. TNF-α Deficiency Prevents Renal Inflammation and Oxidative Stress in Obese Mice. Kidney Blood Press Res. 2017;42(3):416–27.

267. Rashid G, Benchetrit S, Fishman D, Bernheim J. Effect of advanced glycation end-products on gene expression and synthesis of TNF-alpha and endothelial nitric oxide synthase by endothelial cells. Kidney Int. 2004 Sep;66(3):1099–106.

268. Ruiz-Ortega M, Ruperez M, Lorenzo O, Esteban V, Blanco J, Mezzano S, et al. Angiotensin II regulates the synthesis of proinflammatory cytokines and chemokines in the kidney. Kidney Int Suppl. 2002 Dec;(82):S12-22.

269. Quigley JE, Elmarakby AA, Knight SF, Manhiani MM, Stepp DW, Olearzcyk JJ, et al. Obesity induced renal oxidative stress contributes to renal injury in salt-sensitive hypertension. Clin Exp Pharmacol Physiol. 2009 Jul;36(7):724–8.

270. Habibi J, Hayden MR, Sowers JR, Pulakat L, Tilmon RD, Manrique C, et al. Nebivolol attenuates redox-sensitive glomerular and tubular mediated proteinuria in obese rats. Endocrinology. 2011 Feb;152(2):659–68.

271. Fujii H, Kono K, Nakai K, Goto S, Komaba H, Hamada Y, et al. Oxidative and nitrosative stress and progression of diabetic nephropathy in type 2 diabetes. Am J Nephrol. 2010;31(4):342–52.

272. Jha JC, Gray SP, Barit D, Okabe J, El-Osta A, Namikoshi T, et al. Genetic targeting or pharmacologic inhibition of NADPH oxidase nox4 provides renoprotection in long-term diabetic nephropathy. J Am Soc Nephrol. 2014 Jun;25(6):1237–54.

273. Li Y, Qi Y, Kim MS, Xu KZ-Y, Huang TH-W, Rong X, et al. Increased renal collagen cross-linking and lipid accumulation in nephropathy of Zucker diabetic fatty rats. Diabetes Metab Res Rev. 2008 Sep;24(6):498–506.

274. Sureshbabu A, Muhsin SA, Choi ME. TGF-β signaling in the kidney: profibrotic and protective effects. Am J Physiol Renal Physiol. 2016 Apr;310(7):F596–606.

275. Henegar JR, Bigler SA, Henegar LK, Tyagi SC, Hall JE. Functional and structural changes in the kidney in the early stages of obesity. J Am Soc Nephrol. 2001 Jun;12(6):1211–7.

276. Eddy AA. Interstitial fibrosis in hypercholesterolemic rats: role of oxidation, matrix synthesis, and proteolytic cascades. Kidney Int. 1998 May;53(5):1182–9.

277. Williams KJ, Qiu G, Usui HK, Dunn SR, McCue P, Bottinger E, et al. Decorin deficiency enhances progressive nephropathy in diabetic mice. Am J Pathol. 2007 Nov;171(5):1441–50.

278. Ziyadeh FN, Hoffman BB, Han DC, Iglesias-De La Cruz MC, Hong SW, Isono M, et al. Long-term prevention of renal insufficiency, excess matrix gene expression, and glomerular mesangial matrix expansion by treatment with monoclonal antitransforming growth factor-beta antibody in db/db diabetic mice. Proc Natl Acad Sci U S A. 2000 Jul;97(14):8015–20.

279. Dugan LL, You Y-H, Ali SS, Diamond-Stanic M, Miyamoto S, DeCleves A-E, et al. AMPK dysregulation promotes diabetes-related reduction of superoxide and mitochondrial function. J Clin Invest. 2013 Nov;123(11):4888–99.

280. Samuel VT, Shulman GI. Mechanisms for insulin resistance: Common threads and missing links. Cell. 2012.

281. Sharma SG, Bomback AS, Radhakrishnan J, Herlitz LC, Stokes MB, Markowitz GS, et al. The modern spectrum of renal biopsy findings in patients with diabetes. Clin J Am Soc Nephrol. 2013 Oct;8(10):1718–24.

282. Chen X, Han Y, Gao P, Yang M, Xiao L, Xiong X, et al. Disulfide-bond A oxidoreductase-like protein protects against ectopic fat deposition and lipid-related kidney damage in diabetic nephropathy. Kidney Int. 2019 Apr;95(4):880–95.

283. Herman-Edelstein M, Scherzer P, Tobar A, Levi M, Gafter U. Altered renal lipid metabolism and renal lipid accumulation in human diabetic nephropathy. J Lipid Res. 2014 Mar;55(3):561–72.

284. Declèves A-E, Zolkipli Z, Satriano J, Wang L, Nakayama T, Rogac M, et al. Regulation of lipid accumulation by AMK-activated kinase in high fat diet–induced kidney injury.

285. De Vries APJ, Ruggenenti P, Ruan XZ, Praga M, Cruzado JM, Bajema IM, et al. Fatty kidney: Emerging role of ectopic lipid in obesity-related renal disease. Lancet Diabetes Endocrinol [Internet]. 2014;2(5):417–26. Available from: http://dx.doi.org/10.1016/S2213-8587(14)70065-8

286. Yamamoto T, Takabatake Y, Takahashi A, Kimura T. High-Fat Diet-Induced Lysosomal Dysfunction and Impaired Autophagic Flux Contribute to Lipotoxicity in the Kidney. 2016;1–18.

287. Yang X, Okamura DM, Lu X, Chen Y, Moorhead J, Varghese Z, et al. CD36 in chronic kidney disease: novel insights and therapeutic opportunities. Nat Rev Nephrol. 2017 Dec;13(12):769–81.

288. Yang P, Xiao Y, Luo X, Zhao Y, Zhao L, Wang Y, et al. Inflammatory stress promotes the development of obesity-related chronic kidney disease via CD36 in mice. J Lipid Res. 2017 Jul;58(7):1417–27.

289. Feng L, Gu C, Li Y, Huang J. High Glucose Promotes CD36 Expression by Upregulating Peroxisome Proliferator-Activated Receptor γ Levels to Exacerbate Lipid Deposition in Renal Tubular Cells. Biomed Res Int. 2017;2017:1414070.

290. Hua W, Huang H, Tan L, Wan J, Gui H, Zhao L, et al. CD36 Mediated Fatty Acid-Induced Podocyte Apoptosis via Oxidative Stress. PLoS One. 2015;10(5):e0127507.

291. Schlondorff D. Cellular mechanisms of lipid injury in the glomerulus. Am J kidney Dis Off J Natl Kidney Found. 1993 Jul;22(1):72–82.

292. Takemura T, Yoshioka K, Aya N, Murakami K, Matumoto A, Itakura H, et al. Apolipoproteins and lipoprotein receptors in glomeruli in human kidney diseases. Kidney Int. 1993 Apr;43(4):918–27.

293. Decleves A-E, Zolkipli Z, Satriano J, Wang L, Nakayama T, Rogac M, et al. Regulation of lipid accumulation by AMP-activated kinase [corrected] in high fat diet-induced kidney injury. Kidney Int. 2014 Mar;85(3):611–23.

294. Declèves A-E, Zolkipli Z, Satriano J, Wang L, Nakayama T, Rogac M, et al. Regulation of lipid accumulation by AMK-activated kinase in high fat diet–induced kidney injury. Kidney Int [Internet]. 2014;85(3):611–23. Available from: http://linkinghub.elsevier.com/retrieve/pii/S0085253815562443

295. Kang HM, Ahn SH, Choi P, Ko Y-A, Han SH, Chinga F, et al. Defective fatty acid oxidation in renal tubular epithelial cells has a key role in kidney fibrosis development. Nat Med [Internet]. 2014;21(1):37–46. Available from: http://www.nature.com/doifinder/10.1038/nm.3762

296. Sun L, Halaihel N, Zhang W, Rogers H, Levi M. Role of sterol regulatory element-binding protein 1 in regulation of renal lipid metabolism and glomerulosclerosis in diabetes mellitus. J Biol Chem. 2002;277(21):18919–27.

297. Jiang T, Liebman SE, Lucia MS, Li J, Levi M. Role of altered renal lipid metabolism and the sterol regulatory element binding proteins in the pathogenesis of age-related renal disease. Kidney Int. 2005 Dec;68(6):2608–20.

298. Proctor G, Jiang T, Iwahashi M, Wang Z, Li J, Levi M. Regulation of renal fatty acid and cholesterol metabolism, inflammation, and fibrosis in Akita and OVE26 mice with type 1 diabetes. Diabetes. 2006 Sep;55(9):2502–9.

299. Jiang T, Wang Z, Proctor G, Moskowitz S, Liebman SE, Rogers T, et al. Diet-induced Obesity in C57BL / 6J Mice Causes Increased Renal Lipid Accumulation and Glomerulosclerosis via a Sterol Regulatory Element-binding Protein-1c-dependent Pathway *. 2005;280(37):32317–25.

300. Kume S, Uzu T, Araki S-I, Sugimoto T, Isshiki K, Chin-Kanasaki M, et al. Role of Altered Renal Lipid Metabolism in the Development of Renal Injury Induced by a High-Fat Diet. 2007;2715–23.

301. Tanaka Y, Kume S, Araki S, Isshiki K, Chin-Kanasaki M, Sakaguchi M, et al. Fenofibrate, a PPARα agonist, has renoprotective effects in mice by enhancing renal lipolysis. Kidney Int. 2011 Apr;79(8):871–82.

302. Turnbaugh PJ, Ley RE, Mahowald MA, Magrini V, Mardis ER, Gordon JI. An obesity-associated gut microbiome with increased capacity for energy harvest. Nature. 2006 Dec;444(7122):1027–31.

303. Cani PD, Osto M, Geurts L, Everard A. Involvement of gut microbiota in the development of low-grade inflammation and type 2 diabetes associated with obesity. Gut Microbes. 2012;3(4):279–88.

304. Nallu A, Sharma S, Ramezani A, Muralidharan J, Raj D. Gut microbiome in chronic kidney disease: challenges and opportunities. Transl Res. 2017 Jan;179:24–37.

305. Anders H-J, Andersen K, Stecher B. The intestinal microbiota, a leaky gut, and abnormal immunity in kidney disease. Kidney Int. 2013 Jun;83(6):1010–6.

306. Graboski AL, Redinbo MR. Gut-Derived Protein-Bound Uremic Toxins. Toxins (Basel). 2020 Sep;12(9).

307. Kikuchi H, Sasaki E, Nomura N, Mori T, Minamishima YA, Yoshizaki Y, et al. Failure to sense energy depletion may be a novel therapeutic target in chronic kidney disease. Kidney Int. 2019 Jan;95(1):123–37.

308. den Besten G, van Eunen K, Groen AK, Venema K, Reijngoud D-J, Bakker BM. The role of short-chain fatty acids in the interplay between diet, gut microbiota, and host energy metabolism. J Lipid Res. 2013 Sep;54(9):2325–40.

309. Krishnamurthy VMR, Wei G, Baird BC, Murtaugh M, Chonchol MB, Raphael KL, et al. High dietary fiber intake is associated with decreased inflammation and all-cause mortality in patients with chronic kidney disease. Kidney Int. 2012 Feb;81(3):300–6.

310. Fagundes RAB, Soder TF, Grokoski KC, Benetti F, Mendes RH. Probiotics in the treatment of chronic kidney disease: a systematic review. J Bras Nefrol 'orgao Of Soc Bras e Latino-Americana Nefrol. 2018;40(3):278–86.

311. Wang V, Vilme H, Maciejewski ML, Boulware LE. The Economic Burden of Chronic Kidney Disease and End-Stage Renal Disease. Semin Nephrol. 2016 Jul;36(4):319–30.

312. Cornier M-A, Dabelea D, Hernandez TL, Lindstrom RC, Steig AJ, Stob NR, et al. The metabolic syndrome. Endocr Rev. 2008 Dec;29(7):777–822.

313. Nashar K, Egan BM. Relationship between chronic kidney disease and metabolic syndrome: current perspectives. Diabetes Metab Syndr Obes. 2014;7:421–35.

314. Raikou VD, Gavriil S. Metabolic Syndrome and Chronic Renal Disease. Dis (Basel, Switzerland). 2018 Jan;6(1).

315. Thomas G, Sehgal AR, Kashyap SR, Srinivas TR, Kirwan JP, Navaneethan SD. Metabolic syndrome and kidney disease: A systematic review and meta-analysis. Clin J Am Soc Nephrol. 2011;6(10):2364–73.

316. Whaley-Connell A, Sowers JR. Obesity and kidney disease: from population to basic science and the search for new therapeutic targets. Kidney Int [Internet]. 2017;92(2):313–23. Available from: http://dx.doi.org/10.1016/j.kint.2016.12.034

317. Ejerblad E. Obesity and Risk for Chronic Renal Failure. J Am Soc Nephrol [Internet]. 2006;17(6):1695–702. Available from: http://www.jasn.org/cgi/doi/10.1681/ASN.2005060638

318. Bhupathiraju SN, Hu FB. Epidemiology of Obesity and Diabetes and Their Cardiovascular Complications. Circ Res. 2016 May;118(11):1723–35.

319. Maric-Bilkan C. Obesity and diabetic kidney disease. Med Clin North Am. 2013 Jan;97(1):59–74.

320. Jung UJ, Choi M-S. Obesity and its metabolic complications: the role of adipokines and the relationship between obesity, inflammation, insulin resistance, dyslipidemia and nonalcoholic fatty liver disease. Int J Mol Sci. 2014 Apr;15(4):6184–223.

321. DeMarco VG, Aroor AR, Sowers JR. The pathophysiology of hypertension in patients with obesity. Nat Rev Endocrinol. 2014 Jun;10(6):364–76.

322. Kaysen GA. Dyslipidemia in chronic kidney disease: Causes and consequences. Kidney Int [Internet]. 2006;70(SUPPL. 104):S55–8. Available from: http://dx.doi.org/10.1038/sj.ki.5001979

323. Li L, Wang C, Yang H, Liu S, Lu Y, Fu P, et al. Metabolomics reveal mitochondrial and fatty acid metabolism disorders that contribute to the development of DKD in T2DM patients. Mol Biosyst. 2017 Oct;13(11):2392–400.

324. Lee M-J, Feliers D, Mariappan MM, Sataranatarajan K, Mahimainathan L, Musi N, et al. A role for AMP-activated protein kinase in diabetes-induced renal hypertrophy. Am J Physiol Renal Physiol. 2007 Feb;292(2):F617-27.

325. Eid AA, Ford BM, Block K, Kasinath BS, Gorin Y, Ghosh-Choudhury G, et al. AMP-activated protein kinase (AMPK) negatively regulates Nox4-dependent activation of p53 and epithelial cell apoptosis in diabetes. J Biol Chem. 2010 Nov;285(48):37503–12.

326. Han SH, Malaga-Dieguez L, Chinga F, Kang HM, Tao J, Reidy K, et al. Deletion of Lkb1 in Renal Tubular Epithelial Cells Leads to CKD by Altering Metabolism. J Am Soc Nephrol. 2016 Feb;27(2):439–53.

327. Hasanvand A, Amini-Khoei H, Jahanabadi S, Hadian MR, Abdollahi A, Tavangar SM, et al. Metformin attenuates streptozotocin-induced diabetic nephropathy in rats through activation of AMPK signaling pathway. J Nephropathol. 2018;7(1):37–42.

328. Zhou X, Muise ES, Haimbach R, Sebhat IK, Zhu Y, Liu F, et al. PAN-AMPK Activation Improves Renal Function in a Rat Model of Progressive Diabetic Nephropathy. J Pharmacol Exp Ther. 2019 Oct;371(1):45–55.

329. Habib SL, Yadav A, Kidane D, Weiss RH, Liang S. Novel protective mechanism of reducing renal cell damage in diabetes: Activation AMPK by AICAR increased NRF2/OGG1 proteins and reduced oxidative DNA damage. Cell Cycle. 2016 Nov;15(22):3048–59.

330. Liang J, Xu Z-X, Ding Z, Lu Y, Yu Q, Werle KD, et al. Myristoylation confers noncanonical AMPK functions in autophagy selectivity and mitochondrial surveillance. Nat Commun. 2015 Aug;6:7926.

331. Seo-Mayer PW, Thulin G, Zhang L, Alves DS, Ardito T, Kashgarian M, et al. Preactivation of AMPK by metformin may ameliorate the epithelial cell damage caused by renal ischemia. Am J Physiol Renal Physiol. 2011 Dec;301(6):F1346-57.

332. Salatto CT, Miller RA, Cameron KO, Cokorinos E, Reyes A, Ward J, et al. Selective Activation of AMPK beta1-Containing Isoforms Improves Kidney Function in a Rat Model of Diabetic Nephropathy. J Pharmacol Exp Ther. 2017 May;361(2):303–11.

333. Hallows KR, Mount PF, Pastor-Soler NM, Power DA. Role of the energy sensor AMP-activated protein kinase in renal physiology and disease. Am J Physiol Renal Physiol. 2010 May;298(5):F1067-77.

334. Neumann D. Is TAK1 a Direct Upstream Kinase of AMPK? Int J Mol Sci. 2018 Aug;19(8).

335. Pulinilkunnil T, He H, Kong D, Asakura K, Peroni OD, Lee A, et al. Adrenergic regulation of AMP-activated protein kinase in brown adipose tissue in vivo. J Biol Chem. 2011 Mar;286(11):8798–809.

336. Hurley RL, Barré LK, Wood SD, Anderson KA, Kemp BE, Means AR, et al. Regulation of AMP-

activated protein kinase by multisite phosphorylation in response to agents that elevate cellular cAMP. J Biol Chem. 2006 Dec;281(48):36662–72.

337. Coughlan KA, Valentine RJ, Sudit BS, Allen K, Dagon Y, Kahn BB, et al. PKD1 Inhibits AMPKα2 through Phosphorylation of Serine 491 and Impairs Insulin Signaling in Skeletal Muscle Cells. J Biol Chem. 2016 Mar;291(11):5664–75.

338. Lazo-Fernandez Y, Baile G, Meade P, Torcal P, Martinez L, Ibanez C, et al. Kidney-specific genetic deletion of both AMPK alpha-subunits causes salt and water wasting. Am J Physiol Renal Physiol. 2017 Feb;312(2):F352–65.

339. Kohlstedt K, Trouvain C, Boettger T, Shi L, Fisslthaler B, Fleming I. AMP-activated protein kinase regulates endothelial cell angiotensin-converting enzyme expression via p53 and the post-transcriptional regulation of microRNA-143/145. Circ Res. 2013 Apr;112(8):1150–8.

340. Yang X, Mudgett J, Bou-About G, Champy M-F, Jacobs H, Monassier L, et al. Physiological Expression of AMPKgamma2RG Mutation Causes Wolff-Parkinson-White Syndrome and Induces Kidney Injury in Mice. J Biol Chem. 2016 Nov;291(45):23428–39.

341. Viollet B, Horman S, Leclerc J, Lantier L, Foretz M, Billaud M, et al. AMPK inhibition in health and disease. Crit Rev Biochem Mol Biol. 2010;45(4):276–95.

342. Okabe K, Yaku K, Tobe K, Nakagawa T. Implications of altered NAD metabolism in metabolic disorders. J Biomed Sci. 2019 May;26(1):34.

343. Lan F, Cacicedo JM, Ruderman N, Ido Y. SIRT1 modulation of the acetylation status, cytosolic localization, and activity of LKB1. Possible role in AMP-activated protein kinase activation. J Biol Chem. 2008 Oct;283(41):27628–35.

344. Suchankova G, Nelson LE, Gerhart-Hines Z, Kelly M, Gauthier M-S, Saha AK, et al. Concurrent regulation of AMP-activated protein kinase and SIRT1 in mammalian cells. Biochem Biophys Res Commun. 2009 Jan;378(4):836–41.

345. Price NL, Gomes AP, Ling AJY, Duarte F V, Martin-Montalvo A, North BJ, et al. SIRT1 is required for AMPK activation and the beneficial effects of resveratrol on mitochondrial function. Cell Metab. 2012 May;15(5):675–90.

346. Dagon Y, Hur E, Zheng B, Wellenstein K, Cantley LC, Kahn BB. p70S6 kinase phosphorylates AMPK on serine 491 to mediate leptin's effect on food intake. Cell Metab. 2012 Jul;16(1):104–12.

347. Valentine RJ, Coughlan KA, Ruderman NB, Saha AK. Insulin inhibits AMPK activity and phosphorylates AMPK $Ser^{485/491}$ through Akt in hepatocytes, myotubes and incubated rat skeletal muscle. Arch Biochem Biophys. 2014 Nov;562:62–9.

348. Niu M, Xiang L, Liu Y, Zhao Y, Yuan J, Dai X, et al. Adiponectin induced AMP-activated protein kinase impairment mediates insulin resistance in Bama mini-pig fed high-fat and high-sucrose diet. 2017;30(8):1190–7.

349. Bonnard C, Durand A, Vidal H, Rieusset J. Changes in adiponectin, its receptors and AMPK activity in tissues of diet-induced diabetic mice. Diabetes Metab. 2008 Feb;34(1):52–61.

350. Yi W, Sun Y, Gao E, Wei X, Lau WB, Zheng Q, et al. Reduced cardioprotective action of adiponectin in high-fat diet-induced type II diabetic mice and its underlying mechanisms. Antioxid Redox Signal. 2011 Oct;15(7):1779–88.

351. Lyons CL, Roche HM. Nutritional Modulation of AMPK-Impact upon Metabolic-Inflammation. Int J Mol Sci. 2018 Oct;19(10).

352. Steinberg GR, Michell BJ, van Denderen BJW, Watt MJ, Carey AL, Fam BC, et al. Tumor necrosis factor alpha-induced skeletal muscle insulin resistance involves suppression of AMP-kinase signaling. Cell Metab. 2006 Dec;4(6):465–74.

353. Rajani R, Pastor-soler NM, Hallows KR. Role of AMP-activated protein kinase in kidney tubular transport , metabolism , and disease. 2017;

354. Glosse P, Föller M. AMP-Activated Protein Kinase (AMPK)-Dependent Regulation of Renal Transport.

Int J Mol Sci. 2018 Nov;19(11).

355. Spires D, Manis AD, Staruschenko A. Ion channels and transporters in diabetic kidney disease. Curr Top Membr. 2019;83:353–96.

356. Liamis G, Liberopoulos E, Barkas F, Elisaf M. Diabetes mellitus and electrolyte disorders. World J Clin cases. 2014 Oct;2(10):488–96.

357. Benziane B, Björnholm M, Pirkmajer S, Austin RL, Kotova O, Viollet B, et al. Activation of AMP-activated protein kinase stimulates Na+,K+-ATPase activity in skeletal muscle cells. J Biol Chem. 2012 Jul;287(28):23451–63.

358. Xiao J, Zhu S, Guan H, Zheng Y, Li F, Zhang X, et al. AMPK alleviates high uric acid-induced Na(+)-K(+)-ATPase signaling impairment and cell injury in renal tubules. Exp Mol Med. 2019 May;51(5):1–14.

359. Bhalla V, Oyster NM, Fitch AC, Wijngaarden MA, Neumann D, Schlattner U, et al. AMP-activated kinase inhibits the epithelial Na+ channel through functional regulation of the ubiquitin ligase Nedd4-2. J Biol Chem. 2006 Sep;281(36):26159–69.

360. Carattino MD, Edinger RS, Grieser HJ, Wise R, Neumann D, Schlattner U, et al. Epithelial sodium channel inhibition by AMP-activated protein kinase in oocytes and polarized renal epithelial cells. J Biol Chem. 2005 May;280(18):17608–16.

361. Fraser SA, Gimenez I, Cook N, Jennings I, Katerelos M, Katsis F, et al. Regulation of the renal-specific Na+-K+-2Cl- co-transporter NKCC2 by AMP-activated protein kinase (AMPK). Biochem J. 2007 Jul;405(1):85–93.

362. Lazo-Fernández Y, Baile G, Meade P, Torcal P, Martínez L, Ibañez C, et al. Kidney-specific genetic deletion of both AMPK α-subunits causes salt and water wasting. Am J Physiol Renal Physiol. 2017 Feb;312(2):F352–65.

363. Fraser SA, Choy S-W, Pastor-Soler NM, Li H, Davies MRP, Cook N, et al. AMPK couples plasma renin to cellular metabolism by phosphorylation of ACC1. Am J Physiol Renal Physiol. 2013 Sep;305(5):F679-90.

364. Dërmaku-Sopjani M, Almilaji A, Pakladok T, Munoz C, Hosseinzadeh Z, Blecua M, et al. Down-regulation of the Na+-coupled phosphate transporter NaPi-IIa by AMP-activated protein kinase. Kidney Blood Press Res. 2013;37(6):547–56.

365. King JDJ, Fitch AC, Lee JK, McCane JE, Mak D-OD, Foskett JK, et al. AMP-activated protein kinase phosphorylation of the R domain inhibits PKA stimulation of CFTR. Am J Physiol Cell Physiol. 2009 Jul;297(1):C94-101.

366. Deji N, Kume S, Araki S, Soumura M, Sugimoto T, Isshiki K, et al. Structural and functional changes in the kidneys of high-fat diet-induced obese mice. Am J Physiol Renal Physiol [Internet]. 2009;296(1):118–26. Available from: http://www.ncbi.nlm.nih.gov/pubmed/18971213

367. Shimano H, Horton JD, Hammer RE, Shimomura I, Brown MS, Goldstein JL. Overproduction of cholesterol and fatty acids causes massive liver enlargement in transgenic mice expressing truncated SREBP-1a. J Clin Invest. 1996 Oct;98(7):1575–84.

368. Han Y, Hu Z, Cui A, Liu Z, Ma F, Xue Y, et al. Post-translational regulation of lipogenesis via AMPK-dependent phosphorylation of insulin-induced gene. Nat Commun. 2019 Feb;10(1):623.

369. Jung E-J, Kwon S-W, Jung B-H, Oh S-H, Lee B-H. Role of the AMPK/SREBP-1 pathway in the development of orotic acid-induced fatty liver. J Lipid Res. 2011 Sep;52(9):1617–25.

370. Li Y, Xu S, Mihaylova MM, Zheng B, Hou X, Jiang B, et al. AMPK phosphorylates and inhibits SREBP activity to attenuate hepatic steatosis and atherosclerosis in diet-induced insulin-resistant mice. Cell Metab. 2011 Apr;13(4):376–88.

371. Lin Y-C, Wu M-S, Lin Y-F, Chen C-R, Chen C-Y, Chen C-J, et al. Nifedipine Modulates Renal Lipogenesis via the AMPK-SREBP Transcriptional Pathway. Int J Mol Sci. 2019 Mar;20(7).

372. Jiang S, Wang W, Miner J, Fromm M. Cross regulation of sirtuin 1, AMPK, and PPARγ in conjugated

linoleic acid treated adipocytes. PLoS One. 2012;7(11):e48874.

373. Lee WH, Kim SG. AMPK-Dependent Metabolic Regulation by PPAR Agonists. PPAR Res. 2010;2010.

374. Sozio MS, Lu C, Zeng Y, Liangpunsakul S, Crabb DW. Activated AMPK inhibits PPAR-{alpha} and PPAR-{gamma} transcriptional activity in hepatoma cells. Am J Physiol Gastrointest Liver Physiol. 2011 Oct;301(4):G739-47.

375. Kang HM, Ahn SH, Choi P, Ko Y-A, Han SH, Chinga F, et al. Defective fatty acid oxidation in renal tubular epithelial cells plays a key role in kidney fibrosis development HHS Public Access. Nat Med. 2015;21(1):37–46.

376. Sas KM, Nair V, Byun J, Kayampilly P, Zhang H, Saha J, et al. Targeted Lipidomic and Transcriptomic Analysis Identifies Dysregulated Renal Ceramide Metabolism in a Mouse Model of Diabetic Kidney Disease. J Proteomics Bioinform. 2015 Oct;Suppl 14.

377. Bandet CL, Tan-Chen S, Bourron O, Le Stunff H, Hajduch E. Sphingolipid Metabolism: New Insight into Ceramide-Induced Lipotoxicity in Muscle Cells. Int J Mol Sci. 2019 Jan;20(3).

378. Heathcote HR, Mancini SJ, Strembitska A, Jamal K, Reihill JA, Palmer TM, et al. Protein kinase C phosphorylates AMP-activated protein kinase α1 Ser487. Biochem J. 2016 Dec;473(24):4681–97.

379. Declèves A-E, Mathew A V, Armando AM, Han X, Dennis EA, Quehenberger O, et al. AMP-activated protein kinase activation ameliorates eicosanoid dysregulation in high-fat-induced kidney disease in mice. J Lipid Res. 2019 May;60(5):937–52.

380. Rogacka D, Piwkowska A, Audzeyenka I, Angielski S, Jankowski M. Involvement of the AMPK-PTEN pathway in insulin resistance induced by high glucose in cultured rat podocytes. Int J Biochem Cell Biol. 2014 Jun;51:120–30.

381. Guzman J, Jauregui AN, Merscher-Gomez S, Maiguel D, Muresan C, Mitrofanova A, et al. Podocyte-specific GLUT4-deficient mice have fewer and larger podocytes and are protected from diabetic nephropathy. Diabetes. 2014 Feb;63(2):701–14.

382. Brinkkoetter PT, Bork T, Salou S, Liang W, Mizi A, Özel C, et al. Anaerobic Glycolysis Maintains the Glomerular Filtration Barrier Independent of Mitochondrial Metabolism and Dynamics. Cell Rep. 2019 Apr;27(5):1551-1566.e5.

383. Rachubik P, Szrejder M, Rogacka D, Audzeyenka I, Rychłowski M, Angielski S, et al. The TRPC6-AMPK Pathway is Involved in Insulin-Dependent Cytoskeleton Reorganization and Glucose Uptake in Cultured Rat Podocytes. Cell Physiol Biochem Int J Exp Cell Physiol Biochem Pharmacol. 2018;51(1):393–410.

384. Hall G, Wang L, Spurney RF. TRPC Channels in Proteinuric Kidney Diseases. Cells. 2019 Dec;9(1).

385. Wang L, Chang J-H, Buckley AF, Spurney RF. Knockout of TRPC6 promotes insulin resistance and exacerbates glomerular injury in Akita mice. Kidney Int. 2019 Feb;95(2):321–32.

386. Hong Q, Zhang L, Das B, Li Z, Liu B, Cai G, et al. Increased podocyte Sirtuin-1 function attenuates diabetic kidney injury. Kidney Int. 2018 Jun;93(6):1330–43.

387. Rogacka D, Piwkowska A, Audzeyenka I, Angielski S, Jankowski M. SIRT1-AMPK crosstalk is involved in high glucose-dependent impairment of insulin responsiveness in primary rat podocytes. Exp Cell Res. 2016 Dec;349(2):328–38.

388. Shati AA. Salidroside ameliorates diabetic nephropathy in rats by activating renal AMPK/SIRT1 signaling pathway. J Food Biochem. 2020 Apr;44(4):e13158.

389. Rabinovitch RC, Samborska B, Faubert B, Ma EH, Gravel S-P, Andrzejewski S, et al. AMPK Maintains Cellular Metabolic Homeostasis through Regulation of Mitochondrial Reactive Oxygen Species. Cell Rep. 2017 Oct;21(1):1–9.

390. Zhang J, Wang Y, Liu X, Dagda RK, Zhang Y. How AMPK and PKA Interplay to Regulate Mitochondrial Function and Survival in Models of Ischemia and Diabetes. Oxid Med Cell Longev. 2017;2017:4353510.

391. Wan Z, Root-McCaig J, Castellani L, Kemp BE, Steinberg GR, Wright DC. Evidence for the role of AMPK in regulating PGC-1 alpha expression and mitochondrial proteins in mouse epididymal adipose tissue. Obesity (Silver Spring). 2014 Mar;22(3):730–8.

392. Hinchy EC, Gruszczyk A V, Willows R, Navaratnam N, Hall AR, Bates G, et al. Mitochondria-derived ROS activate AMP-activated protein kinase (AMPK) indirectly. J Biol Chem. 2018 Nov;293(44):17208–17.

393. Bullon P, Marin-Aguilar F, Roman-Malo L. AMPK/Mitochondria in Metabolic Diseases. Exp Suppl. 2016;107:129–52.

394. Jornayvaz FR, Shulman GI. Regulation of mitochondrial biogenesis. Essays Biochem. 2010;47:69–84.

395. Galvan DL, Green NH, Danesh FR. The hallmarks of mitochondrial dysfunction in chronic kidney disease. Kidney Int. 2017 Nov;92(5):1051–7.

396. Bhargava P, Schnellmann RG. Mitochondrial energetics in the kidney. Nat Rev Nephrol. 2017 Oct;13(10):629–46.

397. Tang C, Cai J, Dong Z. Mitochondrial dysfunction in obesity-related kidney disease: a novel therapeutic target. Kidney Int [Internet]. 2016;90(5):930–3. Available from: http://dx.doi.org/10.1016/j.kint.2016.07.045

398. Szeto HH, Liu S, Soong Y, Alam N, Prusky GT, Seshan S V. Protection of mitochondria prevents high fat diet-induced glomerulopathy and proximal tubular injury. Kidney Int [Internet]. 2016; Available from: http://dx.doi.org/10.1016/j.kint.2016.06.013

399. Jeong HY, Kang JM, Jun HH, Kim D-J, Park SH, Sung MJ, et al. Chloroquine and amodiaquine enhance AMPK phosphorylation and improve mitochondrial fragmentation in diabetic tubulopathy. Sci Rep. 2018 Jun;8(1):8774.

400. Toyama EQ, Herzig S, Courchet J, Lewis TLJ, Losón OC, Hellberg K, et al. Metabolism. AMP-activated protein kinase mediates mitochondrial fission in response to energy stress. Science. 2016 Jan;351(6270):275–81.

401. Lee S-Y, Kang JM, Kim D-J, Park SH, Jeong HY, Lee YH, et al. PGC1α Activators Mitigate Diabetic Tubulopathy by Improving Mitochondrial Dynamics and Quality Control. J Diabetes Res. 2017;2017:6483572.

402. Jha JC, Banal C, Chow BSM, Cooper ME, Jandeleit-Dahm K. Diabetes and Kidney Disease: Role of Oxidative Stress. Antioxid Redox Signal. 2016 Oct;25(12):657–84.

403. Rius-Perez S, Torres-Cuevas I, Millan I, Ortega AL, Perez S. PGC-1alpha, Inflammation, and Oxidative Stress: An Integrative View in Metabolism. Oxid Med Cell Longev. 2020;2020:1452696.

404. Sharma K. Mitochondrial Hormesis and Diabetic Complications. 2015;64(June 2014):663–72.

405. F GS, Virág L, Jagtap P, Szabó E, Mabley JG, Liaudet L, et al. Diabetic endothelial dysfunction: the role of poly(ADP-ribose) polymerase activation. Nat Med. 2001 Jan;7(1):108–13.

406. Sedeek M, Nasrallah R, Touyz RM, Hébert RL. NADPH oxidases, reactive oxygen species, and the kidney: friend and foe. J Am Soc Nephrol. 2013 Oct;24(10):1512–8.

407. Yang Q, Wu F-R, Wang J-N, Gao L, Jiang L, Li H-D, et al. Nox4 in renal diseases: An update. Free Radic Biol Med. 2018 Aug;124:466–72.

408. Sedeek M, Callera G, Montezano A, Gutsol A, Heitz F, Szyndralewiez C, et al. Critical role of Nox4-based NADPH oxidase in glucose-induced oxidative stress in the kidney: implications in type 2 diabetic nephropathy. Am J Physiol Renal Physiol. 2010 Dec;299(6):F1348-58.

409. Jiang F, Lim HK, Morris MJ, Prior L, Velkoska E, Wu X, et al. Systemic upregulation of NADPH oxidase in diet-induced obesity in rats. Redox Rep. 2011;16(6):223–9.

410. He T, Xiong J, Nie L, Yu Y, Guan X, Xu X, et al. Resveratrol inhibits renal interstitial fibrosis in diabetic nephropathy by regulating AMPK/NOX4/ROS pathway. J Mol Med (Berl). 2016 Dec;94(12):1359–71.

411. Papadimitriou A, Peixoto EBMI, Silva KC, Lopes de Faria JM, Lopes de Faria JB. Increase in AMPK brought about by cocoa is renoprotective in experimental diabetes mellitus by reducing NOX4/TGFβ-1 signaling. J Nutr Biochem. 2014 Jul;25(7):773–84.

412. Papadimitriou A, Peixoto EBMI, Silva KC, Lopes de Faria JM, Lopes de Faria JB. Inactivation of AMPK mediates high phosphate-induced extracellular matrix accumulation via NOX4/TGFß-1 signaling in human mesangial cells. Cell Physiol Biochem Int J Exp Cell Physiol Biochem Pharmacol. 2014;34(4):1260–72.

413. Zhang M, Wang C-M, Li J, Meng Z-J, Wei S-N, Li J, et al. Berberine protects against palmitate-induced endothelial dysfunction: involvements of upregulation of AMPK and eNOS and downregulation of NOX4. Mediators Inflamm. 2013;2013:260464.

414. Kim H-R, Kim S-Y. Perilla frutescens Sprout Extract Protect Renal Mesangial Cell Dysfunction against High Glucose by Modulating AMPK and NADPH Oxidase Signaling. Nutrients. 2019 Feb;11(2).

415. Lee HJ, Lee DY, Mariappan MM, Feliers D, Ghosh-Choudhury G, Abboud HE, et al. Hydrogen sulfide inhibits high glucose-induced NADPH oxidase 4 expression and matrix increase by recruiting inducible nitric oxide synthase in kidney proximal tubular epithelial cells. J Biol Chem. 2017 Apr;292(14):5665–75.

416. Li Y, Xia T, Li R, Tse G, Liu T, Li G. Renal-Protective Effects of the Peroxisome Proliferator-Activated Receptor-γ Agonist Pioglitazone in ob/ob Mice. Med Sci Monit Int Med J Exp Clin Res. 2019 Mar;25:1582–9.

417. Wang Y, An W, Zhang F, Niu M, Liu Y, Shi R. Nebivolol ameliorated kidney damage in Zucker diabetic fatty rats by regulation of oxidative stress/NO pathway: Comparison with captopril. Clin Exp Pharmacol Physiol. 2018 Nov;45(11):1135–48.

418. Eid AA, Lee D-Y, Roman LJ, Khazim K, Gorin Y. Sestrin 2 and AMPK connect hyperglycemia to Nox4-dependent endothelial nitric oxide synthase uncoupling and matrix protein expression. Mol Cell Biol. 2013 Sep;33(17):3439–60.

419. Lin Q, Ma Y, Chen Z, Hu J, Chen C, Fan Y, et al. Sestrin-2 regulates podocyte mitochondrial dysfunction and apoptosis under high-glucose conditions via AMPK. Int J Mol Med. 2020 May;45(5):1361–72.

420. Rajaram RD, Dissard R, Faivre A, Ino F, Delitsikou V, Jaquet V, et al. Tubular NOX4 expression decreases in chronic kidney disease but does not modify fibrosis evolution. Redox Biol. 2019 Sep;26:101234.

421. Muñoz M, López-Oliva ME, Rodríguez C, Martínez MP, Sáenz-Medina J, Sánchez A, et al. Differential contribution of Nox1, Nox2 and Nox4 to kidney vascular oxidative stress and endothelial dysfunction in obesity. Redox Biol. 2020 Jan;28:101330.

422. Kaushal GP, Chandrashekar K, Juncos LA, Shah S V. Autophagy Function and Regulation in Kidney Disease. Biomolecules. 2020 Jan;10(1).

423. Rautou P-E, Mansouri A, Lebrec D, Durand F, Valla D, Moreau R. Autophagy in liver diseases. J Hepatol. 2010 Dec;53(6):1123–34.

424. Fritzen AM, Madsen AB, Kleinert M, Treebak JT, Lundsgaard A-M, Jensen TE, et al. Regulation of autophagy in human skeletal muscle: effects of exercise, exercise training and insulin stimulation. J Physiol. 2016 Feb;594(3):745–61.

425. Yuan J, Zhao X, Hu Y, Sun H, Gong G, Huang X, et al. Autophagy regulates the degeneration of the auditory cortex through the AMPK-mTOR-ULK1 signaling pathway. Int J Mol Med. 2018 Apr;41(4):2086–98.

426. Ahmed M, Hwang JS, Lai TH, Zada S, Nguyen HQ, Pham TM, et al. Co-Expression Network Analysis of AMPK and Autophagy Gene Products during Adipocyte Differentiation. Int J Mol Sci. 2018 Jun;19(6).

427. Dikic I, Elazar Z. Mechanism and medical implications of mammalian autophagy. Nat Rev Mol Cell Biol [Internet]. 2018;19(6):349–64. Available from: http://dx.doi.org/10.1038/s41580-018-0003-4

428. Alers S, Löffler AS, Wesselborg S, Stork B. Role of AMPK-mTOR-Ulk1/2 in the regulation of autophagy: cross talk, shortcuts, and feedbacks. Mol Cell Biol. 2012 Jan;32(1):2–11.

429. Green AS, Chapuis N, Lacombe C, Mayeux P, Bouscary D, Tamburini J. LKB1/AMPK/mTOR signaling pathway in hematological malignancies: from metabolism to cancer cell biology. Cell Cycle. 2011 Jul;10(13):2115–20.

430. Bork T, Liang W, Yamahara K, Lee P, Tian Z, Liu S, et al. Podocytes maintain high basal levels of autophagy independent of mtor signaling. Autophagy. 2019 Dec;1–17.

431. Gwinn DM, Shackelford DB, Egan DF, Mihaylova MM, Mery A, Vasquez DS, et al. AMPK phosphorylation of raptor mediates a metabolic checkpoint. Mol Cell. 2008 Apr;30(2):214–26.

432. Hariharan N, Maejima Y, Nakae J, Paik J, Depinho RA, Sadoshima J. Deacetylation of FoxO by Sirt1 Plays an Essential Role in Mediating Starvation-Induced Autophagy in Cardiac Myocytes. Circ Res. 2010 Dec;107(12):1470–82.

433. Liu WJ, Gan Y, Huang WF, Wu H-L, Zhang X-Q, Zheng HJ, et al. Lysosome restoration to activate podocyte autophagy: a new therapeutic strategy for diabetic kidney disease. Cell Death Dis. 2019 Oct;10(11):806.

434. Kuwahara S, Hosojima M, Kaneko R, Aoki H, Nakano D, Sasagawa T, et al. Megalin-Mediated Tubuloglomerular Alterations in High-Fat Diet-Induced Kidney Disease. J Am Soc Nephrol. 2016 Jul;27(7):1996–2008.

435. Yamahara K, Kume S, Koya D, Tanaka Y, Morita Y, Chin-Kanasaki M, et al. Obesity-mediated autophagy insufficiency exacerbates proteinuria-induced tubulointerstitial lesions. J Am Soc Nephrol. 2013 Nov;24(11):1769–81.

436. Ling NXY, Kaczmarek A, Hoque A, Davie E, Ngoei KRW, Morrison KR, et al. mTORC1 directly inhibits AMPK to promote cell proliferation under nutrient stress. Nat Metab. 2020 Jan;2(1):41–9.

437. Li H, Min Q, Ouyang C, Lee J, He C, Zou M-H, et al. AMPK activation prevents excess nutrient-induced hepatic lipid accumulation by inhibiting mTORC1 signaling and endoplasmic reticulum stress response. Biochim Biophys Acta. 2014 Sep;1842(9):1844–54.

438. Kaushal GP, Chandrashekar K, Juncos LA. Molecular Interactions Between Reactive Oxygen Species and Autophagy in Kidney Disease. Int J Mol Sci. 2019 Aug;20(15).

439. Sohn M, Kim K, Uddin MJ, Lee G, Hwang I, Kang H, et al. Delayed treatment with fenofibrate protects against high-fat diet-induced kidney injury in mice: the possible role of AMPK autophagy. Am J Physiol Renal Physiol. 2017 Feb;312(2):F323–34.

440. Jin Y, Liu S, Ma Q, Xiao D, Chen L. Berberine enhances the AMPK activation and autophagy and mitigates high glucose-induced apoptosis of mouse podocytes. Eur J Pharmacol. 2017 Jan;794:106–14.

441. Wang X, Gao L, Lin H, Song J, Wang J, Yin Y, et al. Mangiferin prevents diabetic nephropathy progression and protects podocyte function via autophagy in diabetic rat glomeruli. Eur J Pharmacol. 2018 Apr;824:170–8.

442. Lim JH, Kim HW, Kim MY, Kim TW, Kim EN, Kim Y, et al. Cinacalcet-mediated activation of the CaMKKbeta-LKB1-AMPK pathway attenuates diabetic nephropathy in db/db mice by modulation of apoptosis and autophagy. Cell Death Dis. 2018 Feb;9(3):270.

443. Wu W, Tian W, Hu Z, Chen G, Huang L, Li W, et al. ULK1 translocates to mitochondria and phosphorylates FUNDC1 to regulate mitophagy. EMBO Rep. 2014 May;15(5):566–75.

444. Laker RC, Drake JC, Wilson RJ, Lira VA, Lewellen BM, Ryall KA, et al. Ampk phosphorylation of Ulk1 is required for targeting of mitochondria to lysosomes in exercise-induced mitophagy. Nat Commun. 2017 Sep;8(1):548.

445. Kaushik S, Cuervo AM. AMPK-dependent phosphorylation of lipid droplet protein PLIN2 triggers its degradation by CMA. Autophagy. 2016;12(2):432–8.

446. Morigi M, Perico L, Benigni A. Sirtuins in Renal Health and Disease. J Am Soc Nephrol [Internet]. 2018;29:1–11. Available from:

http://jasn.asnjournals.org/content/early/2018/04/27/ASN.2017111218.full.pdf

447. Lee IH. Mechanisms and disease implications of sirtuin-mediated autophagic regulation. Exp Mol Med. 2019 Sep;51(9):1–11.

448. Cantó C, Auwerx J. PGC-1alpha, SIRT1 and AMPK, an energy sensing network that controls energy expenditure. Curr Opin Lipidol. 2009 Apr;20(2):98–105.

449. Ruderman NB, Xu XJ, Nelson L, Cacicedo JM, Saha AK, Lan F, et al. AMPK and SIRT1: a long-standing partnership? Am J Physiol Endocrinol Metab. 2010 Apr;298(4):E751-60.

450. Dai H, Sinclair DA, Ellis JL, Steegborn C. Sirtuin activators and inhibitors: Promises, achievements, and challenges. Pharmacol Ther [Internet]. 2018;#pagerange#. Available from: https://doi.org/10.1016/j.pharmthera.2018.03.004

451. Bharathi SS, Zhang Y, Mohsen A-W, Uppala R, Balasubramani M, Schreiber E, et al. Sirtuin 3 (SIRT3) protein regulates long-chain acyl-CoA dehydrogenase by deacetylating conserved lysines near the active site. J Biol Chem. 2013 Nov;288(47):33837–47.

452. Yu W, Dittenhafer-Reed KE, Denu JM. SIRT3 protein deacetylates isocitrate dehydrogenase 2 (IDH2) and regulates mitochondrial redox status. J Biol Chem. 2012 Apr;287(17):14078–86.

453. Pillai VB, Sundaresan NR, Kim G, Gupta M, Rajamohan SB, Pillai JB, et al. Exogenous NAD blocks cardiac hypertrophic response via activation of the SIRT3-LKB1-AMP-activated kinase pathway. J Biol Chem. 2010 Jan;285(5):3133–44.

454. He X, Zeng H, Chen J-X. Emerging role of SIRT3 in endothelial metabolism, angiogenesis, and cardiovascular disease. J Cell Physiol. 2019 Mar;234(3):2252–65.

455. Hirschey MD, Shimazu T, Jing E, Grueter CA, Collins AM, Aouizerat B, et al. SIRT3 deficiency and mitochondrial protein hyperacetylation accelerate the development of the metabolic syndrome. Mol Cell. 2011 Oct;44(2):177–90.

456. Zeng H, Vaka VR, He X, Booz GW, Chen JX. High-fat diet induces cardiac remodelling and dysfunction: Assessment of the role played by SIRT3 loss. J Cell Mol Med. 2015;19(8):1847–56.

457. Morigi M, Perico L, Rota C, Longaretti L, Conti S, Rottoli D, et al. Sirtuin 3-dependent mitochondrial dynamic improvements protect against acute kidney injury. J Clin Invest. 2015;125(2):715–26.

458. Koyama T, Kume S, Koya D, Araki SI, Isshiki K, Chin-Kanasaki M, et al. SIRT3 attenuates palmitate-induced ROS production and inflammation in proximal tubular cells. Free Radic Biol Med [Internet]. 2011;51(6):1258–67. Available from: http://dx.doi.org/10.1016/j.freeradbiomed.2011.05.028

459. Wang Q, Xu J, Li X, Liu Z, Han Y, Xu X, et al. Sirt3 modulate renal ischemia-reperfusion injury through enhancing mitochondrial fusion and activating the ERK-OPA1 signaling pathway. J Cell Physiol. 2019 Dec;234(12):23495–506.

460. Guigas B, Viollet B. Targeting AMPK: From Ancient Drugs to New Small-Molecule Activators. Exp Suppl. 2016;107:327–50.

461. Bruce KD, Byrne CD. The metabolic syndrome: common origins of a multifactorial disorder. Postgrad Med J [Internet]. 2009;85(1009):614–21. Available from: http://www.ncbi.nlm.nih.gov/pubmed/19892897

462. Hsu C, McCulloch CE, Iribarren C, Darbinian J, Go AS. Body mass index and risk for end-stage renal disease. Ann Intern Med. 2006 Jan;144(1):21–8.

463. Hainer V, Toplak H, Mitrakou A. Treatment modalities of obesity: what fits whom? Diabetes Care. 2008 Feb;31 Suppl 2:S269-77.

464. Dietrich MO, Horvath TL. Limitations in anti-obesity drug development: the critical role of hunger-promoting neurons. Nat Rev Drug Discov. 2012 Sep;11(9):675–91.

465. Srivastava RAK, Pinkosky SL, Filippov S, Hanselman JC, Cramer CT, Newton RS. AMP-activated protein kinase: an emerging drug target to regulate imbalances in lipid and carbohydrate metabolism to treat cardio-metabolic diseases. J Lipid Res. 2012 Dec;53(12):2490–514.

466. Després J-P, Lemieux I. Abdominal obesity and metabolic syndrome. Nature. 2006;444(7121):881–7.

467. Ward ZJ, Bleich SN, Cradock AL, Barrett JL, Giles CM, Flax C, et al. Projected U.S. State-Level Prevalence of Adult Obesity and Severe Obesity. N Engl J Med. 2019 Dec;381(25):2440–50.

468. Kovesdy CP, Furth S, Zoccali C. Obesity and kidney disease: Hidden consequences of the epidemic. Vol. 104, Physiology international. Hungary; 2017. p. 1–14.

469. Tonelli M. Effect of Pravastatin on Loss of Renal Function in People with Moderate Chronic Renal Insufficiency and Cardiovascular Disease. J Am Soc Nephrol [Internet]. 2003;14(6):1605–13. Available from: http://www.jasn.org/cgi/doi/10.1097/01.ASN.0000068461.45784.2F

470. Foster MC, Hwang S-J, Porter SA, Massaro JM, Hoffmann U, Fox CS. Fatty kidney, hypertension, and chronic kidney disease: the Framingham Heart Study. Hypertens (Dallas, Tex 1979). 2011 Nov;58(5):784–90.

471. Kume S, Uzu T, Araki S -i., Sugimoto T, Isshiki K, Chin-Kanasaki M, et al. Role of Altered Renal Lipid Metabolism in the Development of Renal Injury Induced by a High-Fat Diet. J Am Soc Nephrol [Internet]. 2007;18(10):2715–23. Available from: http://www.jasn.org/cgi/doi/10.1681/ASN.2007010089

472. De Vries APJ, Ruggenenti P, Ruan XZ, Praga M, Cruzado JM, Bajema IM, et al. Fatty kidney: Emerging role of ectopic lipid in obesity-related renal disease. Lancet Diabetes Endocrinol [Internet]. 2014;2(5):417–26. Available from: http://dx.doi.org/10.1016/S2213-8587(14)70065-8

473. Szrejder M, Piwkowska A. AMPK signalling: Implications for podocyte biology in diabetic nephropathy. Biol cell. 2019 May;111(5):109–20.

474. Declè A-E, Mathew A V, Cunard R, Sharma K. AMPK Mediates the Initiation of Kidney Disease Induced by a High-Fat Diet. J Am Soc Nephrol. 2011;22:1846–55.

475. Stapleton D, Mitchelhill KI, Gao G, Widmer J, Michell BJ, Teh T, et al. Mammalian AMP-activated protein kinase subfamily. J Biol Chem. 1996 Jan;271(2):611–4.

476. Kang JG, Park C-Y. Anti-Obesity Drugs: A Review about Their Effects and Safety. Diabetes Metab J. 2012 Feb;36(1):13–25.

477. Olivier S, Foretz M, Viollet B. Promise and challenges for direct small molecule AMPK activators. Biochem Pharmacol. 2018 Jul;153:147–58.

478. Katzmarzyk PT, Leon AS, Wilmore JH, Skinner JS, Rao DC, Rankinen T, et al. Targeting the metabolic syndrome with exercise: Evidence from the HERITAGE Family Study. Med Sci Sports Exerc. 2003;

479. Ross R, Després J-P. Abdominal Obesity, Insulin Resistance, and the Metabolic Syndrome: Contribution of Physical Activity/Exercise. Obesity [Internet]. 2009;17(n3s):S1–2. Available from: http://doi.wiley.com/10.1038/oby.2009.381

480. Hiraki K, Shibagaki Y, Izawa KP, Hotta C, Wakamiya A, Sakurada T, et al. Effects of home-based exercise on pre-dialysis chronic kidney disease patients: a randomized pilot and feasibility trial. BMC Nephrol. 2017 Jun;18(1):198.

481. Heiwe S, Jacobson SH. Exercise training for adults with chronic kidney disease. Cochrane database Syst Rev. 2011 Oct;(10):CD003236.

482. Qiu Z, Zheng K, Zhang H, Feng J, Wang L, Zhou H. Physical Exercise and Patients with Chronic Renal Failure: A Meta-Analysis. Biomed Res Int. 2017;2017:7191826.

483. Ikizler TA, Robinson-Cohen C, Ellis C, Headley SAE, Tuttle K, Wood RJ, et al. Metabolic Effects of Diet and Exercise in Patients with Moderate to Severe CKD: A Randomized Clinical Trial. J Am Soc Nephrol. 2018 Jan;29(1):250–9.

484. Pierard M, Conotte S, Tassin A, Boutry S, Uzureau P, Boudjeltia KZ, et al. Interactions of exercise training and high-fat diet on adiponectin forms and muscle receptors in mice. Nutr Metab (Lond) [Internet]. 2016;13(1):75. Available from: http://nutritionandmetabolism.biomedcentral.com/articles/10.1186/s12986-016-0138-2

485. Debelle FD, Nortier JL, De Prez EG, Garbar CH, Vienne AR, Salmon IJ, et al. Aristolochic acids induce chronic renal failure with interstitial fibrosis in salt-depleted rats. J Am Soc Nephrol. 2002 Feb;13(2):431–6.

486. Sheehan SM, Korstanje R. Automatic glomerular identification and quantification of histological phenotypes using image analysis and machine learning. Am J Physiol Renal Physiol. 2018 Dec;315(6):F1644–51.

487. Ryu J-E, Jo W, Choi H-J, Jang S, Lee H-J, Woo D-C, et al. Evaluation of Nonalcoholic Fatty Liver Disease in C57BL/6J Mice by Using MRI and Histopathologic Analyses. Comp Med. 2015 Oct;65(5):409–15.

488. Aleidi S, Issa A, Bustanji H, Khalil M, Bustanji Y. Adiponectin serum levels correlate with insulin resistance in type 2 diabetic patients. Saudi Pharm J SPJ Off Publ Saudi Pharm Soc. 2015 Jul;23(3):250–6.

489. Pajvani UB, Hawkins M, Combs TP, Rajala MW, Doebber T, Berger JP, et al. Complex distribution, not absolute amount of adiponectin, correlates with thiazolidinedione-mediated improvement in insulin sensitivity. J Biol Chem. 2004 Mar;279(13):12152–62.

490. Alex S, Boss A, Heerschap A, Kersten S. Exercise training improves liver steatosis in mice. Nutr Metab (Lond). 2015;12:29.

491. Lavie CJ, Pandey A, Lau DH, Alpert MA, Sanders P. Obesity and Atrial Fibrillation Prevalence, Pathogenesis, and Prognosis: Effects of Weight Loss and Exercise. J Am Coll Cardiol. 2017 Oct;70(16):2022–35.

492. Lee S, Kuk JL, Davidson LE, Hudson R, Kilpatrick K, Graham TE, et al. Exercise without weight loss is an effective strategy for obesity reduction in obese individuals with and without Type 2 diabetes. J Appl Physiol. 2005 Sep;99(3):1220–5.

493. Petridou A, Siopi A, Mougios V. Exercise in the management of obesity. Metabolism. 2019 Mar;92:163–9.

494. de Carvalho FP, Moretto TL, Benfato ID, Barthichoto M, Ferreira SM, Costa-Junior JM, et al. Central and peripheral effects of physical exercise without weight reduction in obese and lean mice. Biosci Rep. 2018 Apr;38(2).

495. Chaar LJ, Coelho A, Silva NM, Festuccia WL, Antunes VR. High-fat diet-induced hypertension and autonomic imbalance are associated with an upregulation of CART in the dorsomedial hypothalamus of mice. Physiol Rep. 2016 Jun;4(11).

496. Hariri N, Thibault L. High-fat diet-induced obesity in animal models. Nutr Res Rev [Internet]. 2010;23(2):270–99. Available from: http://journals.cambridge.org/abstract_S0954422410000168

497. Farzanegi P, Dana A, Ebrahimpoor Z, Asadi M, Azarbayjani MA. Mechanisms of beneficial effects of exercise training on non-alcoholic fatty liver disease (NAFLD): Roles of oxidative stress and inflammation. Eur J Sport Sci. 2019 Aug;19(7):994–1003.

498. Castaneda C, Layne JE, Munoz-Orians L, Gordon PL, Walsmith J, Foldvari M, et al. A randomized controlled trial of resistance exercise training to improve glycemic control in older adults with type 2 diabetes. Diabetes Care. 2002 Dec;25(12):2335–41.

499. Ivy JL. Role of exercise training in the prevention and treatment of insulin resistance and non-insulin-dependent diabetes mellitus. Sports Med. 1997 Nov;24(5):321–36.

500. Bird SR, Hawley JA. Update on the effects of physical activity on insulin sensitivity in humans. BMJ open Sport Exerc Med. 2016;2(1):e000143.

501. O'Neill HM. AMPK and Exercise: Glucose Uptake and Insulin Sensitivity. Diabetes Metab J. 2013 Feb;37(1):1–21.

502. Zhu N, Pankow JS, Ballantyne CM, Couper D, Hoogeveen RC, Pereira M, et al. High-molecular-weight adiponectin and the risk of type 2 diabetes in the ARIC study. J Clin Endocrinol Metab. 2010 Nov;95(11):5097–104.

503. Glass OK, Radia A, Kraus WE, Abdelmalek MF. Exercise Training as Treatment of Nonalcoholic Fatty Liver Disease.

504. Chun SK, Lee S, Yang M-J, Leeuwenburgh C, Kim J-S. Exercise-Induced Autophagy in Fatty Liver Disease. Exerc Sport Sci Rev. 2017 Jul;45(3):181–6.

505. Takahashi H, Kotani K, Tanaka K, Egucih Y, Anzai K. Therapeutic Approaches to Nonalcoholic Fatty Liver Disease: Exercise Intervention and Related Mechanisms. Front Endocrinol (Lausanne). 2018;9:588.

506. Mendizábal Y, Llorens S, Nava E. Hypertension in metabolic syndrome: vascular pathophysiology. Int J Hypertens. 2013;2013:230868.

507. Sakamoto S. Prescription of exercise training for hypertensives. Hypertens Res. 2020 Mar;43(3):155–61.

508. Bruder-Nascimento T, Ekeledo OJ, Anderson R, Le HB, Belin de Chantemèle EJ. Long Term High Fat Diet Treatment: An Appropriate Approach to Study the Sex-Specificity of the Autonomic and Cardiovascular Responses to Obesity in Mice. Front Physiol. 2017;8:32.

509. Stump CS. Physical Activity in the Prevention of Chronic Kidney Disease. 2011;85714:164–73.

510. Muller CR, Americo AL V, Fiorino P, Evangelista FS. Aerobic exercise training prevents kidney lipid deposition in mice fed a cafeteria diet. Life Sci. 2018 Oct;211:140–6.

511. Fassett RG, Venuthurupalli SK, Gobe GC, Coombes JS, Cooper MA, Hoy WE. Biomarkers in chronic kidney disease: a review. Kidney Int. 2011 Oct;80(8):806–21.

512. Jeon S-M. Regulation and function of AMPK in physiology and diseases. Exp Mol Med. 2016 Jul;48(7):e245.

513. Al-Rasheed NM, Al-Rasheed NM, Attia HA, Al-Amin MA, Al-Ajmi HN, Hasan IH, et al. Renoprotective Effects of Fenofibrate via Modulation of LKB1/AMPK mRNA Expression and Endothelial Dysfunction in a Rat Model of Diabetic Nephropathy. Pharmacology. 2015;95(5–6):229–39.

514. Rogacka D, Audzeyenka I, Rychlowski M, Rachubik P, Szrejder M, Angielski S, et al. Metformin overcomes high glucose-induced insulin resistance of podocytes by pleiotropic effects on SIRT1 and AMPK. Biochim Biophys acta Mol basis Dis. 2018 Jan;1864(1):115–25.

515. Zhou Y, Lin S, Zhang L, Li Y. Resveratrol prevents renal lipotoxicity in high-fat diet-treated mouse model through regulating PPAR-α pathway. Mol Cell Biochem. 2016;411(1–2):143–50.

516. Juszczak F, Caron N, Mathew A V, Declèves A-E. Critical Role for AMPK in Metabolic Disease-Induced Chronic Kidney Disease. Int J Mol Sci. 2020 Oct;21(21).

517. Lin T-A, Wu VC-C, Wang C-Y. Autophagy in Chronic Kidney Diseases. Cells. 2019 Jan;8(1).

518. Satriano J. Autophagy and metabolic changes in obesity-related chronic kidney disease. 2013;(January 2018).

519. He C, Bassik MC, Moresi V, Sun K, Wei Y, Zou Z, et al. Exercise-induced BCL2-regulated autophagy is required for muscle glucose homeostasis. Nature. 2012 Jan;481(7382):511–5.

520. Klionsky DJ, Klionsky DJ, Abdelmohsen K, Abe A, Abedin MJ, Abeliovich H, et al. Guidelines for the use and interpretation of assays for monitoring autophagy (3rd edition). Autophagy [Internet]. 2016;12(1):1–222. Available from: http://www.tandfonline.com/doi/pdf/10.1080/15548627.2015.1100356?needAccess=true

521. Peng H, Wang Q, Lou T, Qin J, Jung S, Shetty V, et al. Myokine mediated muscle-kidney crosstalk suppresses metabolic reprogramming and fibrosis in damaged kidneys. Nat Commun. 2017 Nov;8(1):1493.

522. Xin C, Liu J, Zhang J, Zhu D, Wang H, Xiong L, et al. Irisin improves fatty acid oxidation and glucose utilization in type 2 diabetes by regulating the AMPK signaling pathway. Int J Obes (Lond). 2016 Mar;40(3):443–51.

523. Vargas-Ortiz K, Pérez-Vázquez V, Macías-Cervantes MH. Exercise and Sirtuins: A Way to

Mitochondrial Health in Skeletal Muscle. Int J Mol Sci. 2019 Jun;20(11).

524. Palacios OM, Carmona JJ, Michan S, Chen KY, Manabe Y, Ward JL 3rd, et al. Diet and exercise signals regulate SIRT3 and activate AMPK and PGC-1alpha in skeletal muscle. Aging (Albany NY). 2009 Aug;1(9):771–83.

525. Kincaid B, Bossy-Wetzel E. Forever young: SIRT3 a shield against mitochondrial meltdown, aging, and neurodegeneration. Front Aging Neurosci. 2013 Sep;5:48.

526. Lombard DB, Zwaans BMM. SIRT3: as simple as it seems? Gerontology. 2014;60(1):56–64.

527. Shi Z, Li C, Yin Y, Yang Z, Xue H, Mu N, et al. Aerobic Interval Training Regulated SIRT3 Attenuates High-Fat-Diet-Associated Cognitive Dysfunction. Biomed Res Int. 2018;2018:2708491.

528. Vargas-Ortiz K, Pérez-Vázquez V, Figueroa A, Díaz FJ, Montaño-Ascencio PG, Macías-Cervantes MH. Aerobic training but no resistance training increases SIRT3 in skeletal muscle of sedentary obese male adolescents. Eur J Sport Sci. 2018 Mar;18(2):226–34.

529. Vargas-Ortiz K, Perez-Vazquez V, Diaz-Cisneros FJ, Figueroa A, Jiménez-Flores LM, Rodriguez-DelaRosa G, et al. Aerobic Training Increases Expression Levels of SIRT3 and PGC-1α in Skeletal Muscle of Overweight Adolescents Without Change in Caloric Intake. Pediatr Exerc Sci. 2015 May;27(2):177–84.

530. Zeng H, Vaka VR, He X, Booz GW, Chen J-X. High-fat diet induces cardiac remodelling and dysfunction: assessment of the role played by SIRT3 loss. J Cell Mol Med. 2015 Aug;19(8):1847–56.

531. Bagnasco S, Good D, Balaban R, Burg M, Bagnasco S, Good D, et al. Lactate production in isolated segments of the rat nephron Lactate production of the rat nephron in isolated segments. 2012;

532. Baumert P, Lake MJ, Stewart CE, Drust B, Erskine RM. Genetic variation and exercise-induced muscle damage: implications for athletic performance, injury and ageing. Eur J Appl Physiol. 2016 Sep;116(9):1595–625.

533. Perico L, Morigi M, Benigni A. Mitochondrial Sirtuin 3 and Renal Diseases. Nephron. 2016;134(1):14–9.

534. Locatelli M, Zoja C, Zanchi C, Corna D, Villa S, Bolognini S, et al. Manipulating Sirtuin 3 pathway ameliorates renal damage in experimental diabetes. Sci Rep. 2020 May;10(1):8418.

535. Duan W-J, Li Y-F, Liu F-L, Deng J, Wu Y-P, Yuan W-L, et al. A SIRT3/AMPK/autophagy network orchestrates the protective effects of trans-resveratrol in stressed peritoneal macrophages and RAW 264.7 macrophages. Free Radic Biol Med. 2016 Jun;95:230–42.

536. Chen L-Y, Wang Y, Terkeltaub R, Liu-Bryan R. Activation of AMPK-SIRT3 signaling is chondroprotective by preserving mitochondrial DNA integrity and function. Osteoarthr Cartil. 2018 Nov;26(11):1539–50.

537. Huh J-E, Shin JH, Jang ES, Park SJ, Park DR, Ko R, et al. Sirtuin 3 (SIRT3) maintains bone homeostasis by regulating AMPK-PGC-1β axis in mice. Sci Rep. 2016 Mar;6:22511.

538. Fu J, Jin J, Cichewicz RH, Hageman SA, Ellis TK, Xiang L, et al. trans-(-)-ε-Viniferin increases mitochondrial sirtuin 3 (SIRT3), activates AMP-activated protein kinase (AMPK), and protects cells in models of Huntington Disease. J Biol Chem. 2012 Jul;287(29):24460–72.

539. Yoshino J, Baur JA, Imai S ichiro. NAD+Intermediates: The Biology and Therapeutic Potential of NMN and NR. Cell Metab [Internet]. 2018;27(3):513–28. Available from: https://doi.org/10.1016/j.cmet.2017.11.002

540. Elhassan YS, Philp AA, Lavery GG. Targeting NAD+ in Metabolic Disease: New Insights Into an Old Molecule. J Endocr Soc [Internet]. 2017;1(7):816–35. Available from: https://academic.oup.com/jes/article-lookup/doi/10.1210/js.2017-00092

541. Canto C, Houtkooper RH, Pirinen E, Youn DY, Oosterveer MH, Cen Y, et al. The NAD + precursor nicotinamide riboside enhances oxidative metabolism and protects against high-fat diet induced obesity. Cell Metab. 2013;15(6):838–47.

542. Yoshino J, Imai S. Mitochondrial SIRT3: a new potential therapeutic target for metabolic syndrome. Mol Cell. 2011 Oct;44(2):170–1.

543. Verdin E. NAD^+ in aging, metabolism, and neurodegeneration. Science. 2015 Dec;350(6265):1208–13.

544. Johnson S, Imai S-I. NAD (+) biosynthesis, aging, and disease. F1000Research. 2018;7:132.

545. Katsyuba E, Romani M, Hofer D, Auwerx J. NAD(+) homeostasis in health and disease. Nat Metab. 2020 Jan;2(1):9–31.

546. Imai S, Guarente L. NAD+ and sirtuins in aging and disease. Trends Cell Biol. 2014 Aug;24(8):464–71.

547. Bai P, Cantó C. The role of PARP-1 and PARP-2 enzymes in metabolic regulation and disease. Cell Metab. 2012 Sep;16(3):290–5.

548. Gupte R, Liu Z, Kraus WL. PARPs and ADP-ribosylation: recent advances linking molecular functions to biological outcomes. Genes Dev. 2017 Jan;31(2):101–26.

549. Bonkowski MS, Sinclair DA. Slowing ageing by design: the rise of NAD(+) and sirtuin-activating compounds. Nat Rev Mol Cell Biol. 2016 Nov;17(11):679–90.

550. Hogan KA, Chini CCS, Chini EN. The Multi-faceted Ecto-enzyme CD38: Roles in Immunomodulation, Cancer, Aging, and Metabolic Diseases. Front Immunol. 2019;10:1187.

551. Malavasi F, Deaglio S, Funaro A, Ferrero E, Horenstein AL, Ortolan E, et al. Evolution and function of the ADP ribosyl cyclase/CD38 gene family in physiology and pathology. Physiol Rev. 2008 Jul;88(3):841–86.

552. Houtkooper RH, Cantó C, Wanders RJ, Auwerx J. The secret life of NAD+: an old metabolite controlling new metabolic signaling pathways. Endocr Rev. 2010 Apr;31(2):194–223.

553. Yoshino J, Mills KF, Yoon MJ, Imai S. Nicotinamide mononucleotide, a key NAD(+) intermediate, treats the pathophysiology of diet- and age-induced diabetes in mice. Cell Metab. 2011 Oct;14(4):528–36.

554. Gariani K, Menzies KJ, Ryu D, Wegner CJ, Wang X, Ropelle ER, et al. Eliciting the mitochondrial unfolded protein response by nicotinamide adenine dinucleotide repletion reverses fatty liver disease in mice. Hepatology. 2016 Apr;63(4):1190–204.

555. Dall M, Penke M, Sulek K, Matz-Soja M, Holst B, Garten A, et al. Hepatic NAD(+) levels and NAMPT abundance are unaffected during prolonged high-fat diet consumption in C57BL/6JBomTac mice. Mol Cell Endocrinol. 2018 Sep;473:245–56.

556. Nielsen KN, Peics J, Ma T, Karavaeva I, Dall M, Chubanava S, et al. NAMPT-mediated NAD(+) biosynthesis is indispensable for adipose tissue plasticity and development of obesity. Mol Metab. 2018 May;11:178–88.

557. Fulco M, Cen Y, Zhao P, Hoffman EP, McBurney MW, Sauve AA, et al. Glucose restriction inhibits skeletal myoblast differentiation by activating SIRT1 through AMPK-mediated regulation of Nampt. Dev Cell. 2008 May;14(5):661–73.

558. Wang L-F, Wang X-N, Huang C-C, Hu L, Xiao Y-F, Guan X-H, et al. Inhibition of NAMPT aggravates high fat diet-induced hepatic steatosis in mice through regulating Sirt1/AMPKα/SREBP1 signaling pathway. Lipids Health Dis. 2017 Apr;16(1):82.

559. Ralto KM, Rhee EP, Parikh SM. NAD(+) homeostasis in renal health and disease. Nat Rev Nephrol. 2020 Feb;16(2):99–111.

560. Martin DR, Lewington AJ, Hammerman MR, Padanilam BJ. Inhibition of poly(ADP-ribose) polymerase attenuates ischemic renal injury in rats. Am J Physiol Regul Integr Comp Physiol. 2000 Nov;279(5):R1834-40.

561. Ogura Y, Kitada M, Monno I, Kanasaki K, Watanabe A, Koya D. Renal mitochondrial oxidative stress is enhanced by the reduction of Sirt3 activity, in Zucker diabetic fatty rats. Redox Rep. 2018;23(1):153–9.

562. Rajman L, Chwalek K, Sinclair DA. Therapeutic Potential of NAD-Boosting Molecules: The In Vivo

Evidence. Cell Metab. 2018 Mar;27(3):529–47.

563. Trammell SA, Yu L, Redpath P, Migaud ME, Brenner C. Nicotinamide Riboside Is a Major NAD+ Precursor Vitamin in Cow Milk. J Nutr. 2016 May;146(5):957–63.

564. Belenky P, Racette FG, Bogan KL, McClure JM, Smith JS, Brenner C. Nicotinamide riboside promotes Sir2 silencing and extends lifespan via Nrk and Urh1/Pnp1/Meu1 pathways to NAD+. Cell. 2007 May;129(3):473–84.

565. Bieganowski P, Brenner C. Discoveries of nicotinamide riboside as a nutrient and conserved NRK genes establish a Preiss-Handler independent route to NAD+ in fungi and humans. Cell. 2004 May;117(4):495–502.

566. Trammell SAJ, Schmidt MS, Weidemann BJ, Redpath P, Jaksch F, Dellinger RW, et al. Nicotinamide riboside is uniquely and orally bioavailable in mice and humans. Nat Commun. 2016 Oct;7:12948.

567. Zhang H, Ryu D, Wu Y, Gariani K, Wang X, Luan P, et al. NAD^+ repletion improves mitochondrial and stem cell function and enhances life span in mice. Science. 2016 Jun;352(6292):1436–43.

568. Brown KD, Maqsood S, Huang J-Y, Pan Y, Harkcom W, Li W, et al. Activation of SIRT3 by the NAD^+ precursor nicotinamide riboside protects from noise-induced hearing loss. Cell Metab. 2014 Dec;20(6):1059–68.

569. Journe F, Chaboteaux C, Dumon J-C, Leclercq G, Laurent G, Body J-J. Steroid-free medium discloses oestrogenic effects of the bisphosphonate clodronate on breast cancer cells. Br J Cancer. 2004 Nov;91(9):1703–10.

570. Alsabeeh N, Chausse B, Kakimoto PA, Kowaltowski AJ, Shirihai O. Cell culture models of fatty acid overload: Problems and solutions. Biochim Biophys acta Mol cell Biol lipids. 2018 Feb;1863(2):143–51.

571. Penke M, Schuster S, Gorski T, Gebhardt R, Kiess W, Garten A. Oleate ameliorates palmitate-induced reduction of NAMPT activity and NAD levels in primary human hepatocytes and hepatocarcinoma cells. Lipids Health Dis. 2017 Oct;16(1):191.

572. Flores-León M, Pérez-Domínguez M, González-Barrios R, Arias C. Palmitic Acid-Induced NAD(+) Depletion is Associated with the Reduced Function of SIRT1 and Increased Expression of BACE1 in Hippocampal Neurons. Neurochem Res. 2019 Jul;44(7):1745–54.

573. Lee HJ, Yang SJ. Nicotinamide riboside regulates inflammation and mitochondrial markers in AML12 hepatocytes. Nutr Res Pract. 2019 Feb;13(1):3–10.

574. Kong X, Wang R, Xue Y, Liu X, Zhang H, Chen Y, et al. Sirtuin 3, a new target of PGC-1alpha, plays an important role in the suppression of ROS and mitochondrial biogenesis. PLoS One. 2010 Jul;5(7):e11707.

575. Wang S, Wan T, Ye M, Qiu Y, Pei L, Jiang R, et al. Nicotinamide riboside attenuates alcohol induced liver injuries via activation of SirT1/PGC-1α/mitochondrial biosynthesis pathway. Redox Biol. 2018 Jul;17:89–98.

576. Zhang T, Liu J, Tong Q, Lin L. SIRT3 Acts as a Positive Autophagy Regulator to Promote Lipid Mobilization in Adipocytes via Activating AMPK. Int J Mol Sci. 2020 Jan;21(2).

577. Liu T, Chen X-M, Sun J-Y, Jiang X-S, Wu Y, Yang S, et al. Palmitic Acid-Induced Podocyte Apoptosis via the Reactive Oxygen Species-Dependent Mitochondrial Pathway. Kidney Blood Press Res. 2018;43(1):206–19.

578. Jiang X-S, Chen X-M, Hua W, He J-L, Liu T, Li X-J, et al. PINK1/Parkin mediated mitophagy ameliorates palmitic acid-induced apoptosis through reducing mitochondrial ROS production in podocytes. Biochem Biophys Res Commun. 2020 May;525(4):954–61.

579. Bause AS, Haigis MC. SIRT3 regulation of mitochondrial oxidative stress. Exp Gerontol. 2013 Jul;48(7):634–9.

580. Klimova N, Long A, Kristian T. Nicotinamide mononucleotide alters mitochondrial dynamics by SIRT3-dependent mechanism in male mice. J Neurosci Res. 2019 Aug;97(8):975–90.

581. Ansari A, Rahman MS, Saha SK, Saikot FK, Deep A, Kim K-H. Function of the SIRT3 mitochondrial deacetylase in cellular physiology, cancer, and neurodegenerative disease. Aging Cell. 2017 Feb;16(1):4–16.

582. Finley LWS, Haigis MC. Metabolic regulation by SIRT3: implications for tumorigenesis. Trends Mol Med. 2012 Sep;18(9):516–23.

583. Ahn B-H, Kim H-S, Song S, Lee IH, Liu J, Vassilopoulos A, et al. A role for the mitochondrial deacetylase Sirt3 in regulating energy homeostasis. Proc Natl Acad Sci U S A. 2008 Sep;105(38):14447–52.

584. Pham TX, Bae M, Kim M-B, Lee Y, Hu S, Kang H, et al. Nicotinamide riboside, an NAD+ precursor, attenuates the development of liver fibrosis in a diet-induced mouse model of liver fibrosis. Biochim Biophys acta Mol basis Dis. 2019 Sep;1865(9):2451–63.

585. Song SB, Jang S-Y, Kang HT, Wei B, Jeoun U-W, Yoon GS, et al. Modulation of Mitochondrial Membrane Potential and ROS Generation by Nicotinamide in a Manner Independent of SIRT1 and Mitophagy. Mol Cells. 2017 Jul;40(7):503–14.

586. Dikalova AE, Itani HA, Nazarewicz RR, McMaster WG, Flynn CR, Uzhachenko R, et al. Sirt3 Impairment and SOD2 Hyperacetylation in Vascular Oxidative Stress and Hypertension. Circ Res. 2017 Aug;121(5):564–74.

587. Arany Z. PGC-1 coactivators and skeletal muscle adaptations in health and disease. Curr Opin Genet Dev. 2008 Oct;18(5):426–34.

588. Pérez-Schindler J, Handschin C. New insights in the regulation of skeletal muscle PGC-1α by exercise and metabolic diseases. Drug Discov Today Dis Model [Internet]. 2013;10(2):e79–85. Available from: http://www.sciencedirect.com/science/article/pii/S1740675713000030

589. Whitham M, Parker BL, Friedrichsen M, Hingst JR, Hjorth M, Hughes WE, et al. Extracellular Vesicles Provide a Means for Tissue Crosstalk during Exercise. Cell Metab. 2018 Jan;27(1):237-251.e4.

590. Thyfault JP, Bergouignan A. Exercise and metabolic health: beyond skeletal muscle. Diabetologia. 2020 Aug;63(8):1464–74.

591. Lee TH-Y, Formolo DA, Kong T, Lau SW-Y, Ho CS-L, Leung RYH, et al. Potential exerkines for physical exercise-elicited pro-cognitive effects: Insight from clinical and animal research. Int Rev Neurobiol. 2019;147:361–95.

592. Ostrowski K, Rohde T, Asp S, Schjerling P, Pedersen BK. Pro- and anti-inflammatory cytokine balance in strenuous exercise in humans. J Physiol. 1999 Feb;515 (Pt 1(Pt 1):287–91.

593. Pedersen BK, Steensberg A, Schjerling P. Muscle-derived interleukin-6: possible biological effects. J Physiol. 2001 Oct;536(Pt 2):329–37.

594. Nechemia-Arbely Y, Barkan D, Pizov G, Shriki A, Rose-John S, Galun E, et al. IL-6/IL-6R axis plays a critical role in acute kidney injury. J Am Soc Nephrol. 2008 Jun;19(6):1106–15.

595. Kato N, Abe S, Suto M, Hiraiwa K. Comparison of renal dysfunction in wild-type, IL-6 KO and iNOS KO mice hind limb tourniquet-reperfusion model. Leg Med (Tokyo). 2009 Apr;11 Suppl 1:S248-51.

596. Miyagi MYS, Seelaender M, Castoldi A, De Almeida DC, Bacurau AVN, Andrade-Oliveira V, et al. Long-term aerobic exercise protects against cisplatin-induced nephrotoxicity by modulating the expression of IL-6 and HO-1. PLoS One. 2014;9(10):2–9.

597. Lemay S, Rabb H, Postler G, Singh AK. Prominent and sustained up-regulation of gp130-signaling cytokines and the chemokine MIP-2 in murine renal ischemia-reperfusion injury. Transplantation. 2000 Mar;69(5):959–63.

598. Nerstedt A, Johansson A, Andersson CX, Cansby E, Smith U, Mahlapuu M. AMP-activated protein kinase inhibits IL-6-stimulated inflammatory response in human liver cells by suppressing phosphorylation of signal transducer and activator of transcription 3 (STAT3). Diabetologia. 2010 Nov;53(11):2406–16.

599. Kelly M, Gauthier M-S, Saha AK, Ruderman NB. Activation of AMP-activated protein kinase by

interleukin-6 in rat skeletal muscle: association with changes in cAMP, energy state, and endogenous fuel mobilization. Diabetes. 2009 Sep;58(9):1953–60.

600. Nadeau L, Aguer C. Interleukin-15 as a myokine: mechanistic insight into its effect on skeletal muscle metabolism. Appl Physiol Nutr Metab = Physiol Appl Nutr Metab. 2019 Mar;44(3):229–38.

601. Sun H, Ma Y, Gao M, Liu D. IL-15/sIL-15Rα gene transfer induces weight loss and improves glucose homeostasis in obese mice. Gene Ther. 2016 Apr;23(4):349–56.

602. Chen N, Li Q, Liu J, Jia S. Irisin, an exercise-induced myokine as a metabolic regulator: an updated narrative review. Diabetes Metab Res Rev. 2016 Jan;32(1):51–9.

603. Arhire LI, Mihalache L, Covasa M. Irisin: A Hope in Understanding and Managing Obesity and Metabolic Syndrome. Front Endocrinol (Lausanne). 2019;10:524.

604. Watt MJ, Miotto PM, De Nardo W, Montgomery MK. The Liver as an Endocrine Organ-Linking NAFLD and Insulin Resistance. Endocr Rev. 2019 Oct;40(5):1367–93.

605. Tanimura Y, Aoi W, Takanami Y, Kawai Y, Mizushima K, Naito Y, et al. Acute exercise increases fibroblast growth factor 21 in metabolic organs and circulation. Physiol Rep. 2016 Jun;4(12).

606. Hanatani S, Izumiya Y, Araki S, Rokutanda T, Kimura Y, Walsh K, et al. Akt1-mediated fast/glycolytic skeletal muscle growth attenuates renal damage in experimental kidney disease. J Am Soc Nephrol. 2014 Dec;25(12):2800–11.

607. Jiang S, Oh D-S, Dorotea D, Son E, Kim D-S, Ha H. Dojuksan ameliorates tubulointerstitial fibrosis through irisin-mediated muscle-kidney crosstalk. Phytomedicine. 2021 Jan;80:153393.

608. Declèves A-E, Sharma K. Obesity and kidney disease: differential effects of obesity on adipose tissue and kidney inflammation and fibrosis. Curr Opin Nephrol Hypertens. 2015 Jan;24(1):28–36.

609. de Las Heras N, Klett-Mingo M, Ballesteros S, Martín-Fernández B, Escribano Ó, Blanco-Rivero J, et al. Chronic Exercise Improves Mitochondrial Function and Insulin Sensitivity in Brown Adipose Tissue. Front Physiol. 2018;9:1122.

610. Geng L, Liao B, Jin L, Huang Z, Triggle CR, Ding H, et al. Exercise Alleviates Obesity-Induced Metabolic Dysfunction via Enhancing FGF21 Sensitivity in Adipose Tissues. Cell Rep. 2019 Mar;26(10):2738-2752.e4.

611. Sonavane M, Hayat F, Makarov M, Migaud ME, Gassman NR. Dihydronicotinamide riboside promotes cell-specific cytotoxicity by tipping the balance between metabolic regulation and oxidative stress. PLoS One. 2020;15(11):e0242174.

612. Hawley JA, Joyner MJ, Green DJ. Mimicking exercise: what matters most and where to next? J Physiol. 2019 Nov;

613. Storder J, Renard P, Arnould T. Update on the role of Sirtuin 3 in cell differentiation: A major metabolic target that can be pharmacologically controlled. Biochem Pharmacol. 2019 Nov;169:113621.

614. Mount P, Davies M, Choy S, Cook N, Power D. Obesity-Related Chronic Kidney Disease—The Role of Lipid Metabolism. 2015;720–32.

615. Beauchamp D, Laurent G, Grenier L, Gourde P, Zanen J, Heuson-Stiennon JA, et al. Attenuation of gentamicin-induced nephrotoxicity in rats by fleroxacin. Antimicrob Agents Chemother. 1997;41(6):1237–45.

616. laurent G, Carlier MB, Rollman B, Van Hoof F, Tulkens P. Mechanism of aminoglycoside-induced lysosomal phospholipidosis: In vitro and in vivo studies with Gentamicin and Amikacin. Biochem Pharmacol. 1982;31(23):3861–70.

617. Singh R, Kaushik S, Wang Y, Xiang Y, Novak I, Komatsu M, et al. Autophagy regulates lipid metabolism. Nature [Internet]. 2009;458(7242):1131–5. Available from: http://dx.doi.org/10.1038/nature07976

618. Singh R, Cuervo AM. Lipophagy: Connecting autophagy and lipid metabolism. Int J Cell Biol. 2012;2012.

619. Slyne J, Slattery C, McMorrow T, Ryan MP. New developments concerning the proximal tubule in diabetic nephropathy: In vitro models and mechanisms. Nephrol Dial Transplant. 2015;30(November):iv60–7.

620. Legouis D, Bataille A, Hertig A, Vandermeersch S, Simon N, Rondeau E, et al. Ex vivo analysis of renal proximal tubular cells. 2015;1–11.

621. Terryn S, Jouret F, Vandenabeele F, Smolders I, Moreels M, Devuyst O, et al. A primary culture of mouse proximal tubular cells, established on collagen-coated membranes. Am J Physiol Renal Physiol. 2007 Aug;293(2):F476-85.

PUBLICATIONS

International Journal of
Molecular Sciences

MDPI

Review

Critical Role for AMPK in Metabolic Disease-Induced Chronic Kidney Disease

Florian Juszczak [1,2,*], Nathalie Caron [2], Anna V. Mathew [3] and Anne-Emilie Declèves [1]

[1] Laboratory of Molecular and Metabolic Biochemistry, Faculty of Medicine and Pharmacy, Research Institute for Health Sciences and Technology, University of Mons (UMONS), 7000 Mons, Belgium; anne-emilie.decleves@umons.ac.be
[2] Molecular Physiology Research Unit (URPhyM), Namur Research Institute for Life Sciences (NARILIS), University of Namur (UNamur), 5000 Namur, Belgium; nathalie.caron@unamur.be
[3] Division of Nephrology, Department of Internal medicine, University of Michigan, Ann Arbor, MI 48109, USA; amat@med.umich.edu
* Correspondence: florian.juszczak@umons.ac.be

Received: 2 October 2020; Accepted: 25 October 2020; Published: 27 October 2020

Abstract: Chronic kidney disease (CKD) is prevalent in 9.1% of the global population and is a significant public health problem associated with increased morbidity and mortality. CKD is associated with highly prevalent physiological and metabolic disturbances such as hypertension, obesity, insulin resistance, cardiovascular disease, and aging, which are also risk factors for CKD pathogenesis and progression. Podocytes and proximal tubular cells of the kidney strongly express AMP-activated protein kinase (AMPK). AMPK plays essential roles in glucose and lipid metabolism, cell survival, growth, and inflammation. Thus, metabolic disease-induced renal diseases like obesity-related and diabetic chronic kidney disease demonstrate dysregulated AMPK in the kidney. Activating AMPK ameliorates the pathological and phenotypical features of both diseases. As a metabolic sensor, AMPK regulates active tubular transport and helps renal cells to survive low energy states. AMPK also exerts a key role in mitochondrial homeostasis and is known to regulate autophagy in mammalian cells. While the nutrient-sensing role of AMPK is critical in determining the fate of renal cells, the role of AMPK in kidney autophagy and mitochondrial quality control leading to pathology in metabolic disease-related CKD is not very clear and needs further investigation. This review highlights the crucial role of AMPK in renal cell dysfunction associated with metabolic diseases and aims to expand therapeutic strategies by understanding the molecular and cellular processes underlying CKD.

Keywords: AMPK; chronic kidney disease; obesity; diabetes; autophagy; mitochondrial homeostasis; lipid metabolism; lipotoxicity; proximal tubule

1. Introduction

Progressive decline in renal function leads to chronic kidney disease (CKD) and, ultimately, end-stage renal disease (ESRD) requiring dialysis or transplantation. As of 2017, 9.1% of the world population has CKD, making CKD a public health problem with an enormous economic impact [1,2]. CKD is associated with metabolic syndrome (MetS), a cluster of metabolic disorders, including hypertension, hyperlipidemia, hyperglycemia, and obesity [3]. MetS contributes to the appearance of albuminuria, the first sign of kidney disease in patients with diabetes [4–6]. Moreover, accumulating studies report that obesity is an independent risk factor of CKD [7–9]. The growing epidemic of obesity contributes to the increased prevalence of type II diabetes and the related kidney complications making diabetic kidney disease the leading cause of ESRD in the developed world [10].

Both obesity- and diabetes-related kidney disease are associated with glomerulomegaly, hemodynamic changes, increased albuminuria as well as similar structural and functional changes in the kidney [11–13]. Although the lesions found in obesity-induced kidney disease are slightly different from nonobese diabetic patients, it is difficult to discriminate between the effects of obesity vs. the concomitant effects of hyperglycemia and insulin resistance in clinical studies, as there is considerable overlap between diabetic and overweight/obese patients [10]. Adiposity and adipose tissue dysfunction, associated with insulin resistance, lead to the release of proinflammatory cytokines and free fatty acids (FA) in the circulation, as well as changes in the production of adipokines (leptin and adiponectin), which likely contribute to the pathogenesis of obesity and diabetes-induced kidney disease [12,14,15]. Obesity enhances the renin-angiotensin-aldosterone system (RAAS), leptin-induced activation of the sympathetic nervous system (SNS), tubular sodium reabsorption, and volume expansion, leading to hypertension [16]. Increased tubular sodium and glucose reabsorption lead to an enhanced consumption of oxygen in the renal cortex, associated with a lower renal oxygenation due to fluid volume expansion and increased blood flow that contributes to hypoxia induction in renal tissue [17,18]. Obesity-induced hypertension accelerates glomerular hyperfiltration, leading to obesity-related glomerulopathy characterized by glomerulomegaly with focal and segmental glomerulosclerosis lesions [19]. Meanwhile, systemic inflammation and dyslipidemia contribute to the initiation of oxidative stress and insulin resistance, leading to renal low-grade inflammation and fibrosis (Figure 1) [20]. Finally, both obesity- and diabetes-induced kidney disease are characterized by ectopic lipid depositions in the kidney and are associated with direct lipotoxicity in rodents and humans [21–27].

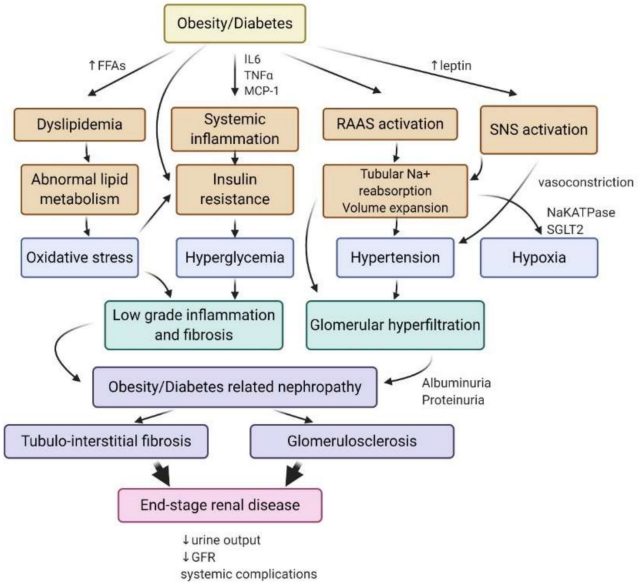

Figure 1. Mechanisms involved in the pathogenesis of diabetes- and obesity-related kidney disease and ultimately end-stage renal disease. Obesity and diabetes initiate systemic disturbances, including systemic inflammation, dyslipidemia, the activation of the SNS, and RAAS that contribute to intrarenal stresses resulting from abnormal lipid metabolism, insulin resistance, and tubular reabsorption of sodium. Hypertension and the associated glomerular hyperfiltration increase albuminuria. Renal oxidative stress and hyperglycemia lead to inflammation and fibrosis that initiate obesity- and diabetes-related nephropathy. Tubulo-interstitial fibrosis and glomerulosclerosis are associated with a progressive decline in the glomerular filtration rate (GFR), loss of nephrons, and ultimately end-stage renal disease. IL6, interleukin 6; TNFα, tumor necrosis factor-α; MCP-1, monocyte chemoattractant protein-1; FFAs, free fatty acids; Na^+-K^+ ATPase, sodium–potassium pump; SGLT2, sodium/glucose cotransporter 2; SNS, sympathetic nervous system; GFR, glomerular filtration rate; RAAS, renin–angiotensin–aldosterone system.

Obesity- and diabetes-related kidney diseases share physiological initiating events and also critical molecular mechanisms of renal cell injury. Studies have demonstrated an essential role of AMP-activated protein kinase (AMPK) dysregulation in obesity- and diabetes-associated kidney disease both in experimental and clinical models [28–33]. In several studies, AMPK activators attenuate diabetic nephropathy and improve high fat-induced kidney disease in mice [24,34–36]. However, therapeutic approaches to prevent or treat kidney disease in patients with obesity and diabetes are not very specific to these altered pathways. The delay in developing therapeutic strategies to modulate AMPK in obesity- and diabetes-induced kidney disease is partially due to the complexity of the underlying physiological and molecular mechanisms. In this review, we discuss the physiological role of AMPK signaling in renal cells and its dysregulation in obesity- and diabetes-related chronic kidney disease.

2. AMP-Activated Protein Kinase (AMPK): Structure, Renal Expression, and Function

AMPK is a heterotrimeric complex composed of three different subunits: α, β, and γ (Figure 2). The catalytic subunit α is present in two different isoforms α1 and α2. The β and γ subunits are the regulatory subunits. There are two β-subunits (β1 and β2) and three γ subunits (γ1, γ2, and γ3). Seven different genes encode these multiple protein isoforms: *PRKA1/2*, *PRKAB1/2*, and *PRKAG1/2/3*. The expression of AMPK subunits is tissue-specific and seems to vary in response to stress, suggesting differential functions of each isoform, which are not well understood. The α subunit contains a kinase domain phosphorylated by upstream kinases on Thr172, an autoinhibitory domain (AID), and a β binding domain, essential for the formation of the heterotrimeric complex. AMPKβ contains a carbohydrate-binding molecule (CBM) that allows AMPK to bind to glycogen and an αγ binding domain. The β subunit is implicated in the relocalization of AMPK in glucose-starved states to the lysosome and the mitochondrial membranes with the goal of mitophagy [37]. The structural characteristics of AMPKγ are the four tandem repeats termed cystathionine β-synthase (CBS) motifs that bind adenine nucleotides. The binding of AMP, rather than ADP or ATP, to the AMPKγ subunit leads to the activation of AMPK [38].

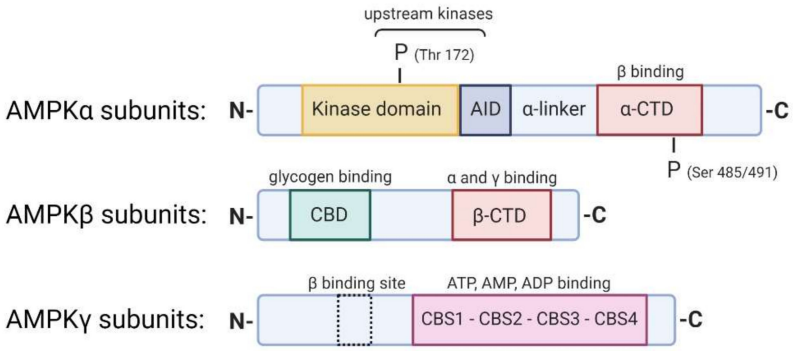

Figure 2. AMPK α, β, and γ subunits. The crystal structure represents the different domains and specific sites of the α, β, and γ subunits that constitute the AMPK heterotrimeric complex. The AMPKα subunits contain a serine/threonine kinase domain at the N-terminus phosphorylated by upstream kinases on the residue Thr172, directly followed by an autoinhibition domain (AID) that maintains the kinase domain inactive in the absence of AMP and a C-terminus domain (α-CTD) that interacts with the β subunits. Phosphorylation of Ser 485/491 residues on the α-CTD negatively regulates AMPK. The AMPKβ subunits have a glycogen-binding domain (CBD) and an α and γ subunit interaction domain (β-CTD). The AMPKγ subunits present four β-synthase (CBS) domains (CBS1-4) that can bind to ATP, AMP, and ADP. AMP binding initiates the allosteric activation of AMPK and promotes phosphorylation of AMPK by upstream kinases.

Renal cells express AMPK extensively. Few studies describe the specific AMPK subunit isoforms expressed in the kidney, as most of the time, the kidney expresses all AMPK isoforms. AMPK is often

studied in total kidney lysates, making it difficult to have specific data regarding subunit expression in the whole kidney. However, specific cell populations in the kidney express AMPK isoforms differentially considering their specific functions in metabolism. According to data from The Human Protein Atlas (HPA), AMPK is mostly expressed in cortical tubular epithelial cells, notably on apical surfaces of distal tubules in mice, as demonstrated with immunostaining for Thr172 Phospho-AMPKα [24,39]. The α2 subunit is the predominant catalytic isoform. However, the α1 subunit is also detectable in the tubule but not detectable in the glomeruli. The human kidney expresses β1, β2, and γ2 isoforms. Salatto et al. showed that human and rodent kidneys predominately express AMPK β1 [40]. The α1 isoform is the predominant isoform in the rat kidney, while the kidney expresses both γ1 and γ2 equally [41]. The skeletal muscle expresses the γ3 subunit, but this subunit is not expressed in the kidney.

2.1. An Allosteric Mechanism Activates AMPK

High AMP:ATP ratios under starvation, hypoxia or exercise are associated to the binding of AMP to the regulatory γ subunit, allosterically activating AMPK. The AMP binding favors the phosphorylation of AMPK by upstream kinases on the α subunits at specific Thr172 residues. Furthermore, AMP binding prevents the dephosphorylation of AMPK by protein phosphatases, PP2A, and PP2C. The two central upstream kinases that phosphorylate AMPK are the serine-threonine liver kinase B1 (LKB1) and the calcium/calmodulin kinase kinase β (CAMKKβ). LKB1 activates AMPK in response to low energy states (e.g., exercise, starvation), while CAMKKβ is sensitive to increases in intracellular Ca^{2+} [38]. The transforming growth factor (TGF)-β-activated kinase-1 (TAK1) is also known to phosphorylate AMPK on Thr172 of the α subunit [42]. Other phosphorylation sites, particularly on Ser485/491 (equivalent rodent sequence is Ser487/491), are targeted by other kinases such as Akt through insulin-related signaling or PKA through c-AMP-related signaling pathways. However, these phosphorylations lead to the negative regulation of AMPK by blocking its phosphorylation at Thr172 by upstream kinases [43–45].

2.2. AMPK Exhibits a Dual Function in Cell Metabolism

First, AMPK decreases ATP consumption by inhibiting anabolic pathways, including lipid, glycogen, and protein synthesis. Secondly, AMPK activates catabolic pathways by increasing lipid oxidation, glucose uptake, autophagy flux, and mitochondrial biogenesis. The following sections will discuss these pathways in the context of obesity- and diabetes-related kidney disease. Energy sensing by AMPK is particularly relevant in renal cells because these cells are strongly dependent on the regulation of energy metabolism for tubular transport.

AMPK regulates the Na^+-K^+-ATPase (NKA), epithelial sodium channel (ENaC), the Na^+-K^+-$2Cl^-$ cotransporter (NKCC), Cystic fibrosis transmembrane conductance regulator (CFTR), and other ion transport proteins in the kidney [41]. AMPK plays an essential role in kidney homeostasis, as evidenced by AMPK knockdown studies. Kidney-specific deletion of both AMPKα subunits displayed salt and water wasting defects [46]. Both AMPKα2 knockout mice and endothelium-specific knockdown of AMPKα2 display an increased angiotensin-converting enzyme (ACE)-levels [47]. Specific renal physiological processes, such as ion transport, blood pressure control, and nitric oxide production, involve AMPK [48]. Tubular epithelial-specific deletion of LKB1, the primary upstream kinase of AMPK, is associated with de-differentiation of tubule epithelial cells, fibrosis, and inflammation, mediated by AMPK and its downstream metabolic effects [33]. On the other hand, uncontrolled sustained activation of AMPK in a Wolff–Parkinson–White Syndrome model led to a disastrous accumulation of glycogen in the kidney and subsequent impairment of renal function [49]. While these genetic studies of AMPK highlight the importance of a tight regulation of AMPK activity in the kidney during physiological conditions, AMPK impairment in the kidney's response to metabolic stress initiates deleterious outcomes.

3. AMPK Activity in Obesity and Diabetes-Induced Chronic Kidney Disease (CKD)

Type II diabetes, obesity, and MetS are characterized by lipid accumulation and hyperglycemia, which is perceived by the cells as a nutrient excess. According to the classic view, the cells respond to this high-energy state by a decreased AMPK activity. However, many cellular and molecular events directly or indirectly linked to metabolic disturbances in the whole body inhibit AMPK [50]. As previously mentioned, AMP: ATP ratio during physiological conditions or adaptations such as exercise or starvation strongly correlate with AMPK activity. In obesity and diabetes, additional mechanisms, independent of the AMP: ATP ratio, might also promote the reduced AMPK activity. With nutrient excess, the energy state of the cell favors an altered redox status with higher NADH production through glycolysis [51]. This increase in NADH, in turn, leads to reduced activity of Sirtuin 1 (SIRT1), an NAD^+-dependent deacetylase, that is a potent activator of LKB1, therefore favoring the dephosphorylated state of AMPK [52–54]. Recently, Kikuchi et al. further demonstrated in CKD-induced by a subtotal nephrectomy in mice that AMPK activity was decreased in renal tissue in spite of high energy demand. CKD-associated acidosis and uremic metabolites were particularly implicated in the sensing failure to upregulate AMPK despite an increased AMP to ATP ratio [55].

Elevated circulating hormones such as insulin and leptin in metabolic diseases downregulate AMPK by inducing inhibitory phosphorylation on different serine residues. For example, insulin decreases AMPK activity through phosphorylation on Ser485 and Ser491 of AMPKα subunits by the Akt pathway. At the same time, leptin induces AMPK inhibition by p70S6 kinase downstream of Akt [56,57]. Additionally, low adiponectin levels in obesity and type II diabetes could also decrease AMPK activation via its receptor, AdipoR1. Adiponectin knockout mice have decreased AMPK activity, while AMPK activity correlates with adiponectin levels in an obesity model [58]. In high-fat and high-sucrose diet models, tissue expression of adiponectin receptors was dysregulated, highlighting a mechanism of adiponectin resistance in peripheral tissues that could also contribute to impaired AMPK activity [59,60]. More recently, the treatment of *db/db* mice with an activator of adiponectin, AdipoRon, showed the upregulation of phosphorylated AMPK in the kidney along with reduced inflammation and lipotoxicity [30]. Finally, obesity and diabetes are associated with inflammation and oxidative stress that are both recognized to inhibit AMPK [61]. The pro-inflammatory cytokine TNFα is known to suppress AMPK activity via the induction of protein phosphatase 2C (PP2C) in skeletal muscle in vitro and in vivo, suppressing fatty acid (FA) oxidation and promoting insulin resistance [62].

4. AMPK in Renal Transport

The role of AMPK in ion transport has been described in earlier reviews [63,64]. However, very little is known about the role of AMPK in renal transport in the setting of obesity and diabetes. Both obesity and insulin resistance are associated with significant changes in tubular transport, leading to electrolyte disorders such as hypomagnesemia, hyper/hyponatremia, hyper/hypokalemia, and hyper/hypocalciuria [65,66]. Interestingly, AMPK interferes with Na^+-handling, notably by activating the primary transport, the NKA [67]. Xiao et al. demonstrated that the AMPK pathway is the principal regulator of NKA signaling as the hyperuricemia-induced renal tubular injury impairs NKA. Moreover, AMPK activation exerts protective effects regarding NKA-mediated mechanisms of tubular injury by regulating NKA expression and reducing lysosomal NKA degradation [68]. However, AMPK activation also downregulates the ENaC expression in the distal tubule [69,70] while it seems to enhance the stimulation of the NKCC that is responsible for sodium reabsorption in the thick ascending limb [46,71]. Nevertheless, the use of knockout mice for AMPK subunits demonstrated only a moderate role for AMPK in renal sodium handling, suggesting that AMPK might only play a secondary modulatory role [72]. Furthermore, AMPK downregulates many other renal transporters such as Na^+-coupled phosphate transporter (NaPi-IIa) or CFTR [73,74]. Therefore, though reduced renal AMPK activity in metabolic diseases may contribute to salt and water imbalance in obesity- or diabetes-related disease, the role of AMPK in renal tubular handling in the metabolic disease associated kidney disease needs further investigation.

5. AMPK and Renal Lipid Metabolism

Diabetic nephropathy and obesity-induced CKD are both linked to renal lipid accumulation and abnormal lipid metabolism (Figure 3) [24,75,76]. Activated AMPK induces the inhibitory phosphorylation of Acetyl-CoA Carboxylase (ACC), the rate-limiting step of FA synthesis, reducing the production of malonyl-CoA. Decreased malonyl-CoA promotes the activation of carnitine palmitoyltransferase-1 (CPT-1), allowing the entry of FA into the mitochondria for β-oxidation. Therefore, a direct consequence of AMPK dysfunction in the kidney is the increase of ACC activity, likely contributing to lipogenesis and ultimately lipid accumulation. Mice fed a high-fat diet confirm dysregulated AMPK and the consequent renal accumulation of cholesterol and triglycerides (TG) [24,77].

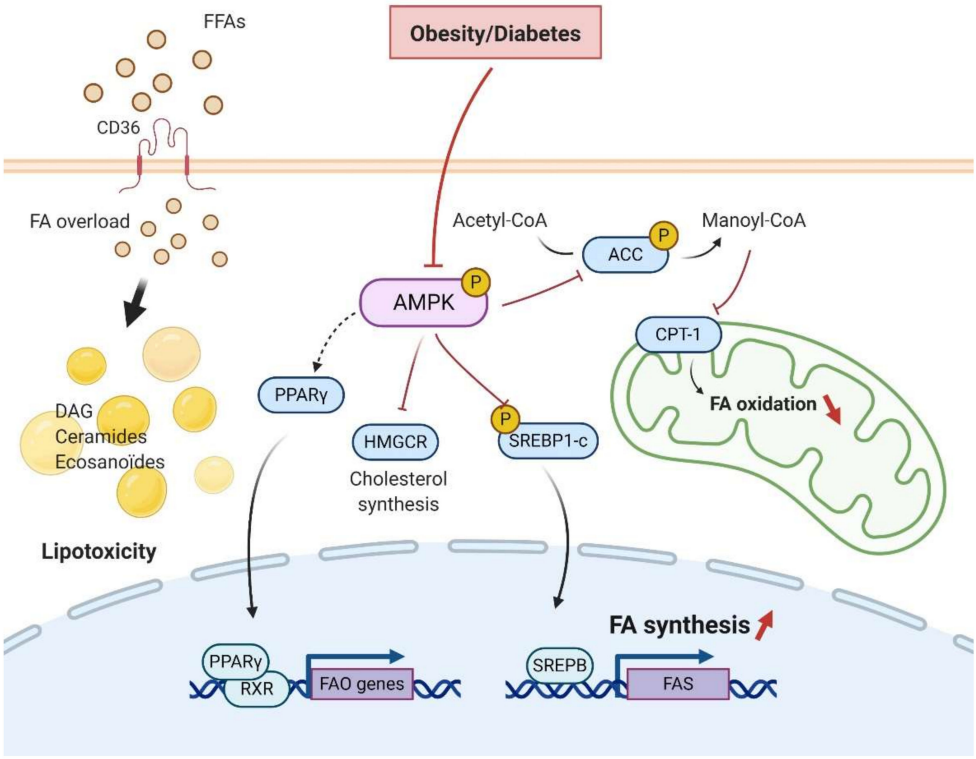

Figure 3. Impaired regulation of lipid metabolism by AMPK in renal cells in obesity/diabetes. Inhibition of AMPK and the increased FA overload lead to a decreased mitochondrial FA oxidation and an enhanced lipogenesis, initiating lipotoxicity in renal cells. Inhibitory phosphorylation of ACC by AMPK is removed, allowing for malonyl-CoA production, leading to inhibition of CPT-1 activity and suppression of FA oxidation in mitochondria. HMGCR and SREBP1-c are enhanced and initiate cholesterol and FA synthesis that contributes to a general increase of lipogenesis, leading to further lipid accumulation in renal cells. Excess FA content associated with impaired AMPK pathway and related lipid metabolism initiates ectopic lipid accumulation in renal cells, including harmful lipid metabolites (DAG, ceramides, and eicosanoids) that cause lipotoxicity. AMPK, AMP-activated protein kinase; ACC, Acetyl-CoA carboxylase; CPT1, Carnitine palmitoyltransferase I; PPARγ, peroxisome proliferator-activated receptor γ; HMGCR, 3-hydroxy-3-methyl-glutaryl-coenzyme A reductase; RXR, retinoid X receptor; SREBP, sterol regulatory element-binding proteins; FAS, fatty acid synthesis; FAO, fatty acid oxidation; DAG diacylglycerol; FFAs, free fatty acids. The arrow indicates whether the regulation is activating (black) or inhibitory (red). The dashed arrow indicates a potential regulation.

Obesity and diabetes increase the expression of Sterol Regulatory Element-binding Proteins (SREBP) that are implicated in fatty acid and cholesterol metabolism [78,79]. SREBP-1c knockout mice fed a high fat diet (HFD) do not accumulate renal lipids [80]. However, transgenic mice overexpressing

SREBP-1a demonstrated elevated renal TG content with glomerulosclerosis and proteinuria [78]. Though this study did not probe AMPK activity, AMPK is a direct upstream kinase of SREBP in the liver [81,82]. Activation of AMPK resulted in inhibition of SREBP1-c and attenuation of lipogenesis in hepatocytes [83]. Indeed, Li et al. demonstrated that SREBP1-c phosphorylation at Ser372 by AMPK in the liver led to the inhibition of the transcriptional activity of SREBP1-c by decreasing its cleavage and nuclear translocation [83]. SREBP family of proteins induces FAS by inducing transcriptional expression of FAS genes [84]. Particularly, SREBP1-c contributes to the increased de novo synthesis of fatty acids by regulating both FAS and ACC expression [85]. Moreover, calcium channel blocker Nifedipine decreased AMPK activity and increased SREBP1/2 and intrarenal lipids [86]. These studies confirm the role of AMPK dysregulation in renal lipid accumulation via the SREBP pathway.

Kume et al. demonstrated an increase in renal TG content and marked neutral lipid accumulations in both the glomeruli and tubular compartment with overexpression of the peroxisome proliferator-activated receptor gamma (PPARγ), while heterozygous PPARγ mice were protected [76]. This study demonstrated decreased AMPK activity, but no link between AMPK and PPARγ was discussed. Interestingly, several independent studies have highlighted a cross-regulation of AMPK and PPARγ, suggesting an expanded regulation of lipid metabolism by AMPK [87–89].

On the other hand, HFD fed mice demonstrated decreased lipolysis and AMPK activity [24]. Cholesteryl esters and phosphatidyl contents but not TG were increased along with a significant increase of lipid droplets in proximal tubular cells (PTC). AICAR, a specific AMPK activator, prevented all these changes. In that study, AMPK activation in HFD mice also prevented cholesterol synthesis by the regulation of the rate-limiting cholesterol synthesis enzyme 3-hydroxy-3-methylglutaryl-CoA reductase (HMGCR) [24]. Other groups also confirmed lipid droplet accumulation in PTC [21–27]. Under physiological conditions, the primary role of PTC is the active reabsorption of filtered sodium. This process requires a large amount of ATP, mostly provided through the mitochondrial β-oxidation of FA. Inhibition of FA oxidation induced increased intracellular lipid depositions, cellular de-differentiation, and cell death in the kidney [90,91]. In PTC, FA can also be taken up via the fatty acid translocase (CD36) and the fatty acid-binding proteins (FABP). FA can then be used to supply energy. CD36 was upregulated in kidney biopsies of diabetic patients [92]. Moreover, CD36 upregulation in the kidney led to the inhibition of AMPK activity and subsequent lipotoxicity [86].

Excess intracellular FA content can lead to the accumulation of toxic lipid metabolites such as diacylglycerol (DAG) and ceramides. Both the DAG and ceramide are known to be involved in insulin resistance and inflammation. Both are endogenous activators of protein kinase C (PKC) and PP2A [93]. Moreover, the downregulation of AMPK activity through the PKC-dependent Ser487 phosphorylation has been demonstrated in human endothelial cells [94]. Using lipidomics, Declèves et al. demonstrated HFD-induced dysregulation of lipid metabolism and particularly highlighted eicosanoids, which are implicated in the inflammatory response in the kidney. Direct activation of AMPK with AICAR reduced arachidonic acid and docosahexaenoic acid-derived metabolites in the kidney, thus improving the eicosanoid pathway and associated lipotoxicity [95]. Therefore, the altered lipid metabolism in the kidney, characterized by an imbalance between FA accumulation and degradation seems primarily mediated by AMPK.

6. AMPK and Renal Glucose Metabolism

In conditions with abundant glucose, AMPK promotes *GLUT4* gene expression, glucose uptake, and glycolysis in insulin-sensitive cells. Several studies have reported the role of AMPK in mediating glucose transport in podocytes and insulin resistance in diabetic nephropathy [96,97]. Indeed, podocytes display a complex cellular morphology that requires a sustained energy supply to maintain cytoskeletal remodeling. In podocytes, the mitochondrial abundance is low and anaerobic glycolysis represents the predominant energy source that makes them uniquely sensitive to insulin [98]. Although insulin-stimulated glucose uptake is mostly independent of AMPK, Rogacka et al. demonstrated that AMPK activity is essential for insulin sensitivity in podocytes.

Moreover, insulin resistance in podocytes cultured in high glucose medium was closely related to AMPK activity [96]. Using pharmacological and genetic approaches, they suggested that the involvement of AMPK in PTEN (phosphatase and tensin homolog) regulation in cultured podocytes was disturbed in high glucose conditions leading to decreased insulin sensitivity. Insulin mediates AMPK regulation through transient receptor potential canonical channel 6 (TRPC6) activation [99]. TRPC6 is a nonselective Ca^{2+} channel protein that is implicated in the pathophysiology of kidney diseases [100]. In diabetic nephropathy, TRPC6 is upregulated, suggesting a putative role of TRPC6 expression in the progression of diabetic nephropathy pathology. Wang et al. investigated the effect of TRPC6 knockout on diabetic kidney disease in the Akita model of type I diabetes [101]. They surprisingly demonstrated a protective effect of TRPC6 downregulation on proteinuria and albuminuria. This role of TRPC6 is contrary to promoting the progression of glomerular impairment associated with insulin resistance in vivo and in podocyte cultures.

Like AMPK, Sirtuin 1 (SIRT1) acts as a nutrient sensor in cells. AMPK and SIRT1 are reciprocally regulated and share common targets. The expression of SIRT1 is significantly reduced in animal models of diabetes and in diabetic patients. Moreover, podocyte-specific overexpression of SIRT1 led to improvements in glomerular and tubular injuries in diabetic mice [102]. SIRT1 downregulates AMPK activity in podocyte cultures. SIRT1 suppresses the stimulation of AMPK by insulin, suggesting that the SIRT1/AMPK pathway is essential in podocytes for proper insulin response [103]. Both AMPK and SIRT1 promote autophagy flux in renal tissue, regulate mitochondrial homeostasis, and antioxidative defense. AMPK mediates the hypoglycemic and renoprotective effects of Salidroside (plant glycoside) by downstream activation of SIRT1 [104].

In the proximal tubule, glucose reabsorption mostly occurs via the Na^+-glucose cotransporter SGLT2 and to a lesser extent via SGLT1 in later segments of the proximal tubule. Glucose leaves the basolateral membrane through GLUT1 and GLUT2 [105]. Although the AMPK regulation of SGLT2 has not been clearly addressed, the use of SGLT2 inhibitors mimics the cellular response to starvation and indirectly activates AMPK, leading to the improvement of nephropathy development [106]. However, it has been demonstrated that AMPK activates SGLT1-dependent glucose transport in colorectal cells and cardiomyocytes that needs to be confirmed in the renal tissue [107,108]. Moreover, AMPK activation increased *GLUT1* gene expression in rat kidneys and is associated with enhanced activity of GLUT2 in murine intestinal tissue [64].

7. AMPK and Renal Mitochondrial Function and Dysfunction

7.1. Mitochondrial Biogenesis and Dynamics

As already mentioned, the kidneys are highly metabolic organs, rich in mitochondria to meet their enormous energy demands. PTCs have a high number of active transporters that require energy to reabsorb ions, glucose, or other nutrients. Maintaining the mitochondrial function is, therefore, essential to sustain the energy demand and kidney function. AMPK activity promotes mitochondrial homeostasis by regulating mitochondrial biogenesis and dynamics and limiting reactive oxygen species (ROS) formation [38,109]. There is a very substantial body of evidence demonstrating the mitochondrial protection exerted by AMPK, notably by activating peroxisome proliferator-activated receptor gamma co-activator 1-alpha (PGC-1α) [110–113]. PGC-1α is a transcriptional co-activator and the master regulator of mitochondrial biogenesis. Upon activation, it migrates to the nucleus to activate different transcription factors, including nuclear respiratory factors 1 and 2 (NRF-1 and -2). These, in turn, activate the expression of nuclear-coded respiratory chain proteins and the expression of mitochondrial transcription factor A (Tfam), driving replication of mitochondrial DNA and transcription [114].

Mitochondrial dysfunction has been well documented in metabolic disease-induced CKD (reviewed in [115,116]) and is a critical player of the pathogenesis [117]. Szeto et al. demonstrated that the use of SS-31, a mitochondrial-targeted antioxidant, preserved mitochondrial structure in HFD mice and led to the improvement of glomerular and tubular injuries. Interestingly, these effects were

attributed to restored AMPK activity, suggesting that mitochondria integrity is essential to maintain AMPK phosphorylation [118]. Even in diabetic nephropathy, the restoration of AMPK activation via AICAR restored mitochondrial function and superoxide production, in association with PGC1-α activation, reduced kidney injury. In another study, treatment with Chloroquine in both in vitro and in vivo diabetic environments enhanced AMPK phosphorylation and led to mitochondrial biogenesis and an improved balance of mitochondrial fusion/fission proteins [119]. Human osteosarcoma cells demonstrate the involvement of AMPK in mitochondrial dynamics (fusion/fission/mitophagy) [120]. Toyama et al. found a new AMPK target protein, the mitochondrial fission factor (MFF), which is the primary receptor for the dynamin-like protein Drp1 involved in the mitochondrial fission mechanism. Later, the same AMPK/MFF/Drp1 axis was dysregulated in mesenchymal stromal cells as well. Renal mitochondrial fragmentation has been observed in both in vitro and in vivo models of diabetic nephropathy that was reversed by both AMPK activators, AICAR and Metformin. Interestingly, in that study, the improvement in mitochondrial fragmentation by AMPK activators was correlated with activation of PGC1-α and the consequent restoration of Drp1 and Mfn1 expression in tubular cells [121].

7.2. AMPK and Oxidative Stress

Oxidative stress plays a crucial role in the development and the progression of diabetic nephropathy and obesity (Figure 4). Because renal cells are metabolically very active and contain many mitochondria, they are highly vulnerable to ROS generation and therefore to oxidative damage [116]. Under physiological conditions, ROS are generated as standard products of aerobic metabolism, acting as intracellular signaling messengers. Therefore, ROS such as the superoxide radical ($O_2^{\bullet -}$) and hydroxyl radical ($^{\bullet}OH$) or even the nonradical hydrogen peroxide (H_2O_2) are continuously produced during cell metabolism and are eliminated by the antioxidant defenses that include superoxide dismutase (SOD), catalase, peroxidases and the glutathione system to prevent cellular protein damage or lipid peroxidation. However, under nutrient stress such as during chronic hyperglycemia or hyperlipidemia, overproduction of ROS due to the disruption of the redox status occurs, leading to renal inflammation, fibrosis, and impairment of organ structure and function [8,122].

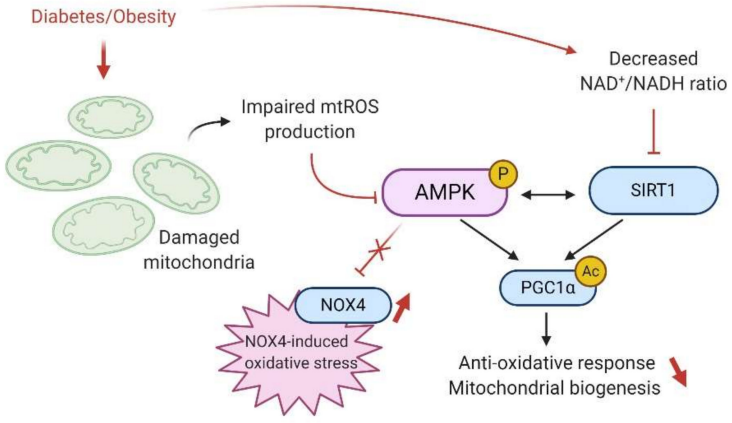

Figure 4. Schematic representation of the proposed mechanism by which diabetes/obesity leads to a decreased antioxidative response mediated by AMPK and enhanced oxidative stress in the renal cell. Regulation of mitochondrial production of reactive oxygen species (ROS) is required for the proper adaptation of the renal cell to metabolic stress. Diabetes and obesity impair renal mitochondrial ROS, which is associated with decreased AMPK. AMPK inhibition and decreased SIRT1 activity lead to a maladaptive antioxidative response through PGC1-α activity suppression, notably decreasing mitochondrial biogenesis. Decreased AMPK also results in increased NOX4-dependent ROS production, further increasing oxidative stress in renal cells. The arrow indicates whether the regulation is activating (black) or inhibitory (red).

In the kidney, the mitochondria are the primary source of ROS production due to a leakage from the mitochondrial electron-transport chain. Regarding AMPK and oxidative stress, it has been well established that AMPK activity plays a crucial role in maintaining redox homeostasis in the cells. AMPK is essential in the suppression of ROS and acts thus as an oxidative stress defense. Different models have described a link between reduced AMPK activity and mitochondrial ROS (mtROS) [112,115–117]. Physiologically, mtROS promotes noncanonical activation of AMPK, triggering antioxidative responses through PGC1-α activation and regulating mitochondria homeostasis by activation of the mitophagy process via AMPK-mediated phosphorylation of the Unc-51 like autophagy activating kinase ULK-1 [109]. AMPK regulates gene expression of several antioxidative genes, including *catalase*, *SOD2*, *UCP2*, and *SIRT3* [123]. Notably, AMPKα or PGC1α deficiency increases oxidative stress in cells and cannot overcome ROS-induced damage and mitochondrial homeostasis disruption [109].

Under pathological conditions, the contribution of ROS to the development and the progression of kidney disease is controversial. For example, Ruggiero et al. demonstrated that the kidneys of mice fed an HFD could maintain mitochondrial biogenesis and bioenergetics, despite evidence of renal oxidative stress, suggesting an adaptive response to the free FA overload [124]. Still, Dugan et al. reported a reduced superoxide production associated with suppression of mitochondrial activity in the type I diabetic model [29]. The decreased mtROS was concomitant with a decreased AMPK activity and led to further inhibition of mitochondria in a feedback loop manner. Interestingly, AICAR treatment restored AMPK activity and the mitochondrial superoxide production reversing the hallmarks of diabetic kidney disease such as glomerular matrix expansion and albuminuria [29]. Sharma et al. proposed that stimulation of mitochondrial function and superoxide production by AMPK agonists would be associated with better outcomes in the diabetic kidney [125]. However, mtROS production inhibits AMPK activity through the SIRT1 pathway. Indeed, mtROS mediate DNA breaks in the nucleus that require the activation of PARP (repair enzyme, poly adenosine diphosphate ribose polymerase), another NAD^+-dependent enzyme. Therefore, upon PARP activation, the pool of cellular NAD^+ is reduced, decreasing NAD^+ availability for SIRT1, reducing the phosphorylation of AMPK through LKB1 activation [126]. In conclusion, the direct link between AMPK and mtROS production has not been fully understood and will require further investigation in the context of diabetes- and obesity-induced CKD.

NADPH oxidases (NOXs) are another important source of ROS in renal cells. NOX-derived ROS are involved in vascular oxidative stress and endothelial dysfunction in obesity. NOX4 is the most abundant NOX isoform in the kidney and predominantly generates H_2O_2 that also plays physiological roles in renal cells [127,128]. Recently, Muñoz et al. demonstrated reduced endothelial NOX4 expression associated with decreased H_2O_2 generation and H_2O_2-mediated vasodilatation in obese rats [129]. NOX4 is upregulated in both diabetic nephropathy and obesity-related CKD [130,131]. The downstream consequences of NOX4 activation in the kidney lead to increased inflammation and fibrosis that is mostly dependent on AMPK signaling. Indeed, AMPK activation reduced NOX4 and ROS production and subsequently inhibiting NFκB and TGF-β-mediated fibrosis. He et al. demonstrated that in renal fibroblast cells and *db/db* mice, high glucose-induced ROS generation is mainly derived from NOX4 and not NOX1 and NOX2. NOX4 activation led to the proliferation and activation of resident fibroblasts and, ultimately, renal fibrosis. Resveratrol treatment in *db/db* mice prevented NOX4 expression primarily due to increased AMPK activity [132]. Similarly, numerous recent studies highlighted the beneficial effects of antioxidants or other compounds against renal injuries implicating AMPK/NOX4/ROS [133–139]. Furthermore, two independent studies reported that Sestrin-2 mediated activation of AMPK inhibits ROS production, podocyte impairment in the hyperglycemic condition, and suppresses NOX4 in glomerular mesangial cells [140,141]. p53 and proapoptotic protein PUMA (p53-up-regulated modulator of apoptosis) in diabetic podocytes and glomeruli are promoted by AMPK/NOX4 dysregulation and reversed by AICAR treatment [32].

Therefore, many studies have demonstrated AMPK dependent NOX4 downregulation in the diabetic kidney, suggesting a protective role of NOX4 in diabetic nephropathy.

8. AMPK and the Regulation of Renal Autophagy and Mitophagy

Autophagy is a complex and highly regulated process of self-degradation of cellular components. In the kidney, basal autophagy flux is essential to maintain cellular homeostasis and renal function. Kidney-specific autophagy-deficient mice revealed evidence of damaged mitochondria, protein aggregates, endoplasmic reticulum stress, podocyte, and proximal tubular cell loss, and progressive impairment of renal function [142]. The role of AMPK in the regulation of the autophagy flux has been extensively investigated in liver, muscle, brain, or adipocytes, whereas only a few studies explore the role of AMPK in renal autophagy [143–146]. AMPK positively regulates the autophagy process through phosphorylation of essential target proteins, mainly through the mechanistic target of rapamycin (mTOR) and ULK-1 [147]. Upon activation, AMPK inhibits mTOR and activates ULK-1, which, in turn, activates autophagy [148]. The inhibition of mTOR by AMPK is either by direct phosphorylation or through phosphorylation of the tuberous sclerosis complex 2 (TSC2) protein that then reduces mTOR activity [149]. Interestingly, the high basal level of autophagy observed in podocytes is mainly regulated by the AMPK/ULK-1 axis rather than the mTOR pathway, suggesting that the activation of autophagy by AMPK might be cell-type dependent in kidneys [150]. Moreover, AMPK phosphorylates Raptor leading to a decrease in mTORC1 activity [151]. Finally, AMPK activity leads to an increased intracellular pool of NAD^+ that allows an increase of SIRT1 activity. SIRT1 targets FOXO1 and FOXO3 in the nucleus and autophagy-related genes *Atg5*, *Atg7*, and *Atg8*, which positively regulate autophagy [152].

Obesity or diabetes can lead to impairment of autophagy flux in renal cells [153,154]. HFD/obesity-induced autophagy impairment has been described in rodent models and obese patients [27,155]. Yamamoto et al. described the stagnation of the autophagy flux as a novel mechanism of renal lipotoxicity in a model of mice fed an HFD. They demonstrated that long term lipid overload was associated with impairments of the lysosomal system and to a consequent accumulation of phospholipids, probably of mitochondrial origin. This lipotoxicity was associated with a sustained mTOR activation, but the association with AMPK was not explored. Excessive fat also induces constitutive activation of mTORC1 that directly inhibits AMPK activity, suggesting a link between mTOR and AMPK [156,157]. However, AMPK-mediated activation of autophagy protects against renal injury, particularly in AKI [158]. Regarding metabolic disease-related CKD, Yamahara et al. demonstrated that obesity significantly suppressed autophagy in PTC of both mice and humans. Notably, they found that AMPK was implicated in FFA-albumin–induced autophagy in PTCs. In PTCs, AMPK downregulation was associated with decreased autophagy induction by albumin-binding FFA, suggesting that AMPK may be essential for maintaining proper autophagy flux. In obesity, AMPK activity remains unaltered by FFA-albumin overload, but its activity failed to decrease the hyperactivation of the mTORC1 signal, which leads to the obesity-mediated exacerbation of proteinuria-induced tubulointerstitial damage. Delayed activation of AMPK with fenofibrate and AICAR was associated with subsequent autophagy activation in the kidney of mice on HFD [24,159]. Antioxidant drugs such as Berberine or Mangiferin improve autophagy flux in diabetic nephropathy through the activation of AMPK [160–162].

There is no direct evidence of the role of AMPK in mitophagy pathways. However, activated ULK-1 translocates to damaged mitochondria and phosphorylates FUN14 domain containing 1 (FUNDC1) protein, which is considered a critical player of mitophagy, allowing the formation of an autophagosome around damaged mitochondria [163]. Therefore, AMPK-induced ULK-1 activation may be a crucial mediator of mitophagy [164]. In the study of Yamamoto et al., the induction of the mitophagy pathway protects PTC from mitochondrial dysfunction. Activation of AMPK with AICAR or Metformin led to an increase of autophagy flux and removal of damaged mitochondria in streptozotocin-induced diabetic nephropathy [121]. Finally, AMPK is implicated in lipophagy, the autophagic degradation of

lipid droplets (LDs). Lipophagy and lipolysis of LDs for intracellular lipid mobilization are preceded by the targeted autophagy of Perilipin2 (PLIN2). This process is controlled by AMPK-dependent phosphorylation of PLIN2, suggesting a new pathway to regulate lipid metabolism by AMPK through the regulation of lipophagy [165]. The precise role of AMPK in the regulation of autophagy, mitophagy, or lipophagy in renal cells needs further investigation. However, AMPK dysregulation inhibits autophagy and participates in the pathogenesis of obesity and diabetic CKD. AMPK activation may be a valuable way of restoring the autophagy process in metabolic disease-induced CKD.

9. AMPK and Sirtuins

The sirtuins are members of the Class III deacetylases. So far, seven forms of sirtuins have been identified (SIRT1-7) [166]. Specifically, SIRT 1 and SIRT3 are induced by caloric restriction and associated with AMPK [167]. The AMPK/SIRT1/PGC1-α pathway acts as a crucial network to maintain mitochondrial homeostasis (already discussed in this review) [168,169]. However, recent studies highlight an AMPK/SIRT3 axis in disease. Deacetylation accounts for a crucial mechanism to regulate the activity of many substrates involved in energy metabolism [170]. SIRT3 is an NAD^+-dependent deacetylase, mainly localized in mitochondria. SIRT3 plays a significant role in mitochondrial homeostasis by regulating the mitochondrial respiratory chain and ATP production. SIRT3 promotes FA oxidation through the deacetylation of long chain acyl-CoA dehydrogenase (LCAD) [171] and also exerts an antioxidant activity by targeting the superoxide dismutase 2 (SOD2) and the isocitrate dehydrogenase (IDH2) [166,172]. More interestingly, the cytosolic form of SIRT3 activates LKB1, which in turn activates AMPK in primary cardiomyocytes [173]. Therefore, reduction in SIRT3 expression in a setting of obesity could, in part, explain the reduction in AMPK activity. Another evidence of the role of SIRT3 in AMPK activation is its involvement in the increase of cytosolic calcium level that, in turn, activates CaMKKβ and promotes AMPK activity. It is thus worth hypothesizing that the AMPK/SIRT3 axis plays a vital role in renal lipotoxicity.

Rodents and humans demonstrate the critical role of SIRT3 in metabolic diseases, highlighting the decrease in SIRT3 activity in several tissues such as the liver, the adipose tissue and the muscle [174,175]. Mice deficient for SIRT3 on an HFD also reveal accelerated hallmarks of MetS [176]. SIRT3 restoration is also beneficial in models of acute kidney injury (AKI) [177–179]. Indeed, maintaining SIRT3 activity was shown to prevent acute damage in renal tubular cells by maintaining the mitochondrial functional integrity and dynamics by normalizing mitochondrial protein acetylation [177,179]. Morigi et al. reported that in mice with cisplatin-induced AKI, tubular cell mitochondrial abnormalities were associated with decreased renal SIRT3 mRNA and protein expression, whereas treatment with AICAR, an activator of AMPK, improved renal function through the restoration of SIRT3 expression and activity. Mitochondrial protein acetylation normalized concomitantly with the upregulation of proximal tubular SIRT3 expression after AICAR treatment providing evidence of the role of AMPK activity in restoring SIRT3 deacetylase activity. These recent data shed light on the AMPK/SIRT3 pathway to maintain cellular homeostasis by improving mitochondrial functional integrity.

10. Conclusions and Future Directions

The downregulation of AMPK activity in obesity- and diabetes-induced CKD has been extensively reported in patients and in vivo and in vitro experimental models. Inhibition of AMPK activity in the kidney results from systemic metabolic dysregulation, signaling factors mediated by other dysfunctional tissues and organs (organ crosstalk), and intrarenal disturbances. Delineating the pleiotropic pathways regulated by AMPK and the potential impact of their dysregulation on renal cell function and metabolism remains a challenge. A better understanding of the AMPK pathway and the consequences of its dysregulation in metabolism-induced kidney diseases is thus essential to improve therapeutic strategies. Here, we present a more comprehensive and exhaustive review of the experimental and clinical evidence supporting the central role of AMPK in the development and progression of diabetes- and obesity-induced CKD. In particular, we summarized relevant data

regarding the altered renal AMPK-mediated molecular mechanisms and critical targets in the context of excessive energy supply. In the kidney, AMPK is essential to maintain ATP levels to meet the high metabolic demands in renal cells to regulate renal transport. Moreover, there is a large body of evidence demonstrating that activating AMPK leads to the prevention of renal lipotoxicity and lipid accumulation by reducing FA synthase. In podocytes, glucose metabolism and associated insulin resistance are both linked with AMPK regulation. Beyond its role in glucose and lipid metabolism and as an energy sensor in the kidney, AMPK alleviates mitochondrial damage by at least four mechanisms (Figure 5): (1) AMPK is strongly implicated in the regulation and the response to ROS production by altered mitochondria, thus preventing damage induced by mtROS; (2) activation of AMPK favors mitochondrial biogenesis to enhance metabolism by inducing AMPK/SIRT1/PGC1-α pathway; (3) AMPK regulates mitochondrial dynamics and quality control, including mitochondrial fission/fusion; and (4) AMPK activity initiates autophagy flux and selectively degrades unhealthy mitochondria. Therefore, inhibition of renal AMPK is associated with poor outcomes and leads to lipotoxicity, insulin resistance, inflammation, fibrosis, and loss of renal function. Therefore, activating AMPK in metabolic disease and the associated renal injury represents a potentially critical therapeutic target [180].

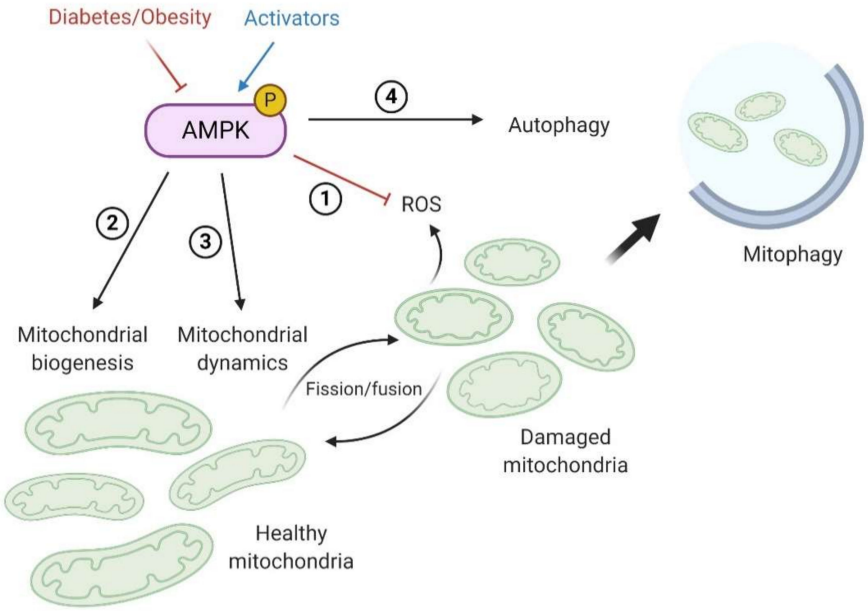

Figure 5. Mechanisms by which AMPK regulates mitochondrial homeostasis in the renal cell. Activation of AMPK in the context of obesity and diabetes leads to improved mitochondrial dysfunction and cellular metabolism by (1) decreasing oxidative stress (ROS) by inducing antioxidative mechanisms; (2) favoring mitochondrial biogenesis to increase mitochondrial density; (3) participating in the dynamic regulation of mitochondrial fission and fusion to facilitate their degradation by mitophagy; and (4) ultimately regulating mitochondrial quality control by the initiation of autophagy and mitophagy.

Dynamic research has extended classical knowledge regarding AMPK beyond energy-sensing towards novel AMPK- related pathways and mechanisms in different models and pathologies. While in vitro studies of renal cells in the context of excess energy supply help investigate cellular and molecular mechanisms, they offer a reductive view of the complex regulation of in vivo AMPK that relies on several factors. However, in animal models of metabolic syndrome, diabetes, and obesity, AMPK activators demonstrate several unintended off-target effects. It is impossible to delineate the exclusive effects of these drugs on the kidney or specific renal cells. Therefore, more studies in models with tissue or cell type-specific genetic deletion or overexpression of AMPK in the context of metabolism-related kidney disease are required to delineate the pleiotropic roles of AMPK presented in this review.

Author Contributions: F.J., N.C., A.V.M. and A.-E.D. researched the data for the article and made substantial contributions to discussions of the content.; F.J. wrote the manuscript; N.C., A.V.M. and A.-E.D. reviewed and edited the manuscript before submission. All authors have read and agreed to the published version of the manuscript.

Funding: This work was funded by grants from the UMONS Research Institute for Health Sciences and Technology (Belgium), the French Diabetes Society and the Fonds de la Recherche Scientifique—FNRS grant number 35265394.

Acknowledgments: The original scientific figures of the review were created in BioRender.com.

Conflicts of Interest: The authors declare no conflict of interest.

References

1. Wang, V.; Vilme, H.; Maciejewski, M.L.; Boulware, L.E. The Economic Burden of Chronic Kidney Disease and End-Stage Renal Disease. *Semin. Nephrol.* **2016**, *36*, 319–330. [CrossRef] [PubMed]
2. Hill, N.R.; Fatoba, S.T.; Oke, J.L.; Hirst, J.A.; O'Callaghan, C.A.; Lasserson, D.S.; Hobbs, F.D.R. Global Prevalence of Chronic Kidney Disease—A Systematic Review and Meta-Analysis. *PLoS ONE* **2016**, *11*, e0158765. [CrossRef] [PubMed]
3. Cornier, M.-A.; Dabelea, D.; Hernandez, T.L.; Lindstrom, R.C.; Steig, A.J.; Stob, N.R.; Van Pelt, R.E.; Wang, H.; Eckel, R.H. The metabolic syndrome. *Endocr. Rev.* **2008**, *29*, 777–822. [CrossRef] [PubMed]
4. Nashar, K.; Egan, B.M. Relationship between chronic kidney disease and metabolic syndrome: Current perspectives. *Diabetes Metab. Syndr. Obes.* **2014**, *7*, 421–435. [CrossRef]
5. Raikou, V.D.; Gavriil, S. Metabolic Syndrome and Chronic Renal Disease. *Diseases* **2018**, *6*, 12. [CrossRef]
6. Thomas, G.; Sehgal, A.R.; Kashyap, S.R.; Srinivas, T.R.; Kirwan, J.P.; Navaneethan, S.D. Metabolic syndrome and kidney disease: A systematic review and meta-analysis. *Clin. J. Am. Soc. Nephrol.* **2011**, *6*, 2364–2373. [CrossRef]
7. Garofalo, C.; Borrelli, S.; Minutolo, R.; Chiodini, P.; De Nicola, L.; Conte, G. A systematic review and meta-analysis suggests obesity predicts onset of chronic kidney disease in the general population. *Kidney Int.* **2017**, *91*, 1224–1235. [CrossRef]
8. Whaley-Connell, A.; Sowers, J.R. Obesity and kidney disease: From population to basic science and the search for new therapeutic targets. *Kidney Int.* **2017**, *92*, 313–323. [CrossRef]
9. Ejerblad, E. Obesity and Risk for Chronic Renal Failure. *J. Am. Soc. Nephrol.* **2006**, *17*, 1695–1702. [CrossRef]
10. Bhupathiraju, S.N.; Hu, F.B. Epidemiology of Obesity and Diabetes and Their Cardiovascular Complications. *Circ. Res.* **2016**, *118*, 1723–1735. [CrossRef]
11. Maric-Bilkan, C. Obesity and diabetic kidney disease. *Med. Clin. N. Am.* **2013**, *97*, 59–74. [CrossRef] [PubMed]
12. Mathew, A.V.; Okada, S.; Sharma, K. Obesity related kidney disease. *Curr. Diabetes Rev.* **2011**, *7*, 41–49. [CrossRef]
13. Goumenos, D.S.; Kawar, B.; El Nahas, M.; Conti, S.; Wagner, B.; Spyropoulos, C.; Vlachojannis, J.G.; Benigni, A.; Kalfarentzos, F. Early histological changes in the kidney of people with morbid obesity. *Nephrol. Dial. Transplant.* **2009**, *24*, 3732–3738. [CrossRef] [PubMed]
14. Jung, U.J.; Choi, M.-S. Obesity and its metabolic complications: The role of adipokines and the relationship between obesity, inflammation, insulin resistance, dyslipidemia and nonalcoholic fatty liver disease. *Int. J. Mol. Sci.* **2014**, *15*, 6184–6223. [CrossRef] [PubMed]
15. Declèves, A.-E.; Sharma, K. Obesity and kidney disease: Differential effects of obesity on adipose tissue and kidney inflammation and fibrosis. *Curr. Opin. Nephrol. Hypertens.* **2015**, *24*, 28–36. [CrossRef]
16. DeMarco, V.G.; Aroor, A.R.; Sowers, J.R. The pathophysiology of hypertension in patients with obesity. *Nat. Rev. Endocrinol.* **2014**, *10*, 364–376. [CrossRef]
17. Jorge, R.-F.; Rodrigo, D.-A.; Maria Ximena, C.-B.; Victor, L.-M.; Emilio, A.-F.; Nehomar, P.-G.; Jose, C.; José, C.; Manuel, C.; Amable, D.; et al. SGLT2 Inhibitors and nephroprotection in diabetic kidney disease: From mechanisms of action to the latest evidence in the literature. *J. Clin. Nephrol.* **2020**, *4*, 044–055. [CrossRef]
18. Hall, J.E.; do Carmo, J.M.; da Silva, A.A.; Wang, Z.; Hall, M.E. Obesity-induced hypertension: Interaction of neurohumoral and renal mechanisms. *Circ. Res.* **2015**, *116*, 991–1006. [CrossRef]

19. D'Agati, V.D.; Chagnac, A.; de Vries, A.P.J.; Levi, M.; Porrini, E.; Herman-Edelstein, M.; Praga, M. Obesity-related glomerulopathy: Clinical and pathologic characteristics and pathogenesis. *Nat. Rev. Nephrol.* **2016**, *12*, 453–471. [CrossRef]
20. Kaysen, G.A. Dyslipidemia in chronic kidney disease: Causes and consequences. *Kidney Int.* **2006**, *70*, S55–S58. [CrossRef]
21. Sharma, S.G.; Bomback, A.S.; Radhakrishnan, J.; Herlitz, L.C.; Stokes, M.B.; Markowitz, G.S.; D'Agati, V.D. The modern spectrum of renal biopsy findings in patients with diabetes. *Clin. J. Am. Soc. Nephrol.* **2013**, *8*, 1718–1724. [CrossRef] [PubMed]
22. Chen, X.; Han, Y.; Gao, P.; Yang, M.; Xiao, L.; Xiong, X.; Zhao, H.; Tang, C.; Chen, G.; Zhu, X.; et al. Disulfide-bond A oxidoreductase-like protein protects against ectopic fat deposition and lipid-related kidney damage in diabetic nephropathy. *Kidney Int.* **2019**, *95*, 880–895. [CrossRef] [PubMed]
23. Herman-Edelstein, M.; Scherzer, P.; Tobar, A.; Levi, M.; Gafter, U. Altered renal lipid metabolism and renal lipid accumulation in human diabetic nephropathy. *J. Lipid Res.* **2014**, *55*, 561–572. [CrossRef]
24. Declèves, A.-E.; Zolkipli, Z.; Satriano, J.; Wang, L.; Nakayama, T.; Rogac, M.; Le, T.P.; Nortier, J.L.; Farquhar, M.G.; Naviaux, R.K.; et al. Regulation of lipid accumulation by AMK-activated kinase in high fat diet–induced kidney injury. *Kidney Int.* **2014**, *85*, 611–623. [CrossRef] [PubMed]
25. De Vries, A.P.J.; Ruggenenti, P.; Ruan, X.Z.; Praga, M.; Cruzado, J.M.; Bajema, I.M.; D'Agati, V.D.; Lamb, H.J.; Barlovic, D.P.; Hojs, R.; et al. Fatty kidney: Emerging role of ectopic lipid in obesity-related renal disease. *Lancet Diabetes Endocrinol.* **2014**, *2*, 417–426. [CrossRef]
26. Zhao, J.; Rui, H.-L.; Yang, M.; Sun, L.-J.; Dong, H.-R.; Cheng, H. CD36-Mediated Lipid Accumulation and Activation of NLRP3 Inflammasome Lead to Podocyte Injury in Obesity-Related Glomerulopathy. *Mediat. Inflamm.* **2019**, *2019*, 3172647.
27. Yamamoto, T.; Takabatake, Y.; Takahashi, A.; Kimura, T. High-Fat Diet-Induced Lysosomal Dysfunction and Impaired Autophagic Flux Contribute to Lipotoxicity in the Kidney. *J. Am. Soc. Nephrol.* **2017**, *28*, 1534–1551. [CrossRef]
28. Li, L.; Wang, C.; Yang, H.; Liu, S.; Lu, Y.; Fu, P.; Liu, J. Metabolomics reveal mitochondrial and fatty acid metabolism disorders that contribute to the development of DKD in T2DM patients. *Mol. Biosyst.* **2017**, *13*, 2392–2400. [CrossRef]
29. Dugan, L.L.; You, Y.-H.; Ali, S.S.; Diamond-Stanic, M.; Miyamoto, S.; DeCleves, A.-E.; Andreyev, A.; Quach, T.; Ly, S.; Shekhtman, G.; et al. AMPK dysregulation promotes diabetes-related reduction of superoxide and mitochondrial function. *J. Clin. Investig.* **2013**, *123*, 4888–4899. [CrossRef]
30. Choi, S.R.; Lim, J.H.; Kim, M.Y.; Kim, E.N.; Kim, Y.; Choi, B.S.; Kim, Y.-S.; Kim, H.W.; Lim, K.-M.; Kim, M.J.; et al. Adiponectin receptor agonist AdipoRon decreased ceramide, and lipotoxicity, and ameliorated diabetic nephropathy. *Metabolism* **2018**, *85*, 348–360. [CrossRef]
31. Lee, M.-J.; Feliers, D.; Mariappan, M.M.; Sataranatarajan, K.; Mahimainathan, L.; Musi, N.; Foretz, M.; Viollet, B.; Weinberg, J.M.; Choudhury, G.G.; et al. A role for AMP-activated protein kinase in diabetes-induced renal hypertrophy. *Am. J. Physiol. Ren. Physiol.* **2007**, *292*, F617–F627. [CrossRef]
32. Eid, A.A.; Ford, B.M.; Block, K.; Kasinath, B.S.; Gorin, Y.; Ghosh-Choudhury, G.; Barnes, J.L.; Abboud, H.E. AMP-activated protein kinase (AMPK) negatively regulates Nox4-dependent activation of p53 and epithelial cell apoptosis in diabetes. *J. Biol. Chem.* **2010**, *285*, 37503–37512. [CrossRef] [PubMed]
33. Han, S.H.; Malaga-Dieguez, L.; Chinga, F.; Kang, H.M.; Tao, J.; Reidy, K.; Susztak, K. Deletion of Lkb1 in Renal Tubular Epithelial Cells Leads to CKD by Altering Metabolism. *J. Am. Soc. Nephrol.* **2016**, *27*, 439–453. [CrossRef] [PubMed]
34. Hasanvand, A.; Amini-Khoei, H.; Jahanabadi, S.; Hadian, M.R.; Abdollahi, A.; Tavangar, S.M.; Mehr, S.E.; Dehpour, A.R. Metformin attenuates streptozotocin-induced diabetic nephropathy in rats through activation of AMPK signaling pathway. *J. Nephropathol.* **2018**, *7*, 37–42. [CrossRef]
35. Zhou, X.; Muise, E.S.; Haimbach, R.; Sebhat, I.K.; Zhu, Y.; Liu, F.; Souza, S.C.; Kan, Y.; Pinto, S.; Kelley, D.E.; et al. PAN-AMPK Activation Improves Renal Function in a Rat Model of Progressive Diabetic Nephropathy. *J. Pharmacol. Exp. Ther.* **2019**, *371*, 45–55. [CrossRef]
36. Habib, S.L.; Yadav, A.; Kidane, D.; Weiss, R.H.; Liang, S. Novel protective mechanism of reducing renal cell damage in diabetes: Activation AMPK by AICAR increased NRF2/OGG1 proteins and reduced oxidative DNA damage. *Cell Cycle* **2016**, *15*, 3048–3059. [CrossRef]

37. Liang, J.; Xu, Z.-X.; Ding, Z.; Lu, Y.; Yu, Q.; Werle, K.D.; Zhou, G.; Park, Y.-Y.; Peng, G.; Gambello, M.J.; et al. Myristoylation confers noncanonical AMPK functions in autophagy selectivity and mitochondrial surveillance. *Nat. Commun.* **2015**, *6*, 7926. [CrossRef]
38. Herzig, S.; Shaw, R.J. AMPK: Guardian of metabolism and mitochondrial homeostasis. *Nat. Rev. Mol. Cell Biol.* **2018**, *19*, 121. [CrossRef]
39. Seo-Mayer, P.W.; Thulin, G.; Zhang, L.; Alves, D.S.; Ardito, T.; Kashgarian, M.; Caplan, M.J. Preactivation of AMPK by metformin may ameliorate the epithelial cell damage caused by renal ischemia. *Am. J. Physiol. Ren. Physiol.* **2011**, *301*, F1346–F1357. [CrossRef]
40. Salatto, C.T.; Miller, R.A.; Cameron, K.O.; Cokorinos, E.; Reyes, A.; Ward, J.; Calabrese, M.F.; Kurumbail, R.G.; Rajamohan, F.; Kalgutkar, A.S.; et al. Selective Activation of AMPK beta1-Containing Isoforms Improves Kidney Function in a Rat Model of Diabetic Nephropathy. *J. Pharmacol. Exp. Ther.* **2017**, *361*, 303–311. [CrossRef]
41. Hallows, K.R.; Mount, P.F.; Pastor-Soler, N.M.; Power, D.A. Role of the energy sensor AMP-activated protein kinase in renal physiology and disease. *Am. J. Physiol. Ren. Physiol.* **2010**, *298*, F1067–F1077. [CrossRef] [PubMed]
42. Neumann, D. Is TAK1 a Direct Upstream Kinase of AMPK? *Int. J. Mol. Sci.* **2018**, *19*, 2412. [CrossRef]
43. Pulinilkunnil, T.; He, H.; Kong, D.; Asakura, K.; Peroni, O.D.; Lee, A.; Kahn, B.B. Adrenergic regulation of AMP-activated protein kinase in brown adipose tissue in vivo. *J. Biol. Chem.* **2011**, *286*, 8798–8809. [CrossRef] [PubMed]
44. Hurley, R.L.; Barré, L.K.; Wood, S.D.; Anderson, K.A.; Kemp, B.E.; Means, A.R.; Witters, L.A. Regulation of AMP-activated protein kinase by multisite phosphorylation in response to agents that elevate cellular cAMP. *J. Biol. Chem.* **2006**, *281*, 36662–36672. [CrossRef] [PubMed]
45. Coughlan, K.A.; Valentine, R.J.; Sudit, B.S.; Allen, K.; Dagon, Y.; Kahn, B.B.; Ruderman, N.B.; Saha, A.K. PKD1 Inhibits AMPKα2 through Phosphorylation of Serine 491 and Impairs Insulin Signaling in Skeletal Muscle Cells. *J. Biol. Chem.* **2016**, *291*, 5664–5675. [CrossRef]
46. Lazo-Fernandez, Y.; Baile, G.; Meade, P.; Torcal, P.; Martinez, L.; Ibanez, C.; Bernal, M.L.; Viollet, B.; Gimenez, I. Kidney-specific genetic deletion of both AMPK alpha-subunits causes salt and water wasting. *Am. J. Physiol. Ren. Physiol.* **2017**, *312*, F352–F365. [CrossRef]
47. Kohlstedt, K.; Trouvain, C.; Boettger, T.; Shi, L.; Fisslthaler, B.; Fleming, I. AMP-activated protein kinase regulates endothelial cell angiotensin-converting enzyme expression via p53 and the post-transcriptional regulation of microRNA-143/145. *Circ. Res.* **2013**, *112*, 1150–1158. [CrossRef] [PubMed]
48. Tain, Y.-L.; Hsu, C.-N. AMP-Activated Protein Kinase as a Reprogramming Strategy for Hypertension and Kidney Disease of Developmental Origin. *Int. J. Mol. Sci.* **2018**, *19*, 1744. [CrossRef]
49. Yang, X.; Mudgett, J.; Bou-About, G.; Champy, M.-F.; Jacobs, H.; Monassier, L.; Pavlovic, G.; Sorg, T.; Herault, Y.; Petit-Demouliere, B.; et al. Physiological Expression of AMPKgamma2RG Mutation Causes Wolff-Parkinson-White Syndrome and Induces Kidney Injury in Mice. *J. Biol. Chem.* **2016**, *291*, 23428–23439. [CrossRef]
50. Viollet, B.; Horman, S.; Leclerc, J.; Lantier, L.; Foretz, M.; Billaud, M.; Giri, S.; Andreelli, F. AMPK inhibition in health and disease. *Crit. Rev. Biochem. Mol. Biol.* **2010**, *45*, 276–295. [CrossRef]
51. Okabe, K.; Yaku, K.; Tobe, K.; Nakagawa, T. Implications of altered NAD metabolism in metabolic disorders. *J. Biomed. Sci.* **2019**, *26*, 34. [CrossRef]
52. Lan, F.; Cacicedo, J.M.; Ruderman, N.; Ido, Y. SIRT1 modulation of the acetylation status, cytosolic localization, and activity of LKB1. Possible role in AMP-activated protein kinase activation. *J. Biol. Chem.* **2008**, *283*, 27628–27635. [CrossRef] [PubMed]
53. Suchankova, G.; Nelson, L.E.; Gerhart-Hines, Z.; Kelly, M.; Gauthier, M.-S.; Saha, A.K.; Ido, Y.; Puigserver, P.; Ruderman, N.B. Concurrent regulation of AMP-activated protein kinase and SIRT1 in mammalian cells. *Biochem. Biophys. Res. Commun.* **2009**, *378*, 836–841. [CrossRef]
54. Price, N.L.; Gomes, A.P.; Ling, A.J.Y.; Duarte, F.V.; Martin-Montalvo, A.; North, B.J.; Agarwal, B.; Ye, L.; Ramadori, G.; Teodoro, J.S.; et al. SIRT1 is required for AMPK activation and the beneficial effects of resveratrol on mitochondrial function. *Cell Metab.* **2012**, *15*, 675–690. [CrossRef] [PubMed]
55. Kikuchi, H.; Sasaki, E.; Nomura, N.; Mori, T.; Minamishima, Y.A.; Yoshizaki, Y.; Takahashi, N.; Furusho, T.; Arai, Y.; Mandai, S.; et al. Failure to sense energy depletion may be a novel therapeutic target in chronic kidney disease. *Kidney Int.* **2019**, *95*, 123–137. [CrossRef]

56. Dagon, Y.; Hur, E.; Zheng, B.; Wellenstein, K.; Cantley, L.C.; Kahn, B.B. p70S6 kinase phosphorylates AMPK on serine 491 to mediate leptin's effect on food intake. *Cell Metab.* **2012**, *16*, 104–112. [CrossRef]
57. Valentine, R.J.; Coughlan, K.A.; Ruderman, N.B.; Saha, A.K. Insulin inhibits AMPK activity and phosphorylates AMPK $Ser^{485}/^{491}$ through Akt in hepatocytes, myotubes and incubated rat skeletal muscle. *Arch. Biochem. Biophys.* **2014**, *562*, 62–69. [CrossRef]
58. Niu, M.; Xiang, L.; Liu, Y.; Zhao, Y.; Yuan, J.; Dai, X.; Chen, H. Adiponectin induced AMP-activated protein kinase impairment mediates insulin resistance in Bama mini-pig fed high-fat and high-sucrose diet. *Asian-Australas. J. Anim. Sci.* **2017**, *30*, 1190–1197. [CrossRef] [PubMed]
59. Bonnard, C.; Durand, A.; Vidal, H.; Rieusset, J. Changes in adiponectin, its receptors and AMPK activity in tissues of diet-induced diabetic mice. *Diabetes Metab.* **2008**, *34*, 52–61. [CrossRef] [PubMed]
60. Yi, W.; Sun, Y.; Gao, E.; Wei, X.; Lau, W.B.; Zheng, Q.; Wang, Y.; Yuan, Y.; Wang, X.; Tao, L.; et al. Reduced cardioprotective action of adiponectin in high-fat diet-induced type II diabetic mice and its underlying mechanisms. *Antioxid. Redox Signal.* **2011**, *15*, 1779–1788. [CrossRef]
61. Lyons, C.L.; Roche, H.M. Nutritional Modulation of AMPK-Impact upon Metabolic-Inflammation. *Int. J. Mol. Sci.* **2018**, *19*, 3092. [CrossRef]
62. Steinberg, G.R.; Michell, B.J.; van Denderen, B.J.W.; Watt, M.J.; Carey, A.L.; Fam, B.C.; Andrikopoulos, S.; Proietto, J.; Görgün, C.Z.; Carling, D.; et al. Tumor necrosis factor alpha-induced skeletal muscle insulin resistance involves suppression of AMP-kinase signaling. *Cell Metab.* **2006**, *4*, 465–474. [CrossRef] [PubMed]
63. Rajani, R.; Pastor-soler, N.M.; Hallows, K.R. Role of AMP-activated protein kinase in kidney tubular transport, metabolism, and disease. *Curr. Opin. Nephrol. Hypertens.* **2017**, *26*, 375–383. [CrossRef]
64. Glosse, P.; Föller, M. AMP-Activated Protein Kinase (AMPK)-Dependent Regulation of Renal Transport. *Int. J. Mol. Sci.* **2018**, *19*, 3481. [CrossRef] [PubMed]
65. Spires, D.; Manis, A.D.; Staruschenko, A. Ion channels and transporters in diabetic kidney disease. *Curr. Top. Membr.* **2019**, *83*, 353–396. [PubMed]
66. Liamis, G.; Liberopoulos, E.; Barkas, F.; Elisaf, M. Diabetes mellitus and electrolyte disorders. *World J. Clin. Cases* **2014**, *2*, 488–496. [CrossRef]
67. Benziane, B.; Björnholm, M.; Pirkmajer, S.; Austin, R.L.; Kotova, O.; Viollet, B.; Zierath, J.R.; Chibalin, A.V. Activation of AMP-activated protein kinase stimulates Na^+,K^+-ATPase activity in skeletal muscle cells. *J. Biol. Chem.* **2012**, *287*, 23451–23463. [CrossRef]
68. Xiao, J.; Zhu, S.; Guan, H.; Zheng, Y.; Li, F.; Zhang, X.; Guo, H.; Wang, X.; Ye, Z. AMPK alleviates high uric acid-induced Na^+-K^+-ATPase signaling impairment and cell injury in renal tubules. *Exp. Mol. Med.* **2019**, *51*, 1–14. [CrossRef]
69. Bhalla, V.; Oyster, N.M.; Fitch, A.C.; Wijngaarden, M.A.; Neumann, D.; Schlattner, U.; Pearce, D.; Hallows, K.R. AMP-activated kinase inhibits the epithelial Na+ channel through functional regulation of the ubiquitin ligase Nedd4-2. *J. Biol. Chem.* **2006**, *281*, 26159–26169. [CrossRef]
70. Carattino, M.D.; Edinger, R.S.; Grieser, H.J.; Wise, R.; Neumann, D.; Schlattner, U.; Johnson, J.P.; Kleyman, T.R.; Hallows, K.R. Epithelial sodium channel inhibition by AMP-activated protein kinase in oocytes and polarized renal epithelial cells. *J. Biol. Chem.* **2005**, *280*, 17608–17616. [CrossRef]
71. Fraser, S.A.; Gimenez, I.; Cook, N.; Jennings, I.; Katerelos, M.; Katsis, F.; Levidiotis, V.; Kemp, B.E.; Power, D.A. Regulation of the renal-specific Na^+-K^+-$2Cl^-$ co-transporter NKCC2 by AMP-activated protein kinase (AMPK). *Biochem. J.* **2007**, *405*, 85–93. [CrossRef] [PubMed]
72. Fraser, S.A.; Choy, S.-W.; Pastor-Soler, N.M.; Li, H.; Davies, M.R.P.; Cook, N.; Katerelos, M.; Mount, P.F.; Gleich, K.; McRae, J.L.; et al. AMPK couples plasma renin to cellular metabolism by phosphorylation of ACC1. *Am. J. Physiol. Ren. Physiol.* **2013**, *305*, F679–F690. [CrossRef]
73. Dërmaku-Sopjani, M.; Almilaji, A.; Pakladok, T.; Munoz, C.; Hosseinzadeh, Z.; Blecua, M.; Sopjani, M.; Lang, F. Down-regulation of the Na^+-coupled phosphate transporter NaPi-IIa by AMP-activated protein kinase. *Kidney Blood Press. Res.* **2013**, *37*, 547–556. [CrossRef] [PubMed]
74. King, J.D.J.; Fitch, A.C.; Lee, J.K.; McCane, J.E.; Mak, D.-O.D.; Foskett, J.K.; Hallows, K.R. AMP-activated protein kinase phosphorylation of the R domain inhibits PKA stimulation of CFTR. *Am. J. Physiol. Cell Physiol.* **2009**, *297*, C94–C101. [CrossRef] [PubMed]
75. Deji, N.; Kume, S.; Araki, S.; Soumura, M.; Sugimoto, T.; Isshiki, K.; Chin-Kanasaki, M.; Sakaguchi, M.; Koya, D.; Haneda, M.; et al. Structural and functional changes in the kidneys of high-fat diet-induced obese mice. *Am. J. Physiol. Ren. Physiol.* **2009**, *296*, 118–126. [CrossRef]

76. Kume, S.; Uzu, T.; Araki, S.-I.; Sugimoto, T.; Isshiki, K.; Chin-Kanasaki, M.; Sakaguchi, M.; Kubota, N.; Terauchi, Y.; Kadowaki, T.; et al. Role of Altered Renal Lipid Metabolism in the Development of Renal Injury Induced by a High-Fat Diet. *J. Am. Soc. Nephrol.* **2007**, *18*, 2715–2723. [CrossRef]
77. Proctor, G.; Jiang, T.; Iwahashi, M.; Wang, Z.; Li, J.; Levi, M. Regulation of renal fatty acid and cholesterol metabolism, inflammation, and fibrosis in Akita and OVE26 mice with type 1 diabetes. *Diabetes* **2006**, *55*, 2502–2509. [CrossRef]
78. Sun, L.; Halaihel, N.; Zhang, W.; Rogers, H.; Levi, M. Role of sterol regulatory element-binding protein 1 in regulation of renal lipid metabolism and glomerulosclerosis in diabetes mellitus. *J. Biol. Chem.* **2002**, *277*, 18919–18927. [CrossRef]
79. Jiang, T.; Liebman, S.E.; Lucia, M.S.; Li, J.; Levi, M. Role of altered renal lipid metabolism and the sterol regulatory element binding proteins in the pathogenesis of age-related renal disease. *Kidney Int.* **2005**, *68*, 2608–2620. [CrossRef]
80. Jiang, T.; Wang, Z.; Proctor, G.; Moskowitz, S.; Liebman, S.E.; Rogers, T.; Lucia, M.S.; Li, J.; Levi, M. Diet-induced Obesity in C57BL/6J Mice Causes Increased Renal Lipid Accumulation and Glomerulosclerosis via a Sterol Regulatory Element-binding Protein-1c-dependent Pathway. *J. Biol. Chem.* **2005**, *280*, 32317–32325. [CrossRef]
81. Han, Y.; Hu, Z.; Cui, A.; Liu, Z.; Ma, F.; Xue, Y.; Liu, Y.; Zhang, F.; Zhao, Z.; Yu, Y.; et al. Post-translational regulation of lipogenesis via AMPK-dependent phosphorylation of insulin-induced gene. *Nat. Commun.* **2019**, *10*, 623. [CrossRef]
82. Jung, E.-J.; Kwon, S.-W.; Jung, B.-H.; Oh, S.-H.; Lee, B.-H. Role of the AMPK/SREBP-1 pathway in the development of orotic acid-induced fatty liver. *J. Lipid Res.* **2011**, *52*, 1617–1625. [CrossRef] [PubMed]
83. Li, Y.; Xu, S.; Mihaylova, M.M.; Zheng, B.; Hou, X.; Jiang, B.; Park, O.; Luo, Z.; Lefai, E.; Shyy, J.Y.-J.; et al. AMPK phosphorylates and inhibits SREBP activity to attenuate hepatic steatosis and atherosclerosis in diet-induced insulin-resistant mice. *Cell Metab.* **2011**, *13*, 376–388. [CrossRef] [PubMed]
84. Dorotea, D.; Koya, D.; Ha, H. Recent Insights Into SREBP as a Direct Mediator of Kidney Fibrosis via Lipid-Independent Pathways. *Front. Pharmacol.* **2020**, *11*, 265. [CrossRef] [PubMed]
85. Kohjima, M.; Higuchi, N.; Kato, M.; Kotoh, K.; Yoshimoto, T.; Fujino, T.; Yada, M.; Yada, R.; Harada, N.; Enjoji, M.; et al. SREBP-1c, regulated by the insulin and AMPK signaling pathways, plays a role in nonalcoholic fatty liver disease. *Int. J. Mol. Med.* **2008**, *21*, 507–511. [CrossRef]
86. Lin, Y.-C.; Wu, M.-S.; Lin, Y.-F.; Chen, C.-R.; Chen, C.-Y.; Chen, C.-J.; Shen, C.-C.; Chen, K.-C.; Peng, C.-C. Nifedipine Modulates Renal Lipogenesis via the AMPK-SREBP Transcriptional Pathway. *Int. J. Mol. Sci.* **2019**, *20*, 1570. [CrossRef]
87. Jiang, S.; Wang, W.; Miner, J.; Fromm, M. Cross regulation of sirtuin 1, AMPK, and PPARγ in conjugated linoleic acid treated adipocytes. *PLoS ONE* **2012**, *7*, e48874. [CrossRef]
88. Lee, W.H.; Kim, S.G. AMPK-Dependent Metabolic Regulation by PPAR Agonists. *PPAR Res.* **2010**, *2010*, 549101. [CrossRef]
89. Sozio, M.S.; Lu, C.; Zeng, Y.; Liangpunsakul, S.; Crabb, D.W. Activated AMPK inhibits PPAR-{alpha} and PPAR-{gamma} transcriptional activity in hepatoma cells. *Am. J. Physiol. Gastrointest. Liver Physiol.* **2011**, *301*, G739–G747. [CrossRef]
90. Kang, H.M.; Ahn, S.H.; Choi, P.; Ko, Y.-A.; Han, S.H.; Chinga, F.; Seo, A.; Park, D.; Tao, J.; Sharma, K.; et al. Defective fatty acid oxidation in renal tubular epithelial cells plays a key role in kidney fibrosis development HHS Public Access. *Nat. Med.* **2015**, *21*, 37–46. [CrossRef]
91. Sas, K.M.; Nair, V.; Byun, J.; Kayampilly, P.; Zhang, H.; Saha, J.; Brosius, F.C., 3rd; Kretzler, M.; Pennathur, S. Targeted Lipidomic and Transcriptomic Analysis Identifies Dysregulated Renal Ceramide Metabolism in a Mouse Model of Diabetic Kidney Disease. *J. Proteom. Bioinform.* **2015**. [CrossRef]
92. Yang, X.; Okamura, D.M.; Lu, X.; Chen, Y.; Moorhead, J.; Varghese, Z.; Ruan, X.Z. CD36 in chronic kidney disease: Novel insights and therapeutic opportunities. *Nat. Rev. Nephrol.* **2017**, *13*, 769–781. [CrossRef] [PubMed]
93. Bandet, C.L.; Tan-Chen, S.; Bourron, O.; Le Stunff, H.; Hajduch, E. Sphingolipid Metabolism: New Insight into Ceramide-Induced Lipotoxicity in Muscle Cells. *Int. J. Mol. Sci.* **2019**, *20*, 479. [CrossRef] [PubMed]
94. Heathcote, H.R.; Mancini, S.J.; Strembitska, A.; Jamal, K.; Reihill, J.A.; Palmer, T.M.; Gould, G.W.; Salt, I.P. Protein kinase C phosphorylates AMP-activated protein kinase α1 Ser487. *Biochem. J.* **2016**, *473*, 4681–4697. [CrossRef]

95. Declèves, A.-E.; Mathew, A.V.; Armando, A.M.; Han, X.; Dennis, E.A.; Quehenberger, O.; Sharma, K. AMP-activated protein kinase activation ameliorates eicosanoid dysregulation in high-fat-induced kidney disease in mice. *J. Lipid Res.* **2019**, *60*, 937–952. [CrossRef] [PubMed]
96. Rogacka, D.; Piwkowska, A.; Audzeyenka, I.; Angielski, S.; Jankowski, M. Involvement of the AMPK-PTEN pathway in insulin resistance induced by high glucose in cultured rat podocytes. *Int. J. Biochem. Cell Biol.* **2014**, *51*, 120–130. [CrossRef] [PubMed]
97. Guzman, J.; Jauregui, A.N.; Merscher-Gomez, S.; Maiguel, D.; Muresan, C.; Mitrofanova, A.; Diez-Sampedro, A.; Szust, J.; Yoo, T.-H.; Villarreal, R.; et al. Podocyte-specific GLUT4-deficient mice have fewer and larger podocytes and are protected from diabetic nephropathy. *Diabetes* **2014**, *63*, 701–714. [CrossRef]
98. Brinkkoetter, P.T.; Bork, T.; Salou, S.; Liang, W.; Mizi, A.; Özel, C.; Koehler, S.; Hagmann, H.H.; Ising, C.; Kuczkowski, A.; et al. Anaerobic Glycolysis Maintains the Glomerular Filtration Barrier Independent of Mitochondrial Metabolism and Dynamics. *Cell Rep.* **2019**, *27*, 1551–1566.e5. [CrossRef]
99. Rachubik, P.; Szrejder, M.; Rogacka, D.; Audzeyenka, I.; Rychłowski, M.; Angielski, S.; Piwkowska, A. The TRPC6-AMPK Pathway is Involved in Insulin-Dependent Cytoskeleton Reorganization and Glucose Uptake in Cultured Rat Podocytes. *Cell. Physiol. Biochem. Int. J. Exp. Cell. Physiol. Biochem. Pharmacol.* **2018**, *51*, 393–410. [CrossRef]
100. Hall, G.; Wang, L.; Spurney, R.F. TRPC Channels in Proteinuric Kidney Diseases. *Cells* **2019**, *9*, 44. [CrossRef]
101. Wang, L.; Chang, J.-H.; Buckley, A.F.; Spurney, R.F. Knockout of TRPC6 promotes insulin resistance and exacerbates glomerular injury in Akita mice. *Kidney Int.* **2019**, *95*, 321–332. [CrossRef] [PubMed]
102. Hong, Q.; Zhang, L.; Das, B.; Li, Z.; Liu, B.; Cai, G.; Chen, X.; Chuang, P.Y.; He, J.C.; Lee, K. Increased podocyte Sirtuin-1 function attenuates diabetic kidney injury. *Kidney Int.* **2018**, *93*, 1330–1343. [CrossRef]
103. Rogacka, D.; Piwkowska, A.; Audzeyenka, I.; Angielski, S.; Jankowski, M. SIRT1-AMPK crosstalk is involved in high glucose-dependent impairment of insulin responsiveness in primary rat podocytes. *Exp. Cell Res.* **2016**, *349*, 328–338. [CrossRef] [PubMed]
104. Shati, A.A. Salidroside ameliorates diabetic nephropathy in rats by activating renal AMPK/SIRT1 signaling pathway. *J. Food Biochem.* **2020**, *44*, e13158. [CrossRef]
105. Vallon, V. Molecular determinants of renal glucose reabsorption. Focus on "Glucose transport by human renal Na+/D-glucose cotransporters SGLT1 and SGLT2". *Am. J. Physiol. Cell Physiol.* **2011**, *300*, C6–C8. [CrossRef] [PubMed]
106. Packer, M. SGLT2 Inhibitors Produce Cardiorenal Benefits by Promoting Adaptive Cellular Reprogramming to Induce a State of Fasting Mimicry: A Paradigm Shift in Understanding Their Mechanism of Action. *Diabetes Care* **2020**, *43*, 508–511. [CrossRef] [PubMed]
107. Castilla-Madrigal, R.; Barrenetxe, J.; Moreno-Aliaga, M.J.; Lostao, M.P. EPA blocks TNF-α-induced inhibition of sugar uptake in Caco-2 cells via GPR120 and AMPK. *J. Cell. Physiol.* **2018**, *233*, 2426–2433. [CrossRef]
108. Di Franco, A.; Cantini, G.; Tani, A.; Coppini, R.; Zecchi-Orlandini, S.; Raimondi, L.; Luconi, M.; Mannucci, E. Sodium-dependent glucose transporters (SGLT) in human ischemic heart: A new potential pharmacological target. *Int. J. Cardiol.* **2017**, *243*, 86–90. [CrossRef]
109. Rabinovitch, R.C.; Samborska, B.; Faubert, B.; Ma, E.H.; Gravel, S.-P.; Andrzejewski, S.; Raissi, T.C.; Pause, A.; St-Pierre, J.; Jones, R.G. AMPK Maintains Cellular Metabolic Homeostasis through Regulation of Mitochondrial Reactive Oxygen Species. *Cell Rep.* **2017**, *21*, 1–9. [CrossRef]
110. Zhang, J.; Wang, Y.; Liu, X.; Dagda, R.K.; Zhang, Y. How AMPK and PKA Interplay to Regulate Mitochondrial Function and Survival in Models of Ischemia and Diabetes. *Oxid. Med. Cell. Longev.* **2017**, *2017*, 4353510. [CrossRef]
111. Wan, Z.; Root-McCaig, J.; Castellani, L.; Kemp, B.E.; Steinberg, G.R.; Wright, D.C. Evidence for the role of AMPK in regulating PGC-1 alpha expression and mitochondrial proteins in mouse epididymal adipose tissue. *Obesity* **2014**, *22*, 730–738. [CrossRef] [PubMed]
112. Hinchy, E.C.; Gruszczyk, A.V.; Willows, R.; Navaratnam, N.; Hall, A.R.; Bates, G.; Bright, T.P.; Krieg, T.; Carling, D.; Murphy, M.P. Mitochondria-derived ROS activate AMP-activated protein kinase (AMPK) indirectly. *J. Biol. Chem.* **2018**, *293*, 17208–17217. [CrossRef] [PubMed]
113. Bullon, P.; Marin-Aguilar, F.; Roman-Malo, L. AMPK/Mitochondria in Metabolic Diseases. *Exp. Suppl.* **2016**, *107*, 129–152. [PubMed]

114. Jornayvaz, F.R.; Shulman, G.I. Regulation of mitochondrial biogenesis. *Essays Biochem.* **2010**, *47*, 69–84. [PubMed]
115. Galvan, D.L.; Green, N.H.; Danesh, F.R. The hallmarks of mitochondrial dysfunction in chronic kidney disease. *Kidney Int.* **2017**, *92*, 1051–1057. [CrossRef] [PubMed]
116. Bhargava, P.; Schnellmann, R.G. Mitochondrial energetics in the kidney. *Nat. Rev. Nephrol.* **2017**, *13*, 629–646. [CrossRef]
117. Tang, C.; Cai, J.; Dong, Z. Mitochondrial dysfunction in obesity-related kidney disease: A novel therapeutic target. *Kidney Int.* **2016**, *90*, 930–933. [CrossRef]
118. Szeto, H.H.; Liu, S.; Soong, Y.; Alam, N.; Prusky, G.T.; Seshan, S. V Protection of mitochondria prevents high fat diet-induced glomerulopathy and proximal tubular injury. *Kidney Int.* **2016**, *90*, 997–1011. [CrossRef] [PubMed]
119. Jeong, H.Y.; Kang, J.M.; Jun, H.H.; Kim, D.-J.; Park, S.H.; Sung, M.J.; Heo, J.H.; Yang, D.H.; Lee, S.H.; Lee, S.-Y. Chloroquine and amodiaquine enhance AMPK phosphorylation and improve mitochondrial fragmentation in diabetic tubulopathy. *Sci. Rep.* **2018**, *8*, 8774. [CrossRef]
120. Toyama, E.Q.; Herzig, S.; Courchet, J.; Lewis, T.L.J.; Losón, O.C.; Hellberg, K.; Young, N.P.; Chen, H.; Polleux, F.; Chan, D.C.; et al. Metabolism. AMP-activated protein kinase mediates mitochondrial fission in response to energy stress. *Science* **2016**, *351*, 275–281. [CrossRef]
121. Lee, S.-Y.; Kang, J.M.; Kim, D.-J.; Park, S.H.; Jeong, H.Y.; Lee, Y.H.; Kim, Y.G.; Yang, D.H.; Lee, S.H. PGC1α Activators Mitigate Diabetic Tubulopathy by Improving Mitochondrial Dynamics and Quality Control. *J. Diabetes Res.* **2017**, *2017*, 6483572. [CrossRef] [PubMed]
122. Jha, J.C.; Banal, C.; Chow, B.S.M.; Cooper, M.E.; Jandeleit-Dahm, K. Diabetes and Kidney Disease: Role of Oxidative Stress. *Antioxid. Redox Signal.* **2016**, *25*, 657–684. [CrossRef] [PubMed]
123. Rius-Perez, S.; Torres-Cuevas, I.; Millan, I.; Ortega, A.L.; Perez, S. PGC-1alpha, Inflammation, and Oxidative Stress: An Integrative View in Metabolism. *Oxid. Med. Cell. Longev.* **2020**, *2020*, 1452696. [CrossRef]
124. Ruggiero, C.; Ehrenshaft, M.; Cleland, E.; Stadler, K. High-fat diet induces an initial adaptation of mitochondrial bioenergetics in the kidney despite evident oxidative stress and mitochondrial ROS production. *Am. J. Physiol. Endocrinol. Metab.* **2011**, *300*, E1047–E1058. [CrossRef]
125. Sharma, K. Mitochondrial Hormesis and Diabetic Complications. *Diabetes* **2015**, *64*, 663–672. [CrossRef] [PubMed]
126. Soriano, F.G.; Virág, L.; Jagtap, P.; Szabó, E.; Mabley, J.G.; Liaudet, L.; Marton, A.; Hoyt, D.G.; Murthy, K.G.; Salzman, A.L.; et al. Diabetic endothelial dysfunction: The role of poly(ADP-ribose) polymerase activation. *Nat. Med.* **2001**, *7*, 108–113. [CrossRef]
127. Sedeek, M.; Nasrallah, R.; Touyz, R.M.; Hébert, R.L. NADPH oxidases, reactive oxygen species, and the kidney: Friend and foe. *J. Am. Soc. Nephrol.* **2013**, *24*, 1512–1518. [CrossRef]
128. Yang, Q.; Wu, F.-R.; Wang, J.-N.; Gao, L.; Jiang, L.; Li, H.-D.; Ma, Q.; Liu, X.-Q.; Wei, B.; Zhou, L.; et al. Nox4 in renal diseases: An update. *Free Radic. Biol. Med.* **2018**, *124*, 466–472. [CrossRef]
129. Muñoz, M.; López-Oliva, M.E.; Rodríguez, C.; Martínez, M.P.; Sáenz-Medina, J.; Sánchez, A.; Climent, B.; Benedito, S.; García-Sacristán, A.; Rivera, L.; et al. Differential contribution of Nox1, Nox2 and Nox4 to kidney vascular oxidative stress and endothelial dysfunction in obesity. *Redox Biol.* **2020**, *28*, 101330. [CrossRef]
130. Sedeek, M.; Callera, G.; Montezano, A.; Gutsol, A.; Heitz, F.; Szyndralewiez, C.; Page, P.; Kennedy, C.R.J.; Burns, K.D.; Touyz, R.M.; et al. Critical role of Nox4-based NADPH oxidase in glucose-induced oxidative stress in the kidney: Implications in type 2 diabetic nephropathy. *Am. J. Physiol. Ren. Physiol.* **2010**, *299*, F1348–F1358. [CrossRef]
131. Jiang, F.; Lim, H.K.; Morris, M.J.; Prior, L.; Velkoska, E.; Wu, X.; Dusting, G.J. Systemic upregulation of NADPH oxidase in diet-induced obesity in rats. *Redox Rep.* **2011**, *16*, 223–229. [CrossRef] [PubMed]
132. He, T.; Xiong, J.; Nie, L.; Yu, Y.; Guan, X.; Xu, X.; Xiao, T.; Yang, K.; Liu, L.; Zhang, D.; et al. Resveratrol inhibits renal interstitial fibrosis in diabetic nephropathy by regulating AMPK/NOX4/ROS pathway. *J. Mol. Med.* **2016**, *94*, 1359–1371. [CrossRef] [PubMed]
133. Papadimitriou, A.; Peixoto, E.B.M.I.; Silva, K.C.; Lopes de Faria, J.M.; Lopes de Faria, J.B. Increase in AMPK brought about by cocoa is renoprotective in experimental diabetes mellitus by reducing NOX4/TGFβ-1 signaling. *J. Nutr. Biochem.* **2014**, *25*, 773–784. [CrossRef]

134. Papadimitriou, A.; Peixoto, E.B.M.I.; Silva, K.C.; Lopes de Faria, J.M.; Lopes de Faria, J.B. Inactivation of AMPK mediates high phosphate-induced extracellular matrix accumulation via NOX4/TGFß-1 signaling in human mesangial cells. *Cell. Physiol. Biochem. Int. J. Exp. Cell. Physiol. Biochem. Pharmacol.* **2014**, *34*, 1260–1272. [CrossRef]
135. Zhang, M.; Wang, C.-M.; Li, J.; Meng, Z.-J.; Wei, S.-N.; Li, J.; Bucala, R.; Li, Y.-L.; Chen, L. Berberine protects against palmitate-induced endothelial dysfunction: Involvements of upregulation of AMPK and eNOS and downregulation of NOX4. *Mediat. Inflamm.* **2013**, *2013*, 260464. [CrossRef]
136. Kim, H.-R.; Kim, S.-Y. Perilla frutescens Sprout Extract Protect Renal Mesangial Cell Dysfunction against High Glucose by Modulating AMPK and NADPH Oxidase Signaling. *Nutrients* **2019**, *11*, 356. [CrossRef] [PubMed]
137. Lee, H.J.; Lee, D.Y.; Mariappan, M.M.; Feliers, D.; Ghosh-Choudhury, G.; Abboud, H.E.; Gorin, Y.; Kasinath, B.S. Hydrogen sulfide inhibits high glucose-induced NADPH oxidase 4 expression and matrix increase by recruiting inducible nitric oxide synthase in kidney proximal tubular epithelial cells. *J. Biol. Chem.* **2017**, *292*, 5665–5675. [CrossRef]
138. Li, Y.; Xia, T.; Li, R.; Tse, G.; Liu, T.; Li, G. Renal-Protective Effects of the Peroxisome Proliferator-Activated Receptor-γ Agonist Pioglitazone in ob/ob Mice. *Med. Sci. Monit. Int. Med. J. Exp. Clin. Res.* **2019**, *25*, 1582–1589. [CrossRef]
139. Wang, Y.; An, W.; Zhang, F.; Niu, M.; Liu, Y.; Shi, R. Nebivolol ameliorated kidney damage in Zucker diabetic fatty rats by regulation of oxidative stress/NO pathway: Comparison with captopril. *Clin. Exp. Pharmacol. Physiol.* **2018**, *45*, 1135–1148. [CrossRef]
140. Eid, A.A.; Lee, D.-Y.; Roman, L.J.; Khazim, K.; Gorin, Y. Sestrin 2 and AMPK connect hyperglycemia to Nox4-dependent endothelial nitric oxide synthase uncoupling and matrix protein expression. *Mol. Cell. Biol.* **2013**, *33*, 3439–3460. [CrossRef]
141. Lin, Q.; Ma, Y.; Chen, Z.; Hu, J.; Chen, C.; Fan, Y.; Liang, W.; Ding, G. Sestrin-2 regulates podocyte mitochondrial dysfunction and apoptosis under high-glucose conditions via AMPK. *Int. J. Mol. Med.* **2020**, *45*, 1361–1372. [CrossRef]
142. Kaushal, G.P.; Chandrashekar, K.; Juncos, L.A.; Shah, S.V. Autophagy Function and Regulation in Kidney Disease. *Biomolecules* **2020**, *10*, 100. [CrossRef]
143. Rautou, P.-E.; Mansouri, A.; Lebrec, D.; Durand, F.; Valla, D.; Moreau, R. Autophagy in liver diseases. *J. Hepatol.* **2010**, *53*, 1123–1134. [CrossRef] [PubMed]
144. Fritzen, A.M.; Madsen, A.B.; Kleinert, M.; Treebak, J.T.; Lundsgaard, A.-M.; Jensen, T.E.; Richter, E.A.; Wojtaszewski, J.; Kiens, B.; Frøsig, C. Regulation of autophagy in human skeletal muscle: Effects of exercise, exercise training and insulin stimulation. *J. Physiol.* **2016**, *594*, 745–761. [CrossRef] [PubMed]
145. Yuan, J.; Zhao, X.; Hu, Y.; Sun, H.; Gong, G.; Huang, X.; Chen, X.; Xia, M.; Sun, C.; Huang, Q.; et al. Autophagy regulates the degeneration of the auditory cortex through the AMPK-mTOR-ULK1 signaling pathway. *Int. J. Mol. Med.* **2018**, *41*, 2086–2098. [CrossRef] [PubMed]
146. Ahmed, M.; Hwang, J.S.; Lai, T.H.; Zada, S.; Nguyen, H.Q.; Pham, T.M.; Yun, M.; Kim, D.R. Co-Expression Network Analysis of AMPK and Autophagy Gene Products during Adipocyte Differentiation. *Int. J. Mol. Sci.* **2018**, *19*, 1808. [CrossRef] [PubMed]
147. Dikic, I.; Elazar, Z. Mechanism and medical implications of mammalian autophagy. *Nat. Rev. Mol. Cell Biol.* **2018**, *19*, 349–364. [CrossRef]
148. Alers, S.; Löffler, A.S.; Wesselborg, S.; Stork, B. Role of AMPK-mTOR-Ulk1/2 in the regulation of autophagy: Cross talk, shortcuts, and feedbacks. *Mol. Cell. Biol.* **2012**, *32*, 2–11. [CrossRef]
149. Green, A.S.; Chapuis, N.; Lacombe, C.; Mayeux, P.; Bouscary, D.; Tamburini, J. LKB1/AMPK/mTOR signaling pathway in hematological malignancies: From metabolism to cancer cell biology. *Cell Cycle* **2011**, *10*, 2115–2120. [CrossRef]
150. Bork, T.; Liang, W.; Yamahara, K.; Lee, P.; Tian, Z.; Liu, S.; Schell, C.; Thedieck, K.; Hartleben, B.; Patel, K.; et al. Podocytes maintain high basal levels of autophagy independent of mtor signaling. *Autophagy* **2019**, 1–17. [CrossRef]
151. Gwinn, D.M.; Shackelford, D.B.; Egan, D.F.; Mihaylova, M.M.; Mery, A.; Vasquez, D.S.; Turk, B.E.; Shaw, R.J. AMPK phosphorylation of raptor mediates a metabolic checkpoint. *Mol. Cell* **2008**, *30*, 214–226. [CrossRef] [PubMed]

152. Hariharan, N.; Maejima, Y.; Nakae, J.; Paik, J.; Depinho, R.A.; Sadoshima, J. Deacetylation of FoxO by Sirt1 Plays an Essential Role in Mediating Starvation-Induced Autophagy in Cardiac Myocytes. *Circ. Res.* **2010**, *107*, 1470–1482. [CrossRef]
153. Liu, W.J.; Gan, Y.; Huang, W.F.; Wu, H.-L.; Zhang, X.-Q.; Zheng, H.J.; Liu, H.-F. Lysosome restoration to activate podocyte autophagy: A new therapeutic strategy for diabetic kidney disease. *Cell Death Dis.* **2019**, *10*, 806. [CrossRef]
154. Kuwahara, S.; Hosojima, M.; Kaneko, R.; Aoki, H.; Nakano, D.; Sasagawa, T.; Kabasawa, H.; Kaseda, R.; Yasukawa, R.; Ishikawa, T.; et al. Megalin-Mediated Tubuloglomerular Alterations in High-Fat Diet-Induced Kidney Disease. *J. Am. Soc. Nephrol.* **2016**, *27*, 1996–2008. [CrossRef]
155. Yamahara, K.; Kume, S.; Koya, D.; Tanaka, Y.; Morita, Y.; Chin-Kanasaki, M.; Araki, H.; Isshiki, K.; Araki, S.; Haneda, M.; et al. Obesity-mediated autophagy insufficiency exacerbates proteinuria-induced tubulointerstitial lesions. *J. Am. Soc. Nephrol.* **2013**, *24*, 1769–1781. [CrossRef] [PubMed]
156. Ling, N.X.Y.; Kaczmarek, A.; Hoque, A.; Davie, E.; Ngoei, K.R.W.; Morrison, K.R.; Smiles, W.J.; Forte, G.M.; Wang, T.; Lie, S.; et al. mTORC1 directly inhibits AMPK to promote cell proliferation under nutrient stress. *Nat. Metab.* **2020**, *2*, 41–49. [CrossRef] [PubMed]
157. Li, H.; Min, Q.; Ouyang, C.; Lee, J.; He, C.; Zou, M.-H.; Xie, Z. AMPK activation prevents excess nutrient-induced hepatic lipid accumulation by inhibiting mTORC1 signaling and endoplasmic reticulum stress response. *Biochim. Biophys. Acta* **2014**, *1842*, 1844–1854. [CrossRef]
158. Kaushal, G.P.; Chandrashekar, K.; Juncos, L.A. Molecular Interactions Between Reactive Oxygen Species and Autophagy in Kidney Disease. *Int. J. Mol. Sci.* **2019**, *20*, 3791. [CrossRef]
159. Sohn, M.; Kim, K.; Uddin, M.J.; Lee, G.; Hwang, I.; Kang, H.; Kim, H.; Lee, J.H.; Ha, H. Delayed treatment with fenofibrate protects against high-fat diet-induced kidney injury in mice: The possible role of AMPK autophagy. *Am. J. Physiol. Ren. Physiol.* **2017**, *312*, F323–F334. [CrossRef]
160. Jin, Y.; Liu, S.; Ma, Q.; Xiao, D.; Chen, L. Berberine enhances the AMPK activation and autophagy and mitigates high glucose-induced apoptosis of mouse podocytes. *Eur. J. Pharmacol.* **2017**, *794*, 106–114. [CrossRef]
161. Wang, X.; Gao, L.; Lin, H.; Song, J.; Wang, J.; Yin, Y.; Zhao, J.; Xu, X.; Li, Z.; Li, L. Mangiferin prevents diabetic nephropathy progression and protects podocyte function via autophagy in diabetic rat glomeruli. *Eur. J. Pharmacol.* **2018**, *824*, 170–178. [CrossRef] [PubMed]
162. Lim, J.H.; Kim, H.W.; Kim, M.Y.; Kim, T.W.; Kim, E.N.; Kim, Y.; Chung, S.; Kim, Y.S.; Choi, B.S.; Kim, Y.-S.; et al. Cinacalcet-mediated activation of the CaMKKbeta-LKB1-AMPK pathway attenuates diabetic nephropathy in db/db mice by modulation of apoptosis and autophagy. *Cell Death Dis.* **2018**, *9*, 270. [CrossRef]
163. Wu, W.; Tian, W.; Hu, Z.; Chen, G.; Huang, L.; Li, W.; Zhang, X.; Xue, P.; Zhou, C.; Liu, L.; et al. ULK1 translocates to mitochondria and phosphorylates FUNDC1 to regulate mitophagy. *EMBO Rep.* **2014**, *15*, 566–575. [CrossRef] [PubMed]
164. Laker, R.C.; Drake, J.C.; Wilson, R.J.; Lira, V.A.; Lewellen, B.M.; Ryall, K.A.; Fisher, C.C.; Zhang, M.; Saucerman, J.J.; Goodyear, L.J.; et al. Ampk phosphorylation of Ulk1 is required for targeting of mitochondria to lysosomes in exercise-induced mitophagy. *Nat. Commun.* **2017**, *8*, 548. [CrossRef] [PubMed]
165. Kaushik, S.; Cuervo, A.M. AMPK-dependent phosphorylation of lipid droplet protein PLIN2 triggers its degradation by CMA. *Autophagy* **2016**, *12*, 432–438. [CrossRef] [PubMed]
166. Morigi, M.; Perico, L.; Benigni, A. Sirtuins in Renal Health and Disease. *J. Am. Soc. Nephrol.* **2018**, *29*, 1–11. [CrossRef]
167. Lee, I.H. Mechanisms and disease implications of sirtuin-mediated autophagic regulation. *Exp. Mol. Med.* **2019**, *51*, 1–11. [CrossRef]
168. Cantó, C.; Auwerx, J. PGC-1alpha, SIRT1 and AMPK, an energy sensing network that controls energy expenditure. *Curr. Opin. Lipidol.* **2009**, *20*, 98–105. [CrossRef]
169. Ruderman, N.B.; Xu, X.J.; Nelson, L.; Cacicedo, J.M.; Saha, A.K.; Lan, F.; Ido, Y. AMPK and SIRT1: A long-standing partnership? *Am. J. Physiol. Endocrinol. Metab.* **2010**, *298*, E751–E760. [CrossRef]
170. Dai, H.; Sinclair, D.A.; Ellis, J.L.; Steegborn, C. Sirtuin activators and inhibitors: Promises, achievements, and challenges. *Pharmacol. Ther.* **2018**, *188*, 140–154. [CrossRef]
171. Bharathi, S.S.; Zhang, Y.; Mohsen, A.-W.; Uppala, R.; Balasubramani, M.; Schreiber, E.; Uechi, G.; Beck, M.E.; Rardin, M.J.; Vockley, J.; et al. Sirtuin 3 (SIRT3) protein regulates long-chain acyl-CoA dehydrogenase by deacetylating conserved lysines near the active site. *J. Biol. Chem.* **2013**, *288*, 33837–33847. [CrossRef]

172. Yu, W.; Dittenhafer-Reed, K.E.; Denu, J.M. SIRT3 protein deacetylates isocitrate dehydrogenase 2 (IDH2) and regulates mitochondrial redox status. *J. Biol. Chem.* **2012**, *287*, 14078–14086. [CrossRef] [PubMed]
173. Pillai, V.B.; Sundaresan, N.R.; Kim, G.; Gupta, M.; Rajamohan, S.B.; Pillai, J.B.; Samant, S.; Ravindra, P.V.; Isbatan, A.; Gupta, M.P. Exogenous NAD blocks cardiac hypertrophic response via activation of the SIRT3-LKB1-AMP-activated kinase pathway. *J. Biol. Chem.* **2010**, *285*, 3133–3144. [CrossRef] [PubMed]
174. He, X.; Zeng, H.; Chen, J.-X. Emerging role of SIRT3 in endothelial metabolism, angiogenesis, and cardiovascular disease. *J. Cell. Physiol.* **2019**, *234*, 2252–2265. [CrossRef]
175. Hirschey, M.D.; Shimazu, T.; Jing, E.; Grueter, C.A.; Collins, A.M.; Aouizerat, B.; Stančáková, A.; Goetzman, E.; Lam, M.M.; Schwer, B.; et al. SIRT3 deficiency and mitochondrial protein hyperacetylation accelerate the development of the metabolic syndrome. *Mol. Cell* **2011**, *44*, 177–190. [CrossRef]
176. Zeng, H.; Vaka, V.R.; He, X.; Booz, G.W.; Chen, J.X. High-fat diet induces cardiac remodelling and dysfunction: Assessment of the role played by SIRT3 loss. *J. Cell. Mol. Med.* **2015**, *19*, 1847–1856. [CrossRef] [PubMed]
177. Morigi, M.; Perico, L.; Rota, C.; Longaretti, L.; Conti, S.; Rottoli, D.; Novelli, R.; Remuzzi, G.; Benigni, A. Sirtuin 3-dependent mitochondrial dynamic improvements protect against acute kidney injury. *J. Clin. Investig.* **2015**, *125*, 715–726. [CrossRef]
178. Koyama, T.; Kume, S.; Koya, D.; Araki, S.I.; Isshiki, K.; Chin-Kanasaki, M.; Sugimoto, T.; Haneda, M.; Sugaya, T.; Kashiwagi, A.; et al. SIRT3 attenuates palmitate-induced ROS production and inflammation in proximal tubular cells. *Free Radic. Biol. Med.* **2011**, *51*, 1258–1267. [CrossRef]
179. Wang, Q.; Xu, J.; Li, X.; Liu, Z.; Han, Y.; Xu, X.; Li, X.; Tang, Y.; Liu, Y.; Yu, T.; et al. Sirt3 modulate renal ischemia-reperfusion injury through enhancing mitochondrial fusion and activating the ERK-OPA1 signaling pathway. *J. Cell. Physiol.* **2019**, *234*, 23495–23506. [CrossRef]
180. Guigas, B.; Viollet, B. Targeting AMPK: From Ancient Drugs to New Small-Molecule Activators. *Exp. Suppl.* **2016**, *107*, 327–350.

International Journal of
Molecular Sciences

MDPI

Article

Delayed Exercise Training Improves Obesity-Induced Chronic Kidney Disease by Activating AMPK Pathway in High-Fat Diet-Fed Mice

Florian Juszczak [1,2,*], Maud Vlassembrouck [1], Olivia Botton [2], Thomas Zwakhals [1], Morgane Decarnoncle [1], Alexandra Tassin [3], Nathalie Caron [2] and Anne-Emilie Declèves [1]

1 Laboratory of Metabolic and Molecular Biochemistry, Faculty of Medicine and Pharmacy, Research Institute for Health Sciences and Technology, University of Mons (UMONS), 7000 Mons, Belgium; maudvlassembrouck@gmail.com (M.V.); Thomas.ZWAKHALS@umons.ac.be (T.Z.); Morgane.decarnoncle@student.umons.ac.be (M.D.); anne-emilie.decleves@umons.ac.be (A.-E.D.)
2 Molecular Physiology Research Unit (URPhyM), Namur Research Institute for Life Sciences (NARILIS), University of Namur (UNamur), 5000 Namur, Belgium; olivia.botton@unamur.be (O.B.); nathalie.caron@unamur.be (N.C.)
3 Laboratory of Respiratory Physiology, Pathophysiology and Rehabilitation, Faculty of Medicine and Pharmacy, Research Institute for Health Sciences and Technology, University of Mons (UMONS), 7000 Mons, Belgium; Alexandra.TASSIN@umons.ac.be
* Correspondence: florian.juszczak@umons.ac.be; Tel.: +32-65373580

Abstract: Exercise training is now recognized as an interesting therapeutic strategy in managing obesity and its related disorders. However, there is still a lack of knowledge about its impact on obesity-induced chronic kidney disease (CKD). Here, we investigated the effects of a delayed protocol of endurance exercise training (EET) as well as the underlying mechanism in obese mice presenting CKD. Mice fed a high-fat diet (HFD) or a low-fat diet (LFD) for 12 weeks were subsequently submitted to an 8-weeks EET protocol. Delayed treatment with EET in obese mice prevented body weight gain associated with a reduced calorie intake. EET intervention counteracted obesity-related disorders including glucose intolerance, insulin resistance, dyslipidaemia and hepatic steatosis. Moreover, our data demonstrated for the first time the beneficial effects of EET on obesity-induced CKD as evidenced by an improvement of obesity-related glomerulopathy, tubulo-interstitial fibrosis, inflammation and oxidative stress. EET also prevented renal lipid depositions in the proximal tubule. These results were associated with an improvement of the AMPK pathway by EET in renal tissue. AMPK-mediated phosphorylation of ACC and ULK-1 were particularly enhanced leading to increased fatty acid oxidation and autophagy improvement with EET in obese mice.

Keywords: high-fat diet; chronic kidney disease; endurance exercise training; AMPK; autophagy; ectopic lipid accumulation

Citation: Juszczak, F.; Vlassembrouck, M.; Botton, O.; Zwakhals, T.; Decarnoncle, M.; Tassin, A.; Caron, N.; Declèves, A.-E. Delayed Exercise Training Improves Obesity-Induced Chronic Kidney Disease by Activating AMPK Pathway in High-Fat Diet-Fed Mice. *Int. J. Mol. Sci.* **2021**, *22*, 0. https://doi.org/

Received: 14 November 2020
Accepted: 26 December 2020
Published: 31 December 2020

1. Introduction

In the general population, obesity is the second most highly predictive factor for end-stage renal disease, independently of diabetes and hypertension [1]. Central obesity is related to caloric excess promoting deleterious cellular responses in targeted organs. Obesity is mainly caused by a sedentary lifestyle commonly characterized by an excess consumption of ultraprocessed food containing high amounts of saturated fat, and a lack of physical activity [2]. The prevalence of obesity is increasing worldwide and predictive projections suggest that nearly 50% of adults will be obese by 2030 [3,4]. The consequences of adiposity include the endocrine activity of the adipose tissue via the production of adipokines, leading to the development of inflammation, oxidative stress, activation of the renin-angiotensin-aldosterone system and increased insulin resistance in the kidney [5]. Clinical and experimental studies have also demonstrated obesity-related glomerulopathy,

which is characterized by glomerulomegaly with thickening of the glomerular basement membrane, mesangial matrix expansion, hyperfiltration-related glomerular filtration barrier injury and, ultimately, focal glomerulosclerosis [6–8]. Furthermore, studies showing ectopic lipid depositions in the kidney have emerged, suggesting a role of fat accumulation in the development and progression of CKD [9–12]. Direct intrarenal effects of obesity involve lipid accumulation and impaired fatty acid β-oxidation (FAO) in kidney cells and tissue [13]. Renal proximal tubular cells (PTC) are metabolically very active, requiring a large amount of ATP, which is mostly provided through the mitochondrial FAO. In a previous work, we demonstrated a robust accumulation of lipids within enlarged multilamellar inclusions (MLI) into the PTC along with impaired tubular function and increased oxidative stress in obese mice [10]. Yamamoto et al. also described the stagnation of the autophagy flux in PTC, associated with the impairment of the lysosomal system. These alterations likely contribute to albuminuria, a progressive decline in renal function and end-stage renal disease. Moreover, evidence of a dysregulation of AMPK activity in podocytes and proximal tubular cells in diabetic and obesity conditions has been demonstrated [14,15]. In addition, pharmacological AMPK activation has been shown to improve pathologic features of the disease [10]. AMPK is a ubiquitous heterotrimeric enzyme that is the master energy sensor in all eukaryotic cells and is abundantly expressed in kidneys [16]. It is a central mediator of energy homeostasis responsive to nutritional and metabolic stresses such as obesity [17]. AMPK also activates autophagy through phosphorylation of ULK-1 in renal cells [18,19]. Therefore, inhibition of AMPK in kidney tissue is associated with poor outcomes.

Despite considerable efforts in the development of new therapeutic strategies, there is still a lack of effective treatment without strong side effects. Current pharmacotherapies that target food intake regulation have side effects (psychiatric and/or cardiovascular side effects) observed for long periods of use and may be associated with weight regain once the medication is stopped [20]. In addition, even though AMPK has been demonstrated to represent a key target for the treatment of metabolic diseases, indirect AMPK activators such as AICAR (5-Aminoimidazole-4-carboxamide ribonucleotide) have been widely investigated during the last decade by our group and others but did not demonstrate adequate and efficient therapeutic effects in clinical use [21]. The ongoing development of direct and specific AMPK activators thus represents an important pharmacological challenge [22]. This highlights the urgent need for alternative therapeutic strategies. Recently, the study of the effects of behavioral interventions such as exercise training in obesity-related diseases has regained interest. Indeed, targeting key pathways that could mediate beneficial effects by exercise represents a safer alternative therapeutic approach for the treatment of chronic metabolic disorders. Exercise training has been shown to exert beneficial outcomes in managing obesity-associated diseases [23,24]. However, there is still a lack of knowledge about the underlying mechanisms. Moreover, the efficacy of exercise-based therapeutic approach in patients presenting CKD remains controversial, mainly due to the experiment biases of the clinical studies regarding exercise training in obese patients with CKD [25–28].

Here, we evaluated for the first time, the potential therapeutic effect of a delayed exercise-based therapy on a treadmill in an obesity-induced CKD mice model. We further investigated the regulation of the AMPK pathway in response to the treatment.

2. Materials and Methods

2.1. Animals and Diet

The study was conformed to APS's guiding principles in the Care and Use of Animals and was approved by the Animal Ethics Committee of the University of Mons (DE-01-01; 09-01-2017). Experiments were performed on eight weeks old C57Bl/6J male mice (Janvier Labs, Le Genest Saint-Isle, France) housed in cages with ad libitum access to water and food and were maintained at 35–40% relative humidity and a temperature of 20–23 °C in a 12:12 h light–dark cycle. Eight-week old male mice were randomized either to a low-fat diet (LFD–10% of total calories from fat; D12450J, Research Diets, New Brunswick,

NJ, USA) or a high-fat diet (HFD–60% of total calories from fat; D12492, Research Diets, New Brunswick, NJ, USA). Food intake and body weight were measured weekly during a 20 weeks exposure period. At week 13, LFD and HFD mice were randomized in either of two additional groups submitted to an endurance exercise training (EET) for eight weeks (LFDT and HFDT) or the untrained control groups (LFD and HFD) (n = 10 in each group). Mice fed a high-fat diet for 12 weeks were previously described to present obesity-related metabolic disturbance as well as characteristic features of obesity-induced CKD [10], and were used to evaluate exercise training protocol as a therapeutic strategy.

2.2. Exercise Training Protocol

After 12 weeks of the experimental protocol, trained groups (LFDT and HFDT) were exercised for a total of eight weeks (five days a week) as previously described in [29]. Briefly, mice were acclimated to a treadmill (Treadmill Control LE8700, Panlab apparatus®, Barcelona, Spain) at a speed of 3 m/min for 5 min and 9 m/min for 10 min during weeks 13 and 14. At the beginning of week 15, a maximal running velocity test was performed for each trained mouse with a gradual speed increase of 1.2 m/min every two min until exhaustion (defined as a maximum of four electric stimulations in one minute). Then, the running velocity (Vmax) was set at 70% of the maximal speed for each mouse. As shown in Supplementary Materials, the maximal running velocity (Vmax) was similar in both trained groups of mice, LFDT and HFDT respectively, indicating that ET had no impact on exercise performance in obese mice (Figure S1). Therefore, mice from LFDT and HFDT were trained with an equivalent running velocity (70% of the Vmax) throughout the EET protocol. The exercise duration started at 10 min/day and was increased by 10 min every week. Sedentary mice were not exposed to exercise training and stayed in their cages during exercise sessions.

2.3. Sample Collection

Mice were euthanized after 20 weeks on the diet. Blood samples were collected by intracardiac puncture and centrifuged at high speed for 20 min at 4 °C. Plasma was collected and stored at −80 °C until use. Liver, heart and kidney were collected, weighed and immediately processed for further analysis. Portions of tissues were snap-frozen in liquid nitrogen for RNA, protein extraction and lipid content quantification. Additional portions of tissues were fixed in Duboscq-Brazil solution for histological analysis.

2.4. Urine Collection and Measurement of Urinary Markers

At weeks 0, 12 and 20 of the protocol, mice were placed into metabolic cages for 24 h-urine collection. A mouse Albuwell ELISA kit and a Creatinine Companion kit (Exocell, Philadelphia, PA, USA) were used to determine the urinary albumin to creatinine level for each mouse at the different timepoints. Total proteinuria was quantified using the Bradford binding assay, as previously described [30]. As an index of oxidative stress, urine samples were also analyzed for hydrogen peroxide by Amplex red assay (Thermo Fisher Scientific, Waltham, MA, USA) and for 8-hydroxy-2-deoxy guanosine (8-OH-dG) by competitive ELISA (Gentaur, Kampenhout, Belgium) following the manufacturer's instructions, and the data were normalized to the urinary creatinine from each mouse.

2.5. Glucose Tolerance Test

After a 12 h-overnight fast and 18 h after the last exercise session, a glucose tolerance test (GTT) was performed at weeks 0, 12 and 20 of the experimental protocol. A dose of 2 g/kg body weight of D-glucose (Roth, Karlsruhe, Germany) was administered intraperitoneally. Blood samples were then obtained from the caudal vein, and the blood glucose level was measured at 0, 30, 60, and 120 min after glucose injection using a One Touch® Verio® glucometer (Zug, Switzerland).

2.6. Biochemical Assays

ELISA. Plasma insulin level was determined by ELISA with the Rat/Mouse Insulin ELISA kit (Merck, Darmstadt, Germany). The homeostasis model assessment (HOMA) for insulin resistance index was determined using a calculator available from the Oxford Centre for Diabetes, Endocrinology and Metabolism (https://www.dtu.ox.ac.uk/homacalculator/). Plasma Adiponectin concentration was measured according to the manufacturer's instructions (Adiponectin: MRP300, R&D Systems, Minneapolis, MN, USA). Plasma TNFα concentration was measured according to the manufacturer's instructions (TNF alpha (mouse) ELISA kit; Gentaur, Kampenhout, Belgium).

Plasma lipid levels. Colorimetric enzymatic tests were performed to measure plasma triglycerides (TG) and cholesterol levels (Diasys, Diagnostic System, Holzheim, Germany) and plasma nonesterified fatty acids (NEFA) level (Wako Pure Chemical Industries, Ltd., Osaka, Japan) following the manufacturer's instructions.

Kidney and liver lipid levels. 90 mg of frozen kidney or liver tissue were prepared as described in [10]. Briefly, renal tissues were homogenized in a dounce homogenizer (Tenbroeck, Kimble/Kontes Glass Co., Vineland, NJ, USA) at 4 °C with nitrogen-sparged acid methanol: [0.2 N HCl/0.2 M NaCl] (4:1 mix) solution. For the first extraction phase, chloroform was added followed by a 30 s vortex to denature and extract proteins. The second extraction phase was performed by adding chloroform/water (2.5:3) to the mix. The samples were centrifuged at 16,000 *g* for 10 min at 4 °C to separate the phases. The lower phase (chloroform) containing lipids was used for measurement of total triglycerides and cholesterol (Diasys, Diagnostic System, Holzheim, Germany) according to the manufacturer's instructions. NEFA level was measured in the same phase using a colorimetric enzymatic test according to the manufacturer's instructions (Wako Pure Chemical Industries, Ltd., Osaka, Japan).

2.7. Morphological Analysis

Paraffin-embedded kidney sections were stained with Periodic Acid Schiff (PAS), Hemalun, and Luxol fast blue for morphological analysis. Morphometry of kidney sections was carried out as previously reported [15]. The glomerular area, mesangial matrix expansion and nuclei count were determined by randomly analyzing 25 glomeruli in the outer cortex in each kidney section using ImageJ based on [31]. In addition, a semiquantitative single-blind analysis was performed to evaluate the frequency of vacuolated tubular cells in renal cortex using an additional lens engrave with a square grid inserted in one of microscope eyepieces. For each paraffin section, 10 square fields (0.084 mm^2/field) were analyzed at $\times$400 magnification. In order to evaluate tubule-interstitial fibrosis, paraffin-embedded kidney sections were stained with picrosirius red (collagen I and III deposits). Ten randomly selected area of each kidney section were then analyzed with imageJ to measure the percentage of positive area. Paraffin-embedded liver sections were stained with hematoxylin and eosin and steatosis was graded as described by Ryu et al., 2015 [32].

2.8. Immunohistochemistry

Paraffin-embedded kidney sections were dewaxed and rehydrated followed by a microwave pretreatment in 1 mM EDTA buffer to unmask antigens present in the renal tissue. Endogenous peroxidase activity was removed by incubation with 3% H_2O_2 for 10 min and blockaded with 10% normal goat serum. Sections were incubated with primary antibody against LAMP-1 (Abcam) overnight at 4 °C. After rinsing in TBS, slides were exposed for 30 min with SignalStain® Boost IHC Detection Reagent (Cell Signaling, Danvers, MA, USA) and bound peroxidase activity was detected with the DAB kit (Agilent DAKO, Heverlee, Belgium). Counterstaining was performed with hemalun and Luxol fast blue. For each section, 10 square fields (0.084 mm^2/field) were observed at $\times$400 magnification in the renal cortex. The randomly selected area of each kidney section were then analyzed with imageJ software. The relative area occupied by positive staining was expressed as a percentage.

2.9. Quantitative Real-Time PCR

Snap-frozen kidney tissues were homogenized, and total RNA was then extracted with Trizol (Sigma-Aldrich, Saint-Louis, MO, USA) and treated with DNAse (Promega, Madison, WI, USA). Then, total RNA concentration was measured using NanoDrop (NanoDrop 1000, Thermo Scientific, Waltham, MA, USA) and 2 µg of total RNA were used for reverse transcription using MLV reverse transcriptase (Promega) following the manufacturer's instructions. Real-time quantitative PCR was performed in order to quantify mRNA level of *Col I*, *Col III*, *TGFβ*, *MCP-1*, *IL-1β*, *TNFα*, *IL-6*, *ACC*, *CPT-1*, *FAS* and *18S* as a housekeeping gene (see Table S1). Quantitative PCR amplification of a triplicate for each gene was performed using the SYBR Green Master Mix (Roche, Basel, Switzerland). Relative gene expressions were calculated using the $2^{-\Delta\Delta CT}$ method.

2.10. Western Blot Analysis

Frozen kidney tissues were homogenized in Cell Lysis Buffer (Cell Signaling, Danvers, MA, USA) with phosphatase and protease inhibitor cocktail (Thermo Fisher Scientific, Waltham, MA, USA) at 4 °C. Samples were subsequently centrifuged at 14,000× *g* for 15 min at 4 °C and supernatants were collected. Protein concentrations were quantified by Pierce BCA assay kit (Thermo Fisher). Next, 40 µg of total lysate were separated on Tris-Glycine 12% or Tris-acetate 3–8% (for high-molecular weight proteins) gels and transferred onto nitrocellulose membranes. The relative amounts of LMW, MMW and HMW Admer in plasma were determined using a nondenaturing PAGE-SDS as described in [29]. Membranes were blocked with 5% BSA for 1 h and primary antibodies against: phospho-ACC and ACC (Cell Signaling), phosphor-LKB1 and LKBA (Cell Signaling) phospho-AMPK and AMPK (Cell Signaling), CPT-1 (Abcam), Adiponectin (Abcam), Beclin-1 (Cell Signaling), p62 (Cell Signaling), phospho-ULK1 (Ser555) and ULK1 (Cell Signaling) and β-actin (Thermo Fisher) were applied in 5% BSA overnight at 4 °C. Finally, membranes were incubated with secondary antibodies (Li-Cor Biosciences, Lincoln, NE, USA) in 1% BSA for 1 h. Proteins were visualized using the Odyssey Infrared Imager (Li-Cor Biosciences). The fluorescence was quantified using the imaging software Odyssey V3.0 from the Odyssey Infrared Imager (Li-Cor Biosciences).

2.11. Statistical Analysis

Results are presented as mean values ± SEM. The level for statistical significance was defined as $p < 0.05$. Analyses were carried out using Prism GraphPad Software version 6 (San Diego, CA, USA). Differences between data groups were evaluated for significance using independent *t*-tests of data, one-way or two-way ANOVA and Newman–Keuls post hoc tests for multiple comparisons.

3. Results

3.1. Delayed Endurance Exercise Training Limits Calorie Intake and Prevents Body and Tissue Weight Gain in HFD Mice

The body weight and the calorie intake along the protocol, as well as tissue weights at week 20, were measured in mice fed an LFD or a HFD. The associated effects of a delayed EET treatment on these parameters were also determined. As observed in Figure 1B, a significant increase in body weight was observed from week five in HFD groups compared to LFD groups. This increase was maintained throughout the experimental protocol in HFD-fed mice compared with LFD-fed mice. This increase was observed along with a higher calorie intake in HFD mice that was significantly increased since the first week of the protocol, compared to LFD (Figure 1D). After the beginning of the EET protocol (week 12), HFDT mice showed a stabilization of the body weight. The BW of HFDT mice was significantly lower as soon as two weeks of EET compared to untrained HFD mice (Figure 1B). Figure 1C presents the percentage of body weight gain in HFD and HFDT from the beginning of EET. The linear regression analysis demonstrated that the slope of HFD was highly significant ($p < 0.0001$) but not in HFDT ($p = 0.2397$) compared with zero.

These results were associated with a decrease in calorie intake at week 20 in HFDT mice compared to HFD (Figure 1D). Figure 1E presents the changes in kidney, liver and heart weights of mice fed a LFD or an HFD with or without EET at the end of the protocol. As shown, the weights of kidneys and heart were higher in mice fed a HFD compared to mice fed a LFD but not in HFDT mice. Interestingly, the important hypertrophy of the liver observed in mice fed a HFD was significantly prevented by the EET.

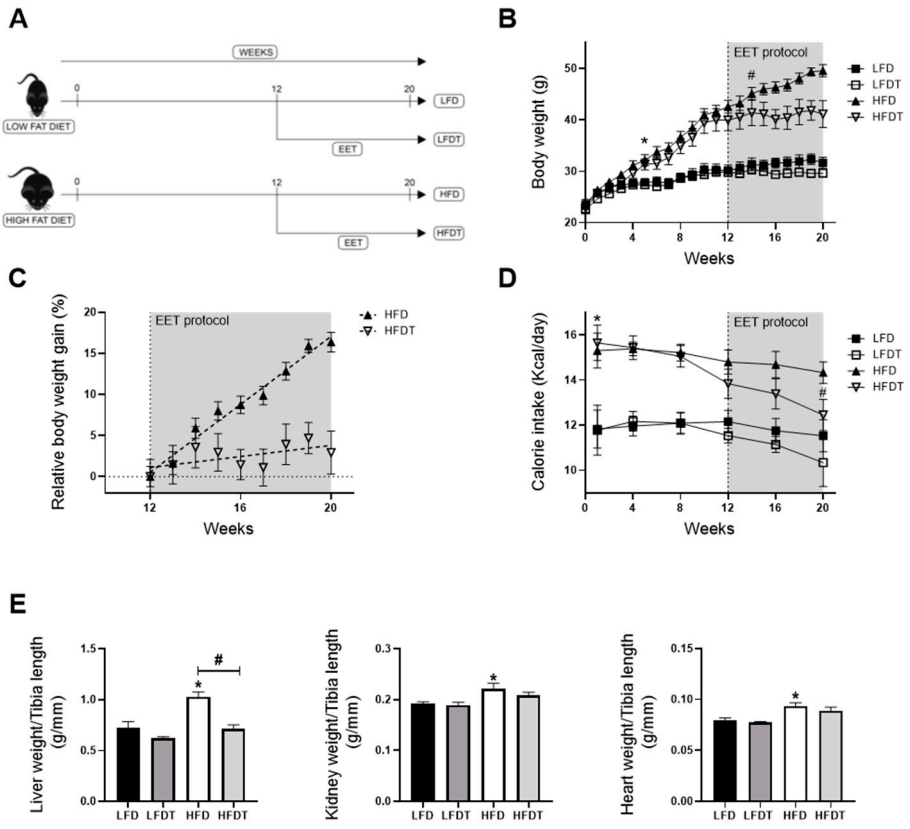

Figure 1. Delayed endurance exercise training (EET) prevents body weight gain and organ hypertrophy induced by HFD in mice. (**A**) Schematic representation of experimental design. Obesity in mice was induced with 12 weeks on a high-fat diet (HFD). Control mice were fed with a low-fat diet (LFD). Mice were subsequently divided in sedentary or trained groups on a treadmill for eight additional weeks (LFD, LFDT, HFD, HFDT). (**B**) Body weight evolution throughout the experimental protocol (20 weeks). Statistical analyses were performed by two-way ANOVA followed by Newman–Keuls post hoc test. (**C**) Relative body weight gain in HFD vs. HFDT mice during EET protocol normalized with body weight at week 12. The slope was determined with simple linear regression analysis. $n = 10$ in each group. (**D**) Calorie intake evolution throughout the experimental protocol. Number of calories consumed per day calculated for each mouse at different time-point (at week 1, 4, 8, 12, 16 and 20 of the experimental protocol). Statistical analyses were performed by two-way ANOVA followed by Newman–Keuls post hoc test. (**E**) Organ weights at week 20. Statistical analyses were performed by one-way ANOVA followed by Newman–Keuls post hoc test. Data are presented as means ± SEM. * $p \leq 0.05$ versus LFD $^{\#}$ $p \leq 0.05$ versus HFD. $n = 10$ in each group.

3.2. Delayed EET Improves Obesity-Related Metabolic Disorders in HFD Mice

HFD feeding in mice is known to induce glucose intolerance, insulin resistance, dyslipidemia and hepatic steatosis. We further characterized the effects of EET on obesity-related disorders in HFD mice. To determine the impact of delayed EET on glucose tolerance, glucose tolerance tests (GTTs) were performed at week 0, before EET (12 weeks) (Figure S2) and at the end of the experimental protocol (20 weeks) (Figure 2A). At week

20, the AUC for HFD fed mice was significantly higher than for LFD groups. However, an improvement of glucose tolerance by EET was demonstrated, as observed by the significant decrease of AUC in HFDT mice compared to the HFD mice (Figure 2A). Consistently, these changes were associated with a significantly higher level of plasma insulin in HFD mice that was decreased by EET in HFDT (Figure 2B). Insulin resistance in HFD mice was confirmed by the calculation of the HOMA-IR (Homeostatic Model Assessment for Insulin Resistance) index (Figure 2C). Serum levels of adiponectin also correlates with insulin sensitivity in obesity and diabetes [33]. Despite this we did not find any changes in the total plasma adiponectin levels in the experimental groups. We evaluated the S_A index (defined as the HMW/(HMW + LMW) ratio of adiponectin multimers in plasma) that was reported as a more relevant indicator of insulin sensitivity [34]. The results demonstrated a reduction of the S_A index in HFD mice (Figure S3) indicating decreased HMW forms in favour of the LMW multimers as demonstrated by Pierard et al., 2016 [29]. This change was particularly reversed following exercise in HFD mice. The plasma levels of cholesterol, triglycerides and NEFA were also measured after EET treatment (Figure 2D). As illustrated, HFD induced a significant elevation of plasma NEFA and cholesterol levels, whereas these increases were counteracted by EET in HFDT mice. Interestingly, there was no change in TG level. Dyslipidaemia commonly leads to hepatic steatosis in HFD mice and is associated with metabolic syndrome consequences. Thus, the liver steatosis score and TG content within the liver tissue were evaluated as markers of nonadipose tissue ectopic lipid accumulation. As illustrated in Figure 2E, histopathologic analyses of liver from HFD mice showed the presence of macrovesicular steatosis (large fat droplets) compared with the LFD groups. This was correlated with the steatosis score evaluation (Figure 2E). In contrast, hepatic steatosis was drastically reduced by EET in HFDT mice. Similarly, hepatic TG accumulation in HFD mice was prevented by EET. The results indicate that a delayed EET protocol applied on obese mice induces a substantial improvement of the metabolic syndrome features and obesity-related disorders. Lastly, we recorded blood pressure during the last week of the protocol. We measured the systolic, diastolic and mean blood pressure. As shown in Table S2, no significant difference was observed in the different experimental groups for each of these measurements.

3.3. Delayed EET Improves Obesity-Related Glomerulopathy and Renal Function

In order to characterize the effects of delayed EET protocol on the pathogenesis of obesity-induced chronic kidney disease, we first evaluated glomerular impairments and renal function. The morphological analysis of glomeruli revealed that mice fed a HFD without EET developed a significant increase of glomerular area along with a dense Periodic-Acid-Schiff (PAS)-positive matrix in the mesangium as well as an increase in nuclei number (Figure 3A–D). This glomerular expansion was prevented by EET in HFD mice. To further determine the effect of a delayed EET on renal function in obese mice, urinary albumin to creatinine ratio (UACR) and total proteinuria were investigated (Figure 3E). After 12 weeks on diet (before EET), both groups of HFD-fed mice presented a significant higher UACR compared to the groups of LFD-fed mice. In contrast, at week 20 (after EET intervention), the UACR in HFDT mice was significantly lower than in HFD mice, demonstrating a decreased albuminuria. The same patterns were found for urinary protein level (Figure 3F). Indeed, mice fed a HFD presented a significant increase in total proteinuria while this increase was prevented by EET. These results demonstrate that the EET protocol is beneficial to counteract the progression of obesity-related glomerulopathy and associated renal dysfunction in obese mice.

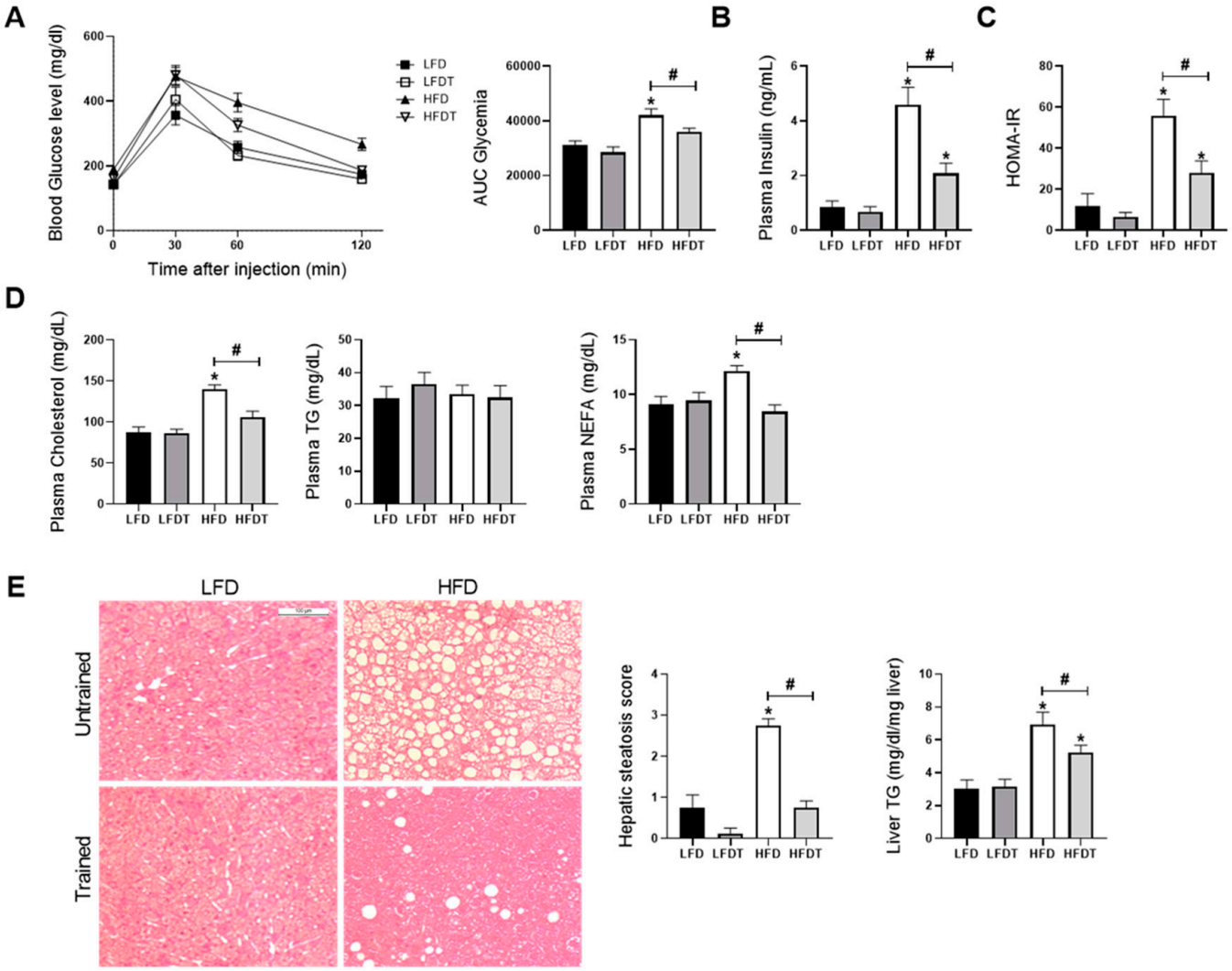

Figure 2. Delayed EET improves obesity-induced metabolic disorders and hepatic steatosis in HFD mice. (**A**) Glucose tolerance test at week 20. Fasted mice were submitted to an intraperitoneal injection of glucose (2 g/kg b.w.). Glycemia was measured before (0) and 30, 60 and 120 min after injection. Histogram represents the area under the curve (AUC) of glycemia from 0 to 120 min. (**B**) Plasma insulin level at week 20. (**C**) HOMA-IR index calculation. (**D**) Plasma levels of cholesterol, triglycerides (TG) and nonesterified fatty acids (NEFA) at week 20. (**E**) Representative photomicrograph (original magnification ×400; scale bar: 100 µm) of H&E staining illustrating hepatic steatosis from liver sections from mice on LFD, LFDT, HFD and HFDT at week 20 of the experimental protocol, steatosis scoring by semiquantitative analyses of lipid accumulation and quantitative analysis of triglycerides (TG) in the liver tissue. Statistical analyses were performed by one-way ANOVA followed by Newman-Keuls post hoc test. Data are presented as means ± SEM. * $p \leq 0.05$ versus LFD $^{\#}$ $p \leq 0.05$ versus HFD. $n = 10$ in each group.

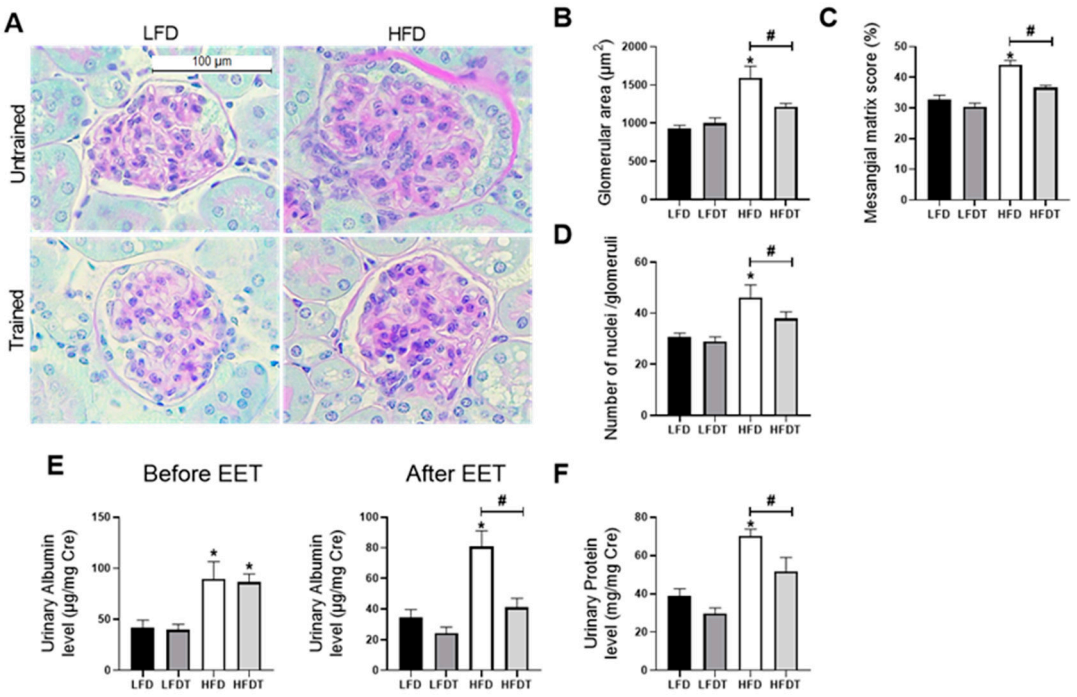

Figure 3. Effects of a delayed EET on renal function and glomerular histology in mice on LFD or HFD. (**A**) Representative photomicrographs (original magnification ×400; scale bar: 100 µm) of Periodic Acid Schiff (PAS) staining illustrating glomerular structure from renal cortex sections from mice on LFD, LFDT, HFD and HFDT. (**B**) Glomerular area. The glomerular tuft area was averaged from 15 glomeruli per kidney section, using one kidney section per animal. (**C**) Mesangial matrix area percentage of total glomerular area. (**D**) Nuclei count. (**E**) Quantitative measurement of urinary albumin to creatinine ratio (UACR) at week 12 (before EET protocol) and at week 20 (after EET protocol) from mice on LFD, LFDT, HFD and HFDT. (**F**) Quantitative analysis of urinary total protein to creatinine ratio at week 20. Statistical analyses were performed by one-way ANOVA followed by Newman–Keuls post hoc test. * $p \leq 0.05$ versus LFD $^{\#}$ $p \leq 0.05$ versus HFD. Data are presented as means ± SEM. n = 10 in each group.

3.4. Delayed EET Ameliorates Renal Fibrosis, Inflammation and Oxidative Stress

Obesity-induced chronic kidney disease is also characterized by an increased tubulo-interstitial fibrosis, inflammation and oxidative stress in HFD mice. To decipher the impact of EET on these key characteristics of the pathological progression, collagen I and III depositions were studied by morphometric analysis in Sirius red-stained renal sections as an index of the fibrotic response. As illustrated in Figure 4A, collagen accumulated in the interstitium of HFD mice. This observation was confirmed by the quantitative analysis of Sirius Red positive staining (Figure 4B). EET treatment significantly reduced collagen I and III deposition. Candidate genes expression involved in renal fibrosis (*TGF-β1*, *collagen type I* and *III*) and inflammation (*TNFα*, *IL-1β*, *IL-6* and *MCP-1*) were also measured by real-time qPCR. As observed in Figure 4E, renal mRNA levels of the profibrotic markers were all significantly decreased with EET in mice fed a HFD as well as for the pro-inflammatory markers in HFD mice. These changes were prevented by EET. The plasma TNFα concentration for systemic inflammation was also evaluated and the data reported an increased concentration of this proinflammatory cytokine in HFD mice that was significantly reduced with exercise. As markers of oxidative stress, the urinary hydrogen peroxide and 8-hydroxy-2′-deoxyguanosine (8-OHdG) levels were measured at week 20. These markers were both significantly higher in HFD mice compared to LFD mice (Figure 4C,D). The increase in urine hydrogen peroxide and 8-OHdG were also prevented by EET. The results demonstrate that EET reduces renal injuries by decreasing oxidative stress, fibrosis and inflammation in obese mice.

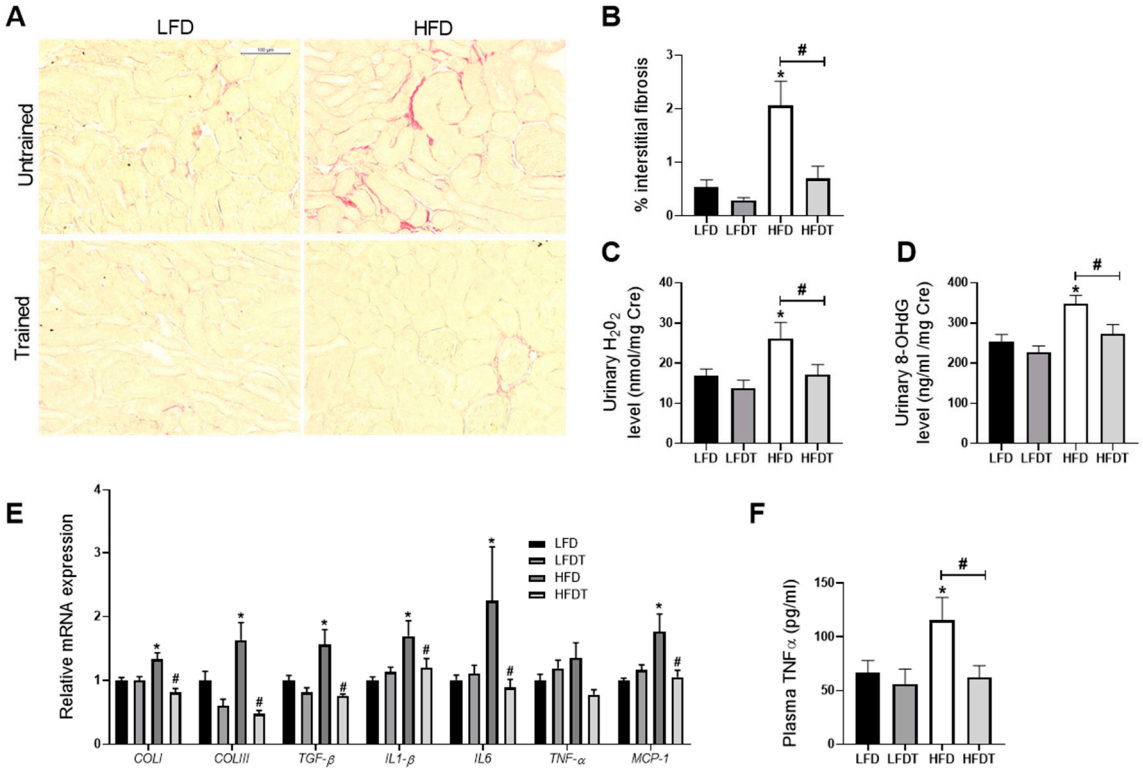

Figure 4. Effects of delayed EET on tubulointerstitial fibrosis, oxidative stress and inflammation from mice on LFD or HFD. (**A**) Representative photomicrographs (original magnification ×400; scale bar: 100 µm) of Sirius Red staining illustrating tubulointerstitial fibrosis in renal cortex. n = 10 in each group. (**B**) Quantitative analysis of the mean percentage of positive staining for Sirius red staining. n = 10 in each group. (**C**) Quantitative analysis of urinary H_2O_2 to creatinine ratio at week 20. n = 10 in each group. (**D**) Quantitative analysis of urinary 8-OHdG to creatinine ratio at week 20. n = 10 in each group. (**E**) Real-time quantitative qPCR for type I collagen (*COLI*), type III collagen (*COLIII*), transforming growth factor β (*TGFβ*), interleukin 1β *(IL-1β)*, tumor necrosis factor α (*TNFα*), interleukin 6 *(IL-6)* and monocyte chemoattractant protein 1 (*MCP-1*). mRNA expressions were performed on kidney tissue from LFD, LFDT, HFD and HFDT mice normalized against 18S. n = 6 in each group. (**F**) TNFα plasmatic level. The TNFαconcentration was measured using indirect ELISA. n = 8 in each group Statistical analyses were performed by one-way ANOVA followed by Newman–Keuls post hoc test. * $p \leq 0.05$ versus LFD $^{\#}$ $p \leq 0.05$ versus HFD. Data are presented as mean ± SEM. n = 10 in each group.

3.5. Delayed EET Reduces Renal Ectopic Lipid Accumulations

The ectopic lipid deposition in the kidney is a key feature of obesity-induced chronic kidney disease which is associated with renal lipotoxicity. We further characterized the effect of delayed EET on tubular lipid accumulation in mice fed a LFD or HFD. As described before by Declèves et al. (2014), vacuolated tubular cells were observed in HFD groups (Figure 5A; black arrows). These tubular alterations in proximal tubules were specifically found in the renal cortex. The quantitative analysis revealed that mice fed a HFD showed a strong increase in vacuolated tubules that was significantly reduced with EET (Figure 5B). Moreover, as illustrated in Figure 5C, cholesterol, TG and NEFA renal tissue content were also measured at week 20. Data demonstrated a significant increase in TG in the HFD group that was prevented by EET. While there was no change in cholesterol content, the level of NEFA was decreased with EET in both the LFDT and the HFDT groups. Thus, EET treatment is associated with a reduced lipid accumulation in the renal tissue in obese mice.

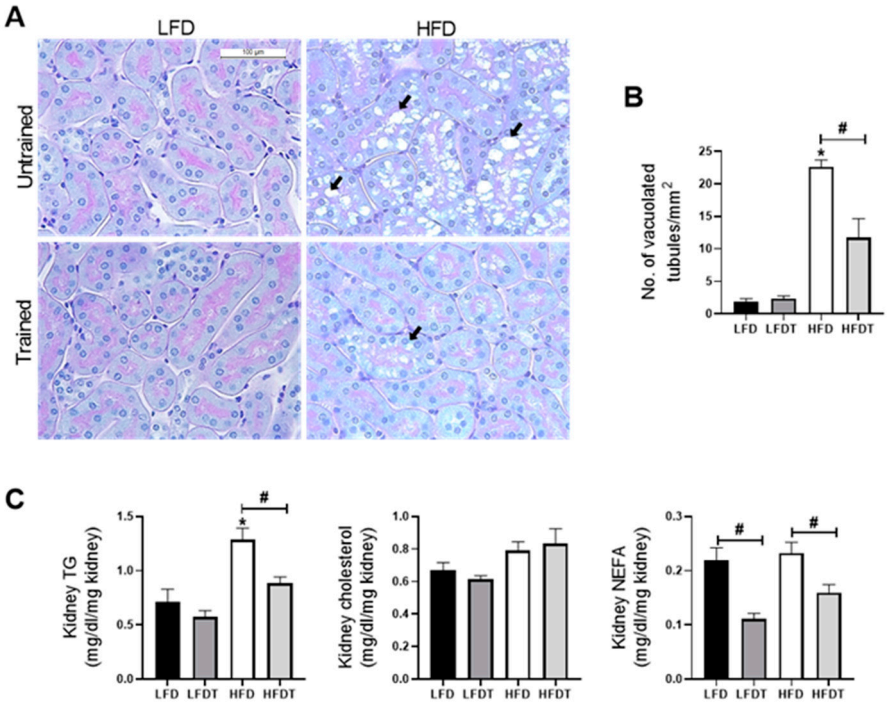

Figure 5. Delayed EET reduces ectopic lipid accumulation in renal tissue induced by HFD in mice. (**A**) Representative photomicrographs (original magnification ×400; scale bar: 100 µm) of PAS staining illustrating vacuolated proximal convoluted tubular cells from renal cortex sections from mice on LFD, LFDT, HFD and HFDT at week 20 (black arrow: intracellular vacuoles). (**B**) Quantitative analysis of number of vacuolated tubules per mm^2. (**C**) Quantitative analysis of cholesterol, triglycerides (TG) and nonesterified fatty acids (NEFA) in renal tissue. Statistical analyses were performed by one-way ANOVA followed by Newman–Keuls post hoc test. * $p \leq 0.05$ versus LFD $^{\#}$ $p \leq 0.05$ versus HFD. Data are presented as means ± SEM. $n = 10$ in each group.

3.6. Delayed EET Enhances AMPK Activity in Renal Tissue of Obese Mice

AMPK pathway dysregulation plays an important role in obesity-associated renal cell dysfunction. To better characterize the effect of a delayed EET on AMPK activity in obese mice, phosphorylation of AMPK and its main downstream target, acetyl-CoA carboxylase (ACC) as well as the main AMPK upstream kinase, the liver kinase B1 (LKB1), were measured by Western blot (Figure 6). As illustrated in Figure 6B, *p*-LKB1 protein level was significantly decreased in HFD mice compared to the control that was prevented by exercise. Moreover, total LKB1 protein level did not change between experimental groups while the *p*-LKB1 to LKB1 ratio was increased in HFDT mice compared to sedentary HFD. Mice fed a HFD exhibited a significant decrease in *p*-AMPK protein level, whereas EET treatment prevented this reduction. Total AMPK protein level was similar in each group while AMPK activity (*p*-AMPK to AMPK ratio) was increased in HFDT mice (Figure 6C). Since AMPK inhibits fatty acid synthesis and promotes fatty acid oxidation by phosphorylation of ACC, *p*-ACC and ACC protein level were also determined (Figure 6D). Consistently, protein level of phospho-ACC was reduced along with a decrease of AMPK activity in HFD group and was significantly increased with EET. Interestingly, total ACC protein level was decreased in both HFD and HFDT groups, participating in the significant increase of the *p*-ACC to ACC ratio in HFDT compared to LFD. We also investigated the protein level of CPT-1 but its expression was not regulated by HFD or EET (Figure 6E). Furthermore, the lipolysis and lipogenic markers mRNA expression were not affected by any treatment (Table S3).

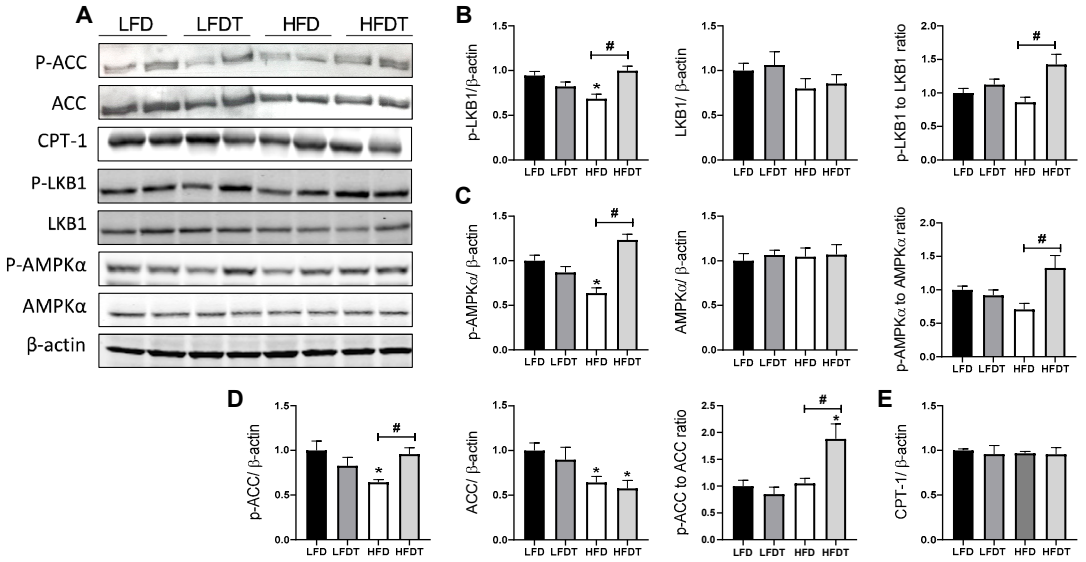

Figure 6. Delayed EET restores AMPK activity in the kidney of HFD mice. (**A**) Western Blot analysis of phosphor-LKB1, LKB1, phospho-AMPK, AMPK, phospho-ACC, ACC and CPT-1 in kidney tissue from mice on LFD, LFDT, HFD and HFDT at week 20. (**B**) Relative densitometry of the immunoblots representing, respectively, phospho-LKB1 protein level normalized with β-actin, LKB1 protein level normalized with β-actin and phospho-LKB1 to LKB1 ratio. (**C**) Relative densitometry of the immunoblots representing, respectively, phospho-AMPK protein level normalized with β-actin, AMPK protein level normalized with β-actin and phospho-AMPK to AMPK ratio. (**D**) Relative densitometry of the immunoblots representing, respectively, phospho-ACC protein level normalized with β-actin, ACC protein level normalized with β-actin and phospho-ACC to ACC ratio. (**E**) Relative densitometry of the immunoblots representing CPT-1 protein level normalized with β-actin. Statistical analyses were performed by one-way ANOVA followed by Newman–Keuls post hoc test. Data are presented as means ± SEM. * $p \leq 0.05$ versus LFD $^{\#}$ $p \leq 0.05$ versus HFD. n = 6–8 in each group.

3.7. Delayed EET Improves Autophagy Flux in Obese Mice by AMPK-Mediated ULK1 Activation

Cellular lipid accumulation and decreased AMPK activity were also associated with an impairment of the autophagy flux. Under physiological conditions, intracellular lipid storage is regulated by an autophagy process that plays a major role to prevent the deleterious effects of a lipid overload on cellular function. AMPK regulates autophagy by phosphorylating ULK-1 that mediates the initiation of autophagy. Thus, we first evaluated p-ULK1 (Ser 555) protein level in response to HFD and EET treatment. Consistently, p-ULK1 was found to be decreased in HFD mice while EET increased p-ULK1 in HFDT compared to HFD (Figure 7B). This result was corroborated with the evaluation of the autophagy marker Beclin-1, p62 for autophagy flux and LAMP-1, a specific marker of lysosomes. Indeed, Western blot analyses revealed that mice fed a HFD exhibited a significant increase in p62 protein level but not with EET (Figure 7C). p62 is a substrate of autophagy that is degraded during this cellular process. An accumulation of p62 in HFD mice revealed a stagnant autophagy process that is normalized by EET in obese mice. Beclin-1 acts during the initiation stage of autophagy by mediating the formation of a double-membrane structure that envelops cytoplasmic material to form the autophagosome. The protein level of Beclin-1 was significantly reduced in HFD and was shown to be restored by EET treatment (Figure 7D). Lastly, we demonstrated by immunohistochemistry an increased positive staining for LAMP-1 in the margins of the lipid vacuoles in proximal tubules that was significantly reduced by EET in the HFDT group (Figure 7E). These data indicate that EET enhances autophagy flux in renal tissues of obese mice possibly by AMPK-mediated phosphorylation of ULK1, ameliorating the progression of obesity-induced CKD.

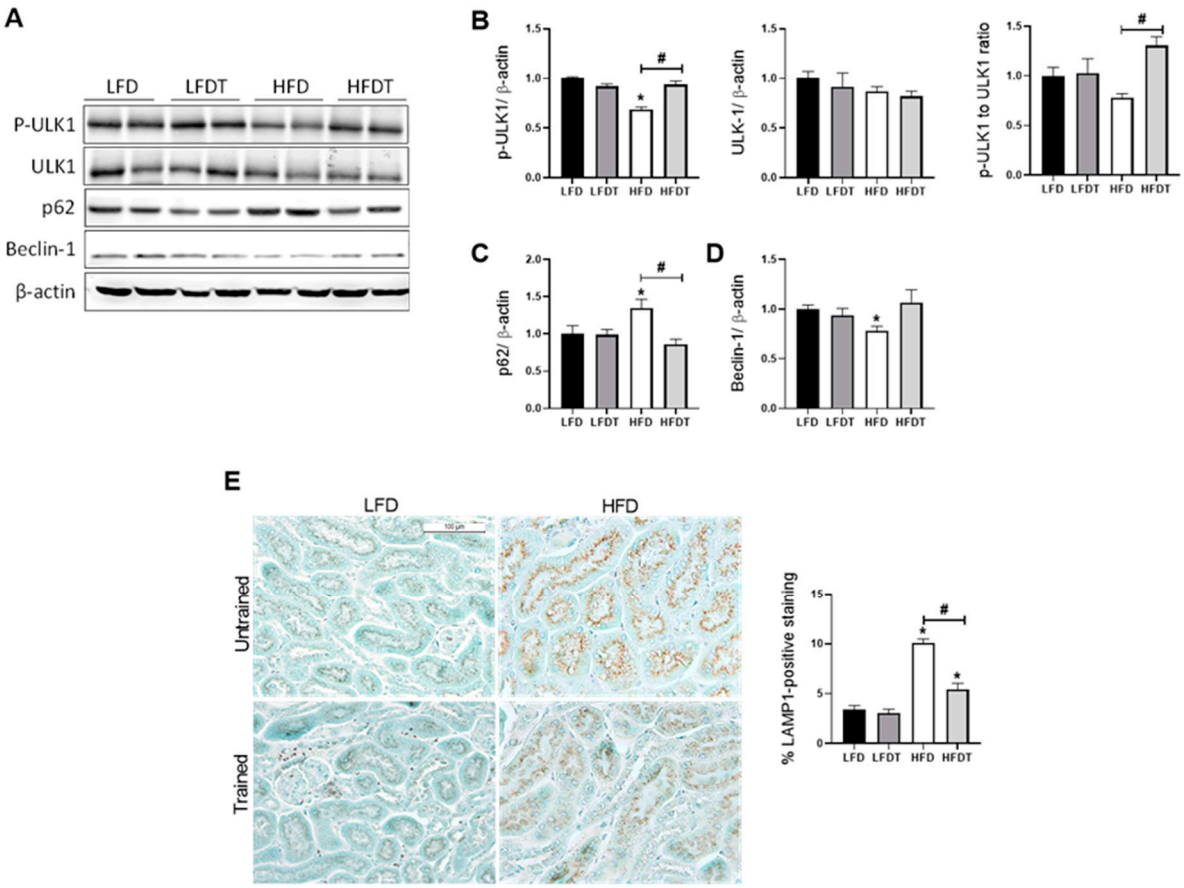

Figure 7. Effects of a delayed EET on autophagy and lysosomal markers in the kidney from mice on LFD or HFD. (**A**) Western Blot analysis of phospho-ULK-1 (Ser 555), ULK-1, p62 and Beclin-1 in kidney tissue from mice LFD, LFDT, HFD and HFDT. (**B**) Relative densitometry of the immunoblots representing, respectively, phosphor-ULK1 (Ser 555) protein level normalized with β-actin, ULK-1 protein level normalized with β-actin and Phospho-ULK1 (Ser 555) to ULK-1 ratio. (**C**) Relative densitometry of the immunoblots representing p62 protein level normalized with β-actin. (**D**) Relative densitometry of the immunoblots representing Beclin-1 protein level normalized with β-actin. (**E**) Representative photomicrograph (original magnification ×400; scale bar: 100 μm) showing lysosomal-associated membrane protein 1 (LAMP1)–positive staining on intracellular vacuoles and related quantitative analysis of LAMP1-positive staining. Statistical analyses were performed by one-way ANOVA followed by Newman–Keuls post hoc test. Data are presented as means ± SEM. * $p \leq 0.05$ versus LFD $^{\#}$ $p \leq 0.05$ versus HFD. n = 6–8 in each group.

4. Discussion

Endurance exercise training (EET) is now considered an interesting therapeutic strategy for managing obesity-related disorders. Emerging studies have demonstrated that EET is an effective strategy to prevent insulin resistance, hepatic steatosis and cardiovascular diseases [35,36]. The expected impact of exercise training treatment in obese patients is in reducing or maintaining body weight. Interestingly, EET has been shown to present beneficial effects without weight loss, suggesting independent effects of EET on obesity-related disorders [37,38]. Particularly, a redistribution of body fat along with a reduced ectopic lipid accumulation and a reduction of inflammation in tissues have been revealed with exercise [39]. Despite evidence that exercise training may improve obesity-related disorders, there is still a lack of knowledge about the underlying cellular and molecular mechanisms. Moreover, in the most experimental studies in obese rodents, animals were concomitantly exposed to EET and HFD, employing EET in a prevention setting and not as a treatment.

In contrast, here, the potential beneficial impact of EET was investigated as a therapeutic strategy on obese mice. Indeed, mice were fed a HFD for 12 weeks to achieve a significant level of metabolic and biochemical changes associated with obesity, including fat mass accumulation, glucose intolerance, insulin resistance, hepatic steatosis, ectopic lipid accumulations and associated chronic kidney disease (CKD) [15,40,41]. Thereafter, EET was applied for eight additional weeks. After 20 weeks on diets, mice exposed to a HFD presented the hallmarks of obesity-related disorders including insulin resistance, glucose intolerance and hyperlipidemia (NEFA and cholesterol). Hepatic steatosis also appeared in HFD mice as demonstrated with histological analysis and TG quantification. Several studies have already demonstrated that exercise training prevented obesity-associated disorders, including diabetes and hepatic steatosis [42–44]. Interestingly, in our model, delayed EET treatment in HFD mice also improved most of the metabolic changes. First, insulin resistance demonstrated in the HFD mice was reversed by EET along with improvement of glucose metabolism in HFD trained mice, as supported by HOMA-IR calculation and GTTs. The decreased insulinemia could be attributed to a lower secretion of insulin required to maintain glucose levels, suggesting a better insulin sensitivity. The exercise-induced changes in insulin sensitivity have been already extensively reported [45]. During exercise, glucose uptake is stimulated by skeletal muscle contraction. This occurs as a result of GLUT4 translocation to the muscle cell membrane [45]. Moreover, chronic exercise enhances insulin sensitivity largely due to activation of AMPK, a master regulator of glucose metabolism in the muscle [46]. The effects of exercise training on insulin resistance were also confirmed by the evaluation of adiponectin multimers distribution. As demonstrated by the S_A index, exercise training was associated with amelioration of the multimers distribution in favor of the HMW forms that are the most biologically active forms of adiponectin regarding glucose homeostasis [47]. EET also reduced dyslipidemia and drastically decreased intrahepatic fat content, consequently reversing HFD-related hepatic steatosis. During exercise, skeletal muscle contraction induces production of a variety of molecules called myokines that mediate beneficial responses in other organs. Experimental studies suggest that both IL-6 and Irisin might be involved in muscle/liver crosstalk mediating improvement of hepatic steatosis. In the liver, EET induces AMPK activity with enhanced mitochondrial function which lead to decreased lipogenesis and increased lipid oxidation. Hepatic AMPK activation also promotes autophagy induction via phosphorylation of ULK-1. As a result, excess lipids are eliminated by lysosomes leading to decreased ectopic lipid accumulations in the liver [48–50]. Furthermore, high blood pressure is another important component of metabolic syndrome, and exercise training is a recognized strategy for the prevention and treatment of hypertension [51,52]. However, in Bruder-Nascimento et al., mice fed a HFD for 24 weeks did not present any change in arterial blood pressure [53]. Similarly, we did not observe in our experimental model any significant difference of the systolic, diastolic or mean arterial blood pressure between LFD and HFD groups, neither between trained nor untrained groups, suggesting that EET has no effect on blood pressure in our experimental conditions.

Even though EET mediates improvement in key features of obesity in humans and animal models, its effects on renal function and metabolism in obesity are not well reported so far. In the general population, obesity is the second most highly prognostic factor to predict end-stage renal disease. However, the underlying mechanisms are complex and include physiological and metabolic aspects. Adiposity could directly impact the kidneys via the proinflammatory environment mediated by adipokines produced by adipose tissue, but also oxidative stress, activation of the renin-angiotensin-aldosterone system and IR [5]. These changes lead to characteristic features of obesity-induced kidney injury including the development of glomerulomegaly and ectopic lipid accumulation in the kidney, leading to renal lipotoxicity. Exercise training has been proposed to be included in renal care at any step of CKD progression [54]. A recent study has even showed that concomitant cafeteria diet exposure and EET prevented lipid depositions in the kidney in mice [55]. To further explore the adaptation of a fatty kidney to EET, we evaluated the effect of an

EET protocol to an HFD-induced CKD mice model. We demonstrated that EET treatment improved key parameters of obesity-induced CKD, as evidenced by improvement of renal function as well as morphological alterations. Notably, increased proteinuria and albuminuria, which reflect both glomerular and tubular impairments, are established predictors of CKD progression [56]. Here, we demonstrated that EET reduced glomerular impairment by reducing mesangial matrix expansion and thus glomerulomegaly. At a tubular level, ectopic lipid depositions in the kidney were markedly decreased, leading to better outcomes regarding CKD progression. Consistently, we demonstrated that EET was associated with reduced interstitial fibrosis, renal inflammation and oxidative stress.

Accumulating studies have demonstrated reduction of AMPK activity in caloric excess conditions [57,58]. Activity of AMPK was reduced in kidneys of diabetic mice and humans [59]. In several studies, pharmacological AMPK activators (5-aminoimidazole-4-carboxamide ribonucleoside, Metformin, Resveratrol, Fenofibrate and AdipoRon) attenuated diabetic nephropathy and obesity-induced CKD [10,60–63]. Consistent with the previous studies, our results showed a decrease in AMPK activity in kidney tissue following a HFD as well as the decreased phosphorylation of its main target ACC and its main upstream kinase LKB1, indicating inhibition of the AMPK pathway. Interestingly, we demonstrated that EET restored the activity of AMPK in obese mice, suggesting a critical role of AMPK regulation in the beneficial effects of EET in obesity-induced CKD. AMPK plays essential roles in glucose and lipid metabolism, cell survival, growth and inflammation. AMPK also exerts a key role in mitochondria homeostasis and has been revealed to regulate autophagy in mammalian cells. Obesity induces AMPK dysregulation by multiple mechanisms independently of the AMP:ATP ratio (reviewed in [64]) including insulin resistance, inflammation, decreased adiponectin, oxidative stress and decreased activity of AMPK upstream kinase. Here, we particularly highlighted the beneficial effects of exercise training on these parameters that may reduce the detrimental intra-renal environment leading to AMPK dysregulation in favor of a proper AMPK signaling.

Under physiological conditions, autophagy is critical for the maintenance of renal function and homeostasis [65]. Autophagy is a complex and highly regulated cellular degradation pathway, well conserved among eukaryotes, that has been intensely documented in many pathological conditions [66]. Both obesity and HFD negatively regulates autophagy in the kidney [67]. In a setting of renal lipid overload, Yamamoto et al. (2016) and our work have demonstrated the impairment of autophagy in proximal tubular cells (PTC) [10,68]. Here, we also highlighted a beneficial role of EET associated with activation of AMPK in preventing impairment of autophagy in PTC and lipid accumulation in these cells. Chronic EET was shown to induce autophagy in vivo in various tissues including muscles, liver, adipose tissue and pancreas [69]. In this study, we investigated whether EET treatment could lead to a restored autophagy flux in renal tissue in an obesity context. We demonstrated that EET regulated autophagy markers by decreasing p62 in obese trained mice and increasing Beclin-1 protein level. Activation of the autophagic flux leads to a decline in p62 level because of its degradation during the process and, contrarily, an accumulation of p62 reflects a stagnant autophagic flux [70]. Moreover, HFD also inhibits autophagy by reducing autophagosome/lysosome fusion [68]. Here, we described an increased lysosomal marker LAMP-1 that was reduced by EET in renal tissue of obese mice. Finally, we demonstrated the AMPK-mediated phosphorylation of ULK-1, an autophagy inducer, by EET in HFD mice. Thus, our data confirmed disturbance of autophagy by HFD and indicated the potential induction of autophagy process by EET via AMPK activation, leading to improvement of renal cell homeostasis. Since autophagy is a highly dynamic process, further investigations are needed to delineate the precise molecular mechanisms of exercise-induced autophagy in the kidney and the particular the role of AMPK in this process. Particularly, the use of ULK-1 knockout mice would be an interesting mechanistical strategy in order to confirm the role of AMPK-dependent autophagy in response to exercise in renal tissue.

Finally, how skeletal muscle communication can prevent or suppress kidney injury is particularly emerging and has not been strongly investigated yet, particularly regarding muscle-kidney cross-talk during exercise. A recent work nicely demonstrated that Irisin, an exerkine, ameliorated tubule cell damage and renal fibrosis in a CKD model [71]. Interestingly, inhibition of AMPK by a specific inhibitor reduced the effects of Irisin in myocytes and hepatocytes, suggesting that Irisin could be implicated in AMPK pathway regulation [72]. However, the particular effects of Irisin on AMPK regulation in the kidney are still unexplored and needs further investigation.

5. Conclusions

Based on our data, exercise training can be considered an interesting strategy for the management of obesity-induced CKD. Kidney function was improved through reducing albuminuria, glomerular hypertrophy, inflammation, oxidative stress and fibrosis, as well as attenuating intra-renal fat content. We demonstrated that these beneficial effects implicate restored AMPK activity and autophagy induction in renal tissue (Figure 8). Exercise training may thus represent an interesting nonpharmacological alternative strategy for AMPK activation in obesity-induced CKD.

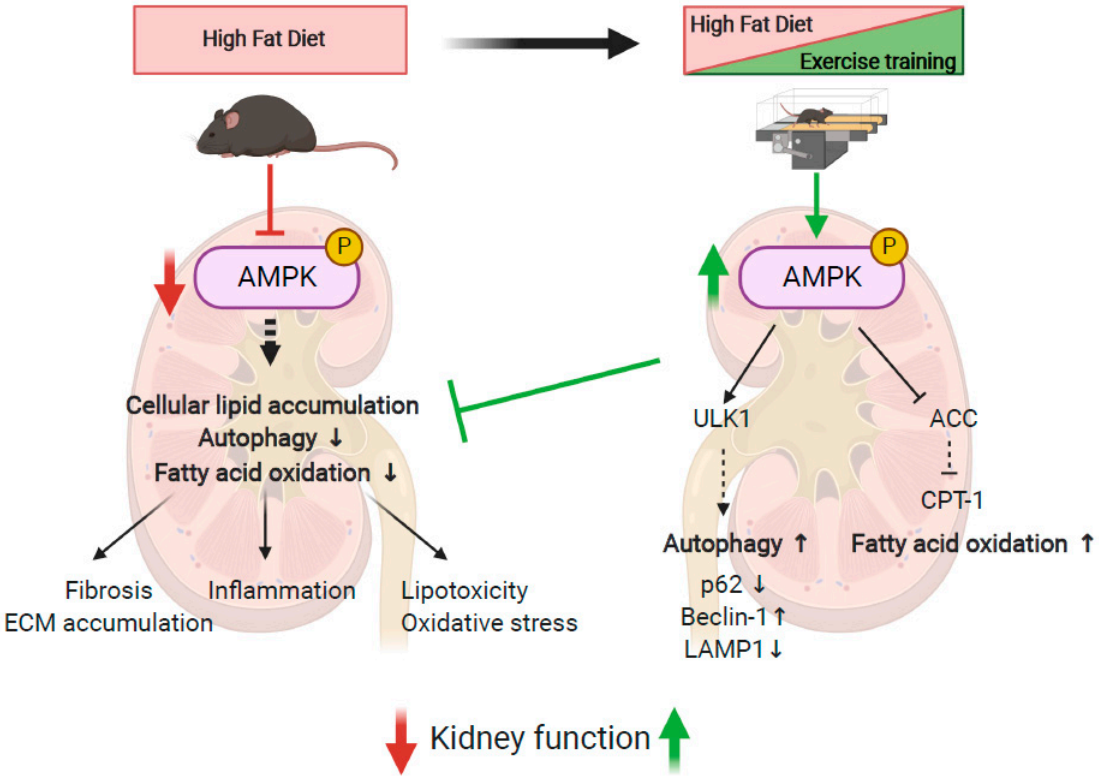

Figure 8. Schematical representation of the effects of HFD and EET on the underlying molecular mechanisms of obesity-induced CKD in mice. Created with Biorender.com.

Supplementary Materials: The following are available online at https://www.mdpi.com/1422-0067/22/1/0/s1, Figure S1: Effects of endurance exercise training on running velocity; Figure S2: Effects of LFD and HFD on glucose tolerance in mice; Table S1: Primer sequences for RT-qPCR analysis of mRNA expression; Table S2: Effects of delayed EET on systolic, diastolic and mean blood pressure in mice fed a LFD, LFDT or HFD and HDFT; Table S3: Effects of delayed EET on renal gene expression in mice fed a LFD, a LFDT, a HFD and a HFDT.

Author Contributions: Among the authors, F.J., N.C. and A.-E.D. conceived the experiments; F.J., M.V. and M.D. performed the experiments and interpreted the data; T.Z. and O.B. provided the technical assistance; N.C., A.T. and A.-E.D. oversaw the experiments which were performed in their respective laboratories; F.J. and A.-E.D. prepared the manuscript. All authors approved the final version of the manuscript and agree to be accountable for all aspects of the work. All persons designated as authors qualify for authorship, and all those who qualify for authorship are listed. All authors have read and agreed to the published version of the manuscript.

Funding: This work was supported by grants from the UMONS Research Institute for Health Sciences and Technology (Belgium) and the FRMH (Fonds pour la Recherche Médicale dans le Hainaut, Belgium).

Institutional Review Board Statement: The study was conformed to APS's guiding principles in the Care and Use of Animals and was approved by the Animal Ethics Committee of the University of Mons (DE-01-01; 09-01-2017).

Data Availability Statement: Data is contained within the article or Supplementary Materials.

Acknowledgments: The authors thank Vincianne Jenart and Jean-François Gaussin for technical support.

Conflicts of Interest: The authors declare no conflict of interest.

References

1. Garofalo, C.; Borrelli, S.; Minutolo, R.; Chiodini, P.; de Nicola, L.; Conte, G. A systematic review and meta-analysis suggests obesity predicts onset of chronic kidney disease in the general population. *Kidney Int.* **2017**, *91*, 1224–1235. [CrossRef] [PubMed]
2. Després, J.-P.; Lemieux, I. Abdominal obesity and metabolic syndrome. *Nature* **2006**, *444*, 881–887. [CrossRef] [PubMed]
3. Blüher, M. Obesity: Global epidemiology and pathogenesis. *Nat. Rev. Endocrinol.* **2019**, *15*, 288–298. [CrossRef] [PubMed]
4. Ward, Z.J.; Bleich, S.N.; Cradock, A.L.; Barrett, J.L.; Giles, C.M.; Flax, C.; Long, M.W.; Gortmaker, S.L. Projected, U.S. State-Level Prevalence of Adult Obesity and Severe Obesity. *N. Engl. J. Med.* **2019**, *381*, 2440–2450. [CrossRef]
5. Kovesdy, C.P.; Furth, S.; Zoccali, C. Obesity and kidney disease: Hidden consequences of the epidemic. *Physiol. Int. Hung.* **2017**, *104*, 1–14. [CrossRef]
6. Tonelli, M. Effect of Pravastatin on Loss of Renal Function in People with Moderate Chronic Renal Insufficiency and Cardiovascular Disease. *J. Am. Soc. Nephrol.* **2003**, *14*, 1605–1613. [CrossRef]
7. Deji, N.; Kume, S.; Araki, S.I.; Soumura, M.; Sugimoto, T.; Isshiki, K.; Kanasaki, M.C.; Sakaguchi, M.; Koya, D.; Haneda, M.; et al. Structural and functional changes in the kidneys of high-fat diet-induced obese mice. *Am. J. Physiol. Renal Physiol.* **2009**, *296*, 118–126. [CrossRef]
8. D'Agati, V.D.; Chagnac, A.; de Vries, A.P.J.; Levi, M.; Porrini, E.; Herman-Edelstein, M.; Praga, M. Obesity-related glomerulopathy: Clinical and pathologic characteristics and pathogenesis. *Nat. Rev. Nephrol.* **2016**, *12*, 453–471. [CrossRef]
9. Foster, M.C.; Hwang, S.-J.; Porter, S.A.; Massaro, J.M.; Hoffmann, U.; Fox, C.S. Fatty kidney, hypertension, and chronic kidney disease: The Framingham Heart Study. *Hypertens* **2011**, *58*, 784–790. [CrossRef]
10. Declèves, A.E.; Zolkipli, Z.; Satriano, J.; Wang, L.; Nakayama, T.; Rogac, M.; Le, T.P.; Nortier, J.L.; Farquhar, M.G.; Naviaux, R.K.; et al. Regulation of lipid accumulation by AMP-activated kinase [corrected] in high fat diet-induced kidney injury. *Kidney Int.* **2014**, *85*, 611–623. [CrossRef]
11. Kume, S.; Uzu, T.; Araki, S.I.; Sugimoto, T.; Isshiki, K.; Kanasaki, M.C.; Sakaguchi, M.; Kubota, N.; Terauchi, Y.; Kadowaki, T.; et al. Role of Altered Renal Lipid Metabolism in the Development of Renal Injury Induced by a High-Fat Diet. *J. Am. Soc. Nephrol.* **2007**, *18*, 2715–2723. [CrossRef] [PubMed]
12. De Vries, A.P.J.; Ruggenenti, P.; Ruan, X.Z.; Praga, M.; Cruzado, J.M.; Bajema, I.M.; D'Agati, V.D.; Lamb, H.J.; Barlovic, D.P.; Hojs, R.; et al. Fatty kidney: Emerging role of ectopic lipid in obesity-related renal disease. *Lancet Diabetes Endocrinol* **2014**, *2*, 417–426. [CrossRef]
13. Kang, H.M.; Ahn, S.H.; Choi, P.; Ko, Y.A.; Han, S.H.; Chinga, F.; Park, A.S.D.; Tao, J.; Sharma, K.; Pullman, J. Defective fatty acid oxidation in renal tubular epithelial cells has a key role in kidney fibrosis development. *Nat. Med.* **2014**, *21*, 37–46. [CrossRef] [PubMed]
14. Szrejder, M.; Piwkowska, A. AMPK signalling: Implications for podocyte biology in diabetic nephropathy. *Biol. Cell* **2019**, *111*, 109–120. [CrossRef] [PubMed]
15. Declèves, A.-E.; Mathew, A.V.; Cunard, R.; Sharma, K. AMPK Mediates the Initiation of Kidney Disease Induced by a High-Fat Diet. *J. Am. Soc. Nephrol.* **2011**, *22*, 1846–1855. [CrossRef] [PubMed]
16. Stapleton, D.; Mitchelhill, K.I.; Gao, G.; Widmer, J.; Michell, B.J.; Teh, T.; House, C.M.; Fernandez, C.S.; Cox, T.; Witters, L.A.; et al. Mammalian AMP-activated protein kinase subfamily. *J. Biol. Chem.* **1996**, *271*, 611–614. [CrossRef]
17. Herzig, S.; Shaw, R.J. AMPK: Guardian of metabolism and mitochondrial homeostasis. *Nat. Rev. Mol. Cell Biol.* **2017**, *19*, 121–135. [CrossRef]

18. Bork, T.; Liang, W.; Yamahara, K.; Lee, P.; Tian, Z.; Liu, S.; Schell, C.; Thedieck, K.; Patel, B.H.K.; Louis, T.P.; et al. Podocytes maintain high basal levels of autophagy independent of mtor signaling. *Autophagy* **2019**, *16*, 1932–1948. [CrossRef] [PubMed]
19. Yamahara, K.; Kume, S.; Koya, D.; Tanaka, Y.; Morita, Y.; Chin-Kanasaki, M.; Araki, H.; Isshiki, K.; Araki, S.; Haneda, M. Obesity-mediated autophagy insufficiency exacerbates proteinuria-induced tubulointerstitial lesions. *J. Am. Soc. Nephrol.* **2013**, *24*, 1769–1781. [CrossRef] [PubMed]
20. Kang, J.G.; Park, C.-Y. Anti-Obesity Drugs: A Review about Their Effects and Safety. *Diabetes Metab. J.* **2012**, *36*, 13–25. [CrossRef] [PubMed]
21. Srivastava, R.A.K.; Pinkosky, S.L.; Filippov, S.; Hanselman, J.C.; Cramer, C.T.; Newton, R.S. AMP-activated protein kinase: An emerging drug target to regulate imbalances in lipid and carbohydrate metabolism to treat cardio-metabolic diseases. *J. Lipid Res.* **2012**, *53*, 2490–2514. [CrossRef] [PubMed]
22. Olivier, S.; Foretz, M.; Viollet, B. Promise and challenges for direct small molecule AMPK activators. *Biochem. Pharmacol.* **2018**, *153*, 147–158. [CrossRef] [PubMed]
23. Katzmarzyk, P.T.; Leon, A.S.; Wilmore, J.H.; Skinner, J.S.; Rao, D.C.; Rankinen, T.; Bouchard, C. Targeting the metabolic syndrome with exercise: Evidence from the HERITAGE Family Study. *Med. Sci. Sports Exerc.* **2003**, *35*, 1703–1709. [CrossRef] [PubMed]
24. Ross, R.; Després, J.-P. Abdominal Obesity, Insulin Resistance, and the Metabolic Syndrome: Contribution of Physical Activity/Exercise. *Obesity* **2009**, *17*, S1–S2. [CrossRef]
25. Hiraki, K.; Shibagaki, Y.; Izawa, K.P.; Hotta, C.; Wakamiya, A.; Sakurada, T.; Yasuda, T.; Kimura, K. Effects of home-based exercise on pre-dialysis chronic kidney disease patients: A randomized pilot and feasibility trial. *BMC Nephrol.* **2017**, *18*, 198. [CrossRef]
26. Heiwe, S.; Jacobson, S.H. Exercise training for adults with chronic kidney disease. *Cochrane Database Syst. Rev.* **2011**, *10*, CD003236. [CrossRef]
27. Qiu, Z.; Zheng, K.; Zhang, H.; Feng, J.; Wang, L.; Zhou, H. Physical Exercise and Patients with Chronic Renal Failure: A Meta-Analysis. *BioMed Res. Int.* **2017**, *2017*, 7191826. [CrossRef]
28. Ikizler, T.A.; Cohen, C.R.; Ellis, C.; Headley, S.A.E.; Tuttle, K.; Wood, R.J.; Evans, E.E.; Milch, C.M.; Moody, K.A.; Germain, M.; et al. Metabolic Effects of Diet and Exercise in Patients with Moderate to Severe CKD: A Randomized Clinical Trial. *J. Am. Soc. Nephrol.* **2018**, *9*, 250–259. [CrossRef]
29. Pierard, M.; Conotte, S.; Tassin, A.; Boutry, S.; Uzureau, P.; Boudjeltia, K.Z.; Legrand, A. Interactions of exercise training and high-fat diet on adiponectin forms and muscle receptors in mice. *Nutr. Metab. (Lond.)* **2016**, *13*, 75. [CrossRef]
30. Debelle, F.D.; Nortier, J.L.; de Prez, E.G.; Garbar, C.H.; Vienne, A.R.; Salmon, I.J.; Deschodt-Lanckman, M.M.; Vanherweghem, L.J. Aristolochic acids induce chronic renal failure with interstitial fibrosis in salt-depleted rats. *J. Am. Soc. Nephrol.* **2002**, *13*, 431–436.
31. Sheehan, S.M.; Korstanje, R. Automatic glomerular identification and quantification of histological phenotypes using image analysis and machine learning. *Am. J. Physiol. Renal Physiol.* **2018**, *315*, F1644–F1651. [CrossRef] [PubMed]
32. Ryu, R.-E.; Jo, W.; Choi, H.; Jang, S.; Lee, H.; Woo, D.C.; Kim, J.K.; Kim, K.W.; Yu, E.S.; Son, W. Evaluation of Nonalcoholic Fatty Liver Disease in C57BL/6J Mice by Using MRI and Histopathologic Analyses. *Comp. Med.* **2015**, *65*, 409–415. [PubMed]
33. Aleidi, S.; Issa, A.; Bustanji, H.; Khalil, M.; Bustanji, Y. Adiponectin serum levels correlate with insulin resistance in type 2 diabetic patients. *Saudi Pharm. J.* **2015**, *23*, 250–256. [CrossRef] [PubMed]
34. Pajvani, B.; Hawkins, M.; Combs, T.P.; Rajala, M.W.; Doebber, T.; Berger, J.P.; Wagner, J.A.; Wu, M.; Knopps, A.; Xiang, A.H.; et al. Complex distribution, not absolute amount of adiponectin, correlates with thiazolidinedione-mediated improvement in insulin sensitivity. *J. Biol. Chem.* **2004**, *279*, 12152–12162. [CrossRef] [PubMed]
35. Alex, S.; Boss, A.; Heerschap, A.; Kersten, S. Exercise training improves liver steatosis in mice. *Nutr. Metab. (Lond.)* **2015**, *12*, 29. [CrossRef] [PubMed]
36. Lavie, C.J.; Pandey, A.; Lau, D.H.; Alpert, M.A.; Sanders, P. Obesity and Atrial Fibrillation Prevalence, Pathogenesis, and Prognosis: Effects of Weight Loss and Exercise. *J. Am. Coll. Cardiol.* **2017**, *70*, 2022–2035. [CrossRef]
37. Lee, S.; Kuk, J.L.; Davidson, L.E.; Hudson, R.; Kilpatrick, K.; Graham, T.; Ross, R. Exercise without weight loss is an effective strateg.y for obesity reduction in obese individuals with and without Type 2 diabetes. *J. Appl. Physiol.* **2005**, *99*, 1220–1225. [CrossRef]
38. Petridou, A.; Siopi, A.; Mougios, V. Exercise in the management of obesity. *Metabolism* **2019**, *92*, 163–169. [CrossRef]
39. De Carvalho, F.P.; Moretto, T.L.; Benfato, I.D.; Barthichoto, M.; Ferreira, S.M.; Júnior, J.M.C.; de Oliveira, C.A.M. Central and peripheral effects of physical exercise without weight reduction in obese and lean mice. *Biosci. Rep.* **2018**, *38*, BSR20171033. [CrossRef]
40. Chaar, L.J.; Coelho, A.; Silva, N.M.; Festuccia, W.L.; Antunes, V.R. High-fat diet-induced hypertension and autonomic imbalance are associated with an upregulation of CART in the dorsomedial hypothalamus of mice. *Physiol. Rep.* **2016**, *4*, e12811. [CrossRef]
41. Hariri, N.; Thibault, L. High-fat diet-induced obesity in animal models. *Nutr. Res. Rev.* **2010**, *23*, 270–299. [CrossRef] [PubMed]
42. Farzanegi, P.; Dana, A.; Ebrahimpoor, Z.; Asadi, M.; Azarbayjani, M.A. Mechanisms of beneficial effects of exercise training on non-alcoholic fatty liver disease (NAFLD): Roles of oxidative stress and inflammation. *Eur. J. Sport Sci.* **2019**, *19*, 994–1003. [CrossRef] [PubMed]
43. Castaneda, C.; Layne, J.E.; Munoz-Orians, L.; Gordon, P.L.; Walsmith, J.; Foldvari, M.; Roubenoff, R.; Tucker, K.L.; Nelson, M.E. A randomized controlled trial of resistance exercise training to improve glycemic control in older adults with type 2 diabetes. *Diabetes Care* **2002**, *25*, 2335–2341. [CrossRef]

44. Ivy, J.L. Role of exercise training in the prevention and treatment of insulin resistance and non-insulin-dependent diabetes mellitus. *Sports Med.* **1997**, *24*, 321–336. [CrossRef] [PubMed]
45. Bird, S.R.; Hawley, J.A. Update on the effects of physical activity on insulin sensitivity in humans. *BMJ Open Sport Exerc. Med.* **2016**, *2*, e000143. [CrossRef] [PubMed]
46. O'Neill, H.M. AMPK and Exercise: Glucose Uptake and Insulin Sensitivity. *Diabetes Metab. J.* **2013**, *37*, 1–21. [CrossRef] [PubMed]
47. Zhu, N.; Pankow, J.S.; Ballantyne, C.M.; Couper, D.; Hoogeveen, R.C.; Pereira, M.; Duncan, B.B.; Schmidt, M.I. High-molecular-weight adiponectin and the risk of type 2 diabetes in the ARIC study. *J. Clin. Endocrinol. Metab.* **2010**, *95*, 5097–5104. [CrossRef]
48. Glass, O.K.; Radia, A.; Kraus, W.E.; Abdelmalek, M.F. Exercise Training as Treatment of Nonalcoholic Fatty Liver Disease. *J. Funct.* **2017**, *2*, 35. [CrossRef]
49. Chun, S.K.; Lee, S.; Yang, M.-J.; Leeuwenburgh, C.; Kim, J.-S. Exercise-Induced Autophagy in Fatty Liver Disease. *Exerc. Sport Sci. Rev.* **2017**, *45*, 181–186. [CrossRef]
50. Takahashi, H.; Kotani, K.; Tanaka, K.; Egucih, Y.; Anzai, K. Therapeutic Approaches to Nonalcoholic Fatty Liver Disease: Exercise Intervention and Related Mechanisms. *Front. Endocrinol.* **2018**, *9*, 588. [CrossRef]
51. Mendizábal, Y.; Llorens, S.; Nava, E. Hypertension in metabolic syndrome: Vascular pathophysiology. *Int. J. Hypertens.* **2013**, *2013*, 230868. [CrossRef] [PubMed]
52. Sakamoto, S. Prescription of exercise training for hypertensives. *Hypertens. Res.* **2020**, *43*, 155–161. [CrossRef] [PubMed]
53. Nascimento, T.B.; Ekeledo, O.J.; Anderson, R.; Le, H.B.; de Chantemèle, E.J.B. Long Term High Fat Diet Treatment: An Appropriate Approach to Study the Sex-Specificity of the Autonomic and Cardiovascular Responses to Obesity in Mice. *Front. Physiol.* **2017**, *8*, 32.
54. Stump, C.S. Physical Activity in the Prevention of Chronic Kidney Disease. *Cardiorenal Med.* **2011**, *1*, 164–173. [CrossRef]
55. Muller, C.R.; Americo, A.L.V.; Fiorino, P.; Evangelista, F.S. Aerobic exercise training prevents kidney lipid deposition in mice fed a cafeteria diet. *Life Sci.* **2018**, *211*, 140–146. [CrossRef]
56. Fassett, R.G.; Venuthurupalli, S.K.; Gobem, G.C.; Coombes, J.S.; Cooper, M.A.; Hoy, W.E. Biomarkers in chronic kidney disease: A review. *Kidney Int.* **2011**, *80*, 806–821. [CrossRef] [PubMed]
57. Viollet, B.; Horman, S.; Leclerc, J.; Lantier, L.; Foretz, M.; Billaud, M.; Giri, S.; Andreelli, F. AMPK inhibition in health and disease. *Crit. Rev. Biochem. Mol. Biol.* **2010**, *45*, 276–295. [CrossRef] [PubMed]
58. Jeon, S.-M. Regulation and function of AMPK in physiology and diseases. *Exp. Mol. Med.* **2016**, *48*, e245. [CrossRef] [PubMed]
59. Dugan, L.L.; You, Y.H.; Ali, S.S.; Stanic, M.D.; Miyamoto, S.; de Cleves, A.E.; Andreyev, A.; Quach, T.; Ly, S.; Shekhtman, G.; et al. AMPK dysregulation promotes diabetes-related reduction of superoxide and mitochondrial function. *J. Clin. Investig.* **2013**, *123*, 4888–4899. [CrossRef]
60. Al-Rasheed, N.M.; Al-Rasheed, N.M.; Attia, H.A.; Al-Amin, M.A.; Al-Ajmi, H.N.; Hasan, I.H.; Mohamad, R.A.; Sinjilawi, N.A. Renoprotective Effects of Fenofibrate via Modulation of LKB1/AMPK mRNA Expression and Endothelial Dysfunction in a Rat Model of Diabetic Nephropathy. *Pharmacology* **2015**, *95*, 229–239. [CrossRef]
61. Rogacka, D.; Audzeyenka, I.; Rychłowski, M.; Rachubik, P.; Szrejder, M.; Angielski, S.; Piwkowsk, A. Metformin overcomes high glucose-induced insulin resistance of podocytes by pleiotropic effects on SIRT1 and AMPK. *Biochim. Biophys. Acta Mol. Basis Dis.* **2018**, *1864*, 115–125. [CrossRef] [PubMed]
62. Zhou, Y.; Lin, S.; Zhang, L.; Li, Y. Resveratrol prevents renal lipotoxicity in high-fat diet-treated mouse model through regulating PPAR-α pathway. *Mol. Cell Biochem.* **2016**, *411*, 143–150. [CrossRef] [PubMed]
63. Choi, S.R.; Lim, J.H.; Kim, M.Y.; Kim, E.N.; Kim, Y.; Choi, B.S.; Kim, Y.; Kim, H.W.; Lim, K.M.; Kim, M.J. Adiponectin receptor agonist AdipoRon decreased ceramide, and lipotoxicity, and ameliorated diabetic nephropathy. *Metabolism* **2018**, *85*, 348–360. [CrossRef] [PubMed]
64. Juszczak, F.; Caron, N.; Mathew, A.V.; Declèves, A.-E. Critical Role for AMPK in Metabolic Disease-Induced Chronic Kidney Disease. *Int. J. Mol. Sci.* **2020**, *21*, 7994. [CrossRef]
65. Lin, T.-A.; Wu, V.C.-C.; Wang, C.-Y. Autophagy in Chronic Kidney Diseases. *Cells* **2019**, *8*, 61. [CrossRef]
66. Dikic, I.; Elazar, Z. Mechanism and medical implications of mammalian autophagy. *Nat. Rev. Mol. Cell Biol.* **2018**, *19*, 349–364. [CrossRef]
67. Satriano, J.; Sharma, K. Autophagy and metabolic changes in obesity-related chronic kidney disease. *Nephrol. Dial. Transplant.* **2013**, *28*, iv29–iv36. [CrossRef]
68. Yamamoto, T.; Takabatake, Y.; Takahashi, A.; Kimura, T. High-Fat Diet-Induced Lysosomal Dysfunction and Impaired Autophagic Flux Contribute to Lipotoxicity in the Kidney. *J. Am. Soc. Nephrol.* **2016**, 1–18. [CrossRef]
69. He, C.; Bassik, M.C.; Moresi, V.; Sun, K.; Wei, Y.; Zou, Z.; An, Z.; Loh, J.; Fisher, J.; Sun, Q. Exercise-induced BCL2-regulated autophagy is required for muscle glucose homeostasis. *Nature* **2012**, *481*, 511–515. [CrossRef]
70. Klionsky, D.J.; Abdelmohsen, K.; Abe, A.; Abedin, M.J.; Abeliovich, H.; Arozena, A.A.; Adachi, H.; Adams, C.M.; Adams, P.D.; Adeli, K.; et al. Guidelines for the use and interpretation of assays for monitoring autophagy (3rd edition). *Autophagy* **2016**, *12*, 1–222. [CrossRef]

71. Peng, H.; Wang, Q.; Lou, T.; Qin, J.; Jung, S.; Shetty, V.; Li, F.; Wang, Y.; Feng, X.H.; Mitch, W.E.; et al. Myokine mediated muscle-kidney crosstalk suppresses metabolic reprogramming and fibrosis in damaged kidneys. *Nat. Commun.* **2017**, *8*, 1493. [CrossRef] [PubMed]
72. Xin, C.; Liu, J.; Zhang, J.; Zhu, D.; Wang, H.; Xiong, L.; Lee, Y.; Ye, J.; Lian, K.; Xu, C.; et al. Irisin improves fatty acid oxidation and glucose utilization in type 2 diabetes by regulating the AMPK signaling pathway. *Int. J. Obes. (Lond.)* **2016**, *40*, 443–451. [CrossRef] [PubMed]

Supplementary

Delayed Exercise Training Improves Obesity-Induced Chronic Kidney Disease by Activating AMPK Pathway in High-Fat Diet-Fed Mice

Florian Juszczak [1,2,*], Maud Vlassembrouck [1], Olivia Botton [2], Thomas Zwakhals [1], Morgane Decarnoncle [1], Alexandra Tassin [3], Nathalie Caron [2] and Anne-Emilie Declèves [1]

[1] Laboratory of Metabolic and Molecular Biochemistry, Faculty of Medicine and Pharmacy, Research Institute for Health Sciences and Technology, University of Mons (UMONS), 7000 Mons, Belgium; maudvlassembrouck@gmail.com (M.V.); Thomas.ZWAKHALS@umons.ac.be (T.Z.); Morgane.decarnoncle@student.umons.ac.be (M.D.); anne-emilie.decleves@umons.ac.be (A.-E.D.)
[2] Molecular Physiology Research Unit (URPhyM), Namur Research Institute for Life Sciences (NARILIS), University of Namur (UNamur), 5000 Namur, Belgium; olivia.botton@unamur.be (O.B.); nathalie.caron@unamur.be (N.C.)
[3] Laboratory of Respiratory Physiology, Pathophysiology and Rehabilitation, Faculty of Medicine and Pharmacy, Research Institute for Health Sciences and Technology, University of Mons (UMONS), 7000 Mons, Belgium; anne-emilie.decleves@umons.ac.be
* Correspondence: florian.juszczak@umons.ac.be; Tel.: +3265373580

Citation: Juszczak, F.; Vlassembrouck, M.; Botton, O.; Zwakhals, T.; Decarnoncle, M.; Tassin, A.; Caron, N.; Declèves, A.-E. Delayed exercise training improves obesity-induced chronic kidney disease by activating AMPK pathway in high-fat diet-fed mice. *Int. J. Mol. Sci.* **2020**, *22*, x. https://doi.org/10.3390/xxxxx

Received: 14 November 2020
Accepted: 26 December 2020
Published: date

Publisher's Note: MDPI stays neutral with regard to jurisdictional claims in published maps and institutional affiliations.

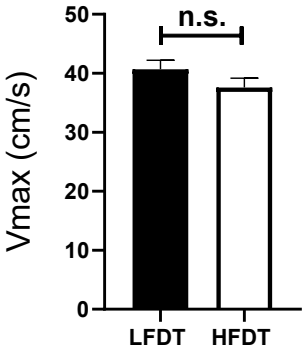

Figure S1. Effects of endurance exercise training on running velocity. Representation of maximal running velocity performance after 14 weeks on diet. *t-test*. Data are presented as means ± SEM. *ns* = non-significant. *n=10* in each group.

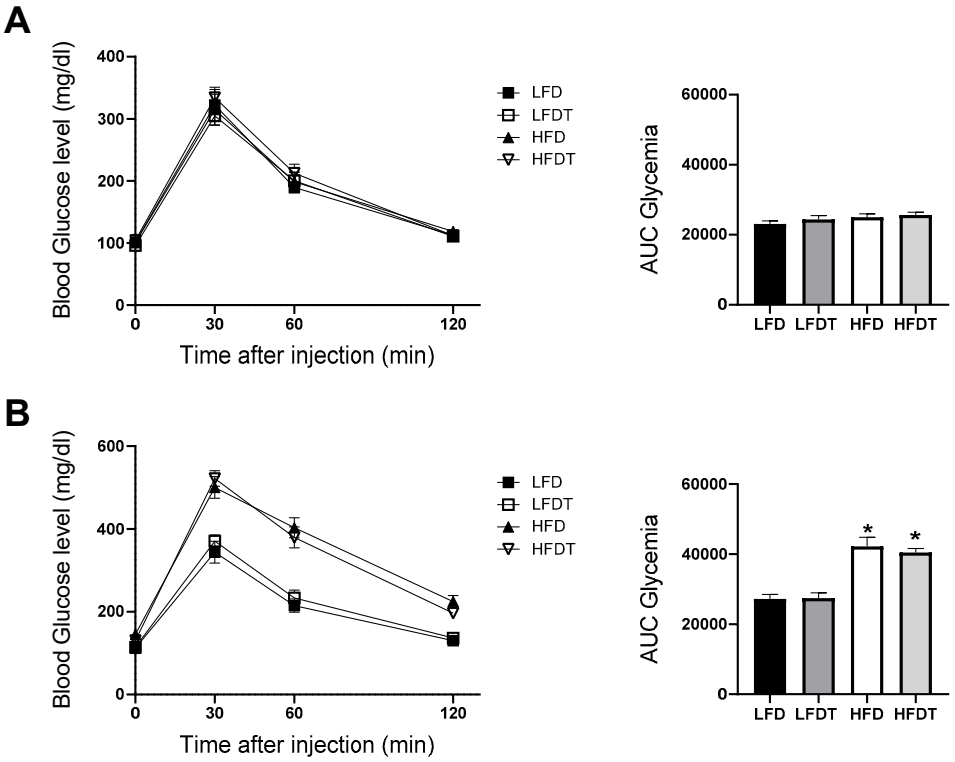

Figure S2. Effects of LFD and HFD on glucose tolerance in mice. Glucose tolerance test at week 0 (**A**) and week 12 (**B**). Fasted mice were submitted to an intraperitoneal injection of glucose (2 g/ kg b.w.). Glycemia was measured before (0) and 30, 60 and 120 min after injection. Histogram represents the area under the curve (AUC) of glycemia from 0 to 120 min

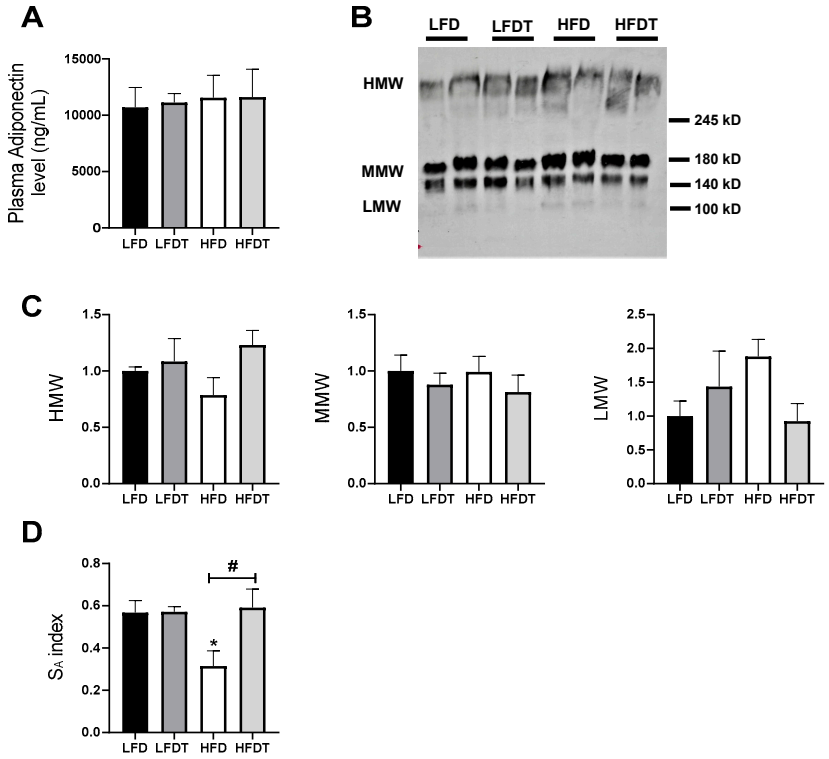

Figure S3. Total plasma adiponectin and adiponectin multimers distribution analysis at week 20. **A**. Ad plasmatic level. The total plasma Ad concentration was measured using indirect ELISA. **B**. Representative immunoblots of Adiponectin multimers expression in plasma sample. **C**. Relative densitometry of the immunoblots representing respectively HMW (High Molecular Weight), MMW (Medium Molecular Weight) and LMW (Low Molecular Weight) multimers of Adiponectin normalized with total Adiponectin protein level. **D**. S_A index was calculated as the ratio HMW/(HMW + LMW). Data are presented as means ± SEM. * $P \leq 0.05$ versus LFD $^{\#}$ $P \leq 0.05$ versus HFD. *n=6-8* in each group.

Table S1. Primer sequences for RT-qPCR analysis of mRNA expression

Gene		Primer Sequences (5'-3')
COLI	Fw	CTTGCCCCATTCATTTGTCT
	Rv	GCAGGTTCACCTACTCTGTTCT
COLIII	Fw	TGAGTCGAATTGGGGAGAAT
	Rv	TCCCCTGGAATCTGTGAATC
TGFβ	Fw	TGGAGCAACATGTGGAACTC
	Rv	GTCAGCAGCCGGTTACCA
MCP-1	Fw	CTTCTGGGCCTGCTGTTCA
	Rv	CCAGCCTACTCATTGGGATCA
IL1β	Fw	AGTTGACGGACCCCAAAAG
	Rv	AGCTGGATGCTCTCATCAGG
TNFα	Fw	TACTGAACTTCGGGGTGATTGGTCC
	Rv	CAGCCTTGTCCCTTGAAGAGAACC
IL6	Fw	GCTACCAAACTGGATATAATCAGGA
	Rv	CCAGGTAGCTATGGTACTCCAGAA
ACC (Acaca)	Fw	ATGGGCGGAATGGTCTCTTTC
	Rv	TGGGGACCTTGTCTTCATCAT
FAS (FASN)	Fw	GGAGGTGGTGATAGCCGGTAT
	Rv	TGGGTAATCCATAGAGCCCAG
CPT-1 (CPT1a)	Fw	CTCCGCCTGAGCCATGAAG
	Rv	CACCAGTGATGATGCCATTCT
18S	Fw	CGCCGCTAGAGGTGAAATTCT
	Rv	CGAACCTCCGACTTTCGTTCT

Table S2. Effects of delayed EET on systolic, diastolic and mean blood pressure in mice fed a LFD, LFDT or HFD and HDFT**.**

	LFD	**LFDT**	**HFD**	**HFDT**
Systolic blood pressure *(mmHg)*	128,6 ± 10,99	138,0 ± 4,988	119,5 ± 10,86	119,3 ± 5,850
Diastolic blood pressure *(mmHg)*	106,8 ± 10,60	117,6 ± 2,584	96,33 ± 8,750	101,7 ± 6,035
Mean blood pressure *(mmHg)*	117,7 ± 10,78	127,8 ± 3,763	107,9 ± 9,768	110,5 ± 5,570

Measurement were performed during the last week of the experimental protocol (week 20). Systemic, diastolic and mean blood pressures were measured using a non-invasive CODA tail-cuff blood pressure occlusion system (Kent Scientific, Torrington, USA). During the week 20, measurements were taken for each animal that were acclimatized for a 1-hour period before experiments into restraining chambers. The animals were placed onto a preheated pad maintained at 30°C in a designed quiet area and blood pressure measurements were initiated when tail temperature reached 30°C (measured using an infrared sensor) and recorded at least 5 times. Mice were acclimated for at least 3 consecutive days before baseline blood pressure measurements. No statistical difference was found by One-way ANOVA analysis. *n=5* in each group.

Table S3. Effects of delayed EET on renal gene expression in mice fed a LFD, a LFDT, a HFD and a HFDT.

	LFD	**LFDT**	**HFD**	**HFDT**
Lipid metabolism markers				
ACC	1,000 ± 0,0918	0,9636 ± 0,1356	1,067 ± 0,1404	1,028 ± 0,0796
FAS	1,000 ± 0,0265	1,023 ± 0,1480	1,218 ± 0,2496	1,112 ± 0,1884
CPT-1	1,000 ± 0,0326	0,9017 ± 0,1308	0,8483 ± 0,1201	1,222 ± 0,2337

Real-time quantitative qPCR for Acetyl-CoA carboxylase (*ACC*), Fatty acid synthase (*FAS*) and Carnitine palmitoyltransferase I (*CPT1*). mRNA expressions were performed on kidney tissue from LFD, LFDT, HFD and HFDT mice normalized against 18S. Statistical analyses were performed by one-way ANOVA followed by Newman–Keuls post hoc test. Data are presented as means ± SEM. * $P \leq 0.05$ versus LFD $^{\#}$ $P \leq 0.05$ versus HFD. *n=6* in each group.